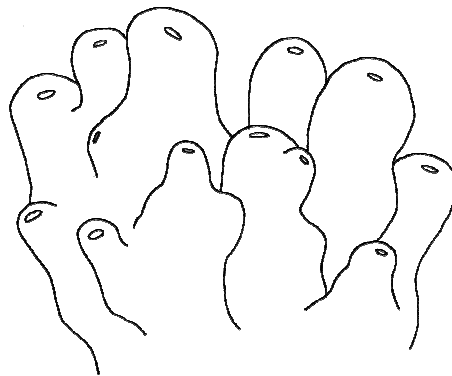


**Secondary metabolites from marine sponges,
with focus on the chemical ecology and biochemical characterisation of the
stress-induced biotransformation of *Aplysina* alkaloids**

Sekundärmetabolite mariner Schwämme,
mit Schwerpunkt auf der chemischen Ökologie und biochemischen Charakterisierung der
stressinduzierten Biotransformation von *Aplysina*-Alkaloiden



Inaugural - Dissertation
zur Erlangung des naturwissenschaftlichen Doktorgrades
der Mathematisch-Naturwissenschaftlichen Fakultät
der Heinrich-Heine-Universität Düsseldorf

vorgelegt von Annika Putz
aus Münster

Düsseldorf, März 2009

Aus dem Institut für Pharmazeutische Biologie und Biotechnologie
der Heinrich-Heine Universität Düsseldorf

Gedruckt mit der Genehmigung der Mathematisch-Naturwissenschaftlichen Fakultät der
Heinrich-Heine-Universität Düsseldorf

Referent: Prof. Dr. Peter Proksch

Koreferent: Prof. Dr. Lutz Schmitt

Tag der mündlichen Prüfung: 04.05.2009

Für meine Eltern

Contents

Introduction	1
Marine natural products.....	1
Ecological functions of marine secondary metabolites	2
Chemical defence systems.....	3
<i>Aplysina</i> sponges	4
Secondary metabolites	5
Chemical ecology	7
System under investigation.....	8
Stress-induced biotransformation of <i>Aplysina</i> alkaloids	9
Aims of this thesis	12
Part I: Isolation of secondary metabolites from marine sponges.....	13
Methods	13
General materials and methods.....	13
Isolation of secondary metabolites	19
Biological activity	30
Results	38
Identification of isolated compounds	38
Biological activity	64
Part II: Chemical ecology of Mediterranean sponges	71
Methods	71
Quantification of sponge metabolites	71
<i>Aplysina</i> depth profile.....	71
Transplantation of <i>Aplysina</i> sponges to different depths.....	74
Transplantation of three Mediterranean sponges to different light conditions...	74
Data analysis.....	75
Results	76
<i>Aplysina</i> depth profile.....	76
Transplantation of <i>Aplysina</i> sponges to different depths.....	80
Transplantation of three Mediterranean sponges to different light conditions...	84
Part III: Stress-induced biotransformation in <i>Aplysina</i> sponges	89
Methods	89
General materials and methods.....	89

Isolation of the substrate aerophobin-2 (2) from <i>Aplysina aerophoba</i>	97
Purification of the isoxazoline cleaving enzyme	98
Results	125
Differential centrifugation.....	125
Washing membranes with sodium carbonate.....	126
Solubilisation of cell membranes	128
Ion exchange chromatography	134
Gel filtration	136
Affinity chromatography.....	140
Labelling of the isoxazoline cleaving enzyme & detection via Western blot..	149
Trypsin digestion and mass analysis of the isoxazoline cleaving enzyme.....	155
Discussion	156
Secondary metabolites from marine sponges.....	156
Chemical ecology.....	162
<i>Aplysina</i>	162
<i>Dysidea avara</i> and <i>Agelas oroides</i>	165
Related studies	166
Stress-induced biotransformation of <i>Aplysina</i> alkaloids.....	167
Purification of the isoxazoline cleaving enzyme	168
Characterisation of the isoxazoline cleaving enzyme	171
Conclusion and perspectives	172
Summary	174
Zusammenfassung.....	176
References	178
Abbreviations	188
Appendix	190
List of isolated compounds	190
Quantified metabolites: Calibration curves, UV spectra, molecular weight....	194
NMR spectra of isolated compounds	204
Supplementary data on <i>Aplysina</i> peptide sequences.....	220
Acknowledgments.....	227
Publications	229
Curriculum vitae.....	230
Erklärung.....	231

Introduction

Marine natural products

Nature has provided a broad arsenal of structurally diverse and pharmacologically active compounds that serve as highly effective drugs or lead structures for the development of novel synthetically derived drugs to combat a multitude of diseases. Traditionally, terrestrial organisms represented the richest source of natural drugs, such as plants (e.g. paclitaxel (Taxol[®]) from *Taxus brevifolia* which was later found to be produced by the endophytic fungus *Taxomyces andreanae* (Stierle et al. 1993)), or microorganisms (e.g. penicillins from *Penicillium notatum*). However, research in the field of marine derived natural products is comparably young, with the first serious attempts to utilise the vast potential of marine organisms as sources of bioactive metabolites starting in the late 1960s (Proksch et al. 2002). Usually, the isolation of prostaglandin derivatives from the Caribbean gorgonian *Plexaura homomalla* (Weinheimer and Spraggins 1969) is considered as starting point of marine chemistry, although Bergmann and Feeney (1951) already discovered unusual nucleoside derivatives in the sponge *Tethya crypta* in the 1950s. Later, nucleoside drugs for the chemotherapy of viral infections such as Ara-A (Vidarabin[®]) were developed based on the model of the above mentioned compounds. Since then, more than 18,000 different marine natural products have been isolated (MarinLit 2007), proving the constant, rapid growth of this field. Considering the fact that over 70 % of the earth surface is covered by oceans providing the habitat for rich biodiversity, aspiration in marine bioprospecting as viable counterpart to the discovery of bioactive compounds from the terrestrial environment seems justified, especially behind the background that presently close to 20 different marine natural products or natural product derivatives are involved in clinical studies (Putz and Proksch accepted). Recently, a toxin derived from marine *Conus* snails was introduced into the drug market as new analgesic (Prialt[®]). Another compound, the anticancer drug ET-743 (Yondelis[®]) from the marine tunicate *Ecteinascidia turbinata* is currently in phase II and III clinical trials (Proksch et al. 2006). Interestingly, the majority of marine natural products involved in clinical or preclinical trials is produced by invertebrates, i.e. sponges, tunicates, bryozoans or mollusks, which is in contrast to the compounds derived from the terrestrial

environment where plants by far exceed animals with respect to the production of bioactive metabolites (Proksch et al. 2002).

Ecological functions of marine secondary metabolites

Since the production of secondary metabolites requires the investment of valuable resources in terms of nutrients and energy, they impose a considerable cost to the producing organism. Therefore, trade-offs between defensive chemistry and other physiological processes such as growth emerge (Donaldson et al. 2006). It is therefore likely to assume an ecological function of these compounds. With this respect, the fact that bioactive metabolites are predominantly found in sessile or slow-moving marine organisms that lack physical defence structures such as algae and most marine invertebrates (Blunt et al. 2008) thus appears to reflect the ecological importance of these compounds for the respective organism.

In the marine environment, overall threats involve inter- as well as intraspecific interactions. The soft bodies of sessile or slow-moving invertebrates such as sponges often live exposed and exhibit conspicuous colours despite the lack of protecting shells or other physical defence structures, thus making them prone to face a high risk of predation. Many of these organisms compensate for their lack of a physical defence in terms of a chemical defence. Numerous studies of marine natural products have indicated the significance of these metabolites against predatory or herbivorous fish or other predators (Paul and Puglisi 2004; Paul et al. 2006).

Furthermore, competition for space is generally intense on marine hard bottom substrates, and appears to be most pronounced on tropical reefs characterised by high biodiversity and remarkable population density unmatched in any other marine ecosystem (Jackson 1977; Branch 1984; Porter and Targett 1988; Sale 1991). Therefore, allelopathic effects through biosynthesis and exudation of toxic compounds appear to play a crucial role in structuring benthic marine ecosystems (Putz and Proksch accepted).

In the marine environment, fouling is a ubiquitous biological phenomenon (Fusetani 2004), which is referred to as growth of animals and plants on artificial (man made) or natural surfaces (rocks, reefs, but also the surfaces of animals and algae). Fouling organisms include micro- (e.g. bacteria, diatoms and protozoa) as well as macroorganisms (algae and invertebrates) (Bakus et al. 1986; Davis et al. 1989; Bakus et al. 1990; Ortlepp et al. 2007). Especially for filter-feeding organisms such as corals

and sponges, fouling may be disadvantageous or even life-threatening if inhalant canals are blocked by epibionts, resulting in a reduced feeding capacity. In addition, epibionts might compete with their hosts for food. However, surfaces of marine invertebrates are usually remarkably free of fouling organisms, supporting the assumption that this is achieved by secretion of anti-fouling compounds. The latter is further confirmed by the anti-fouling potential found for a wide range of marine natural products (reviewed in e.g. Fusetani 2004; Paul and Ritson-Williams 2008).

Interestingly, an obvious chemical similarity or even identity is often found between natural products derived from marine invertebrates and those known to occur in microorganisms such as bacteria and microalgae (Putz and Proksch accepted). Since marine invertebrates, especially sponges, often house a large number of microorganisms in their tissues, it appears tempting to assume that in many cases, associated microorganisms are the true producers of bioactive natural compounds. This could for instance be shown for the highly toxic protein phosphatase inhibitor okadaic acid which had originally been isolated from sponges of the genus *Halichondria* (Tachibana et al. 1981), whose production was later attributed to dinoflagellates of the genus *Prorocentrum* (Murakami et al. 1982). Direct proof for a microbial origin of bioactive invertebrate metabolites is, however, hampered by the fact that most invertebrate-associated microorganisms cannot not be successfully cultivated (e.g. Friedrich et al. 2001).

Chemical defence systems

Most chemical defence strategies reported so far for marine invertebrates or algae are constitutive and rely on preformed toxic or deterrent compounds that are present in tissues and either liberated upon wounding or constantly exuded (Walker et al. 1985). However, chemical ecological studies in the terrestrial environment have repeatedly shown that the defence of plants may be highly dynamic rather than static. Stress-induced defence strategies are dynamic and involve e.g. the accelerated biosynthesis of constitutively present compounds upon tissue damage or attack by pathogens (Marak et al. 2002; Bezemer et al. 2004; Alves et al. 2007). Another example for a stress-induced defence in plants is the de novo biosynthesis of phytoalexins especially in response to invading fungi (Pedras et al. 2000; Heil and Bostock 2002). Apart from the induced defence strategies, activated defence systems represent a further highly dynamic defence reaction (Paul and Van Alstyne 1992). Activated defence mechanisms are fast

and occur mostly within seconds after cell compartmentalisation is disturbed. Protoxins get into contact with liberating enzymes that catalyse a biotransformation of protoxins yielding the actual defence metabolite. The most prominent example from the terrestrial environment is found in cyanogenic plants. After the plant tissue is wounded, β -glucosidases catalyse the hydrolysis of cyanogenic glycosides to form chemically unstable cyanohydrins that in turn are transformed into the defence metabolite hydrocyanic acid (Conn 1979; Wajant and Effenberger 1996).

However, activated defence mechanisms are not only known from plants, but also from the marine environment. The first example in the marine habitat was described for tropical green algae of the genus *Halimeda* that contain halimedatetraacetate as major metabolite. Upon tissue damage, halimedatetraacetate is (probably enzyme-catalysed) converted into the chemically highly reactive halimedatriol (Paul and Van Alstyne 1992) that causes an increase of feeding deterrence towards herbivorous fishes (Paul and Van Alstyne 1988). For sponges, the wound-induced biotransformation of isoxazoline alkaloids in *Aplysina* sponges was the first example proposed as an activated chemical defence strategy (Teeyapant and Proksch 1993) which will be described in detail in the next chapter.

***Aplysina* sponges**

Sponges of the genus *Aplysina* are known for their structurally diverse brominated isoxazoline alkaloids (Cimino et al. 1983; Ciminiello et al. 1994a; Ciminiello et al. 1994b, 1995; Ciminiello et al. 1996a; Ciminiello et al. 1996b; Ciminiello et al. 1997; Ciminiello et al. 1999, 2000; Thoms et al. 2003a) which act as potent chemical defence against predators and microorganisms (Teeyapant et al. 1993b; Weiss et al. 1996; Encarnación-Dimayuga et al. 2003; Kelly et al. 2003; Thoms et al. 2004). *Aplysina* species occur in the Mediterranean Sea, the Atlantic Ocean, and in the Caribbean Sea (Pawlik et al. 1995) where they often contribute to the dominant sponges present. The Mediterranean Sea is home to two *Aplysina* species: *Aplysina aerophoba* which occurs in water depths as low as 1 m (Riedl 1983; Pansini 1997; Thoms et al. 2003b), and *Aplysina cavernicola* which prefers shaded caves and deeper habitats (40 m or lower) (Wilkinson and Vacelet 1979; Thoms et al. 2003b).

Secondary metabolites

Both *A. aerophoba* and *A. cavernicola* contain aerophobin-2 (2) and aplysinamisin-1 (1) as brominated isoxazoline alkaloids, with the latter compound not always being found in *A. aerophoba* (Teeyapant et al. 1993a; Ciminiello et al. 1997; Thoms et al. 2003a; Thoms et al. 2004) (Figure 1, Table 1). Both species differ, however, chemically with regard to the occurrence of aerothionin (4), isofistularin-3 (3) and their yellowish pigments.

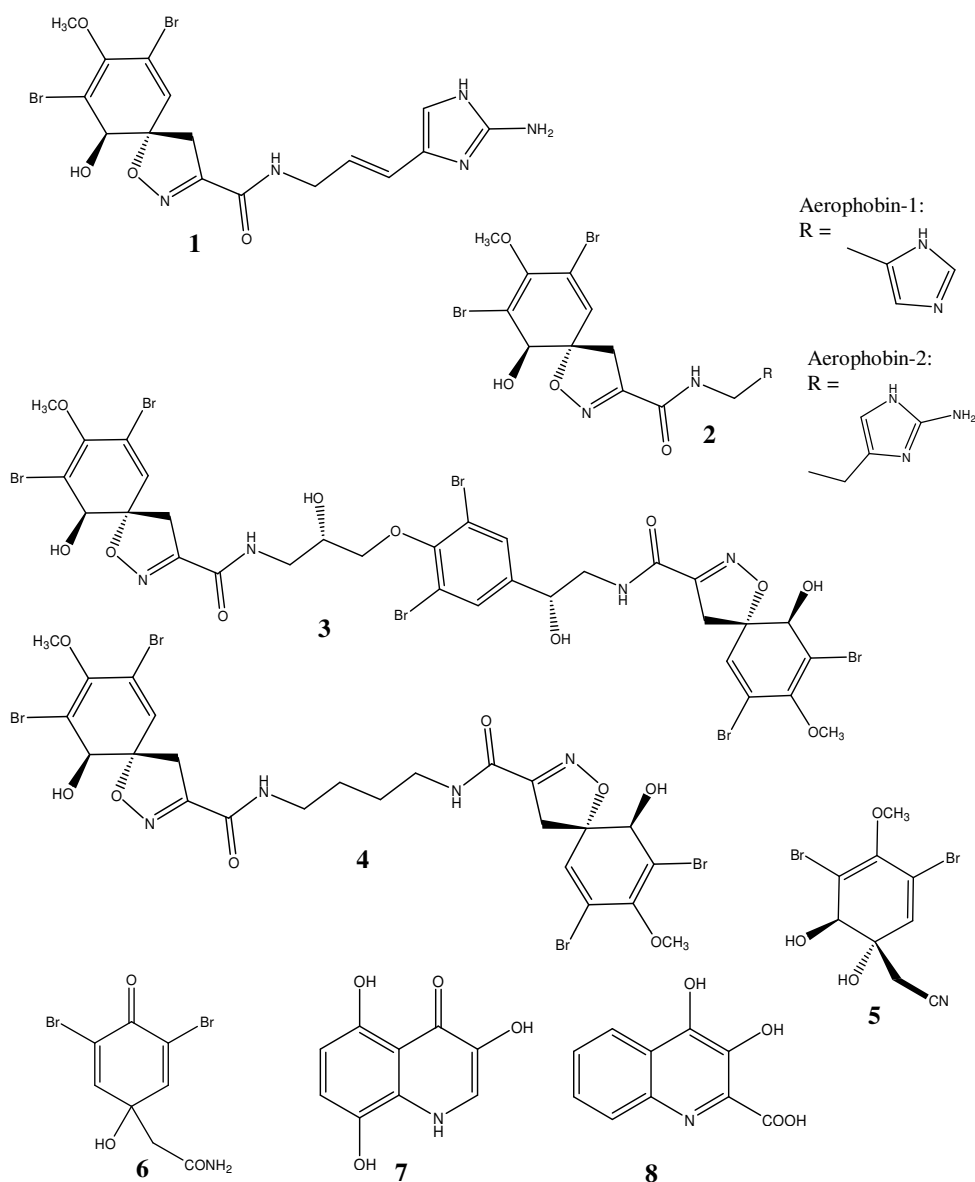


Figure 1. Structures of *Aplysina* metabolites: aplysinamisin-1 (1), aerophobin-2 (2), isofistularin-3 (3), aerothionin (4), aeroplysin-1 (5), dienone (6), uranidine (7), and 3,4-dihydroxyquinoline-2-carboxylic acid (8).

Table 1. Characteristic alkaloids of *Aplysina aerophoba* and *Aplysina cavernicola*.

	<i>A. aerophoba</i>	<i>A. cavernicola</i>
Aplysinamisin-1 (1)		X
Aerophobin-2 (2)	X	
Isofistularin-3 (3)	X	
Aerothionin (4)		X
Pigment uranidine (7)	X	
Pigment 3,4-dihydroxyquinoline -2-carboxylic acid (8)		X

A. aerophoba typically contains isofistularin-3 (3) and lacks detectable amounts of aerothionin (4) (Cimino et al. 1983; Ciminiello et al. 1997) (Table 1). Its highly unstable yellow pigment uranidine (7) polymerises rapidly when exposed to air and yields a black polymer (Cimino et al. 1984). This phenomenon is the reason for the name “aerophoba” (fearing air) which refers to the blackening of sponge tissue when exposed to air. In contrast, *A. cavernicola* shows no blackening of its tissues when exposed to air and contains aerothionin (4) as one of its major isoxazoline alkaloids. Instead of uranidine (7) the chemically rather stable pigment 3,4-dihydroxyquinoline-2-carboxylic acid (8) is accumulated (Thoms et al. 2003a; Thoms et al. 2004) (Table 1).

Morphologically, Vacelet 1959 distinguished *A. aerophoba* and *A. cavernicola* by surface texture, digitations, lateral projections and colour shade, with *A. aerophoba* being characterised by an auburn to darkly yellow colour, and *A. cavernicola* by a bright yellow colour. However, none of these characteristics proved to be a reliable marker, since *Aplysina* sponges are known to change their habitus when exposed to different ecological conditions (Wilkinson and Vacelet 1979; Klöppel et al. 2008).

Two brominated *Aplysina* compounds, aerothionin (4) and homoaerothionin, have been localised within the spherules of spherulous cells in the closely related tropical species *Aplysina fistularis* (Thompson et al. 1983). In *Aplysina*, spherulous cells are concentrated at the surface of sponge tissues, just beneath the exopinacoderm and the endopinacoderm of excurrent canals. Spherulous cells are widely distributed in demosponges, and share one characteristic: they degenerate and apparently release their cell contents into the intercellular matrix (Donadey and Vacelet 1977). The defensive role of the brominated alkaloids is further confirmed by the inclusion of spherulous cells in a collagenous envelope around spawned oocytes, a phenomenon described for *A. cavernicola* and *A. aerophoba* (Gallissan and Vacelet 1976). Later, Turon et al. (2000)

likewise demonstrated that brominated compounds of *A. aerophoba* are localised in the spherulous cells by coupling X-ray microanalysis with cryofixation techniques.

Chemical ecology

Aplysina sponges compensate for their lack of a physical defence with an effective chemical defence in terms of large amounts of isoxazoline alkaloids (Teeyapant et al. 1993b; Weiss et al. 1996; Encarnación-Dimayuga et al. 2003; Kelly et al. 2003; Thoms et al. 2004). However, sessile organisms living in steep environmental gradients are expected to face spatially variable selection (Jormalainen and Honkanen 2004). Aquatic littoral habitats provide such gradients on a relatively small spatial scale (Jormalainen and Honkanen 2004). Depth gradients generate heterogeneity in several ways, involving for example light quality, temperature, sea surge, nutrient availability and changing risk of predation. Such environmental factors have previously been shown to influence absolute content and/or composition of secondary metabolites of marine invertebrates and algae (Thompson et al. 1987; Harvell et al. 1993; Maida et al. 1993; Yates and Peckol 1993; Becerro et al. 1995; Jormalainen and Honkanen 2004; Page et al. 2005; Abdo et al. 2007).

Relatively few studies documented intraspecific variability in secondary metabolites through time and space (Thompson et al. 1987; Harvell et al. 1993; Maida et al. 1993; Yates and Peckol 1993; Becerro et al. 1995; Jormalainen and Honkanen 2004; Page et al. 2005; Abdo et al. 2007). This reveals that studies analysing the chemical defence of marine organisms thus have to take into account that secondary metabolite contents and patterns of individuals may not be stable, but are rather subject to considerable quantitative and/or qualitative variation. For sponges, evidence for adaptation of secondary metabolite production to changing biotic and/or abiotic environmental factors is so far fragmentary (Thompson et al. 1987; Harvell et al. 1993; Maida et al. 1993; Yates and Peckol 1993; Becerro et al. 1995; Jormalainen and Honkanen 2004; Page et al. 2005; Abdo et al. 2007). In order to shed more light on this issue, the influence of environmental factors such as depth and light on secondary metabolite content and patterns of three Mediterranean sponge species was investigated in this thesis.

System under investigation

Sponges of the genus *Aplysina* represent a suitable model system for studies of chemical ecology. *A. aerophoba* and *A. cavernicola* both occur in the Mediterranean Sea where they contribute to the dominant sponge species present. Especially *A. aerophoba* can be easily sampled due to its preferred habitat in shallow water, sometimes even as low as 1 m depth. Furthermore, *Aplysina* sponges contain large amounts of metabolites, facilitating the isolation of compounds from the sponge tissue, and accounting for the fact that secondary metabolites are well described and documented. *Aplysina* sponges thus represent an optimal system to investigate chemo-ecological effects *in situ*.

For the same reasons, *Agelas oroides* and *Dysidea avara* which likewise occur in the Mediterranean are suitable model species to investigate effects of ecological factors on secondary metabolite production. *Agelas oroides* sponges contain the well known major metabolites oroidin (11) and 4,5-dibromo-1*H*-pyrrole-carboxylic acid (12, Figure 2), and derivatives of the latter in minor amounts (Forenza et al. 1971; Fattorusso and Tagliatalata-Scafati 2000). Almost no bioactivity of these two major metabolites could be found in terms of cytotoxicity, antiplasmodial and anti-histaminic activity (Cafieri et al. 1997; König et al. 1998). However, both oroidin (11) and 4,5-dibromo-1*H*-pyrrole-carboxylic acid (12) were found to be involved in the chemical defence of *Agelas* sponges by acting as feeding deterrents against fish (Chanas et al. 1996; Assmann et al. 2000; Richelle-Maurer et al. 2003)

Avarol (9) and its oxidated form avarone (10, Figure 2) represent major metabolites of the sponge *Dysidea avara* (Minale et al. 1974). Avarol (9) is a cytostatically active compound and possesses antimicrobial properties (Cariello et al. 1982; Müller et al. 1984; Sarma et al. 1993), potentially indicating an ecological role in the prevention of biofouling. Both avarol (9) and avarone (10) inhibit the catalytic functions of human immunodeficiency virus type 1 (HIV-1) reverse transcriptase (RT) indiscriminately (Loya and Hizi 1990). As for the *Agelas oroides* metabolites, avarol (9) and avarone (10) are easily detectable and quantifiable via HPLC, thus facilitating chemo-ecological studies.

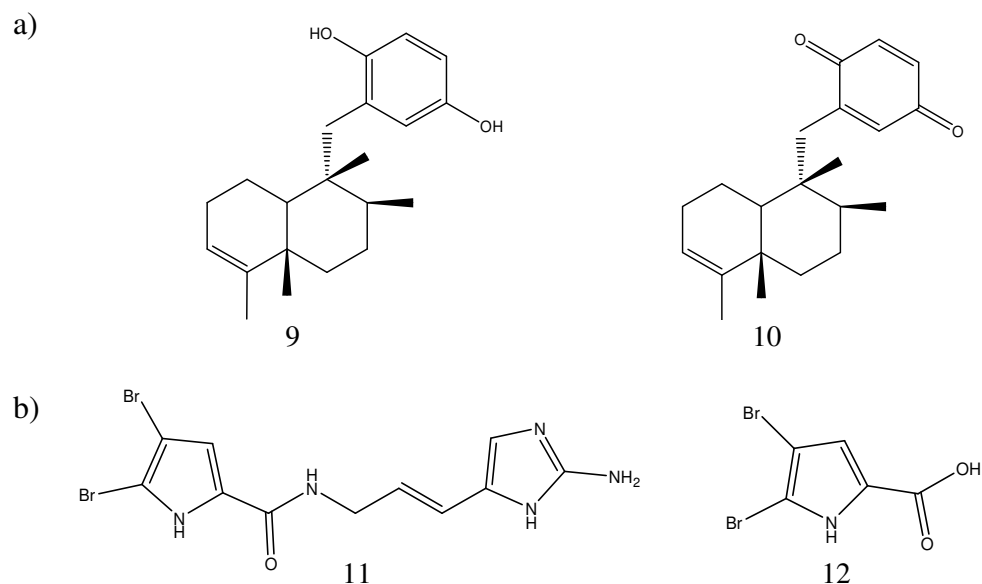


Figure 2. Major secondary metabolites of a) *Dysidea avara*: avarol (9) and avarone (10), and b) *Agelas oroides*: oroidin (11) and 4,5-dibromo-1*H*-pyrrol-2-carboxylic acid (12).

Stress-induced biotransformation of *Aplysina* alkaloids

All *Aplysina* species known are prone to a wound-induced bioconversion of brominated isoxazoline alkaloids giving rise to the nitrile aeroplysinin-1 (5) which in turn is transformed into a dienone (6) (Teeyapant and Proksch 1993; Ebel et al. 1997; Thoms et al. 2006). The bioconversion products aeroplysinin-1 (5) and dienone (6) show pronounced antibiotic activity against numerous marine and terrestrial bacteria (Teeyapant et al. 1993b; Weiss et al. 1996; Debitus et al. 1998). In contrast, their isoxazoline precursors exhibit no or only weak antibiotic activity, but rather act as feeding deterrents against fishes (Thoms et al. 2004).

Several PhD theses confirmed that the cleavage of isoxazoline *Aplysina* alkaloids is an enzyme catalysed reaction by inactivating sponge proteins by heat or treatment with acid. Since the biotransformation product aeroplysinin-1 (5) was not found in samples where proteins were denatured, it was concluded that the biotransformation taking place in *Aplysina* is an enzymatically catalysed reaction (Teeyapant 1994; Ebel 1998; Fendert 2000).

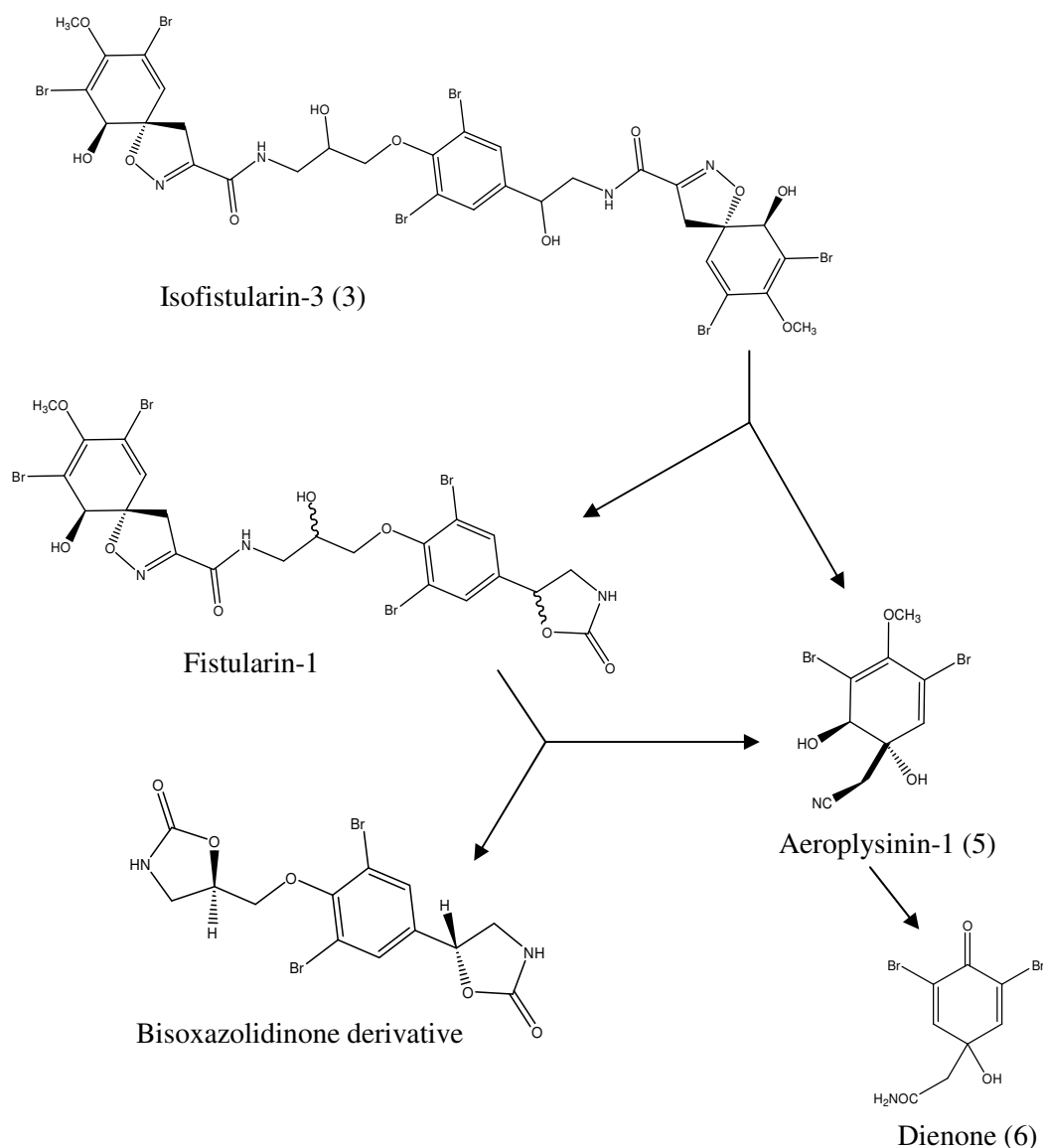


Figure 2. Biotransformation of the isoxazoline alkaloids as described by Teeyapant und Proksch (1993) with isofistularin-3 (3) as example.

The cleavage of the isoxazoline alkaloids represents an unusual enzyme catalysed hydrolysis reaction, to which no biochemical equivalent is known up to now. A similar reaction is known in the field of organic chemistry, the so-called abnormal Beckmann fragmentation (McCarty 1970). During the course of this reaction, the C-C bond of an α -oximinoketone is split, yielding a nitrile, an alcohol and, upon addition of water, a carboxylic acid derivative (Figure 3). Figure 3 reveals the parallels between the cleavage of isoxazoline alkaloids and the abnormal Beckmann fragmentation. The brominated isoxazoline alkaloids can be understood as α -oximinoketones, where the keto function is part of an amide partial structure and the imino group is part of the heterocycle. The oxygen-substituent of the α -oximinoketones represents either a hydroxy- or an O-alkyl group, in the case of the isoxazoline alkaloids it is part of the

heterocycle. During the course of the biotransformation of sponge alkaloids the C-C bond between the carbonyl function and the isoxazoline ring is split, and a nitrile, aeroplysinin 1 (5), emerges, which is in analogy to the abnormal Beckmann fragmentation. The oxygen substituent of the oximino function is not split as water or alcohol, but remains linked to the nitrile aeroplysinin-1 (5) as alcoholic hydroxy function at the carbon at position 1.

During the abnormal Beckmann fragmentation, a carboxylic acid is derived from the keto function of the α -oximinoketones by attachment of water. This is also assumed to happen in the case of the isoxazoline alkaloids. However, the emerging structure is highly instable and thus only the respective decarboxylation product, in the example shown in Figure 4 histamine, is detectable.

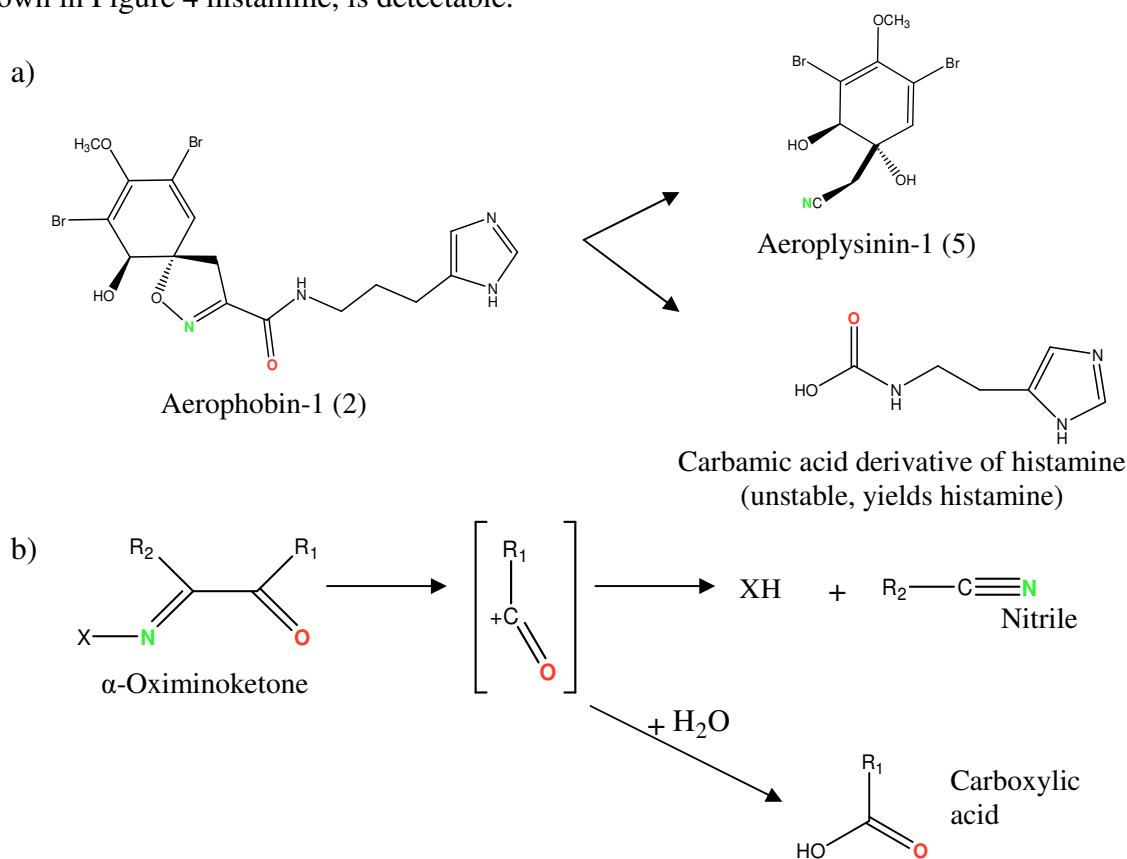


Figure 4. Parallels between a) the cleavage of the isoxazoline alkaloids and b) the abnormal Beckmann fragmentation (McCarty 1970).

Further experiments were conducted to characterise the isoxazoline cleaving enzyme (Teeyapant 1994; Ebel 1998; Fendert 2000). All of these employed the protein raw extract of *Aplysina* sponges since the enzyme could not be purified up to now. The protein raw extract is gained by grinding freeze dried sponge tissue with buffer in a

mortar, centrifugation of this mixture, and purification of the supernatant over a desalting (PD10) column. The optimal temperature determined for enzyme activity was 50 °C, and optimal pH at pH 5.8. The isoxazoline cleaving enzyme appears to be highly specific towards its substrates, the isoxazoline *Aplysina* alkaloids. By offering different natural and synthetic compounds as substrate analogs, three structural characteristics relevant for enzyme activity could be identified, (1) the presence of an intact spirocyclohexadienisoaxazoline ring system, (2) the acid amide side chain, (3) the hydroxyl group at position C-1 and the bromination pattern (Fendert 2000). For the second biotransformation step, where aeroplysinin-1 (5) is transformed into a dienone (6), the involvement of a nitrile hydratase was concluded due to the structural differences of these two metabolites (Ebel 1998; Fendert 2000).

The fact that no biochemical equivalent of the cleavage of isoxazoline alkaloids is known up to now raises questions about the nature of the enzyme catalysing such a reaction. In my thesis, I therefore attempted the purification and characterisation of this unusual protein.

Aims of this thesis

The objective of this study was threefold:

- (I) Isolation and structure elucidation of bioactive compounds from sponges collected in the Mediterranean (Turkey and Croatia) and in the Andaman Sea (Thailand).
- (II) Investigation of the influence of environmental parameters such as depth and light on secondary metabolite contents of three Mediterranean sponge species, i.e. sponges of the genus *Aplysina*, *Dysidea avara*, and *Agelas oroides*.
- (III) Purification and characterisation of the isoxazoline cleaving enzyme in *Aplysina aerophoba*.

The Methods and Results section of this thesis is therefore divided into three parts (I to III) dealing with the respective topics.

Part I:

Isolation of secondary metabolites from marine sponges

Methods

General materials and methods

This chapter summarises chemicals, materials and standard techniques which cannot be contributed to a particular experiment, but were commonly involved in most approaches.

Chemicals and materials

Eppendorf pipettes 10/20/100/200/1000	Eppendorf
Round filters 595 Ø 90 mm/200 mm	Schleicher & Schuell
Formic acid	Riedel-de Haen
Orthophosphoric acid (85 %)	VWR
HPLC methanol	VWR
HPLC acetonitrile	VWR

Water employed for biochemical experiments was cleaned via ion exchange prior to usage (NANOpure, Barnstead) and will be referred to as ultrapure water in the following.

Equipment

Rotary evaporator Rotavapor R200	Büchi
Heating bath B-490	Büchi
Vacuum pump CVC2	Vacuubrand
Ultrasonic bath Sonorex RK 510H	Bandelin
Vacuum centrifuge SpeedVac SPD 111V	Savant
Cooling trap RVT 400	Savant
Freeze dryer Lyovac GT2	Steris
UV lamp and RLC detection table	Camag
Digital scales 2354/TE1502S	Sartorius

Analytical scale MC1	Sartorius
-86 °C freezer	Forma Scientific
Digital pH-meter 420 Aplus	Orion
Heating-plate/magnetic stirrer Combi Mag	IKA
Centrifuge Biofuge pico	Heraeus
Fraction collector Retriever II	Isco

Standard procedures

Liquid-liquid extraction

When dealing with complex raw extracts, liquid-liquid extraction provides a preliminary separation of compounds accumulating in the two phases. Dry methanol raw extracts were reconstituted in 90 % methanol, transferred into a separation funnel, and taken up with an equal volume of hexane. Partitioning was repeated at least twice. Both methanol and hexane phase were dried completely via rotary evaporation. The dry methanol phase was then reconstituted in ultrapure water and mixed with an equal volume of ethyl acetate. Partitioning was repeated at least three times until the ethyl acetate phase was almost colourless or exhausted. Both water and ethyl acetate phase were dried completely via rotary evaporation. Metabolic profile was checked via TLC and HPLC.

Column chromatography

Column chromatography was generally used as further separation step following liquid-liquid extraction. A technique commonly employed was size exclusion chromatography which separates molecules according to their size (or more accurately their hydrodynamic diameter). Smaller molecules are able to enter the pores of the media and, therefore, take longer to elute, whereas larger molecules are excluded from the pores and elute faster. Further separation steps involved normal phase or reversed phase chromatography. In normal phase chromatography, the stationary phase is polar and the mobile phase nonpolar. Reversed phase chromatography is an elution procedure where the mobile phase is significantly more polar than the stationary phase. Table I.1 gives an overview over the chromatography media used for column chromatography. Fractions were collected with the help of a fraction collector.

Table I.1. Chromatography media employed in secondary metabolite isolation.

Medium	Company	Separation principle
Sephadex G25 (LH20), 25-100 μm	Amersham Biosciences	Size exclusion, adsorption
Silica gel 60 RP18, 40 – 63 μm	Merck	Reversed phase
Silica gel 60 M, 40 – 63 μm	Machery-Nagel	Normal phase
LiChroprep Diol, 40 – 63 μm	Merck	Normal phase

Thin layer chromatography

Extracts as well as fractions obtained by column chromatography were investigated via TLC (silica gel 60, F₂₅₄). TLC plates were developed in a saturated chamber over a distance of approx. 8 cm, in a solvent system appropriate to the separation problem which is described for the respective specific methods below. Detection was achieved under a UV lamp at 254 and 366 nm. Afterwards, TLC plates were commonly sprayed with an anisaldehyde or ninhydrin spray reagent and heated for approx. 5 min on a heating plate at 110 °C.

Anisaldehyde spray reagent:	85 ml methanol (distilled)
	10 ml acetic acid (100 %, Merck)
	5 ml sulphuric acid (conc., Merck)
	0.5 ml 4-methoxybenzaldehyde (Merck)
Ninhydrin spray reagent:	100 ml n-butanol (Riedel-de Haen)
	3 ml acetic acid (100 %, Merck)
	0.3 mg ninhydrin (Riedel-de Haen)

Preliminary experiments involved alternative TLC materials suited for the determination of an appropriate solvent system for consecutive column chromatography. Materials employed for TLC are listed in Table I.2.

Table I.2. TLC materials employed in secondary metabolite isolation.

Medium	Company	Separation principle
Silica gel 60 F ₂₅₄ , 0.20 mm	Merck	Normal phase
Diol F _{254s} , 0.20 mm	Merck	Normal phase
RP-18 F _{254s} , 0.25 mm	Merck	Reversed phase

Analytical HPLC

An analytical HPLC system consisting of an HPLC coupled to a photo diode array detector (UV-Vis) was employed for identification and quantification of compounds in extracts and fractions. The respective solvent system and standard gradient used is given in Table I.3. In some cases, a shorter gradient was used with exactly half the times as given in Table I.3. Routine detection was at 235, 254, 280 and 320 nm. Comparison of the online-UV spectra with a spectra library facilitated the identification of known compounds. Samples were solved either in 100 % HPLC methanol or in a methanol/ultrapure water mixture, and centrifuged prior to analysis in order to avoid particles that occlude the HPLC column. Analytical HPLC system specifications are described below.

Table I.3. Solvent system and standard gradient employed for analytical HPLC. Flow rate: 1 ml/min.

Time (min)	0.02% phosphoric acid, pH 2 (%)	Methanol (%)
0	90	10
5	90	10
35	0	100
45	0	100
50	90	10
60	90	10

Pump	P 580, Dionex
Autosampler	ASI-100, Dionex
Column oven	STH 585, Dionex
Column	Eurospher 100-C18, 5 μ m, 125 x 4 mM i.d., Knauer
Detector	UVD 340 S, Dionex
Software	Chromleon V6.3

Semi-preparative HPLC

Semi-preparative HPLC was applied in order to separate compound mixtures obtained after initial fractionation via various chromatography media. A binary solvent system served for compound separation consisting of methanol or acetonitrile as organic solvents, and ultrapure water as aqueous phase. Depending on the separation problem, either a gradient or an isocratic solvent mixture was employed. Samples were solved in the same solvent mixture as used for compound separation. Flow rate was 5 ml/min. Sample amount never exceeded 3 mg per run to avoid declined separation due to overloading the column. Sample concentration commonly was 100 μ g/ μ l of which 15 μ l were injected using a 20 μ l injection loop.

Semi-preparative HPLC system specifications:

Pump	L-7100, Merck/Hitachi
Column	Eurospher 100-C18, 10 μ m, 300 x 8 mM i.d., Knauer
Detector	UV detector L-7400, Merck/Hitachi
Printer	Flatbed recorder Kipp & Zonen

Preparative HPLC

For larger sample amounts obtained by prior column chromatographic separation, a preparative HPLC system was employed for further purification which gave good separation for sample volumes of 22-88 mg per run. Compound separation was achieved by using either a gradient or an isocratic solvent mixture consisting of methanol or acetonitrile as organic solvents, and ultrapure water as aqueous phase. Samples were solved in the same solvent mixture as used for compound separation. Commonly, 1 ml of a 50 mg/ml sample solution was applied via a 1 ml injection loop. Flow rate was 20 ml/min. Preparative HPLC system specifications were as follows:

Pump	PrepStar 218, Varian
Column	Microsorb 60-8 C18, 250 x 21.4 mM i.d., Varian Dynamax
Detector	UV detector ProStar 320, Varian
Software	Varian Star (v. 6)

HPLC-MS

HPLC coupled with ESI-MS allows for the separation of substance mixtures and subsequent determination of the relative molecular mass of the separated compounds. Since not all compounds show UV-absorption and are thus not detectable via HPLC-DAD, HPLC-MS further yields the possibility to prove the purity of isolated compounds. Molecular weight was determined in order to confirm the identity of known compounds in pure fractions as well as in raw extracts. Routine detection was in positive as well as in negative sample mode. The respective solvent system and standard gradient employed is given in Table I.4. Samples were solved either in 100 % HPLC methanol or in a methanol/ultrapure water mixture, and centrifuged prior to analysis in order to avoid particles occluding the column.

Since electron spray ionisation was not applicable to certain compounds, alternative ionisation methods were necessary, i.e. fast atom bombardment (FAB, Sectorfield mass spectrometer Finnigan MAT 8200) or matrix-assisted laser desorption/ionisation

(MALDI, Bruker Ultraflex TOF). These measurements were taken in the Anorganic Chemistry department of the HHU Düsseldorf.

Some compounds were analysed via a FTIRMS-Orbitrap spectrometer (ThermoFinnigan) by Dr. Edrada-Ebel (Strathclyde Institute of Pharmacy and Biomedical Sciences, University of Strathclyde, Glasgow, Scotland) in order to obtain exact masses or MS-MS fragmentation. HPLC-MS system specifications are described below.

Table I.4. Solvent system and standard gradient employed for HPLC-MS. Flow rate: 0.4 ml/min.

Time (min)	0.1 % formic acid (%)	Acetonitrile (%)
0	90	10
2	90	10
35	0	100
45	0	100
47	90	10
60	90	10

HPLC	HP 1100, Agilent
MS	Finnigan LCQ ^{Deca} , Thermoquest
Ion source	ESI and APCI, Thermoquest
Pump	Edwards 30, BOC
Injector	G 1313 A ALS 1100, Agilent
Column	Knauer Eurospher 100; C-18A
Detector	G 1315 B DAD 1100, Agilent
Software	Xcalibur, version 1.4

Optical rotation

Molecules with a chiral centre are able to rotate the orientation of linearly polarised light. Optical rotation is defined by the rotation angle α by which the linearly polarised light is rotated after passing through a solution. The specific rotation $[\alpha]_D^{20}$ refers to a solution of a concentration of 1 g/ 100 ml, measured at 20 °C with light of the sodium D line ($\lambda = 589.3$ nm), and a bulb layer thickness of 10 cm. In addition to temperature, the wavelength of the light which is rotated, and the concentration of the solution measured, optical rotation is also influenced by the solvent in which the measured compound is dispensed.

For this work, all optical rotation measurements were taken at the sodium D line with a bulb thickness of 10 cm by a Polarimeter 341 LC (Perkin Elmer).

Nuclear Magnetic Resonance (NMR)

NMR spectra were measured with a DRX-500-spectrometer (Bruker) in the Institute of Inorganic Chemistry (HHU Düsseldorf). Deuterated solvents included methanol (CD₃OD, euriso-top) or dimethyl sulfoxide (DMSO-*d*₆, euriso-top). Data were processed with the 1D- or 2D WinNMR Software (Bruker and MestReNova). Chemical shifts are given in ppm relative to tetramethylsilane (TMS), and coupling constants in Hertz (Hz). One-dimensional (¹H- and ¹³C-NMR) as well as two-dimensional (H, H-COSY, H, C- correlations such as HMBC and HMQC) experiments were employed. Comparison of chemical shifts, integrals and coupling constants with literature data allowed for structure elucidation of isolated compounds.

Amounts of some samples were too low to yield suitable NMR spectra by measurement via the DRX-500-spectrometer (Bruker) in the Institute of Inorganic Chemistry of the HHU Düsseldorf. Thus, these substances were analysed by Dr. Wray using DPX 300 and DMX 600 spectrometers (Bruker, Helmholtz Centre for Infection Research, Braunschweig).

Isolation of secondary metabolites

Isolation of secondary metabolites involved sponges from the Mediterranean (Croatia and Turkey), and samples collected in the Andaman Sea (Thailand). The isolation procedure for each sponge species employed is given below.

For *Aplysina*, *Dysidea avara* and *Agelas oroides*, the aim was to isolate major metabolites for the generation of calibration curves in order to identify and quantify these components in raw extracts as described in Part II (Chemical ecology).

Aplysina aerophoba

Dried methanol extracts of *Aplysina aerophoba* and *Aplysina cavernicola*, collected in Rovinj, Croatia in April 2006, served to isolate secondary metabolites. Samples were transported and stored frozen prior to exhaustive extraction in methanol. Extracts were dissolved in ultrapure water, transferred into a separation funnel and mixed with the same volume of ethyl acetate in order to collect sponge secondary metabolites in the nonpolar phase. Exhaustive liquid-liquid extraction with ethyl acetate was repeated three to five times. Both water and ethyl acetate phase were evaporated with a rotary

evaporator. A preliminary separation of secondary metabolites was achieved by application of the dried ethyl acetate extract to a sephadex column (2.5 x 26 cm) with methanol (100 %) as solvent. Fractions were collected with a fraction collector, and approx. 20 µl of each fraction were spotted on TLC (silica gel, solvent system: ethyl acetate/methanol/ultrapure water/acetic acid 100/13.5/9/1) in order to identify and combine similar fractions. TLC detection was under a UV lamp at 254 nm. Combined fractions were dried via rotary evaporation, and redissolved in HPLC methanol. Identification of compounds was achieved by comparing their online-UV spectra with the respective spectra stored in the HPLC database, and by determining the molecular weight via HPLC-MS. This isolation procedure yielded several fractions with pure or almost pure compounds (Figure I.1).

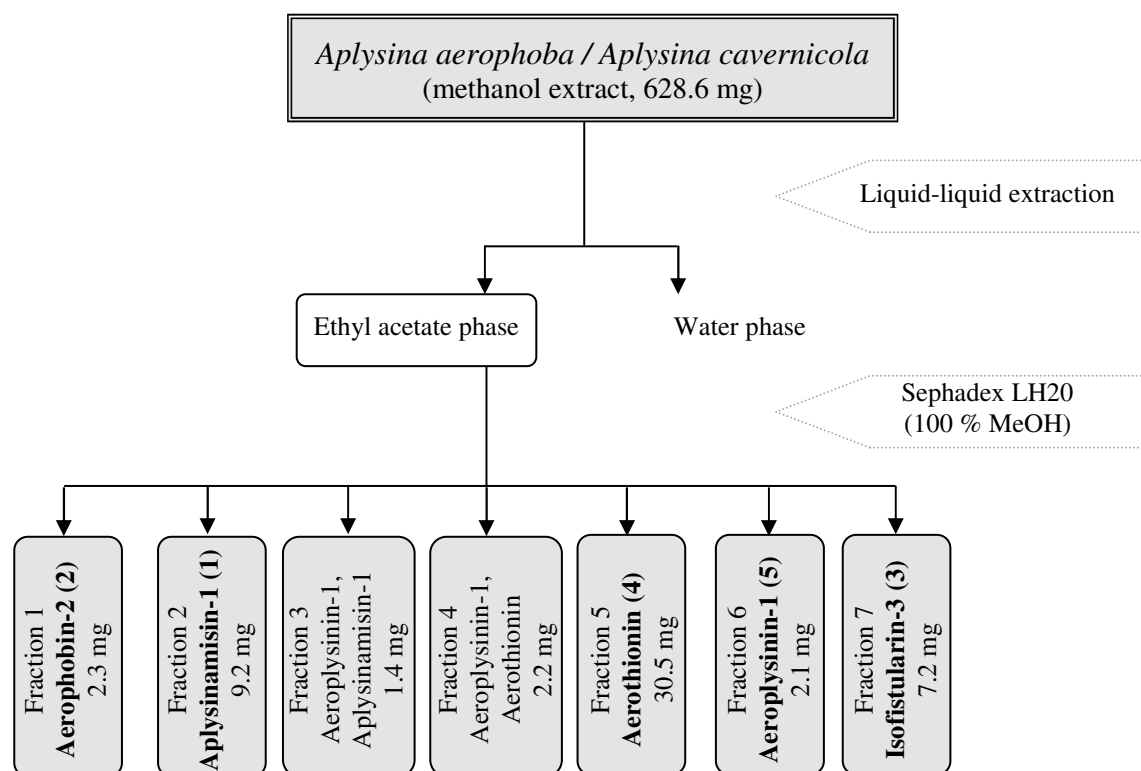


Figure I.1. Isolation scheme of *Aplysina* metabolites.

Dysidea avara

Dysidea avara individuals were sampled in Rovinj, Croatia in April 2006. Samples were transported and stored frozen prior to exhaustive extraction in methanol. The dry methanol extracts of several individuals were combined and dissolved in ultrapure water. The solution was then transferred into a separation funnel and mixed with the

same volume of ethyl acetate. Liquid-liquid extraction with ethyl acetate was repeated three to five times until the ethyl acetate phase was almost colourless. Both water and ethyl acetate phase were evaporated with a rotary evaporator. A first separation of secondary metabolites was achieved by application of the dried ethyl acetate phase to a silica gel column (2.5 x 43 cm) with a solvent system consisting of dichloromethane/methanol (98/2). Fractions were collected with a fraction collector, and approx. 20 µl of each fraction were spotted on TLC (silica gel, solvent system: dichloromethane/methanol 98/2) in order to combine similar fractions. TLC detection was under a UV lamp at 254 nm, and with anisaldehyde spray reagent. Combined fractions were dried via rotary evaporation, and redissolved in HPLC methanol. The fraction containing avarol (9) was still contaminated with other compounds and thus further purified by a sephadex column (2.5 x 43 cm) with a solvent system consisting of dichloromethane/methanol (1/1). Fractions were collected with a fraction collector, spotted on TLC and similar fractions combined. One of these fractions yielded avarol (9) as a pure compound (Figure I.2).

Avarone (10) was obtained by oxidation of the purified avarol (9): 16 mg silver oxide (Ag_2O , kindly provided by Prof. Weber, Institute for Pharmaceutical and Medicinal Chemistry) were dissolved in 1 ml acetone (Merck, Uvasol for spectroscopy). A solution of 3.5 mg avarol (9) in 1 ml acetone was added to the silver oxide solution under constant stirring in an argon atmosphere at room temperature, direct light was avoided. In order to survey the completion of the oxidation process, approx. 20 µl of the solution were taken after 10 min, 20 min, 30 min and 60 min and applied to TLC plates (silica gel, solvent system hexane/ethyl acetate/acetonitrile 75/10/5). After 60 min, avarol (9) was not detectable any more, avarone (10) represented the only compound present. The solution was then filtered in order to remove silver residuals, and subsequently dried under nitrogen. The same procedure was repeated with larger amounts, yielding 38.8 mg avarone (10) obtained from 44.0 mg avarol (9). The identity of both avarol (9) and avarone (10) was confirmed by comparing online-UV spectra, molecular weight, optical rotation and $^1\text{H-NMR}$ signals with the according literature data.

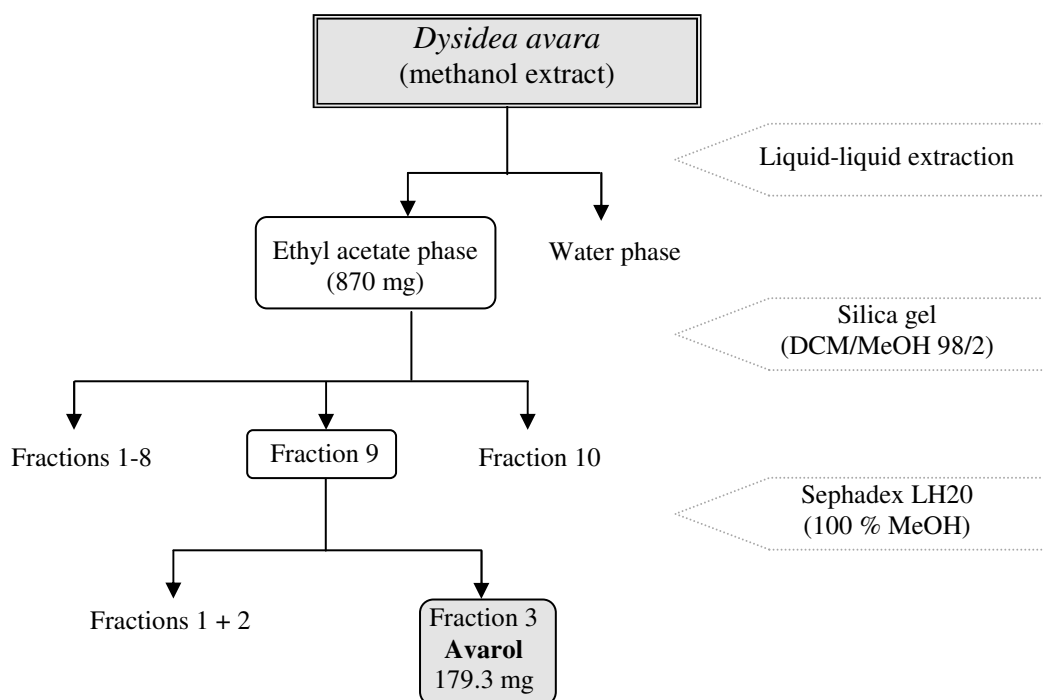


Figure I.2 . Isolation scheme of avarol (9) from *Dysidea avara*.

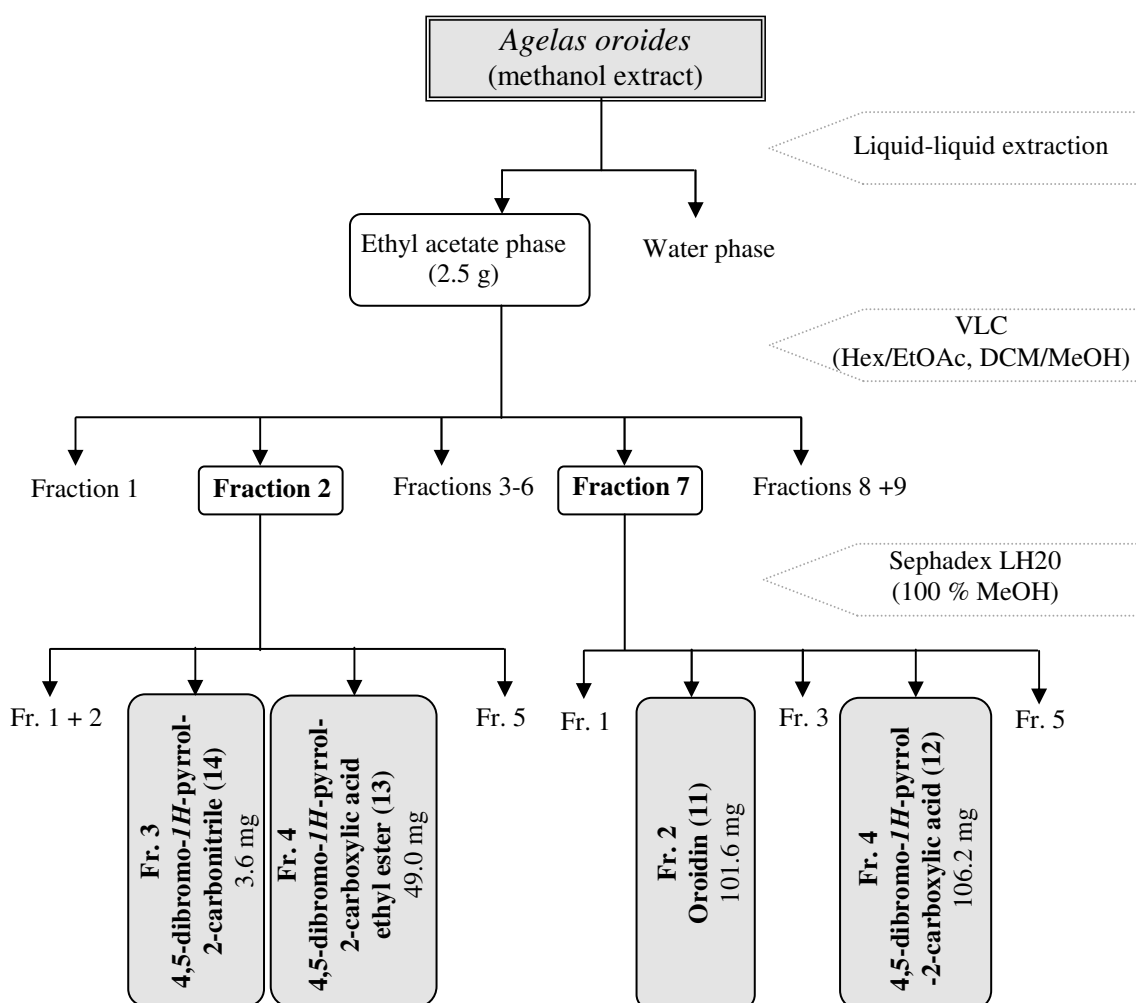
Agelas oroides

Agelas oroides samples were collected in the Mediterranean Sea close to Fethiye, Turkey, in March 2006. Samples were transported and stored in 70 % ethanol prior to exhaustive extraction in methanol. The dried methanol extract was dissolved in ultrapure water, transferred into a separation funnel and mixed with the same volume of ethyl acetate. Liquid-liquid extraction with ethyl acetate was repeated three to five times until the ethyl acetate phase was almost colourless. The resulting ethyl acetate extract was dissolved in methanol and loaded in portions to silica gel, stirred until dryness, and taken to complete dryness in the desiccator. The dry sample was then submitted to vacuum liquid chromatography (VLC), i.e. a silica gel column (6 x 10 cm) with a solvent system consisting of hexane/ethyl acetate and dichloromethane/methanol which is shown in Table I.5. Both VLC fractions 2 and 7 were selected for further purification by sephadex columns (2.3 x 55 cm, 100 % methanol). Fractions were collected with a fraction collector, and approx. 20 μ l of each fraction were spotted on TLC (silica gel, solvent system: dichloromethane/methanol 98/2) in order to combine similar fractions. TLC detection was under a UV lamp at 254 nm, and with ninhydrin spray reagent.

Table I.5. Solvent system as applied for vacuum liquid chromatography.

Fraction	Hexane (%)	Ethyl acetate (%)
1	100	0
2	75	25
3	50	50
4	25	75
Fraction	Dichloromethane (%)	Methanol (%)
5	100	0
6	75	25
7	50	50
8	25	75
9	0	100

Combined fractions were dried via rotary evaporation, and redissolved in HPLC methanol. In total four compounds could be isolated (Figure I.3). The identity of these was confirmed by comparing online-UV spectra, molecular weight, and NMR signals (^1H , ^{13}C , DEPT and HMBC) with the according literature data.

Figure I.3. Isolation scheme for *Agelas oroides* metabolites.

Ircinia variabilis

Sponge samples were collected in the Mediterranean Sea close to Mersin, Turkey in September 2005. Samples were transported and stored in 70 % ethanol prior to exhaustive extraction in methanol. The dried methanol extract was treated by liquid-liquid extraction between ethyl acetate and water as described above. The ethyl acetate extract was taken up in dichloromethane/methanol (1/1) and loaded to a sephadex column (2.0 x 30 cm, dichloromethane/methanol 1/1). Fractions were collected with a fraction collector, and approx. 20 μ l of each fraction were spotted on TLC (silica gel, solvent system: dichloromethane/methanol 97/3) in order to combine similar fractions. TLC detection was under a UV lamp at 254 nm, and by subsequent treatment with anisaldehyde spray reagent. Combined fractions were dried via rotary evaporation, and redissolved in HPLC methanol for HPLC analysis. Fraction 3 was further purified by a silica column (2 x 30 cm, dichloromethane/methanol 97/3), of which fraction 7 yielded fasciculatin (20) of ample purity. All purification steps are summarised in Figure I.4. The identity of this compound was confirmed by comparing online-UV spectra, molecular weight, and NMR signals (^1H , ^{13}C and H,H-COSY) with the according literature data.

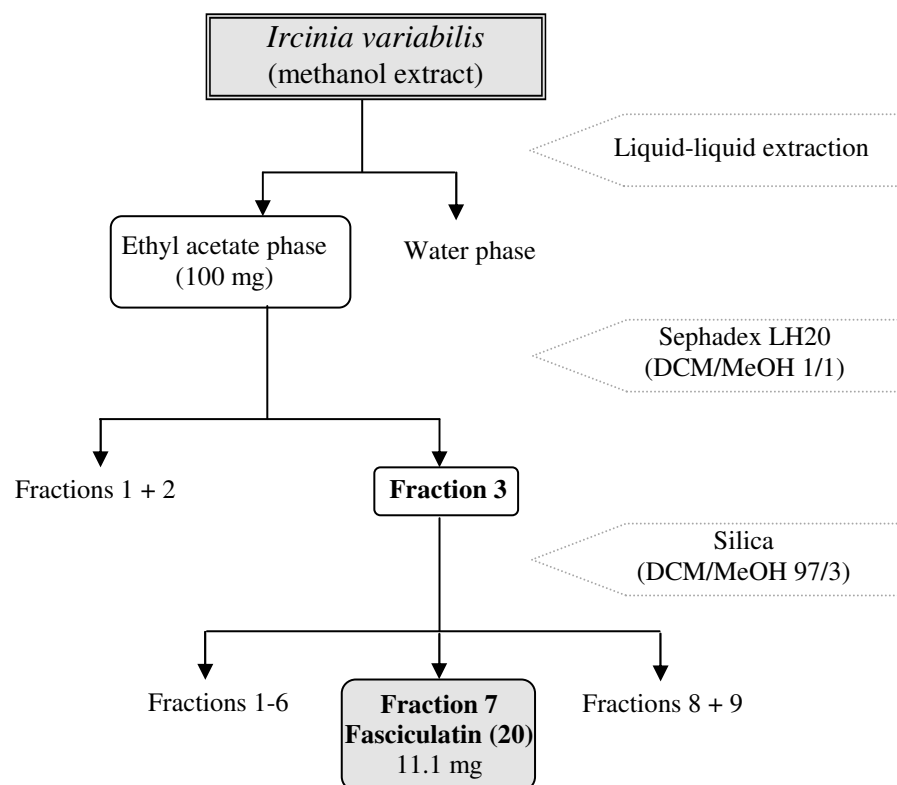


Figure I.4. Isolation scheme for *Ircinia variabilis* metabolites.

Ircinia fasciculata

Ircinia fasciculata individuals were collected in the Mediterranean Sea close to Fethiye, Turkey in March 2006. Samples were transported and stored in 70 % ethanol prior to exhaustive extraction in methanol. The dried methanol extract was treated by liquid-liquid extraction between ethyl acetate and water as described above. The ethyl acetate phase was dissolved in methanol and loaded to a sephadex column (3.0 x 88 cm, 100 % methanol). Fractions were collected with a fraction collector, and approx. 20 μ l of each fraction were spotted on TLC (silica gel, solvent system: hexane/ethyl acetate/dichloromethane 65/30/5) in order to combine similar fractions. TLC detection was under a UV lamp at 254 nm, and with anisaldehyde spray reagent.

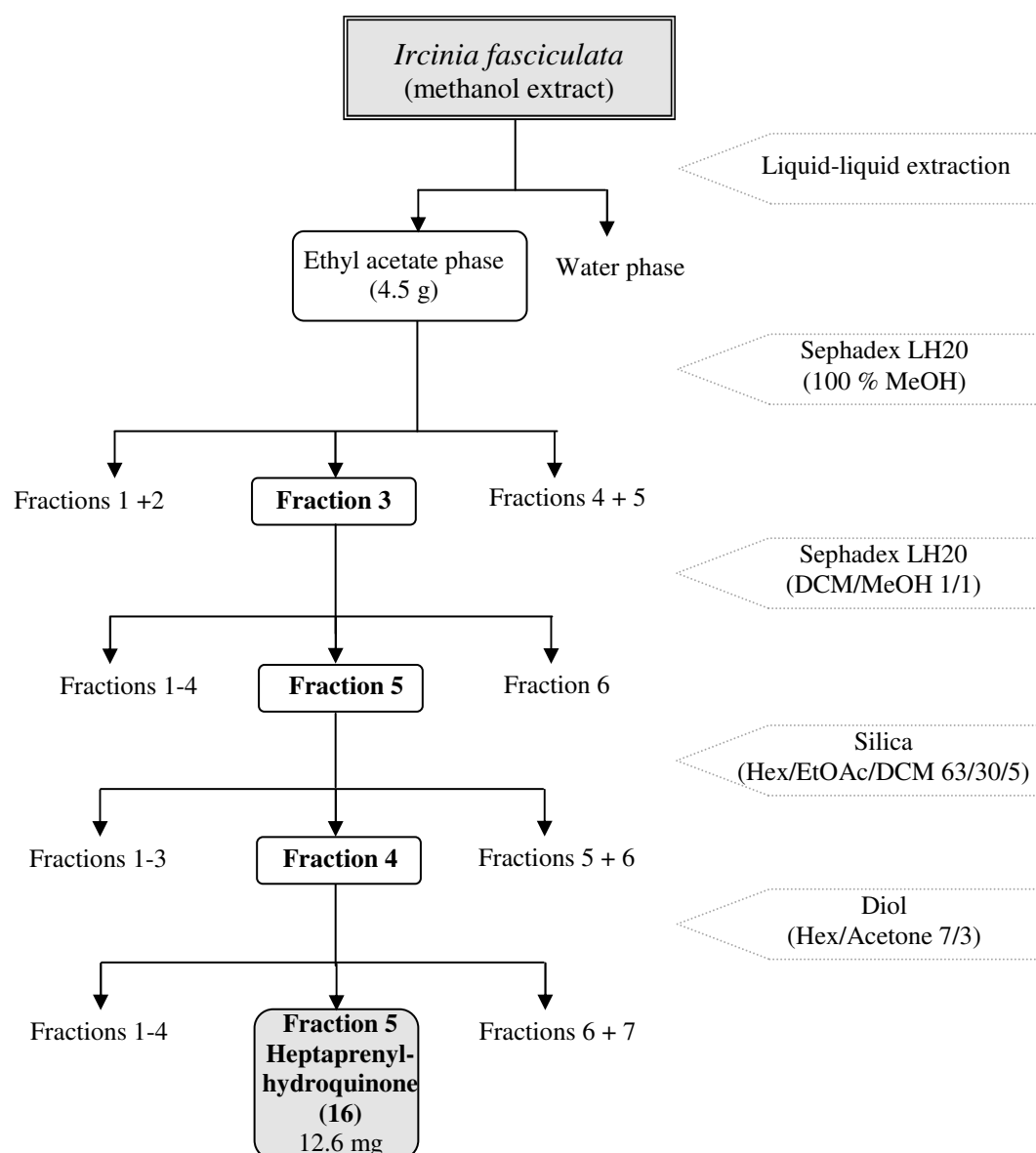


Figure I.5. Isolation scheme for *Ircinia fasciculata* metabolites.

Combined fractions were dried via rotary evaporation, and redissolved in HPLC methanol for HPLC analysis. Fraction 3 was further purified by a sephadex column (3.5 x 51 cm, dichloromethane/methanol 1/1). Since fractions were still complex, employment of a silica column (2.0 x 30 cm, hexane/ethyl acetate/dichloromethane 65/30/5) and a diol column (1.5 x 16 cm, hexane/acetone 7/3) was required to obtain a pure compound. All purification steps are summarised in Figure I.5. By comparing online-UV spectra, molecular weight, and $^1\text{H-NMR}$ signals with the according literature data the isolated compound could be identified as heptaprenylhydroquinone (16).

Sarcotragus muscarum

Sponge samples were collected in the Mediterranean Sea close to Mersin, Turkey in September 2005. Samples were transported and stored in 70 % ethanol prior to exhaustive extraction in methanol. The dried methanol extract was treated by liquid-liquid extraction between 90 % methanol and hexane. The methanol part was then dried, redissolved in ultrapure water, and liquid-liquid extraction was repeated against ethyl acetate. The resulting ethyl acetate extract was dissolved in methanol and loaded to a sephadex column (3.0 x 85 cm, 100 % methanol). Fractions were collected with a fraction collector, and approx. 20 μl of each fraction were spotted on TLC (silica gel, solvent system hexane/ethyl acetate/dichloromethane 75/20/5) in order to combine similar fractions. TLC detection was under a UV lamp at 254 nm, and with anisaldehyde spray reagent. Combined fractions were dried via rotary evaporation, and redissolved in HPLC methanol for HPLC analysis. Fraction 4 yielded a mixture of two compounds (18 and 19) which were separated from each other by semipreparative HPLC (Solvent system methanol/water, gradient as given in Table I.6).

Table I.6. Gradient used for the separation of the ambigol A derivatives.

Time (min)	Water (%)	Methanol (%)
0	30	70
5	30	70
25	0	100
30	0	100
35	30	70
40	30	70

Fraction 2 of the sephadex column was solved in methanol and loaded in portions to silica gel, stirred until dryness, and taken to complete dryness in the desiccator. The dry sample was then submitted to vacuum liquid chromatography (VLC), a silica gel

column (6 x 10 cm) with a solvent system consisting of hexane/ethyl acetate and dichloromethane/methanol which is shown in Table I.7.

Table I.7. Solvent system as applied for vacuum liquid chromatography.

Fraction	Hexane (%)	Ethyl acetate (%)
1	100	0
2	80	20
3	60	40
4	40	60
5	20	80
6	0	100
Fraction	Dichloromethane (%)	Methanol (%)
7	100	0
8	80	20
9	60	40
10	40	60
11	20	80
12	0	100

Of these, fraction 3 was applied to a sephadex column (3.0 x 66 cm, methanol/dichloromethane 1/1) where the major compounds accumulated in fraction 4 which were subsequently purified via a diol column (2.5 x 39 cm, hexane/acetone 9/1). Semipreparative HPLC of fraction 6 (isocratic, 100 % methanol) finally succeeded in obtaining two pure compounds, hexa- (15) and nonaprenylhydroquinone (17). All purification steps are summarised in Figure I.6. By comparing online-UV spectra, molecular weight, and NMR signals (¹H, H,H-COSY and HMBC) with the according literature data the structure of these isolated compounds could be confirmed.

Dysidea granulosa

Sponge samples were collected in the Andaman Sea close to Laoliang Island, Thailand in March 2007. Samples were cooled on ice during transport, stored at -20 °C upon arrival in the laboratory, and were subsequently exhaustively extracted in methanol. The dried methanol extract was treated by liquid-liquid extraction between ethyl acetate and water as described above. The ethyl acetate extract was dissolved in methanol and loaded to a sephadex column (3.0 x 58 cm, 100 % methanol). Fractions were collected with a fraction collector, and approx. 20 µl of each fraction were spotted on TLC (silica gel, solvent system hexane/acetone 8/2) in order to combine similar fractions. TLC detection was under a UV lamp at 254 nm, and with anisaldehyde spray reagent.

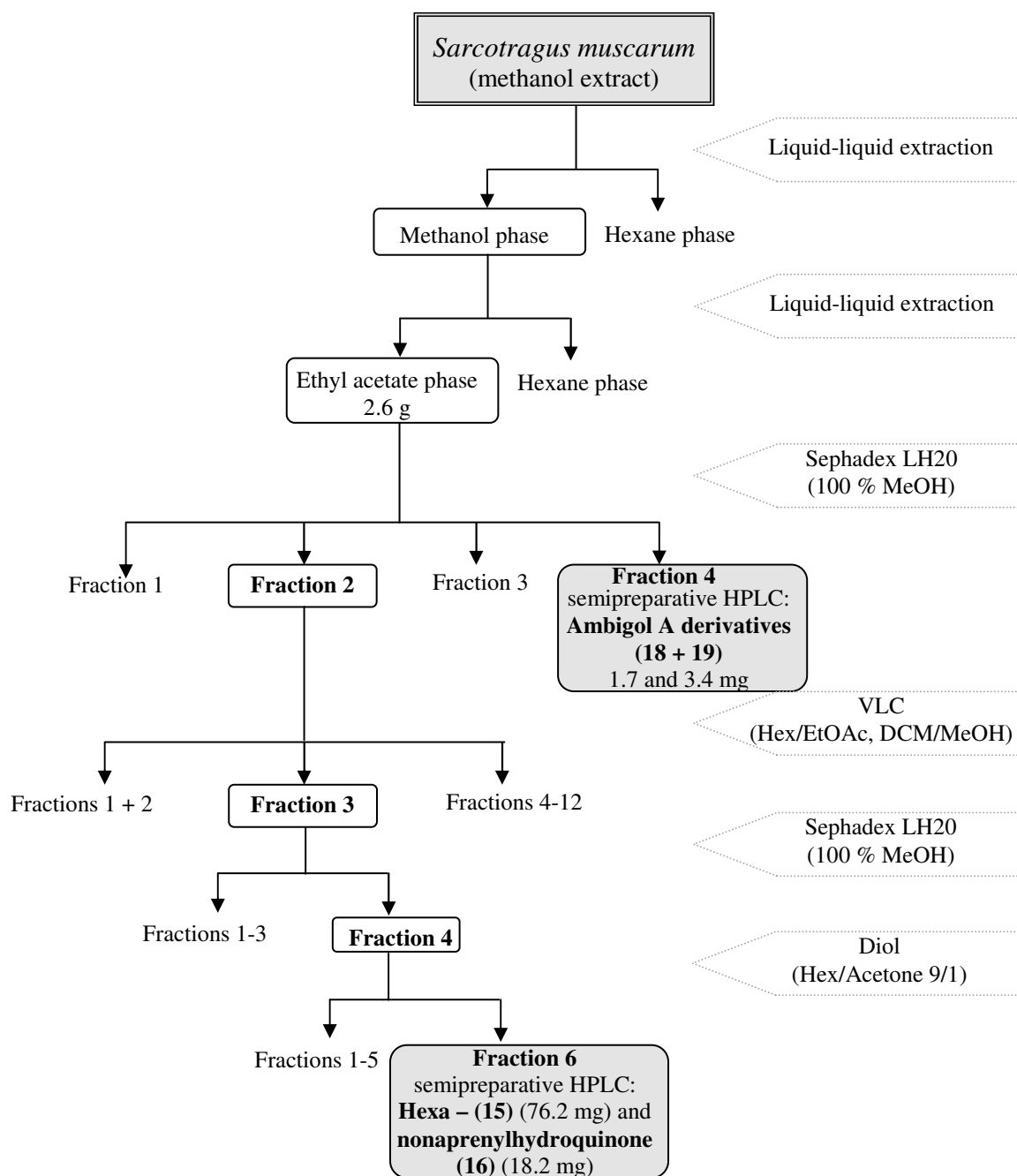


Figure I.6. Isolation scheme for *Sarcotragus muscarum* metabolites.

Combined fractions were dried via rotary evaporation, and redissolved in HPLC methanol for HPLC analysis. Fraction 10 was further purified by a sephadex column (2.5 x 66 cm, dichloromethane/methanol 1/1), of which fraction 4 contained a mixture of two compounds. After application to a diol column (2.5 x 66 cm, hexane/acetone 9/1) these two compounds could be obtained in ample purity. All purification steps are summarised in Figure I.7. The identity of 4,5,6-tribromo-2-(2',4'-dibromophenoxy)phenol (21) and 4,6-dibromo-2-(2',4'-dibromo-phenoxy)-

phenol (22) was confirmed by comparing online-UV spectra, molecular weight, and NMR signals (^1H , ^{13}C and HMBC) with the according literature data.

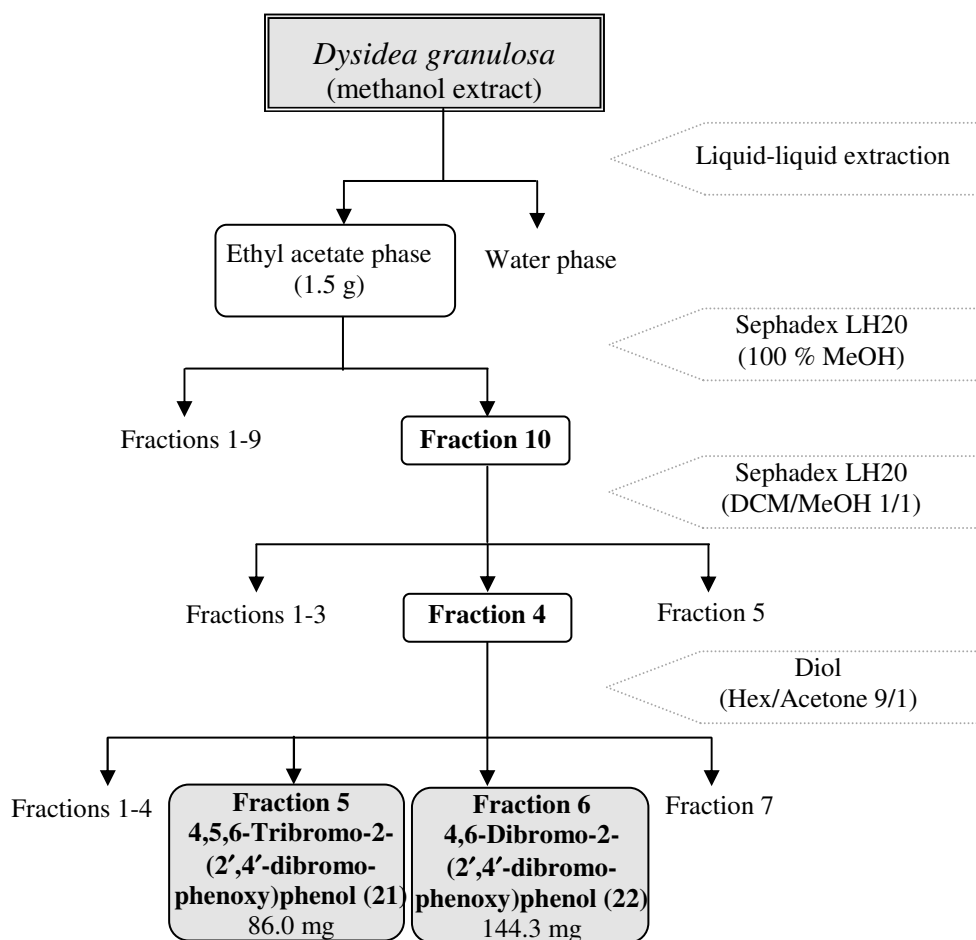


Figure I.7. Isolation scheme for *Dysidea granulosa* metabolites.

Haliclona spec

Haliclona specimens were collected in the Andaman Sea close to Laoliang Island, Thailand in March 2007. Samples were cooled on ice during transport, stored at $-20\text{ }^{\circ}\text{C}$ upon arrival in the laboratory, and subsequently exhaustively extracted in methanol. The dried methanol extract was treated by liquid-liquid extraction between ethyl acetate and water as described above. The ethyl acetate extract was dissolved in methanol and loaded to a sephadex column (3.0 x 36 cm, 100 % methanol). Fractions were collected with a fraction collector, and approx. 20 μl of each fraction were spotted on TLC (silica gel, solvent system hexane/acetone 8/2) in order to combine similar fractions. TLC detection was under a UV lamp at 254 nm, and with anisaldehyde spray reagent. Combined fractions were dried via rotary evaporation, and redissolved in HPLC methanol for HPLC analysis. Fraction 2 yielded papuamine (23). The purification

procedure is summarised in Figure I.8. The identity of papuamine (23) was confirmed by comparing online-UV spectra, molecular weight, optical rotation and NMR signals (^1H and ^{13}C) with the according literature data. Since the fraction containing papuamine (23) was still contaminated by minor amounts of fatty acids, the dry fraction was dissolved in 0.5 N sulphuric acid (pH 2) and submitted to liquid extraction against ethyl acetate. After removal of the ethyl acetate phase, pH of the aqueous phase was adjusted to pH 11 with ammonia (25 %, Grüssing GmbH, Filsum), and liquid extraction against ethyl acetate was repeated. The purified alkaloid papuamine (23) was obtained in the latter ethyl acetate fraction.

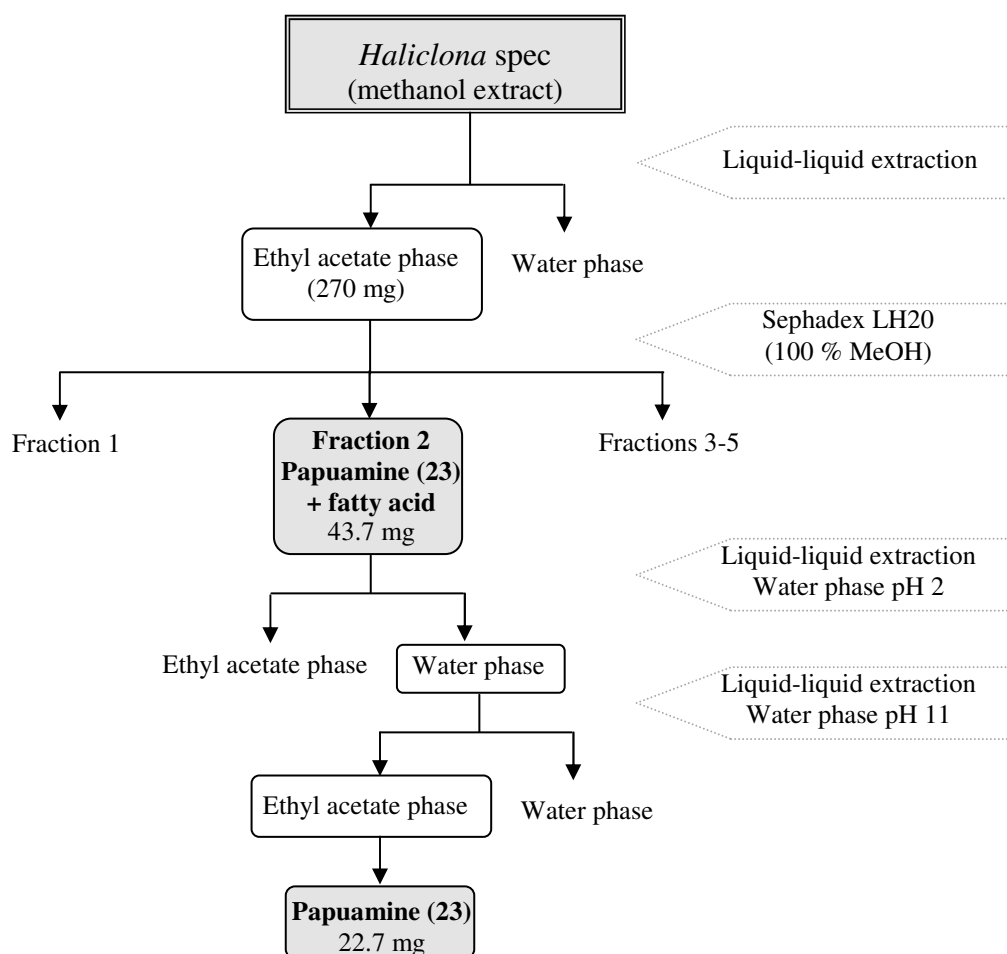


Figure I.8. Isolation scheme for *Haliclona spec* metabolites.

Biological activity

Compounds that could be obtained in ample amounts were tested for their biological activity, i.e. cytotoxic properties and protein kinase inhibition.

Cytotoxicity assay

In order to test for the cytotoxic activity of crude extracts as well as isolated compounds, the 3-(4,5-Dimethylthiazol-2-yl)-2,5-diphenyltetrazolium bromide (MTT) assay was employed as a standard colorimetric assay for measuring cellular proliferation. In living cells, the yellow MTT (a tetrazole) is reduced to purple formazan in the mitochondria. This formazan product is dissolved in dimethyl sulfoxide (DMSO) or other detergents, yielding a coloured solution. The absorption of this solution is directly related to the number of viable cells. By comparing the amount of formazan product produced by untreated control cells with the formazan amount of cells treated with a substance, the cytotoxic effect of the compound in question can be deduced.

In this study, MTT assays were carried out by the group of Prof. Müller at the Institute of Physiological Chemistry and Pathology, University of Mainz. Cytotoxicity was tested against L5178Y mouse lymphoma cells. Cells were grown in Eagle's minimal essential medium supplement with 10 % horse serum in roller tube culture. The medium contained 100 units/ml penicillin and 100 µg/ml streptomycin. Cells were maintained in a humidified atmosphere at 37 °C with 5 % CO₂. Stock solutions of test compounds were prepared in ethanol 96 % (v/v). Exponentially growing cells were harvested, counted and diluted appropriately. Of the cell suspension, 50 µl containing 3750 cells were pipetted into 96-well microtiter plates. Subsequently, 50 µl of a solution of the test samples containing the appropriate concentration was added to each well (either 3 or 10 µg/ml). Residual ethanol present in the wells did not affect the experiments. The test plates were incubated at 37 °C with 5 % CO₂ for 72 h. A solution of MTT was prepared at 5 mg/ml in phosphate buffered saline (PBS; 1.5 mM KH₂PO₄, 6.5 mM Na₂HPO₄, 137 mM NaCl, 2.7 mM KCl; pH 7.4) of which 20 µl were pipetted into each well. After an incubation period of 3 h 45 at 37 °C in a humidified incubator with 5 % CO₂, the medium was centrifuged (15 min, 20 °C, 210 x g). Cells were lysed with 200 µl DMSO to liberate the formazan product. After thorough mixing, absorbance was measured at 520 nm using a scanning microtiter-well spectrophotometer. Cell survival was calculated using the formula:

$$\text{Survival [\%]} = 100 \times \frac{\text{absorbance of treated cells} - \text{absorbance of culture medium}}{\text{absorbance of untreated cells} - \text{absorbance of culture medium}}$$

All experiments were carried out in triplicates and repeated three times. As controls, media with 0.1 % EGMME/DMSO were included.

EC₅₀ values were determined for samples showing strong inhibition of cell growth.

Protein kinase assays

Protein kinase assays were carried out by ProQinase GmbH (Freiburg, Germany). Kinases are ATP dependent enzymes that add phosphate groups to proteins. Phosphorylation is the key regulatory mechanism of numerous signal transduction pathways involved in the regulation of cell growth, differentiation, and response to changes in the extracellular environment (e.g. (Meijer et al. 2000)). Consequently, kinases are major targets for potential novel drugs treating diseases such as cancer and various inflammatory disorders. The inhibitory potency of crude extracts or purified compounds was determined using 24 protein kinases (see Table I.9). The IC₅₀ profile of extracts or compounds showing an inhibitory potency of ≥ 40 % with at least one of the 24 kinases at an assay concentration of 1×10^{-06} g/ml was determined. IC₅₀ values were measured by testing 10 concentrations of each sample in singlicate (n = 1).

Extracts or compounds were provided as 1×10^{-03} g/ml stock solutions in 100 % DMSO (1000 or 500 μ l) in micronic boxes stored at -20 °C. Prior to the assays, 100 μ l of the stock solutions were transferred into separate microtiter plates and subjected to serial, semi-logarithmic dilution using 100 % DMSO as a solvent resulting in 10 different concentrations. 100 % DMSO was used as control. Subsequently, 7×5 μ l of each concentration were aliquoted and diluted with 45 μ l H₂O just a few minutes prior to transfer into the assay plate to minimise precipitation. Plates were shaken thoroughly and then used for the transfer of 5 μ l compound solution into the assay plates.

Recombinant protein kinases

All protein kinases were expressed in Sf9 insect cells as human recombinant GSTfusion proteins or His-tagged proteins by means of the baculovirus expression system. Kinases were purified by affinity chromatography using either Glutathione-agarose (GSH-agarose, Sigma) or Ni-NTA-agarose (Qiagen). Purity was checked by

SDS–PAGE/silver staining and the identity of each kinase was verified by Western blot analysis with kinase specific antibodies or by mass spectrometry.

Protein kinase assay

A proprietary protein kinase assay (³³PanQinase[®] Activity Assay) was used for measuring the kinase activity of the protein kinases. All kinase assays were performed in 96-well FlashPlates[™] from Perkin Elmer/NEN (Boston, USA) in a 50 µl reaction volume. The reaction mixture was pipetted in the following order: 20 µl assay buffer, 5 µl ATP solution in H₂O, 5 µl test compound in 10 % DMSO and 10 µl substrate/10 µl enzyme solution (premixed). The assay for all enzymes contained 60 mM HEPES-NaOH (pH 7.5), 3 mM MgCl₂, 3 mM MnCl₂, 3 µM Na-orthovanadate, 1.2 mM DTT, 50 µg/ml PEG20000, 1 µM [γ-³³P]-ATP. The reaction mixtures were incubated at 30 °C for 80 min and stopped with 50 µl 2 % (v/v) H₃PO₄. The plates were aspirated and washed two times with 200 µl of 0.9 % (w/v) NaCl or 200 µl H₂O. Incorporation of ³³P_i was determined with a microplate scintillation counter (Microbeta Trilux, Wallac). All assays were performed with a BeckmanCoulter/Sagian robotic system.

Table I.9. List of protein kinases and their substrates.

Family	Kinase	Substrate	Mechanism	Disease
Serine / threonine kinases	AKT1/PKB alpha	GCS3(14-27)	Apoptosis	Gastric cancer (Staal 1987)
	ARK5	Autophos.	Apoptosis	Colorectal cancer (Kusakai et al. 2004)
	Aurora A	tetra(LRRWSLG)	Proliferation	Pancreatic cancers (Li et al. 2003)
	Aurora B	tetra(LRRWSLG)	Proliferation	Breast cancer (Keen and Taylor 2004)
	CDK2/Cyclin A	Histone H1	Proliferation	Pancreatic cancer (Iseki et al. 1998)
	CDK4/Cyclin D1	Rb-CTF	Proliferation	Breast cancer (Yu et al. 2006)
	CK2-alpha1	p53-CTM	Proliferation	Rhabdomyosarcoma (Izeradjene et al. 2004)
	COT	Autophos.	Proliferation	Breast cancer (Sourvinos et al. 1999)
	PLK-1	Casein	Proliferation	Prostate cancer (Weichert et al. 2004)
	B-RAF-VE	MEK1-KM	Proliferation	Thyroid cancer (Ouyang et al. 2006)
	SAK	Autophos.	Proliferation	Colorectal cancer (Macmillan et al. 2001)

Receptor tyrosine kinase	EGFR	Poly(Glu,Tyr) _{4:1}	Proliferation	Glioblastoma multiforme (NationalCancerInstitute 2005)
	EPHB4	Poly(Glu,Tyr) _{4:1}	Angiogenesis	Prostate cancer (Xia et al. 2005)
	ERBB2	Poly(Glu,Tyr) _{4:1}	Proliferation	Gastric carcinomas (Lee et al. 2005)
	FLT3	Poly (Ala,Glu,Lys,Tyr) _{6:2:4:1}	Proliferation	Leukemia (Menezes et al. 2005)
	IGF1-R	Poly(Glu,Tyr) _{4:1}	Apoptosis	Breast cancer (Zhang and Yee 2000)
	INS-R	Poly (Ala,Glu,Lys,Tyr) _{6:2:4:1}	“counter kinase”	Ovarian cancer (Kalli et al. 2002)
	MET	Poly (Ala,Glu,Lys,Tyr) _{6:2:4:1}	Metastasis	Lung cancer (Qiao et al. 2002)
	PDGFR-beta	Poly (Ala,Glu,Lys,Tyr) _{6:2:4:1}	Proliferation	Prostate cancer (Hofer et al. 2004)
	TIE-2	Poly(Glu,Tyr) _{4:1}	Angiogenesis	Rheumatoid arthritis (DeBusk et al. 2003)
	VEGF-R2	Poly(Glu,Tyr) _{4:1}	Angiogenesis	Pancreatic cancers (Li et al. 2003)
	VEGF-R3	Poly(Glu,Tyr) _{4:1}	Angiogenesis	Breast cancer (Garces et al. 2006)
	Soluble tyrosine kinase	FAK	Poly(Glu,Tyr) _{4:1}	Metastasis
SRC		Poly(Glu,Tyr) _{4:1}	Metastasis	Colon cancer (Dehm et al. 2001)

Prenylated hydroquinones

Since three prenylated hydroquinones could be isolated just differing by the number of isoprenic units attached to the aromatic ring, further experiments assessing biological activity were conducted by Dr. Wim Wätjen at the Institute of Toxicology, HHU Düsseldorf, in order to infer the influence of isoprenic chain length on selected bioactivities.

Antioxidative activity

Trolox equivalent antioxidative capacity (TEAC) was measured spectrophotometrically analysing the decolourisation of a stable radical cation ABTS (2,2'-azino-bis(3-ethylbenz-thiazoline-6-sulfonic acid)) at 734 nm in comparison to the synthetic antioxidant Trolox (Re et al. 1999). Absorption was measured after 4 min of mixing the pterocarpanes with the ABTS solution.

Cytotoxic activity

For cell culture, H4IIE rat hepatoma were grown in Dulbecco's Modified Eagle Medium (DMEM) containing 4.5 g/l glucose and 2 mmol/l L-glutamine, supplemented with 10 % fetal bovine serum (FBS). The cell culture medium contained 100 units/ml penicillin and 100 µg/ml streptomycin and was changed twice per week. The cells were maintained in a humidified atmosphere at 37 °C with 5 % CO₂. The effect of isolated compounds on cell viability was determined using the MTT assay (Mosmann 1983). The cells were plated on 96-multiwell plates with 10000 cells per well. Subsequently, cells were allowed to attach for 24 h and then treated with different concentrations of the prenylated hydroquinones for 24 h. After this treatment the medium was changed and the cells were incubated for 3 h under cell culture conditions with 20 µg/ml MTT. After incubation, cells were lysed with ethanol/water/acetic acid 50/49/1. The concentration of reduced MTT as a marker for cell viability was measured photometrically at 560 nm.

Determination of NF-κB inhibiting activity

H4IIE cells were stably transfected with HiFect transfection reagent (Amaxa) according to the manufacturer's protocol. Briefly, H4IIE cells were seeded at a density of 1.5×10^5 per 35 mM petri dish and incubated over night. Cells were transfected with 1.6 µg pNF-κB-SEAP and 0.4 µg pTK-Hyg by using 10 µl HiFect transfection reagent in 1 ml serum free DMEM medium. 48 h after transfection cells were split 1/5 into 100 mM petri dishes and stably transfected cell clones (H4IIE-SEAP) were selected with 400 µg/ml hygromycin. For the reporter gene assay, H4IIE-SEAP cells were seeded at a density of 2×10^5 cells per 12-well plates and incubated for 48 h. Cells were preincubated with 0.5 or 1 µM of hexa- (15) and 5 or 10 µM hepta- (16) and nonaprenylhydroquinone (17) for 1 h and then stimulated with 5 ng/ml TNF-α for 24 h. Activity of the reporter enzyme (SEAP) in the medium was measured using a chemiluminescence-based detection method. In brief, 30 µl conditioned cell culture medium was mixed with 30 µl of 1 × dilution buffer (50 mM Tris, 150 mM NaCl, pH 7.4) and incubated for 30 min at 65 °C to heat-inactivate endogenous alkaline phosphatase activity. Samples were mixed with 30 µl assay buffer (2 M diethanolamine, 28 mM L-homoarginine) and 30 µl chemiluminescent disodium 3-(4-methoxy Spiro{1,2-dioxetane-3,2'-(5'-chloro)tricyclo[3.3.1.1^{3,7}]decan}-4-yl) phenyl phosphate (CSPD)

substrate. After 15 min incubation at dark, SEAP activity was measured in a plate luminometer (Victor 1420, Wallac). In each experiment it was verified that inhibition of SEAP activity was not caused by cytotoxic effects (MTT assay). Data are given as mean \pm SD of at least three independent experiments.

Antimicrobial activity

The antimicrobial activity of pure compounds was assessed by SeaLife Pharma, Tulln, Austria, against a range of gram-positive as well as gram-negative bacteria, *Escherichia coli*, *Enterococcus faecalis*, *Staphylococcus aureus*, *Streptococcus pyogenes*, *Pseudomonas aeruginosa* and *Klebsiella pneumoniae*. All these microorganisms have in common that they are potential human pathogens and that multidrug resistant strains exist, thus rendering them a relevant test system for a primary screen when aiming at finding potential new antibiotics against these microorganisms.

Primary screening

In a primary screening, active substances were identified for further investigation of toxicity and the MIC (minimum inhibitory concentration)-test. Substances were dissolved in 200 μ l DMSO, and mixed with 800 μ l culture water to yield a stock solution of 1 mg/ml. Final concentrations in the assay were 250, 125, and 62.5 μ g/ml, which were achieved by diluting stock solutions with "Müller Hinton Bouillon". Substances were tested in 96 well plates and overlaid with a microbe solution of 10^5 CFU/ml. The plates were cultivated for 24 h at 35 °C. The test was analysed by checking microbial growth visibly by eye and via measurement of the optical density at 650 nm. Substances that inhibit minimum 80 % (in relation to a positive control) were considered for subsequent toxicity and MIC-tests.

Toxicity against HeLa cells

In order to examine the toxic profile of substances that proved to be active in the primary screening, substances were dissolved in 200 μ l DMSO, and mixed with 800 μ l culture water to yield a stock solution of 1 mg/ml. Final concentrations in the assay were 250, 125, and 62.5 μ g/ml. HeLa cells were seeded in a 96 well plate (5×10^3 cells per well) and cultivated overnight to a confluence of nearly 60-70 %. The cells were then overlaid with the substances diluted in media and incubated for 48 h. Subsequently,

the viability of cells was assessed by staining with crystal violet and detection of the absorbance at 450 nm (average of five independent measurements).

MIC-test of positive substances

In order to examine the minimum inhibitory concentration of substances that proved to be active in the primary screening, substances were dissolved in 200 μ l DMSO, and mixed with 800 μ l culture water to yield a stock solution of 1 mg/ml. The test was performed in 96 well plates with a classical MIC test. Substances were diluted from 250 to 0.24 μ g/ml and overlaid with the microbes (10^5 CFU/ml). Plates were cultivated for 24 h at 35 °C. Microbial growth was detected visibly by eye and via measurement of the optical density at 650 nm.

Results

Structure elucidation of the isolated compounds will be first presented and succeeded by data on cytotoxic potential of these compounds as tested in the MTT and the protein kinase assay, and antimicrobial activity.

Identification of isolated compounds

This chapter summarises data on compounds isolated from sponges obtained from the Mediterranean Sea and Andaman Sea in Thailand. The compounds isolated from *Aplysina* sponges, *Dysidea avara* and *Agelas oroides* involve major metabolites that were already previously described in the literature (Compounds 1-10, structures were presented in the Introduction chapter). They served to establish the calibration curves for quantifying these metabolites in raw extracts as described in Part II on the chemical ecology of Mediterranean sponges. All data which include UV spectra, molecular weights, retention times under the standard HPLC conditions employed, and NMR spectra are presented in the appendix together with their calibration curves needed for their quantitative analysis.

Data of all other compounds are listed below according to their biological source.

Agelas oroides

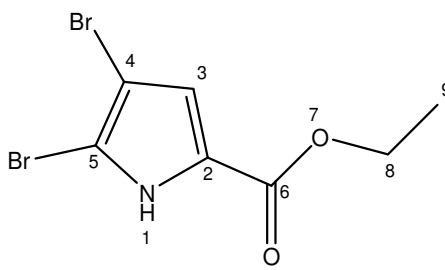
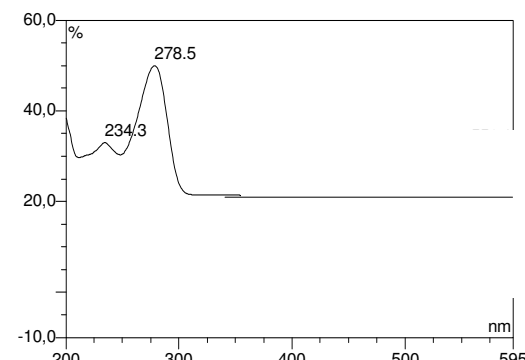
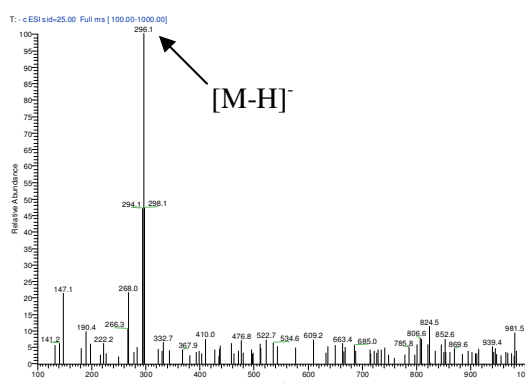
Apart from the already known major metabolites oroidin (11) and 4,5-dibromo-1*H*-pyrrol-2-carboxylic acid (12), two further known compounds were obtained from *Agelas oroides* in minor quantities.

Structure elucidation of 4,5-dibromo-1*H*-pyrrol-2-carboxylic acid ethyl ester (13)

The known compound 4,5-dibromo-1*H*-pyrrol-2-carboxylic acid ethyl ester (13) was isolated from the *Agelas oroides* methanol extract as a red powder. The compound showed UV absorbances at λ_{\max} (MeOH) 234 and 279 nm (Table I.11). ESI-MS exhibited the molecular ion peaks at m/z 294, 296, and 298 [M-H]⁻ in a ratio of 1:2:1 typical for dibrominated compounds (table I.11). ¹³C-NMR and DEPT spectra (appendix Figure A8a and b) exhibited typical resonances at δ_C 107.8 (s), 99.3 (s), 117.5 (d) and 124.4 (s) suggesting the presence of a trisubstituted pyrrol ring. This was confirmed by the ¹H-NMR spectrum (appendix Figure A7) showing signals at δ_H 13.11

(1H, s) and 6.88 (1H, s) corresponding to NH-1 and H-3. The remaining $^1\text{H-NMR}$ signals at 4.22 (2H, dd, $J = 7.1, 14.2$ Hz) and at 1.15 (3H, t, $J = 7.1$ Hz) indicated the presence of a carboxylic acid ethyl ester. This observation was concordant with the signals at δ_{C} 60.6 (t) and 14.6 (q) in the $^{13}\text{C-NMR}$ and DEPT spectra. DEPT signals identified the signal at δ_{C} 60.6 (t) as a CH_2 group. No published NMR data could be found for the 4,5-dibromo-1*H*-pyrrol-2-carboxylic acid ethyl ester (13), although this compound has been previously described (Handy et al. 2004; Handy and Zhang 2006). Therefore, comparison of $^1\text{H-NMR}$ and $\text{C}^{13}\text{-NMR}$ data with those from the literature for 4,5-dibromo-1*H*-pyrrol-2-carboxylic acid methyl ester (König et al. 1998) led to the identification of compound 13 as 4,5-dibromo-1*H*-pyrrol-2-carboxylic acid ethyl ester (Table I.13).

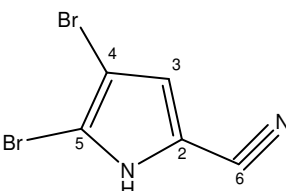
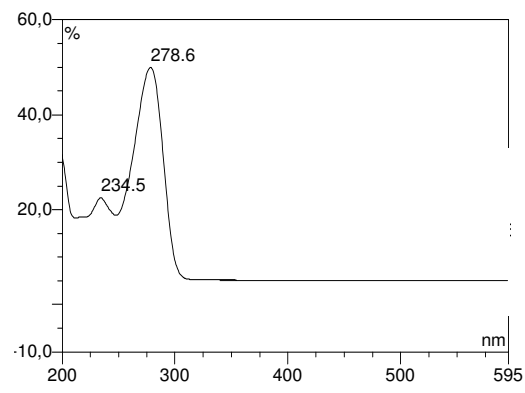
Table I.11. Analytical data of 4,5-dibromo-1*H*-pyrrol-2-carboxylic acid ethyl ester (13).

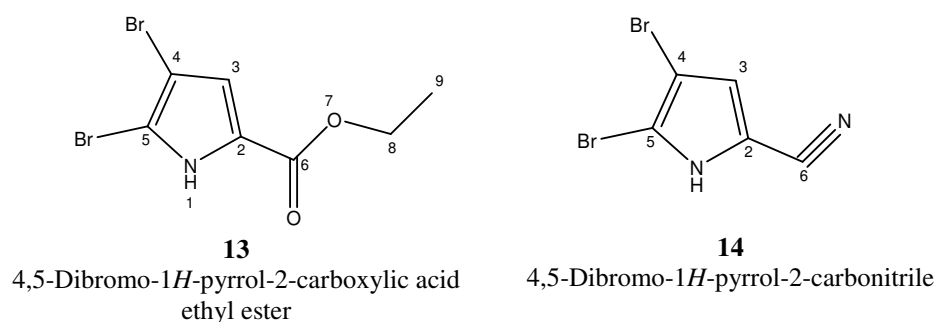
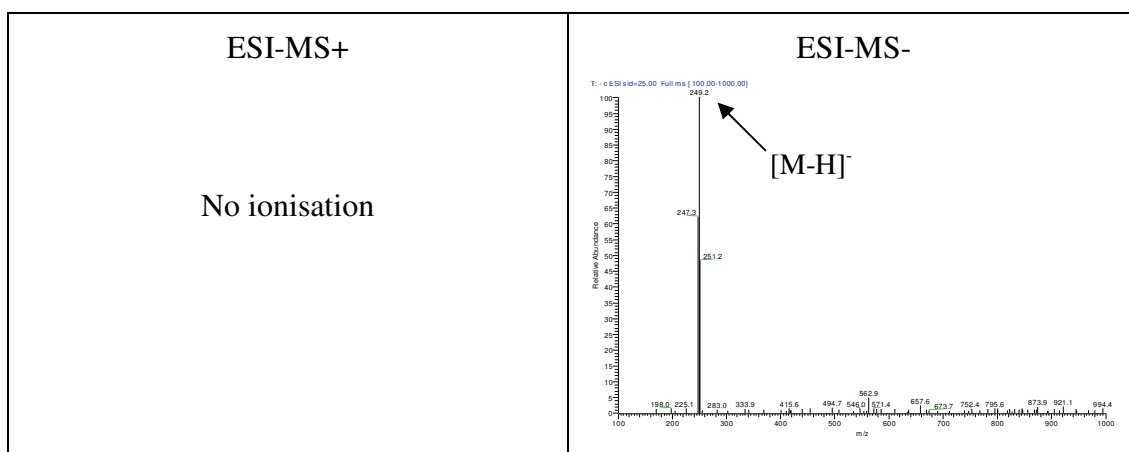
4,5-dibromo-1 <i>H</i> -pyrrol-2-carboxylic acid ethyl ester (13)	
Synonym(s)	Ethyl 4,5-dibromo-1 <i>H</i> -pyrrol-2-carboxylate
Amount	49.0 mg
Physical description	Red powder
Molecular formula	$\text{C}_7\text{H}_7\text{Br}_2\text{NO}_2$
Molecular weight	296 g/mol
Retention time HPLC	30.3 min (standard gradient)
<p style="text-align: center;">Structure</p> 	<p style="text-align: center;">UV spectrum</p> 
<p style="text-align: center;">ESI-MS+</p> <p style="text-align: center;">No ionisation</p>	<p style="text-align: center;">ESI-MS-</p> 

Structure elucidation of 4,5-dibromo-1*H*-pyrrol-2-carbonitrile (14)

The known compound 4,5-dibromo-1*H*-pyrrol-2-carbonitrile (14) was obtained from *Agelas oroides* methanol extract as a red-brown powder. UV absorbances were at λ_{\max} (MeOH) 235 and 279 nm (Table I.12). ESI-MS showed the molecular ion peak at m/z 247, 249, and 251 [M-H]⁻ in a ratio of 1:2:1 characteristic for a dibrominated compound (Table I.12). ¹H-NMR data (appendix Figure A9) showed signals at δ_{H} 13.16 (1H, s) and 6.90 (1H, s) corresponding to NH-1 and H-3 of a trisubstituted pyrrol ring. In combination with the mass spectral data, the absence of further proton signals indicated the presence of a carbonitrile moiety in the side chain. The HMBC spectrum (appendix Figure A10) showed correlations of H-3 to C-2 and C-5, thereby confirming the structure of the pyrrol ring (Table I.13b). However, no correlation of H-3 to C-6 was detectable. The HMBC spectra could not confirm the presence of a carbonitrile at C-2, which might be attributed to the very small quantity of compound available for NMR measurements (3.6 mg). Nevertheless, comparison of ¹H-NMR data, UV- and mass spectra with literature data (König et al. 1998) strongly supported the structure of 4,5-dibromo-1*H*-pyrrol-2-carbonitrile (14) (Table I.13a).

Table I.12. Analytical data of 4,5-dibromo-*H*-pyrrol-2-carbonitrile (14).

4,5-dibromo- <i>H</i> -pyrrol-2-carbonitrile (14)	
Synonym(s)	5-Cyano-2,3-dibromopyrrol
Amount	3.6 mg
Physical description	Red-brown powder
Molecular formula	C ₅ H ₂ Br ₂ N ₂
Molecular weight	249 g/mol
Retention time HPLC	27.3 min (standard gradient)
Structure	UV spectrum
	

Table I.13a. ¹H-NMR data (500 MHz) of compounds 13 and 14.

No	13 δ_{H} (m, <i>J</i> in Hz) (DMSO- <i>d</i> ₆)	13^{a*} δ_{H} (m, <i>J</i> in Hz) (CDCl ₃)	14 δ_{H} (DMSO- <i>d</i> ₆)	14^a δ_{H} (CDCl ₃)
1	13.11 (s)	9.32 (s)	13.16 (s)	9.35 (br)
3	6.88 (s)	6.87 (d, 2.9)	6.90 (s)	6.84 (d, 2.9)
8	4.22 (dd, 7.1, 14.2)	3.86 (s)	-	-
9	1.25 (t, 7.1)	-	-	-

^a (König et al. 1998)), ¹H-NMR (300 MHz)* Literature data for 4,5-dibromo-1*H*-pyrrol-2-carboxylic acid methyl esterTable I.13b. ¹³C-NMR data (125 MHz) of compounds 13 and 14, and HMBC data of compound 14.

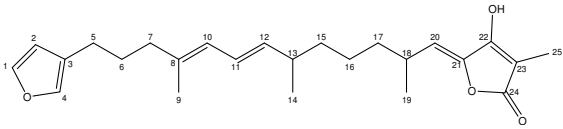
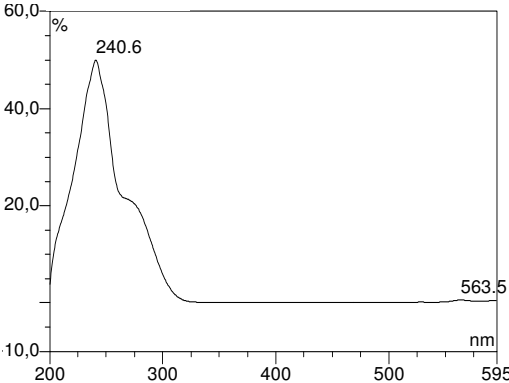
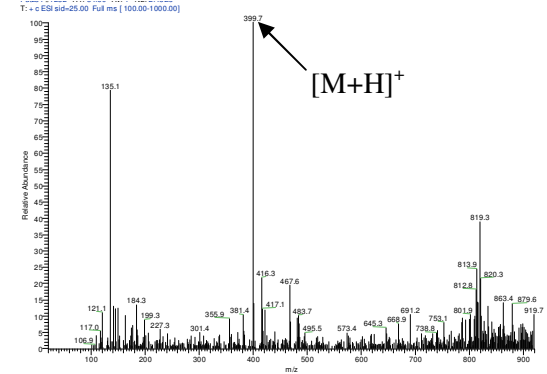
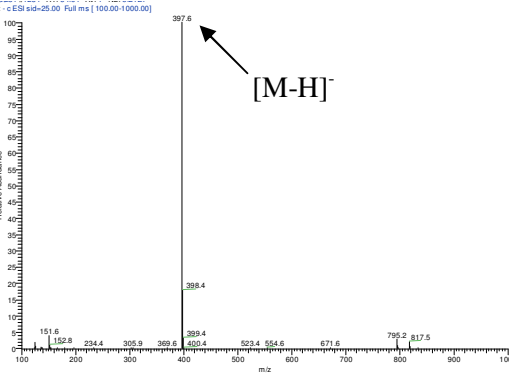
No	13 δ_{C} (DMSO- <i>d</i> ₆)	13^{a*} δ_{C} (CDCl ₃)	HMBC (DMSO- <i>d</i> ₆)	14^b δ_{C} (DMSO- <i>d</i> ₆)	14^a δ_{C} (CDCl ₃)
2	124.4 (s)	123.8 (s)	-	107.2 (s)	112.8 (s)
3	117.5 (d)	117.9 (d)	2, 5	123.4 (d)	122.6 (d)
4	99.3 (s)	100.8 (s)	-	-	100.1 (s)
5	107.8 (s)	106.7 (s)	-	117.6 (s)	107.7 (s)
6	159.2 (s)	159.9 (s)	-	-	104.3 (s)
7	-	-	-	-	-
8	60.6 (t)	52.0 (q)	-	-	-
9	14.6 (q)	-	-	-	-

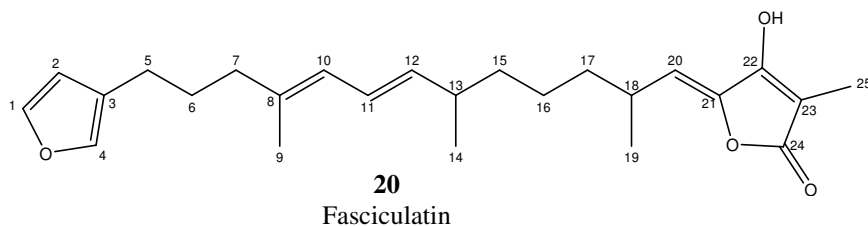
^a (König et al. 1998)), ¹³C-NMR (75 MHz)* Literature data for 4,5-dibromo-1*H*-pyrrol-2-carboxylic acid methyl ester
^b derived from HMBC spectrum

Ircinia variabilisStructure elucidation of fasciculatin (20)

The known compound fasciculatin (20) represents the major metabolite in the *Ircinia variabilis* methanol extract and was obtained as brown oil. UV absorbance was at λ_{\max} (MeOH) 249 nm (Table I.14). ESI-MS showed the molecular ion peak at m/z 397 $[M-H]^-$ (Table I.14). $^1\text{H-NMR}$ data (appendix Figure A23) exhibited signals at δ_{H} 7.34 (1H, t, $J = 1.6$ Hz), 7.20 (1H, t, $J = 1.0$ Hz) and 6.27 (1H, br s) corresponding to H-1, H-2 and H-4 of a mono-substituted furan ring, which was confirmed by ^{13}C resonances at δ_{C} 143.9, 111.9, 126.4 and 140.1 (appendix Figure A25). $^1\text{H-NMR}$ signals at δ_{H} 6.17 (1H, dd, $J = 15.1, 10.7$), 5.77 (1H, d, $J = 10.7$), 5.42 (1H, dd, $J = 15.1, 7.9$) and 5.24 (1H, d, $J = 9.8$) indicated the presence of five olefinic carbons which corresponded to ^{13}C signals at δ_{C} 139.2, 136.6, 126.5, 126.3 and 115.6. Coupling constants of H-11 and H-12 revealed a *trans*-olefinic function. The ^{13}C signal at δ_{C} 173.8 further alluded to the presence of a carboxylic group. The H,H-COSY spectrum (appendix Figure A24) showed correlations of H-1, H-2 and H-4, thereby confirming the structure of the furan ring. Correlations between H-4 and H-5 proved the attachment of the side chain to the furan. H,H-COSY data further supported the structure of the side chain which indicated spin systems for H-5 to H-7, H-9 to H-15, and H-17 to H-20. Careful inspection of ^1H -, ^{13}C - and H,H-COSY NMR data, UV- and mass spectra in comparison with literature data (Rifai et al. 2005) strongly supported the structure for fasciculatin (20) (Table I.15). This was further confirmed by the fact that the optical rotation of the isolated compound $[\alpha]_{\text{D}}^{17} -13.3^\circ$ (c 0.43, CHCl_3) was almost identical with the value given in literature $[\alpha]_{\text{D}}^{17} -12^\circ$ (c 0.43, CHCl_3) (Rifai et al. 2005).

Table I.14. Analytical data of fasciculatin (20).

Fasciculatin (20)	
Synonym(s)	5-(13-Furan-3-yl-2,6,10-trimethyl-trideca-7,9-dienylidene)-4-hydroxy-3-methyl-5 <i>H</i> -furan-2-one
Amount	11.1 mg
Physical description	Brown oil
Molecular formula	C ₂₅ H ₃₄ O ₄
Molecular weight	398 g/mol
[α] _D ¹⁷	-13.3° (c 0.43, CHCl ₃)
Retention time HPLC	35.3 min (standard gradient)
<p style="text-align: center;">Structure</p> 	<p style="text-align: center;">UV spectrum</p> 
<p style="text-align: center;">ESI-MS+</p> 	<p style="text-align: center;">ESI-MS-</p> 

Table I.15. ¹H- (500 MHz) and ¹³C-NMR (125 MHz) and H,H-COSY data of compound 20.

No	20 δ_{H} (m, <i>J</i> in Hz) (CDCl ₃)	20^a δ_{H} (m, <i>J</i> in Hz) (CDCl ₃)	20 δ_{C} (CDCl ₃)	20^a δ_{C} (CDCl ₃)	20 H,H-COSY (CDCl ₃)
1	7.34 (t, 1.6)	7.27 (t, 1.6)	143.9 (d)	142.6 (d)	2, 4
2	6.26 (br s)	6.19 (dd, 1.7, 0.7)	111.9 (d)	111.0 (d)	1
3	-	-	126.4 (s)	125.0 (s)	
4	7.20 (t, 1.0)	7.13 (t, 1.0)	140.1 (d)	138.8 (d)	1, 5
5	2.38 (t, 7.6)	2.32 (t, 7.6)	23.8 (t)	24.3 (t)	4, 6, 7
6	1.66 (t, 7.9)	1.61 (t, 8.0)	28.1 (t)	28.0 (t)	5
7	2.06 (t, 7.3)	1.99 (t, 7.4)	40.4 (t)	39.3 (t)	5
8	-	-	136.6 (s)	136.0 (s)	
Me-9	1.70 (d, 0.9)	1.65 (d, 0.9)	16.5 (q)	16.5 (q)	10
10	5.77 (d, 10.7)	5.70 (d, 10.7)	126.5 (d)	125.0 (d)	9, 11
11	6.17 (dd, 15.1, 10.7)	6.10 (dd, 15.0, 10.7)	126.3 (d)	124.7 (d)	10, 12
12	5.40 (dd, 15.1, 7.9)	5.36 (dd, 15.0, 7.9)	139.2 (d)	138.5 (d)	11, 13
13	2.13 (m)	2.08 (br)	38.1 (d)	36.8 (d)	12, 14
Me-14	0.97 (d, 6.9)	0.90 (d, 6.7)	21.2 (q)	20.6 (q)	13, 15
15, 16, 17	1.16-1.36 (m)	1.10-1.30 (m)	38.3 (15, 17); 25.2 (16) (t)	37.1 (15, 17); 25.1 (16) (t)	14 (15) 18 (17)
18	2.78 (m)	2.71 (m)	30.8 (d)	30.8 (d)	17, 19, 20
Me-19	1.04 (d, 6.9)	0.97 (d, 6.7)	21.5 (q)	20.7 (q)	18
20	5.25 (d, 9.8)	5.23 (d, 10.1)	115.6 (d)	115.8 (d)	18
21	-	-	145.3 (s)	142.8 (s)	
22	-	-	-	162.1 (s)	
23	-	-	98.4 (s)	99.1 (s)	
24	-	-	173.8 (s)	172.0 (s)	
Me-25	1.72 (s)	1.73 (s)	6.1 (q)	6.2 (q)	

^a (Rifai et al. 2005), ¹H NMR 300 MHz, ¹³C-NMR 75 MHz

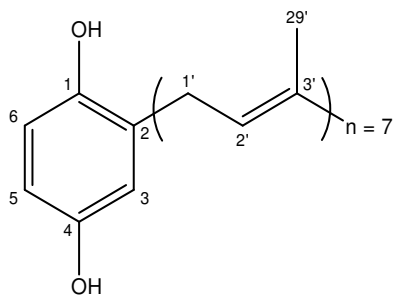
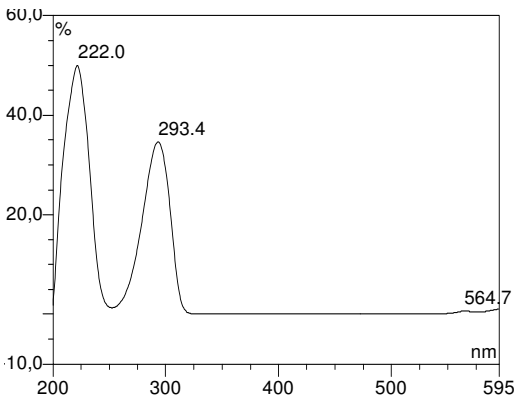
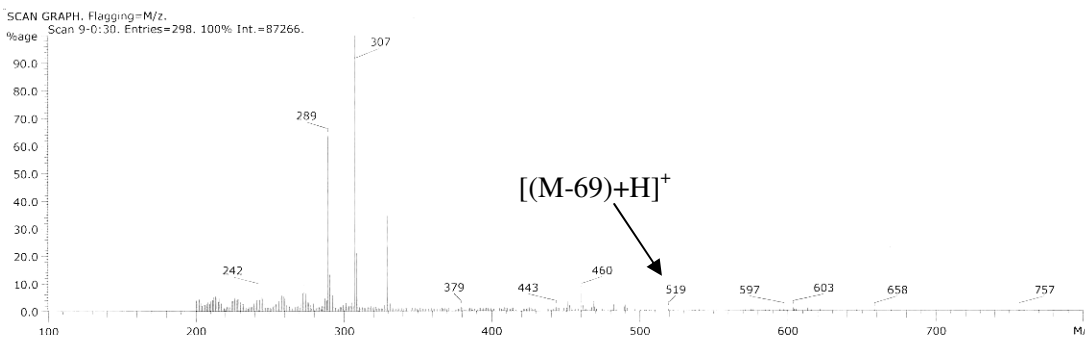
Ircinia fasciculata

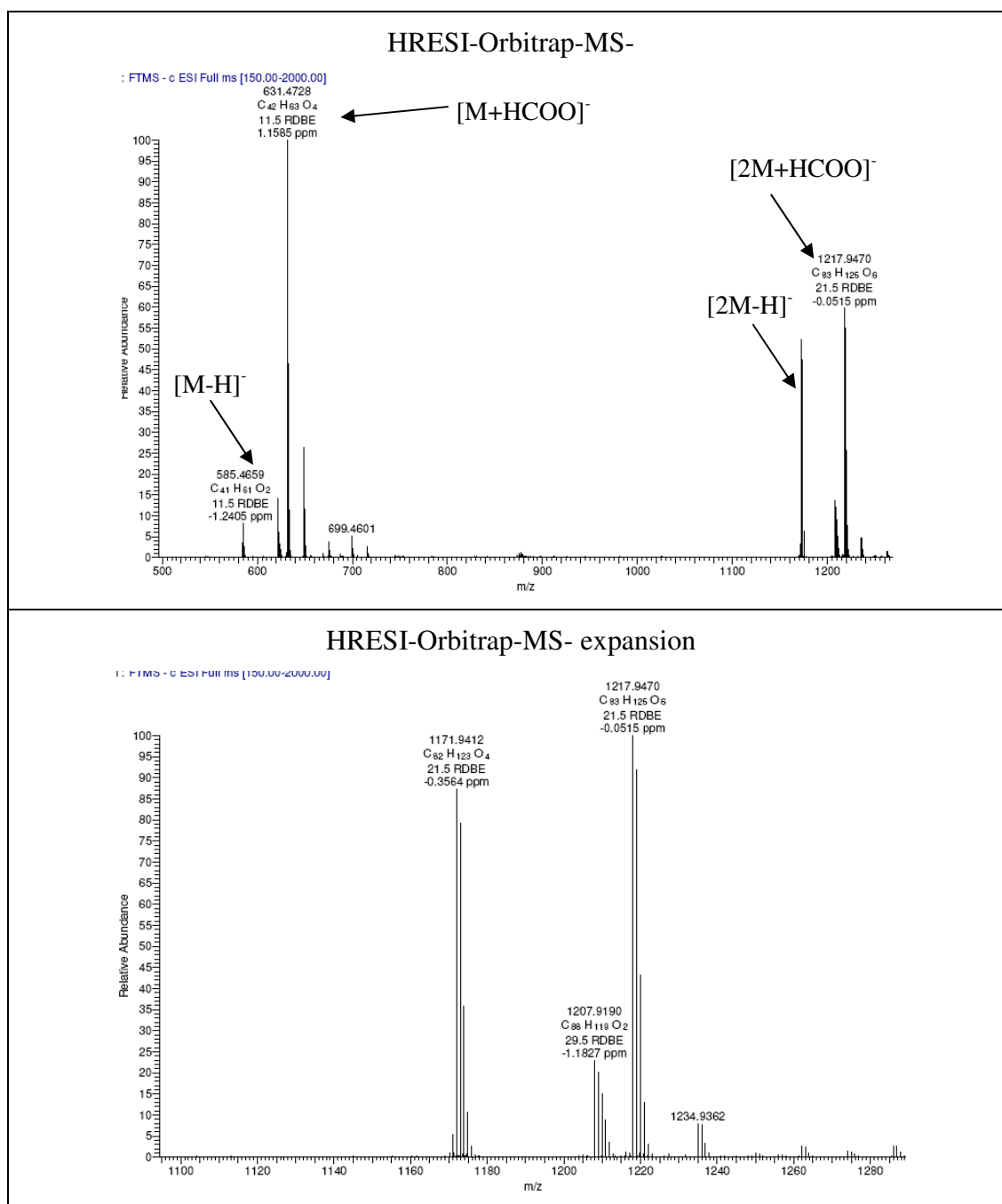
Structure elucidation of heptaprenylhydroquinone (16)

The known compound heptaprenylhydroquinone (16) represents another major metabolite in the *Ircinia fasciculata* methanol extract and was obtained as a brown oil. UV absorbance was at λ_{max} (MeOH) 222 and 293 nm (Table I.16). FAB-MS failed to detect the expected molecular ion peak of heptaprenylhydroquinone (16) at m/z 587 [M+H]⁺. Instead, it exhibited an ion peak at m/z 519 [M+H]⁺ which corresponds to hexaprenylhydroquinone (15) and a series of peaks at m/z M⁺-69-(68)_n arising from

successive loss of isoprene units (Table I.16). However, HRESI-MS showed the expected molecular ion peak at m/z 585.4659 $[M-H]^-$ (Table I.16). The $^1\text{H-NMR}$ spectrum (appendix Figure A15) was identical to that of hexaprenylhydroquinone isolated from *Sarcotragus muscarum* (15, presented below), the only difference were peak integrals, indicating one additional isoprene unit of compound 17 when compared to hexaprenylhydroquinone (15, Table 19a).

Table I.16. Analytical data of heptaprenylhydroquinone (16).

Heptaprenylhydroquinone (16)	
Synonym(s)	Heptaprenyl p-quinol; 2-heptaprenyl-1,4-benzenediol; 2-(3,7,11,15,19,23,27-heptamethyl-2,6,10,14,18,22,26-octacosaeptaeny)-1,4-benzenediol
Amount	12.6 mg
Physical description	Brown oil
Molecular formula	$\text{C}_{41}\text{H}_{62}\text{O}_2$
Molecular weight	586.4659 g/mol
Retention time HPLC	39.5 min (standard gradient)
Structure	UV spectrum
	
FAB-MS	
	



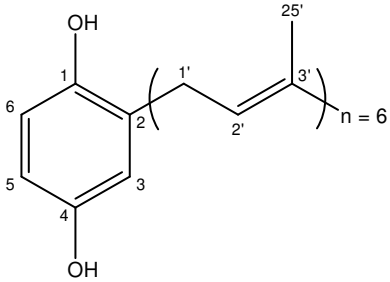
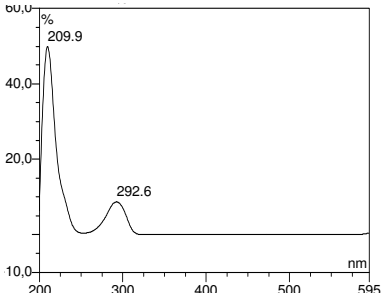
Sarcotragus muscarum

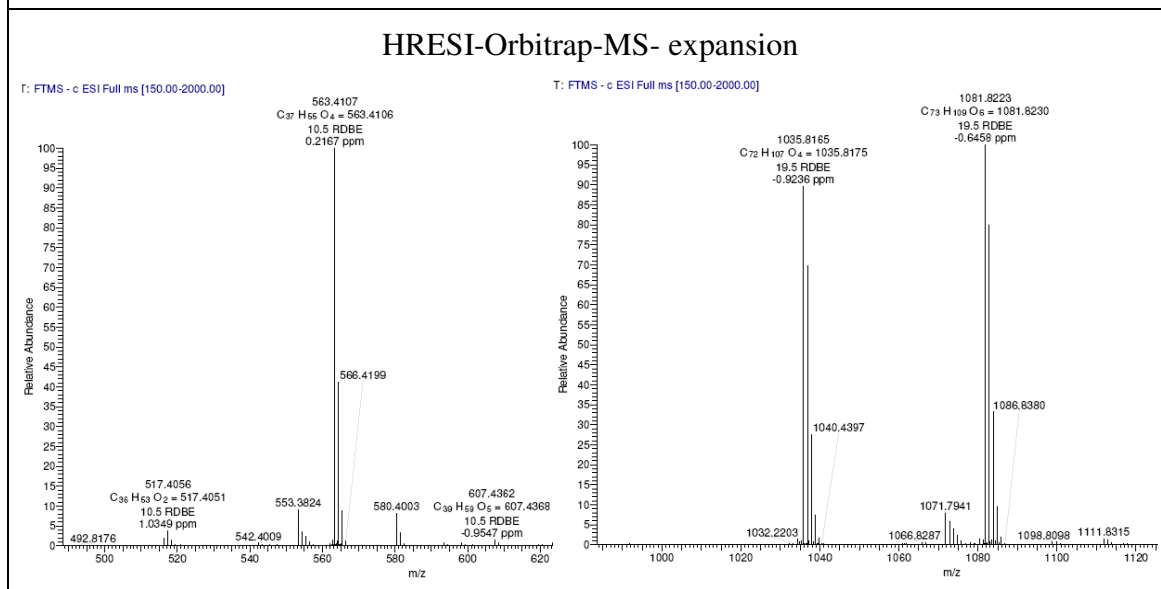
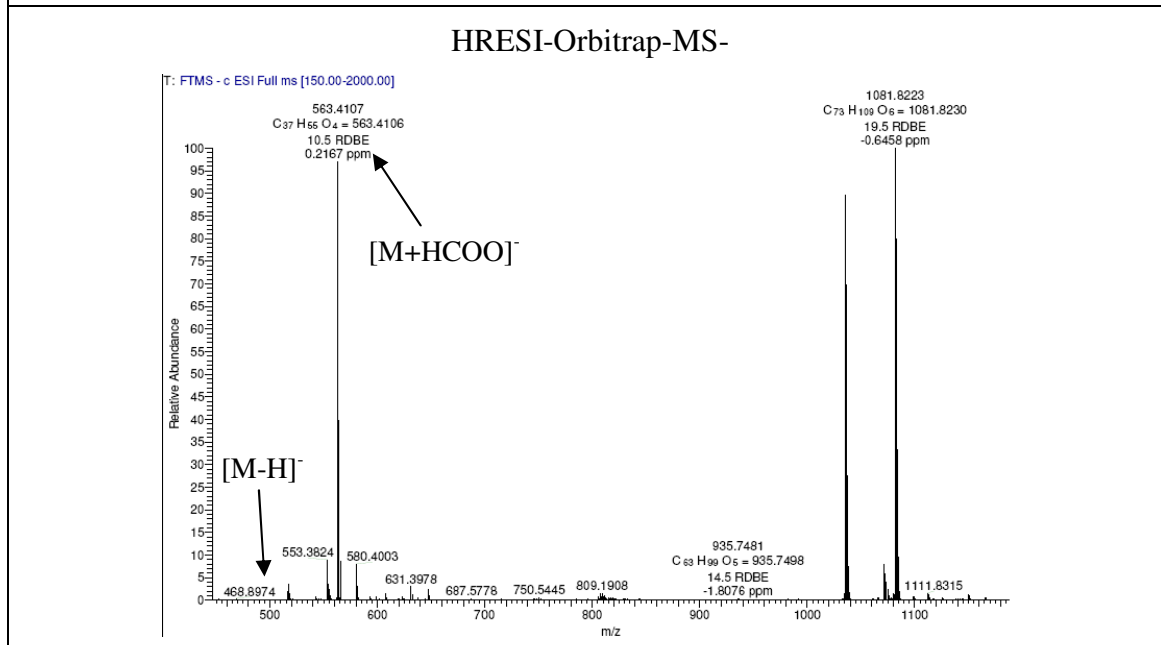
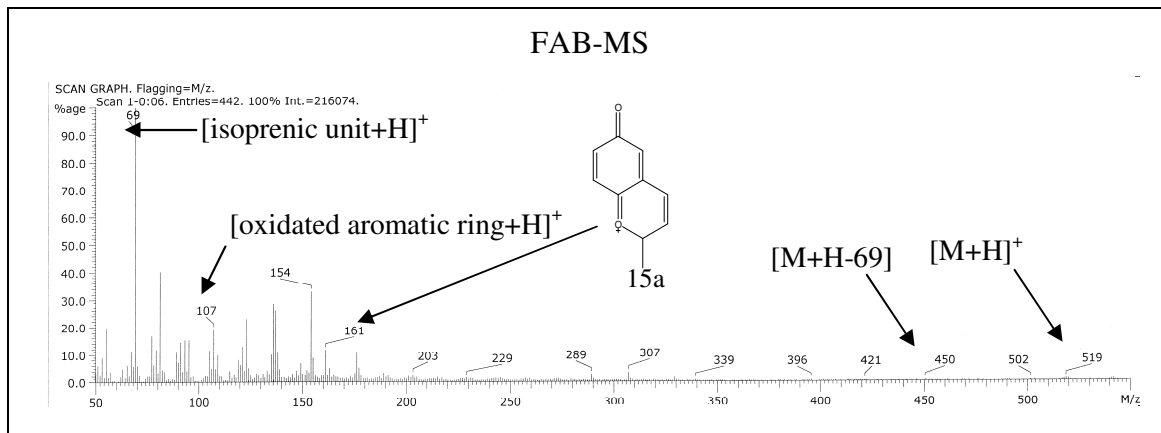
Structure elucidation of hexaprenylhydroquinone (15)

The known compound hexaprenylhydroquinone (15) represents one of the major metabolites in the *Sarcotragus muscarum* methanol extract and was obtained as a brown oil. UV absorbance was at λ_{\max} (MeOH) 210 and 293 nm (Table I.17). FAB-MS showed the molecular ion peak at m/z 519 $[M+H]^+$ and a series of peaks at m/z M^+-69 - $(68)n$ arising from successive loss of isoprene units (Table I.17). The peak at m/z 161

corresponds to the ion 15a (Table I.17) characteristic of prenylated 1,4-benzoquinones (Cimino et al. 1972). HRESI-MS displayed the expected molecular ion peak at m/z 517.4056 $[M-H]^-$ (Table I.17). $^1\text{H-NMR}$ data (appendix Figure A11) exhibited signals at δ_{H} 6.52 (1H, d, $J = 2.8$ Hz), 6.42 (1H, dd, $J = 2.8, 8.5$ Hz) and 6.56 (1H, d, $J = 8.5$) corresponding to H-3, H-5 and H-6 of a hydroquinone, to which a side chain of isoprenic units was attached. This could be inferred by signals δ_{H} 3.23 (2H, d, $J = 7.3$ Hz), 5.31 (1H, t, $J = 7.3$ Hz), 2.13 (2H, t, $J = 6.8$) and 1.69 (3H, s) representing the isoprene unit attached directly to the ring (H-1', H-2', H-4' and Me-25'), and the slightly shifted signals of the remaining isoprene units. Peak integrals allowed for the determination of the number of isoprene units attached to the hydroquinone (Table I.19a). H,H-COSY and HMBC correlations (appendix Figure A12 and A13, Table I.19b) confirmed the structure of a prenylated hydroquinone. Careful inspection of $^1\text{H-NMR}$, H,H-COSY and HMBC data, UV- and mass spectra and comparison with literature data (Cimino et al. 1972; Wakimoto et al. 1999) strongly supported the structure of hexaprenylhydroquinone (15) (Table I.19a and b). Since the $^1\text{H-NMR}$ spectrum of hexaprenylhydroquinone isolated by Cimino et al. 1972 was measured at 100 MHz, $^1\text{H-NMR}$ chemical shifts described for sulfated octaprenylhydroquinone published more recently by Wakimoto et al. 1999 which was measured in 600 MHz were used for the comparison of ^1H chemical shifts of compounds 15, 16 and 17 (Table I.19a).

Table I.17. Analytical data of hexaprenylhydroquinone (15).

Hexaprenylhydroquinone (15)	
Synonym(s)	2-Hexaprenyl-1,4-benzenediol; 2-(3,7,11,15,19,23-hexamethyl-2,6,10,14,18,22-tetracosahexaenyl)-1,4-benzenediol
Amount	76.2 mg
Physical description	Brown oil
Molecular formula	$\text{C}_{36}\text{H}_{54}\text{O}_2$
Molecular weight	518.4056 g/mol
Retention time HPLC	38.9 min (standard gradient)
Structure	UV spectrum
	

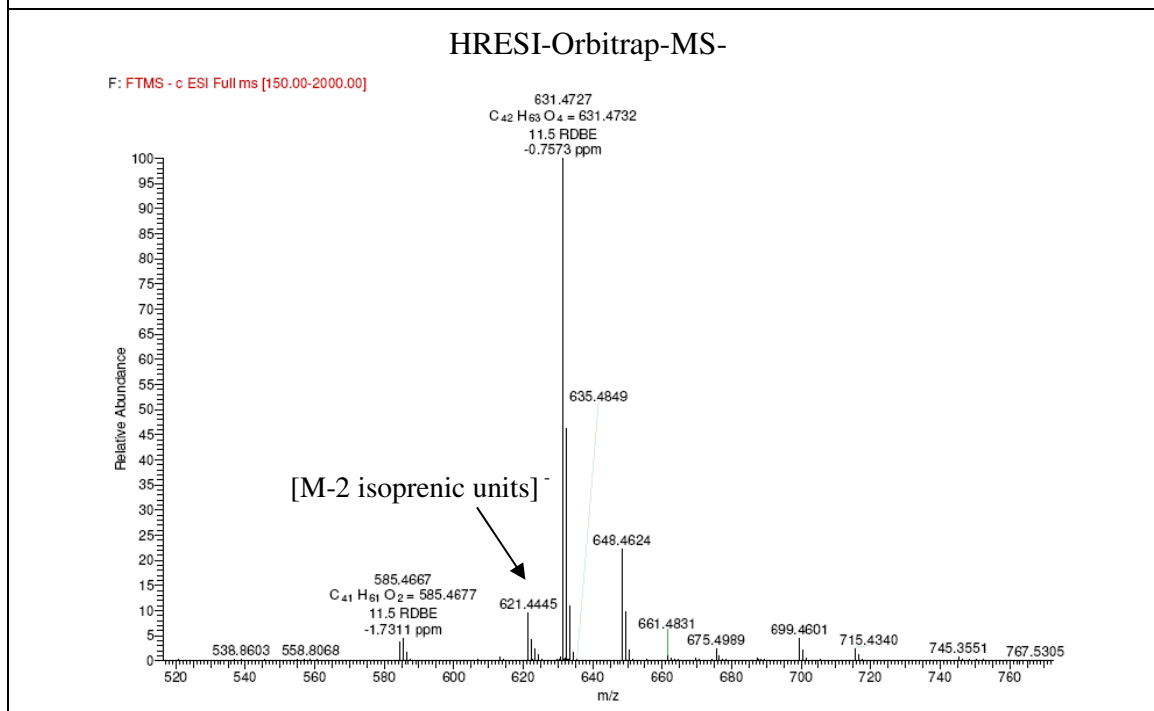
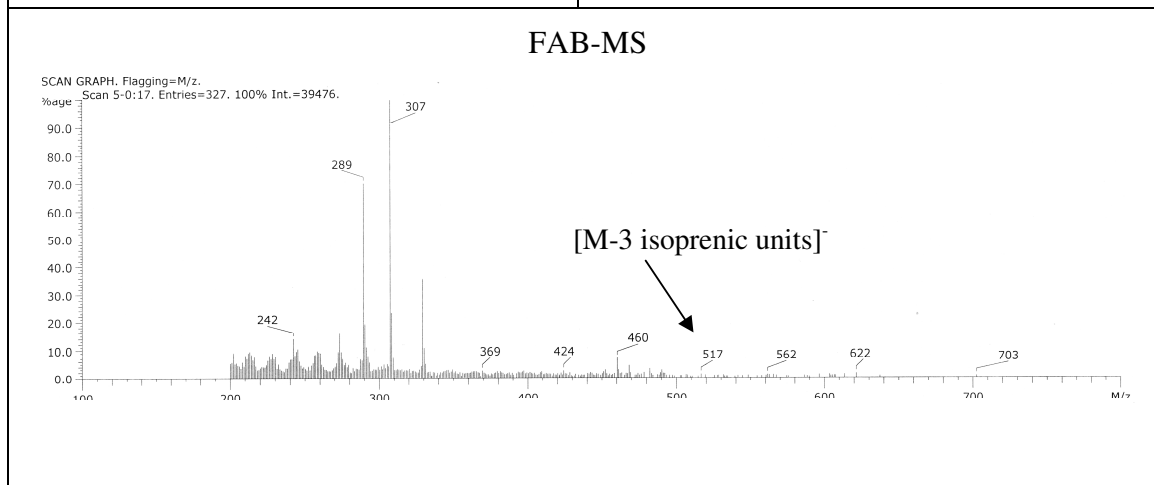
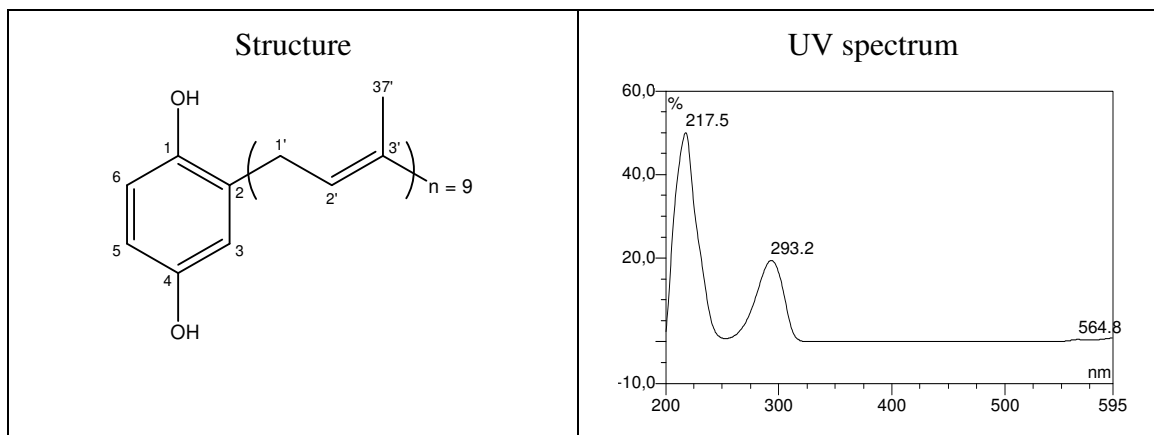


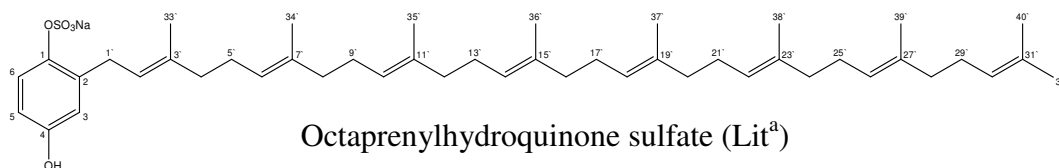
Structure elucidation of nonaprenylhydroquinone (17)

Together with the hexaprenylhydroquinone (15), the known compound nonaprenylhydroquinone (17) represents one of the major metabolites in the *Sarcotragus muscarum* methanol extract and was obtained as brown oil. UV absorbance was at λ_{max} (MeOH) 218 and 293 nm (Table I.18). FAB-MS did not show the molecular ion peak expected at m/z 722 $[\text{M-H}]^-$. Instead, a fragment peak at m/z 517 $[\text{M-H}]^-$ and a series of peaks at m/z $\text{M}^+ - 69 - (68)n$ arising from successive loss of isoprene units (Table I.18) was detected. HRESI-MS displayed the fragment peak at m/z 585.4667 $[\text{M-H}]^-$, identical to that of heptaprenylhydroquinone (16, Table I.18). Molecular weight was thus detectable neither by FAB-MS nor by HRESI-MS. The $^1\text{H-NMR}$ spectrum (appendix Figure A14) was identical to that of hexaprenylhydroquinone (15), the single difference were peak integrals which indicated three additional isoprene units of compound 16 when compared to hexaprenylhydroquinone (15, Table I.19a). Since retention time under HPLC standard conditions was different from compounds 15 and 17, and peak integrals proved to be reliable in quantifying the number of isoprene units attached to the hydroquinone, compound 17 differed from compounds 15 and 16. Compound 17 was thus identified as nonaprenylhydroquinone, even though the molecular weight of this compound could not be confirmed by MS.

Table I.18. Analytical data of nonaprenylhydroquinone(17).

Nonaprenylhydroquinone (17)	
Synonym(s)	2-Nonaprenyl-1,4-benzenediol; 2-(3,7,11,15,19,23,27,31,35-nonamethyl- 2,6,10,14,18,22,26,30,34-hexatriacontanonaenyl)-1,4- benzenediol
Amount	18.2 mg
Physical description	Brown oil
Molecular formula	$\text{C}_{51}\text{H}_{78}\text{O}_2$
Molecular weight	723 g/mol
Retention time HPLC	43.5 min (standard gradient)



Table I.19a. ¹H-NMR data (500 MHz) of compounds 15, 16 and 17.

Since the ¹H-NMR spectrum of prenylated hydroquinones isolated by Cimino et al. 1972 was measured at 100 MHz, ¹H-NMR chemical shifts described for sulfated octaprenylhydroquinone published more recently by Wakimoto et al. 1999 which was measured in 600 MHz were used for the comparison of ¹H chemical shifts of compounds 15, 16 and 17

No	15 δ _H (m, J in Hz), no. of H (CD ₃ OD)	16 δ _H (m, J in Hz), no. of H (CD ₃ OD)	17 δ _H (m, J in Hz), no. of H (CD ₃ OD)	Lit^a δ _H (m, J in Hz), no. of H (CD ₃ OD)
3	6.52 (d, 2.8), 1H	6.52 (d, 2.8), 1H	6.52 (d, 2.8), 1H	6.60 (d, 3.0), 1H
5	6.42 (dd, 2.8, 8.5), 1H	6.42 (dd, 2.8, 8.5), 1H	6.42 (dd, 2.8, 8.5), 1H	6.52 (dd, 3.0, 9.0), 1 H
6	6.56 (d, 8.5), 1H	6.56 (d, 8.5), 1H	6.56 (d, 8.5), 1H	7.18 (d, 9.0), 1H
1'	3.23 (d, 7.3), 2H	3.23 (d, 7.3), 2H	3.23 (d, 7.3), 2H	3.43, 2H
2'	5.31 (t, 7.3), 1H	5.31 (t, 7.3), 1H	5.31 (t, 7.3), 1H	5.32, 1H
4'	2.13 (t, 6.8), 2H	2.13 (t, 6.8), 2H	2.13 (t, 6.8), 2H	2.05, 2H
CH ₂ 8', 12', 16' etc	2.06 (m), 8H	2.06 (m), 10H	2.06 (m), 14H	1.97, 12H
CH ₂ 5', 9', 13' etc	1.97 (t, 7.3), 10H	1.97 (t, 7.3), 12H	1.97 (t, 7.3), 16H	2.07, 14H
CH 6', 10', 14' etc	5.09 (m), 5H	5.09 (m), 6H	5.09 (m), 8H	5.09, 7H
Me-32' (terminal methyl group)	1.65 (s), 3H	1.65 (s), 3H	1.65 (s), 3H	1.65, 3H
Me-33' / equivalent	1.69 (s), 3H	1.69 (s), 3H	1.69 (s), 3H	1.71, 3H
CH ₃ groups	1.58 (s), 15H	1.58 (s), 18H	1.58 (s), 24H	1.58, 21H

^a (Wakimoto et al. 1999), ¹H-NMR (600 MHz)

Structure elucidation of brominated ambigol A derivative 1 (18) and 2 (19)

Brominated ambigol A derivatives (compounds 18 and 19) represent minor metabolites in the *Sarcotragus muscarum* methanol extract and were obtained as white powder. Both compounds are new and thus have not been described previously.

Brominated ambigol A derivative 1 (18) shows UV absorbances at λ_{max} (MeOH) 221 and 291 nm (Table I.20). HRESI-MS displayed molecular ion peaks at *m/z* 822, 824,

826, 828, 830, 832, 834 and 836 [M-H]⁻ in a ratio of 1:7:21:35:35:21:7:1 characteristic for a molecule containing seven bromine atoms (Table I.20).

Table I.19b. H,H-COSY and HMBC correlations of compound 15.

No	15	
	H,H-COSY (CD ₃ OD)	HMBC (CD ₃ OD)
3	5	1, 2, 4
5	3, 6	3
6	5	3
1'	2', 25'	1, 2, 3, 6, 2'
2'	1', 4', 6', 25'	
4'	2'	2'
CH ₂ 8', 12', 16' etc	CH ₂ 5', 9' etc; CH ₃ groups	CH ₂ 5', 9' etc; CH 6', 10' etc; C 3', 7' etc; CH ₃ groups
CH ₂ 5', 9', 13' etc	CH 6', 10' etc; CH ₂ 8', 12' etc	C 3', 7' etc; CH 6', 10' etc; CH ₂ groups 8', 12' etc
CH groups 6', 10', 14' etc	2', CH ₂ 5', 9' etc	CH ₂ groups 5', 9' etc; CH ₂ groups 8', 12' etc; CH ₃ groups
Me-32' (terminal methyl group) = 24'	21', 22'	22', 23', 30'
Me-33' / equivalent = 25'	1', 2'	2', 3', 4'
CH ₃ groups	CH ₂ 8', 12' etc	CH ₂ 5', 9' etc; CH 6', 10' etc; CH ₂ groups 8', 12'; C 3', 7' etc

¹H-NMR data (appendix Figure A16) exhibited signals at δ_{H} 7.72 (1H, d, $J = 2.4$ Hz), 7.31 (1H, dd, $J = 2.4, 8.8$ Hz) and 6.57 (1H, d, $J = 8.8$ Hz) corresponding to H-3'', H-5'' and H-6'' of a trisubstituted benzene ring, which was confirmed by ¹³C signals at δ_{C} 117.5, 132.5, 136.4 representing C-6'', C-5'' and C-3'', and at δ_{C} 114.8 and 113.3 indicating the existence of two brominated carbon atoms (appendix Figure A17). The weak signal at δ_{C} 154.8 was assigned to C-1'' which represents part of an ether structure. The structure of this ring system was confirmed by HMBC correlations (appendix Figure A18, Table I.22b). Signals at δ_{H} 7.62 (1H, d, $J = 2.4$ Hz) and 7.08 (1H, d, $J = 2.4$ Hz) revealed the presence of a second, fourfold substituted benzene ring (appendix Figure A16) which was evidenced by ¹³C signals at δ_{C} 135.9 and 134.8 for C-4' and C-6', respectively, and 112.8 and 111.9 characteristic for the brominated carbons (appendix Figure A17). ¹³C signals for C-1' and C-2' were not clearly detectable, but could be deduced from the HMBC spectrum by their crosspeaks with H-4' and H-6' (appendix Figure A18, Table I.22b).

Table I.20. Analytical data of brominated ambigol A derivative 1 (18).

Brominated ambigol A derivative 1 (18)	
Synonym(s)	4,5,6,3',5'-Pentabromo-3-(2,4-dibromo-phenoxy)-biphenyl-2,2'-diol
Amount	3.4 mg
Physical description	White powder
Molecular formula	C ₁₈ H ₇ Br ₇ O ₃
Molecular weight	829.4539 g/mol
Retention time HPLC	35.1 min (standard gradient)
Structure proposal	UV spectrum
HREI-MS-	
HRESI-Orbitrap-MS- expansion	

Since the signal for C-2' was found at δ_c 152.5 the attachment of a hydroxyl group was concluded (appendix Figure A18). HMBC correlations confirmed the structure of the second ring system (Figures A21, A22, Table I.22b). Taken together, all NMR data seemed to identify compound 18 as a brominated diphenyl ether.

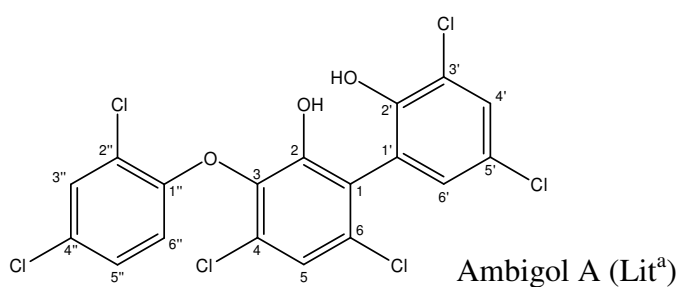
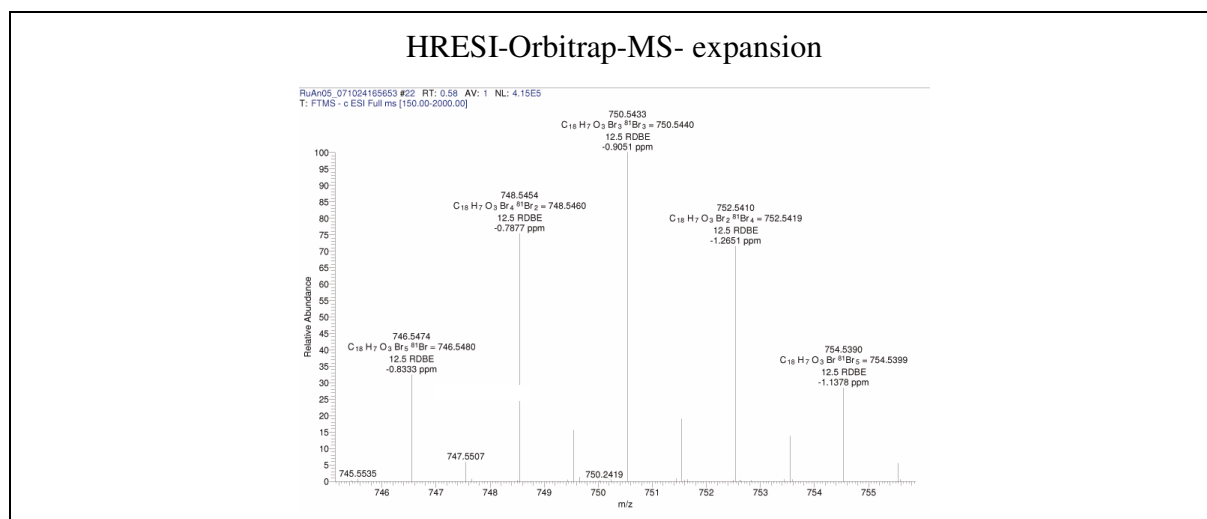
However, these data were not in congruence with HRESI-MS data detecting the major molecular ion peak at m/z 828.4539 $[M-H]^-$ and clearly showing a peak pattern characteristic for a compound containing seven bromine atoms. It was therefore concluded that the two aromatic ring systems inferred from NMR data are connected via a third, completely substituted aromatic ring system which would thus not show any signals in the 1H -NMR spectrum. The ^{13}C signals for this third ring system were neither in the ^{13}C -NMR nor in the HMBC spectrum detectable. In order to achieve an unequivocal proof of the existence of such a ring system, an INADEQUATE spectrum showing C-C correlations would be required, which could not be recorded due to the insufficient amount of substance isolated to accomplish such experiments. In conclusion, NMR data showed a good match with the data for ambigol A published by (Falch et al. 1993) (Table I.22a). Compound 18 is comparable to ambigol A except for the bromine substituents instead of chlorine units. Furthermore, the central ring system is completely substituted, which is not the case for ambigol A where one proton appears as a singlett at δ_H 7.21 in the 1H -NMR spectrum (Table I.22a) (Falch et al. 1993). Based on NMR and HRESI-MS data, the proposed structure of compound 18 seems probable, but could not be further confirmed by NMR due to a lack of data for the central ring system.

Brominated ambigol A derivative 2 (19) displays UV absorbances at λ_{max} (MeOH) 220 and 291 nm (Table I.21). HRESI-MS showed molecular ion peaks at m/z 744, 746, 748, 750, 752, 754 and 756 $[M-H]^-$ in an isotopic ratio of 1:6:15:20:15:6:1 characteristic for a molecule containing six bromine atoms (Table I.21). 1H -NMR data (appendix Figure A19) exhibited signals at δ_H 7.72 (1H, d, $J = 2.4$ Hz), 7.31 (1H, dd, $J = 2.4, 8.8$ Hz) and 6.56 (1H, d, $J = 8.8$ Hz) attributed to H-3'', H-5'' and H-6'' of a trisubstituted benzene ring, and corresponding ^{13}C signals at δ_c 117.5, 132.5, 136.4, 114.8, 113.3 and 154.8 (appendix Figure A20). Signals at δ_H 7.29 (1H, dd, $J = 2.5, 8.7$ Hz), 7.06 (1H, d, $J = 2.5$ Hz) and 6.77 (1H, d, $J = 8.7$ Hz) revealed the presence of a second, trisubstituted benzene ring (appendix Figure A19) which was implicated by ^{13}C signals at δ_c 135.9, 134.8 and 118.2 for C-3', C-4' and C-6', respectively, and 111.5 for the brominated carbon (appendix Figure A20). The ^{13}C signals for C-1' were not clearly detectable. The

structure of both ring systems was confirmed by H,H-COSY and HMBC spectra (appendix Figures A21 and A22, Table I.22 b). Taken together, all NMR data were identical to those of compound 18, apart from position C-3' which carries a bromine atom in compound 18 but is not substituted in compound 19. These data were in congruence with HRESI-MS data featuring the major molecular ion peak at m/z 750.5436 $[M-H]^-$ and clearly showing a peak pattern characteristic for a compound containing six bromine atoms. As for compound 18, the presence of the central ring could not be proven due to very low yield.

Table I.21. Analytical data of brominated ambigol A derivative 2 (19).

Brominated ambigol A derivative 2 (19)	
Synonym(s)	4,5,6,5'-Tetrabromo-3-(2,4-dibromo-phenoxy)-biphenyl-2,2'-diol
Amount	1.7 mg
Physical description	White powder
Molecular formula	$C_{18}H_8Br_6O_3$
Molecular weight	751.5436 g/mol
Retention time HPLC	33.9 min (standard gradient)
Structure proposal	UV spectrum

Table I.22a. ¹H- (600 MHz) and ¹³C-NMR (150 MHz) data of compounds 18 and 19.

No	18		19		Lit ^a	
	δ_{H} (m, <i>J</i> in Hz), (CD ₃ OD)	δ_{C} (CD ₃ OD)	δ_{H} (m, <i>J</i> in Hz), (CD ₃ OD)	δ_{C} (CD ₃ OD)	δ_{H} (m, <i>J</i> in Hz), (CD ₃ OD)	δ_{C} (CD ₃ OD)
1	-	-	-	-	-	125.9 (s)
2	-	-	-	-	-	152.3 (s)
3	-	-	-	-	-	139.3 (s)
4	-	-	-	-	-	128.9 (s) ^b
5	-	-	-	-	7.21 (s)	121.8 (d)
6	-	-	-	-	-	132.8 (s) ^b
1'	-	128.0 (s)	-	130.6 (s)	-	126.5 (s)
2'	-	152.5 (s)	-	155.1 (s)	-	151.6 (s)
3'	-	112.8 (s)	6.77 (d, 8.7)	118.2 (d)	-	123.6 (s)
4'	7.62 (d, 2.4)	135.9 (d)	7.29 (dd, 2.5, 8.7)	133.2 (d)	7.44 (d, 2.6)	130.1 (d)
5'	-	111.9 (s)	-	111.5 (s)	-	124.9 (s)
6'	7.08 (d, 2.4)	134.8 (d)	7.06 (d, 2.5)	134.9 (d)	7.13 (d, 2.6)	131.1 (d)
1''	-	154.8 (s)	-	154.8 (s)	-	153.3 (s)
2''	-	113.3 (s)	-	113.2 (s)	-	124.7 (s)
3''	7.72 (d, 2.4)	136.4 (d)	7.72 (d, 2.4)	132.6 (d)	7.54 (d, 2.5)	131.1 (d)
4''	-	114.8 (s)	-	114.9 (s)	-	128.6 (s)
5''	7.31 (dd, 2.4, 8.8)	132.5 (d)	7.31 (dd, 2.4, 8.8)	136.4 (d)	7.22 (dd, 2.5, 8.9)	128.8 (d)
6''	6.57 (d, 8.8)	117.2 (d)	6.56 (d, 8.8)	117.1 (d)	6.72 (d, 8.9)	117.0 (d)

^a (Falch et al. 1993) ¹H NMR (500 MHz), ¹³C-NMR (125 MHz)^b Assignments interchangeable

Table I.22b. HMBC data of compounds 18 and 19 and H,H-COSY of compound 19.

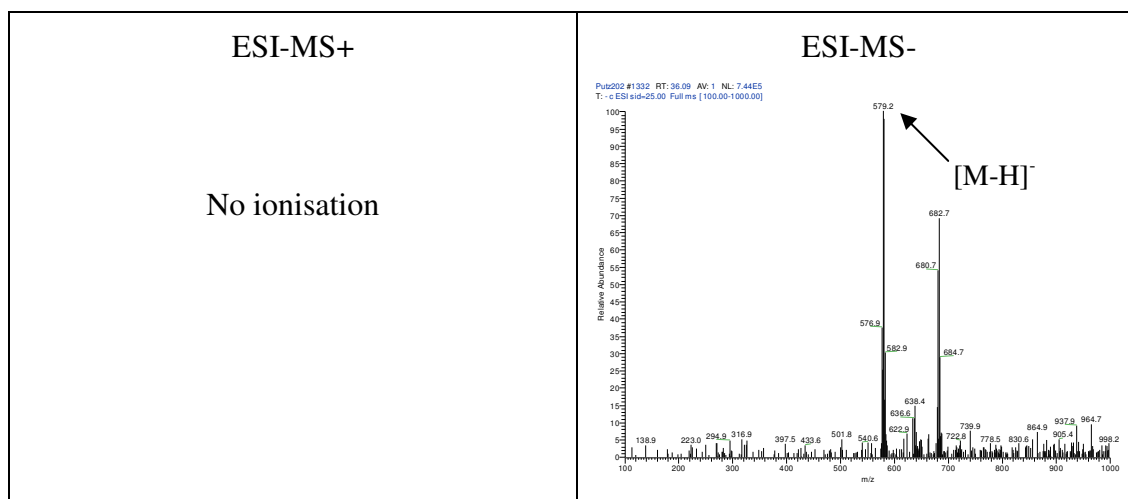
No	18 HMBC (CD ₃ OD)	HMBC (CD ₃ OD)	19 H,H-COSY (CD ₃ OD)
1'			
2'			
3'		1', 2', 4', 5', 6'	4', 6'
4'	2', 3', 5', 6'	2', 5', 6'	3', 6'
5'			
6'	1', 2', 3', 4', 5'	1', 2', 3', 4', 5'	3', 4'
1''			
2''	3'', 5'', 6''	3'', 5'', 6''	5''
3''	1'', 2'', 4'', 5''	1'', 2'', 4'', 5'', 6''	6'', 5''
4''			
5''	1'', 2'', 3'', 4'', 6''	1'', 2'', 3'', 4'', 6''	3''
6''			

*Dysidea granulosa*Structure elucidation of 4,5,6-tribromo- (21) and 4,6-dibromo-2-(2',4'-dibromophenoxy)phenol (22)

4,5,6-tribromo- (21) and 4,6-dibromo-2-(2',4'-dibromophenoxy)phenol (22) represent the two major metabolites in the *Dysidea granulosa* methanol extract and were obtained as white powder. Both compounds have been previously described.

Table I.23. Analytical data of 4,5,6-tribromo-2-(2',4'-dibromophenoxy)phenol (21).

4,5,6-tribromo-2-(2',4'-dibromophenoxy)phenol (21)	
Synonym(s)	2,4-Dibromo-6-(2,3,4-tribromo-phenoxy)-phenol
Amount	86.0 mg
Physical description	White powder
Molecular formula	C ₁₂ H ₅ Br ₅ O ₂
Molecular weight	580 g/mol
Retention time HPLC	34.6 min (standard gradient)
Structure	UV spectrum

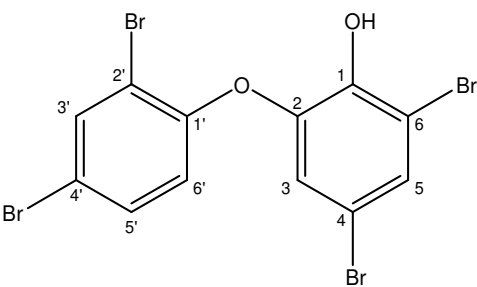
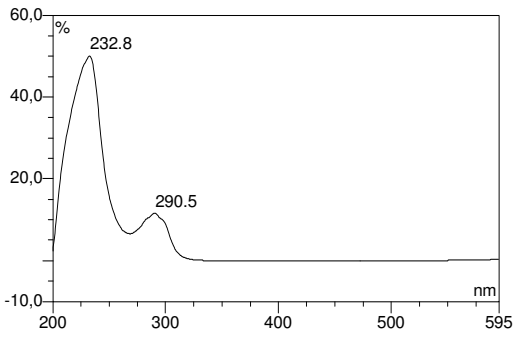
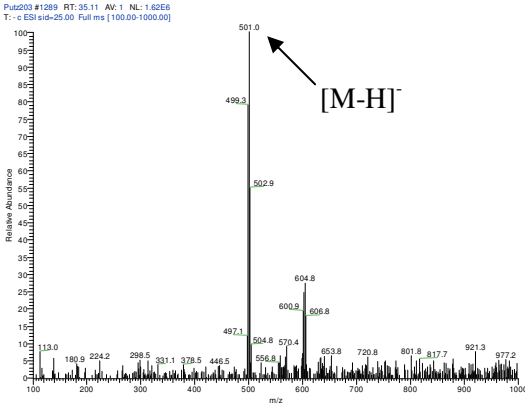


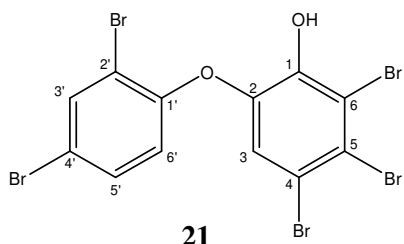
4,5,6-tribromo-2-(2',4'-dibromophenoxy)phenol (21) showed UV absorbances at λ_{\max} (MeOH) 236 and 290 nm (Table I.23). ESI-MS displayed molecular ion peaks at m/z 575, 577, 579, 581, 583, and 585 $[M-H]^-$ in an isotopic ratio of 1:5:10:10:5:1 characteristic for a molecule containing five bromine atoms (Table I.23). $^1\text{H-NMR}$ data (appendix Figure A25) exhibited signals at δ_{H} 7.77 (1H, d, $J = 2.4$ Hz), 7.32 (1H, dd, $J = 2.3, 8.8$ Hz) and 6.41 (1H, d, $J = 8.8$ Hz) corresponding to H-3', H-5' and H-6' of a trisubstituted benzene ring, which was confirmed by ^{13}C signals at δ_{C} 136.8, 132.5, 121.9 representing C-3', C-5' and C-6', and at δ_{C} 115.6 and 113.4 proving the existence of two brominated carbon atoms (appendix Figure A26). The signal at δ_{C} 154.2 was assigned to C-1' which represents part of the ether structure. The peak at δ_{H} 7.36 (1H, s) revealed the presence of a second benzene ring with five substituents (appendix Figure A25) which was also indicated by ^{13}C signals at δ_{C} 122.9 for C-3, 122.8 (2x) and 116.8 for three brominated carbons, and 152.3 for C-1 (appendix Figure A26). The structure of both ring systems was confirmed by HMBC correlations (appendix Figure A27, Table I.25b). In summary, ESI-MS and NMR data confirmed the structure of compound 21 as brominated diphenyl ether. Comparison with literature data (Fu and Schmitz 1996) identified compound 21 as 4,5,6-tribromo-2-(2',4'-dibromophenoxy)phenol (Table I.25a).

4,6-dibromo-2-(2',4'-dibromophenoxy)phenol (22) showed UV absorbances at λ_{\max} (MeOH) 236 and 290 nm (Table I.24). ESI-MS featured molecular ion peaks at m/z 497, 499, 501, 503, and 505 $[M-H]^-$ in an isotopic ratio of 1:4:6:4:1 typical for a molecule containing four bromine atoms (Table I.24). $^1\text{H-NMR}$ data (appendix Figure A28) exhibited signals at δ_{H} 7.76 (1H, d, $J = 2.3$ Hz), 7.32 (1H, dd, $J = 2.3, 8.8$ Hz) and 6.41 (1H, d, $J = 8.8$ Hz) corresponding to H-3', H-5' and H-6' of a trisubstituted benzene

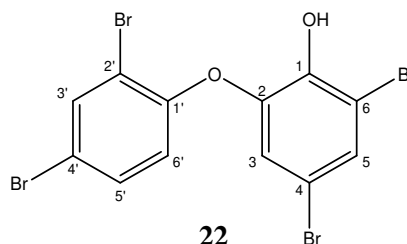
ring identical to compound 21. This observation was confirmed by ^{13}C signals (appendix Figure A29). Signals at δ_{H} 7.30 (1H, d, $J = 2.2$) and δ_{H} 7.11 (1H, d, $J = 2.3$) revealed the presence of a second benzene ring with four substituents (appendix Figure A28) which was corroborated by ^{13}C signals (appendix Figure A29). The structure of both ring systems was confirmed by HMBC correlations (appendix Figure A30, Table I.25b). Taken together, ESI-MS and NMR data confirmed the structure of compound 22 as brominated diphenyl ether identical to compound 21 except for C-5 which carried a bromine atom in compound 21, and was not substituted in compound 22 (Table I.25a). Compound 22 could thus be identified as 4,6-dibromo-2-(2',4'-dibromophenoxy)phenol (Fu and Schmitz 1996).

Table I.24. Analytical data of 4,6-dibromo-2-(2',4'-dibromo-phenoxy)phenol (22).

4,6-dibromo-2-(2',4'-dibromo-phenoxy)phenol (22)	
Synonym(s)	2,4-Dibromo-6-(2,4-dibromo-phenoxy)-phenol
Amount	144.3 mg
Physical description	White powder
Molecular formula	$\text{C}_{12}\text{H}_6\text{Br}_4\text{O}_2$
Molecular weight	501 g/mol
Retention time HPLC	33.8 min (standard gradient)
Structure	UV spectrum
	
ESI-MS+	ESI-MS-
No ionisation	

**21**

4,5,6-tribromo-2-
(2',4'-dibromophenoxy)phenol

**22**

4,6-dibromo-2-
(2',4'-dibromophenoxy)phenol

Table I.25a. ¹H- (500 MHz) and ¹³C-NMR (125 MHz) data of compounds 21 and 22.

No	21		22		21^a	
	δ_{H} (m, <i>J</i> in Hz), (CD ₃ OD)	δ_{C} (CD ₃ OD)	δ_{H} (m, <i>J</i> in Hz), (CD ₃ OD)	δ_{C} (CD ₃ OD)	δ_{H} (m, <i>J</i> in Hz), (DMSO- <i>d</i> ₆)	δ_{C} (DMSO- <i>d</i> ₆)
1		152.3 (s)		153.5 (s)		150.2 (s)
2		141.5 (s)		140.4 (s)		143.8 (s)
3	7.36 (s)	122.9 (d)	7.30 (d, 2.2)	127.1 (d)	7.15 (s)	122.1 (d)
4		122.8 (s)		120.7 (s)		121.8 (s)
5		122.8 (s)	7.11 (d, 2.3)	120.1 (d)		121.8 (s)
6		116.8(s)		116.8 (s)		116.5 (s)
1'		154.2 (s)		154.5 (s)		152.1 (s)
2'		113.4 (s)		113.3 (s)		114.6 (s)
3'	7.77 (d, 2.4)	136.8 (d)	7.76 (d, 2.3)	136.7 (d)	7.91 (d, 2.4)	135.5 (d)
4'		115.6 (s)		115.4 (s)		115.7 (s)
5'	7.32 (dd, 2.3, 8.8)	132.5 (d)	7.32 (dd, 2.3, 8.8)	132.4 (d)	7.50 (dd, 2.4, 8.6)	132.3 (d)
6'	6.41 (d, 8.8)	121.9 (d)	6.41 (d, 8.8)	119.2 (d)	6.87 (d, 8.6)	121.3 (d)

^a (Fu and Schmitz 1996), ¹H NMR (500 MHz), ¹³C-NMR (125 MHz)

Table I.25b. HMBC data of compounds 21 and 22.

No	21	22
	HMBC (CD ₃ OD)	HMBC (CD ₃ OD)
1		
2		
3	1, 2, 4, 5, 6	1, 2, 4, 5, 6
4		
5		1, 2, 3, 4, 6
6		
1'		
2'		
3'	1', 2', 4', 5'	1', 2', 4', 5'
4'		
5'	1', 3', 4', 6'	1', 3', 4', 6'
6'	1', 2', 3', 4', 5'	1', 2', 3', 4', 5'

*Haliclona spec*Structure elucidation of papuamine (23)

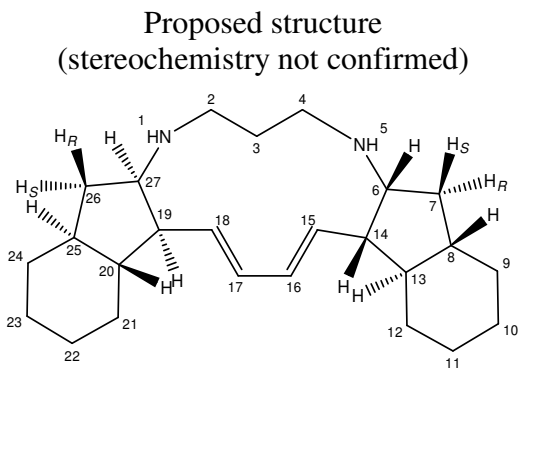
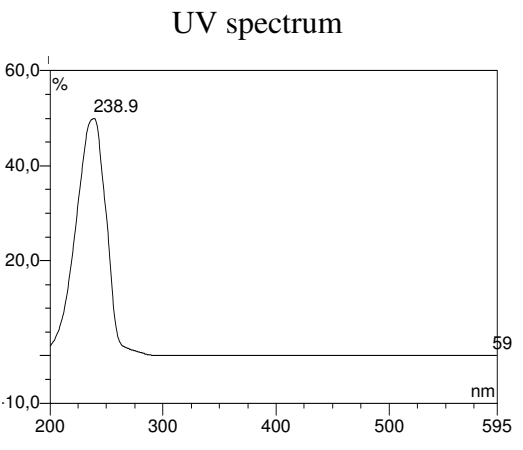
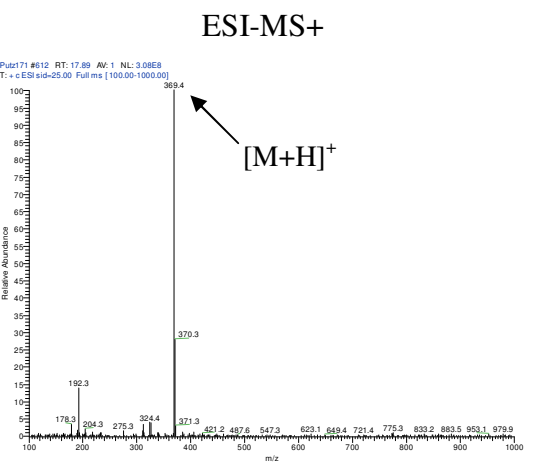
Papuamine (23) was the major metabolite in the *Haliclona* methanol extract and was obtained as yellow oil. It has been described previously from the same genus.

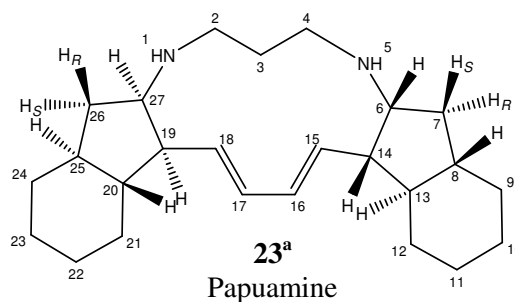
Papuamine (23) showed UV absorbance at λ_{\max} (MeOH) 239 nm (Table I.26). ESI-MS exhibited the molecular ion peak at m/z 369 $[M+H]^+$ (Table I.26). $^1\text{H-NMR}$ data (appendix Figure A31) featured signals at δ_{H} 6.48 (H-16/H-17, dd, $J = 9.4, 19.8$ Hz) and 5.86 (H-15/H-18, br dd, $J = 14.3$ Hz) and corresponding ^{13}C signals at δ_{C} 135.9 and 130.6 (appendix Figure A32), indicating the presence of four olefinic carbons. Coupling constants of H-16/H-17 and H-15/H-18 revealed a *trans*-olefinic function. The existence of the two cyclohexane rings was assigned from the signals at δ_{H} 1.86 (2H, br dd, $J = 9.8$ Hz), 1.05 (4H, m), 1.27 (4H, m) and 1.36 (4H, m, overlapping with signals of H-7_S, H-26_R of the cyclopentane ring) and ^{13}C signals at δ_{C} 44.8, 32.3, 30.9, 47.2 and 25.2. Two cyclopentane rings were derived from δ_{H} signals at 3.51 (2H, dd, $J = 7.7, 16.2$ Hz), 2.59 (2H, dd, $J = 9.2, 20.0$ Hz), 2.39 (2H, m; H-7_R/H-26_S) and 1.36 (4H, m, overlapping with signals of H-11a/H-22a of the cyclopropane rings), and corresponding ^{13}C signals (Table I.27). Proton signals at 3.12 (2H, m), 2.93 (2H, br dd, $J = 13.8$ Hz) and respective ^{13}C signals at δ_{C} 49.7 (partly concealed by the solvent peak) indicated the existence of two nitrogen atoms. Compound 23 proved to be a symmetrical molecule, whose symmetry axis runs directly through C-3 whose signal at δ_{H} 1.90 (2H, m) integrates for just two protons instead of four (which was the case for all other protons except for the olefinic protons in the $^1\text{H-NMR}$ spectrum of compound 23). Comparison with literature data (Baker et al. 1988) revealed minor deviations for $^1\text{H-NMR}$ data (Table I.27), which might be attributed to differences between instruments employed for measurement of spectra (300 vs. 500 MHz). ^{13}C signals likewise showed deviations from the data published for papuamine (Table I.27), which could potentially be due to the different deuterated solvents used in $^{13}\text{C-NMR}$ measurements (CD_3OD vs. CDCl_3 used by Baker et al. 1988). The $[\alpha]_{\text{D}}^{20}$ value of compound 23 (-155.5° , c 0.46, MeOH) was identical to that published for papuamine (Baker et al. 1988), $[\alpha]_{\text{D}} -150^\circ$, c 1.5, MeOH). Shortly after the first description of papuamine (23), haliclonadamine, an unsymmetrical diastereoisomer of papuamine was isolated by Fahy et al. 1988, who determined the structure of this compound by X-ray analysis. The $[\alpha]_{\text{D}}^{20}$ value for

haliclونadamine was published by McDermott et al. 1996 ($[\alpha]_D -5.0^\circ$, c 0.12, CHCl_3), and therefore differed from the $[\alpha]_D^{20}$ value measured for compound 23, which was taken as indication to refer to compound 23 as papuamine.

However, the $[\alpha]_D^{20}$ value of papuamine published by McDermott et al. 1996 ($[\alpha]_D -346^\circ$, c 0.46, MeOH) differed from that described by Baker et al. 1988 ($[\alpha]_D -150^\circ$, c 1.5, MeOH). Since papuamine and haliclونadamine, respectively, contain more than one chiral center, looking at the optical rotation alone will not conclude the stereochemistry. Since the structure of compound 23 was not confirmed by X-ray analysis, INADEQUATE or 2D-NOE experiments as done in the literature (Baker et al. 1988), the stereochemistry of compound 23 was not confirmed.

Table I.26. Analytical data of papuamine (23).

Papuamine (23)	
Synonym(s)	-
Amount	22.7 mg
Physical description	Yellow oil
Molecular formula	$\text{C}_{25}\text{H}_{40}\text{N}_2$
Molecular weight	368 g/mol
$[\alpha]_D^{20}$	- 155.5° (c 0.46, MeOH)
Retention time HPLC	23.0 min (standard gradient)
<p>Proposed structure (stereochemistry not confirmed)</p> 	<p>UV spectrum</p> 
<p>ESI-MS+</p> 	<p>ESI-MS-</p> <p>No ionisation</p>

Table I.27. ¹H- (500 MHz) and ¹³C-NMR (125 MHz) data of compound 23.

No	23		23^a	
	δ_{H} (m, <i>J</i> in Hz), (CD ₃ OD)	δ_{C} (CD ₃ OD)	δ_{H} (m, <i>J</i> in Hz), (CD ₃ OD)	δ_{C} (CDCl ₃)
16, 17	5.48 (dd, 9.4, 19.8)	135.9 (d)	6.22 (dd, 10.5, 15.8)	131.9 (d)
15, 18	5.86 (br dd, 14.3)	130.6 (d)	5.71 (dd, 8.3, 15.8)	129.4 (d)
6, 27	3.51 (dd, 7.7, 16.2)	62.2 (d)	3.05 (br dd, 8.2, 8.2, 8.8)	60.9 (d)
2y, 4y	3.12 (m)	49.7 ^b (t)	2.64 (m)	
2z, 4z	2.93 (br d, 13.8)		2.22 (m)	
14, 19	2.59 (dd, 9.2, 20.0)	50.6 (d)	2.21 (m)	50.0 (d)
7R, 26S	2.39 (m)	39.5 (d)	2.17 (m)	43.6 (d)
9e, 24e	1.94 (m)	32.3 (t)	1.82 (m)	40.4 (t)
12e, 21e	1.94 (m)	30.9 (t)	1.78 (m)	31.3 (t)
10e, 23e	1.93 (m)	25.2 (t)	1.70 (m)	26.1 (t)
11e, 22e	1.93 (m)	25.2 (t)	1.68 (m)	26.0 (t)
3	1.90 (m)	27.2 (t)	1.60 (m)	30.1 (t)
8, 25	1.86 (br d, 9.8)	44.8 (t)	1.23 (m)	46.0 (t)
7S, 26R	1.36 (m)	39.5 (d)	1.20 (m)	43.6 (d)
11a, 22a	1.36 (m)		1.20 (m)	
13, 20	1.27 (m)	47.2 (d)	1.19 (m)	48.9 (d)
10a, 23a	1.27 (m)		1.19 (m)	
9a, 24a,	1.05 (m)		0.9 (m)	
12a, 21a				

^a (Baker et al. 1988) ¹H NMR 300 MHz, ¹³C-NMR 100 MHz^b concealed by solvent signal

Biological activity

All compounds of which isolated amounts were ample were subjected to bioassays in order to determine cytotoxicity. While in the MTT assay, general cytotoxicity is assessed towards the L5178Y mouse lymphoma cell line, protein kinase inhibitory profiles give a more specific result about the cytotoxic properties of a compound.

Cytotoxicity assay

The two compounds isolated from *Dysidea avara*, avarol (9) and avarone (10), showed strong growth inhibition towards L5178Y mouse lymphoma cells (Table I.24). The same applies to the prenylated hydroquinones obtained from *Sarcotragus muscarum* and *Ircinia fasciculata* (15-17). Fasciculatin (20), isolated from *Ircinia variabilis*) and compounds derived from *Agelas oroides* (11-14) showed little or no inhibitory effects, thus EC₅₀ values were not determined. Of the two brominated diphenyl ethers (*Dysidea granulosa*), the one with five bromines (21) showed strong, the other one with four bromines (22) moderate inhibitory effects. Papuamine (23) isolated from *Haliclona spec* was strongly active in the MTT assay.

Table I.24. Cytotoxicity test results for compounds isolated from various marine sponges.

Compound	L5178Y growth [%] (Conc 10 µg/ml)*	EC ₅₀ (µg/ml)*	EC ₅₀ (µmol/l)
Avarol (9)	- 2.1	0.3	1.0
Avarone (10)	- 1.2	1.8	5.8
Hexaprenylhydroquinone (15)	0.8	1.5	2.9
Heptaprenylhydroquinone (16)	- 0.2	2.1	3.6
Nonaprenylhydroquinone (17)	1.3	1.7	2.4
Fasciculatin (20)	119.9	-	-
Oroidin (11)	71.9	-	-
4,5-dibromo-1 <i>H</i> -pyrrol -2-carboxylic acid (12)	104.0	-	-
4,5-dibromo-1 <i>H</i> -pyrrol-2-carboxylic acid ethyl ester (13)	38.1	-	-
4,5-dibromo-1 <i>H</i> -pyrrol-2-carbonitrile (14)	37.5	-	-
4,5,6-tribromo-2- (2',4'-dibromophenoxy)phenol (21)	0.1	0.2	0.3
4,6-dibromo-2- (2',4'-dibromophenoxy)phenol (22)	12.6	2.0	5.9
Papuamine (23)	- 0.5	0.2	0.5

*Data provided by Prof. Müller, University of Mainz.

Protein kinase assay

The protein kinase assay aims at detecting inhibitory effects of the compounds tested on selected kinases and thus gives an estimate of the specificity of cytotoxicity. IC₅₀ values were only determined for those compounds that exhibited strong inhibitory effects on a comparably small number of kinases. Two of the compounds isolated from *Agelas oroides*, 4,5-dibromo-1*H*-pyrrol-2-carboxylic acid ethyl ester (13) and 4,5-dibromo-1*H*-pyrrol-2-carbonitrile (14), displayed no or only weak inhibitory effects, thus IC₅₀ was not determined. Oroidin (11) and 4,5-dibromo-1*H*-pyrrol-2-carboxylic acid (12) showed moderate activities. The same applies for fasciculatin (20), which is in line with the results of the MTT assay. For papuamine (23) derived from *Haliclona* IC₅₀ was not determined although this compound was strongly active. However, since inhibitory effects were unspecific involving a wide range of kinases, it did not meet the criteria of finding compounds with strong as well as specific activity. In contrast to its oxidated form avarone (10), avarol (9) showed good activity in the kinase assay. The prenylated hydroquinones (15-17) likewise displayed specific activity, where nonaprenylhydroquinone (17) was slightly more active than hexa- and heptaprenylhydroquinone (15, 16).

Table I.25. Protein kinase assay results for isolated compounds*.

Compound tested	EGF-R	EPHB4	ERBB2	FAK	IGF1-R	SRC	VEGF-R2	VEGF-R3	AKT1	ARK5	Aurora-A	Aurora-B	PAK4	PRK1	CDK2/CvcA	CDK4/CvcD1	CK2-alpha1	FLT3	INS-R	MET	PDGFR-beta	PLK1	SAK	TIE2	COT	B-RAF-VE	
Avarol (9)	M	0	0	0	0	0	0	0	0	0	A	A	0	0	0	0	0	0	0	A	M	0	0	0	0	0	0
Avarone (10)	0	0	0	0	0	0	0	0	0	0	0	0	0	0	0	0	0	0	0	0	0	0	0	0	0	0	0
Hexaprenylhydr. (15)	A	0	M	0	0	0	0	0	0	0	M	M	0	0	0	0	0	M	0	0	0	0	M	0	0	0	0
Heptaprenylhydr. (16)	A	M	M	0	0	M	0	0	0	0	0	0	0	0	0	0	0	M	0	0	0	0	M	M	A	0	
Nonaprenylhydr. (17)	S	M	A	0	0	M	0	M	0	0	M	M	0	0	0	0	0	M	0	0	0	0	M	M	A	A	
Fasciculatin (20)	M	0	M	M	M	M	M	M	0	0	M	M	0	0	0	M	0	M	0	0	0	0	M	M	M	M	
Oroidin (11)	M	0	0	0	0	M	0	0	0	0	M	M	0	0	0	0	0	0	0	0	0	0	A	0	0	0	
x-carboxylic acid (12)	M	M	M	0	M	0	M	0	0	0	M	M	0	M	0	0	0	0	0	0	0	0	M	0	M	M	
x-carb.ac.ethyl ester (13)											Not selected for IC ₅₀																
x-carbonitrile (14)											Not selected for IC ₅₀																
3,4,6-y (21)	M	M	M	0	M	0	M	0	0	0	M	M	0	M	0	M	0	0	M	M	M	0	S	0	M	M	
4,6-z (22)	M	M	M	M	M	M	M	0	M	M	M	M	0	M	M	M	0	0	M	M	M	0	M	0	M	0	
Papuamine (23)											Not selected for IC ₅₀																

x = 4,5-dibromo-1*H*-pyrrol-2-, y = tribromo-2-(2',4'-dibromophenoxy)phenol, z = dibromo-2-(2',4'-dibromophenoxy)phenol 1.

S: strongly active (IC₅₀ (M) < 1⁻⁰⁷), **A**: active (IC₅₀ (M) 1⁻⁰⁶ – 1⁻⁰⁷), **M**: moderately active (IC₅₀ (M) 1⁻⁰⁵ – 1⁻⁰⁶), **0**: not active (IC₅₀ (M) > 1⁻⁰⁵).

*Data provided by ProQinase, Freiburg.

The inhibitory effects of the two brominated diphenyl ethers isolated from *Dysidea granulosa* (21, 22) revealed in the kinase assay were in congruence with activities found in the MTT assay: 4,5,6-tribromo-2-(2',4'-dibromophenoxy)phenol (21) with five bromine atoms showed stronger inhibitory effects than 4,6-dibromo-2-(2',4'-dibromophenoxy)phenol (22) with four bromines, and inhibited a smaller range of kinases, thus indicating a slightly higher specificity.

Prenylated hydroquinones

Further experiments were conducted at the Institute of Toxicology, HHU Düsseldorf for the three hydroquinones differing in the number of isoprenic units in order to determine whether the length of the chain has an impact on biological activity. All data given below were provided by Dr. W. Wätjen.

Antioxidative activity

The antioxidative potential of the prenylated hydroquinones was analysed in the TEAC assay showing a strong antioxidative potential similar to the synthetic vitamin E derivative Trolox. However, the radical-scavenging effects of quercetin, a main flavonoid which is widely used due to its antioxidative properties, were even more prominent (10 μ M quercetin caused a reduction of absorption to 0.102 ± 0.018 , not shown in Figure I.11).

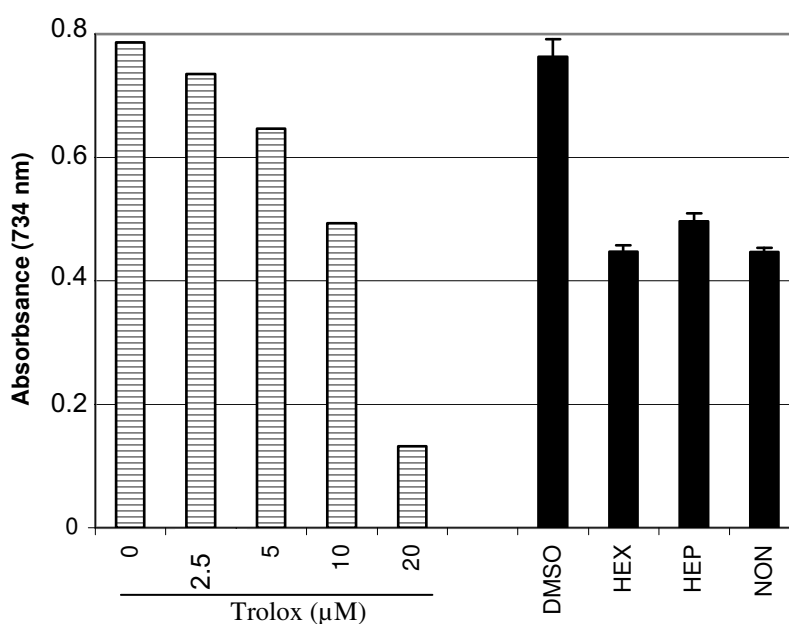


Figure I.11. Antioxidative capacity of the isolated compounds hexa- (15, HEX), hepta- (16, HEP) and nonaprenylhydroquinone (17, NON) was measured spectrophotometrically at 734 nm in comparison to the synthetic antioxidant Trolox. Data are means \pm SD ($n > 3$); * $p < 0.05$ vs. control (DMSO).

Cytotoxic activity

The toxic potential of the isolated prenylhydroquinones was analysed in H4IIE hepatoma cells using the MTT reduction assay (Figure I.12). The EC₅₀-value for hexaprenylhydroquinone (15) was found to be in the low micromolar range (2.5 μ M). The EC₅₀-values for hepta- (16) and nonaprenylhydroquinone (17) were found to be about tenfold higher (EC₅₀-values: approx. 25 μ M).

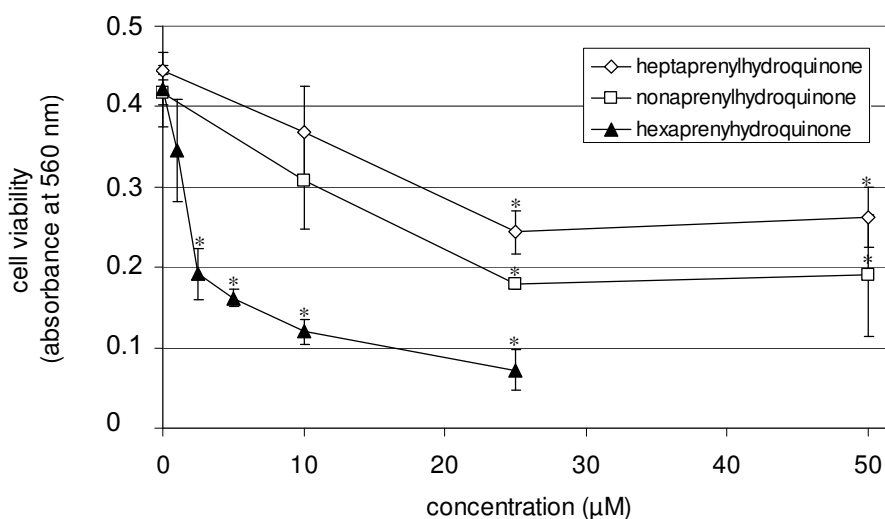


Figure I.12. H4IIE cells were incubated with the prenylated hydroquinones for 24 h, then MTT reduction was measured as a marker of cell viability (absorbance at 560 nm). Data are means \pm SD (n = 2-5), * p < 0.05 vs. corresponding control (DMSO).

NF- κ B inhibiting activity

The transcription factor NF- κ B regulates a variety of physiological processes including cell growth and oxidative stress response, but also apoptosis. For these reasons, it was analysed whether the prenylated hydroquinones interfere with the activation of NF- κ B caused by the cytokine TNF- α (H4IIE cells stably transfected with pNF- κ B-SEAP reporter plasmid). Incubation with TNF- α (5 ng/ml, 24 h) increased SEAP activity about 3.3-fold. 1 h preincubation with 1 μ M of hexaprenylhydroquinone (15) or 10 μ M of heptaprenylhydroquinone (16) and nonaprenylhydroquinone (17) significantly lowered NF- κ B-activity after stimulation by TNF- α to $73 \pm 7.7\%$ and $72 \pm 5.3\%$ of TNF- α stimulated value, respectively. On the other hand, basal NF- κ B activity was not modulated by these substances (Figure I.13). As positive control the known NF- κ B inhibitor CAPE (caffeic acid ethylphenylester) was used. Incubation of H4IIE cells with 40 μ M CAPE for 1 h inhibited basal NF- κ B dependent transcriptional

activity and, furthermore, it completely blocked TNF- α induced SEAP activity to control levels.

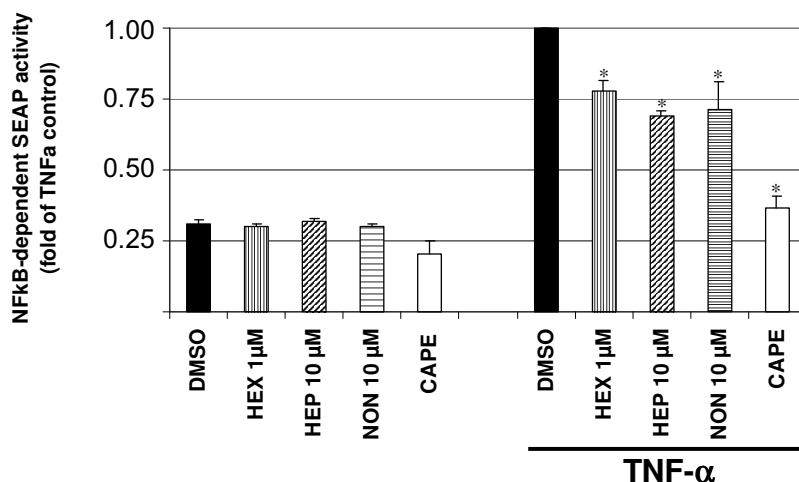


Figure I.13. H4IIE cells stably transfected with pNF- κ B-SEAP reporter plasmid were preincubated for 1 h with isolated compounds (hexaprenylhydroquinone (15, HEX): 1 μ M, heptaprenylhydroquinone (16, HEP) and nonaprenylhydroquinone (17, NON): 10 μ M) or 40 μ M of the NF- κ B inhibitor CAPE and then stimulated with 5 ng/ml TNF- α for 24 h. Cell culture supernatants were assayed for SEAP activity, results are expressed as fold activity of the TNF- α stimulated cells (means \pm SD, n = 3).

Antimicrobial activity

Data on the antimicrobial activity of pure compounds against *Escherichia coli*, *Enterococcus faecalis*, *Staphylococcus aureus*, *Streptococcus pyrogenes*, *Pseudomonas aeruginosa* and *Klebsiella pneumoniae* were kindly provided by SeaLife Pharma, Tulln, Austria.

Primary screening

In a primary screening, antimicrobially active substances were identified for further investigation of toxicity and the MIC (minimum inhibitory concentration)-tests. Table I.26 shows the antimicrobial activity of substances ($\geq 80\%$ growth inhibition). Both avarol (9) and avarone (10) were active against *Enterococcus faecalis*. Avarol (9) further inhibited growth of *Streptococcus pyrogenes*, and avarone (10) of *Staphylococcus aureus*. The prenylated hydroquinones (15-17) did not show antimicrobial properties, except for nonaprenylhydroquinone (17) which was active against *S. aureus*. Likewise, the two brominated diphenyl ethers (21 and 22) obtained from *Dysidea granulosa* were inactive. Fasciculatin (20) inhibited growth of *S. aureus* and *S. pyrogenes*. Two of the compounds isolated from *Agelas oroides*, oroidin (11) and

4,5-dibromo-1*H*-pyrrol-2-carboxylic acid (12) showed pronounced activity against *Escherichia coli*, *E. faecalis*, *S. aureus*, and *S. pyrogenes*, and oroidin (11) also against *Pseudomonas aeruginosa*. Papuamine (23) was active against all microbial strains tested.

Table I.26. Antimicrobial properties of pure compounds*. "x": significant antimicrobial activity ($\geq 80\%$ growth inhibition). Final substance concentrations in the assay were 250, 125, and 62.5 $\mu\text{g/ml}$.

Compound	<i>E. coli</i>	<i>K. pneumoniae</i>	<i>E. faecalis</i>	<i>S. aureus</i>	<i>S. pyrogenes</i>	<i>P. aeruginosa</i>
Avarol (9)			x		x	
Avarone (10)			x	x		
Hexaprenylhydroquinone (15)						
Heptaprenylhydroquinone (16)						
Nonaprenylhydroquinone (17)				x		
Fasciculatin (20)				x	x	
Oroidin (11)	x		x	x	x	x
4,5-dibromo-1 <i>H</i> -pyrrol-2-carboxylic acid (12)	x		x	x	x	
4,5-dibromo-1 <i>H</i> -pyrrol-2-carboxylic acid ethyl ester (13)						
4,5,6-tribromo-2-(2',4'-dibromophenoxy)phenol (21)						
4,6-dibromo-2-(2',4'-dibromophenoxy)phenol (22)						
Papuamine (23)	x	x	x	x	x	x

*Data provided by SeaLife Pharma, Tulln, Austria.

Toxicity against HeLa cells

Based on the results of the primary screening, active substances were chosen to test the toxicity of these compounds towards HeLa cells. Avarol (9), avarone (10), nonaprenylhydroquinone (17), fasciculatin (20), and papuamine (23) were toxic at concentrations of $> 62\ \mu\text{g/ml}$, oroidin (11) and 4,5-dibromo-1*H*-pyrrol-2-carboxylic acid (12) at concentrations of $> 125\ \mu\text{g/ml}$. Good toxicity profiles were thus found for oroidin (11) and 4,5-dibromo-1*H*-pyrrol-2-carboxylic acid (12).

MIC-test of positive substances

Substances that were active in the primary screening were also employed in the MIC (minimum inhibitory concentration)-test. Table I.27 summarizes the outcome of the MIC-tests. Based on these results, avarol (9), avarone (10), fasciculatin (20), oroidin (11), 4,5-dibromo-1*H*-pyrrol-2-carboxylic acid (12), and papuamine (23) were identified as substances with significant antimicrobial activity against the strains tested.

Table I.27. Results of the MIC-tests*. Numbers are concentrations in µg/ml where an activity could be seen (> 70 % inhibition). n: no effect seen upon repetition.

Compound	<i>E. coli</i>	<i>K. pneumoniae</i>	<i>E. faecalis</i>	<i>S. aureus</i>	<i>S. pyrogenes</i>	<i>P. aeruginosa</i>
Avarol (9)			> 62.5		> 7.8	
Avarone (10)			> 7.8	> 62.5	> 7.8	
Nonaprenylhydroquinone (17)				n		
Fasciculatin (20)				> 3.9	> 3.9	
Oroidin (11)	> 125		> 31.2	> 31.2	> 31.2	> 125
4,5-dibromo-1 <i>H</i> -pyrrol-2-carboxylic acid (12)	> 125		> 62.5	> 31.2	> 31.2	> 125
Papuamine (23)	> 7.8	> 3.9	> 7.8	> 7.8	> 3.9	> 31.2

*Data provided by SeaLife Pharma, Tulln, Austria.

Part II:

Chemical ecology of Mediterranean sponges

Methods

Chemicals, equipment and standard procedures generally employed are summarised in the Methods chapter of Part I of this thesis. Methods specific for the respective experiments dealing with the chemical ecology of Mediterranean sponges are outlined in the following.

Quantification of sponge metabolites

For the quantification of secondary metabolites via HPLC, it was necessary to establish calibration curves for the respective pure compounds. The isolation procedure for each sponge species employed (*Aplysina aerophoba* / *Aplysina cavernicola*, *Dysidea avara* and *Agelas oroides*) is given in Part I Methods. Calibration curves were generated by triple measurement: three aliquots of 2 mg each were solved in 800 μ l HPLC methanol yielding a concentration of 2.5 mg/ml. Of this solution, 400 μ l were taken for HPLC. The remaining 400 μ l were diluted to a concentration of 1.25 mg/ml, of which 400 μ l were taken for HPLC. For further samples, 200 μ l, 80 μ l and 40 μ l of the latter dilution were replenished to a total volume of 400 μ l. Calibration curves, retention times under standard HPLC conditions, UV spectra, and molecular weight of these compounds are summarised in the appendix.

***Aplysina* depth profile**

Aplysina sponges were sampled in April 2006 (22 individuals in total) and in August 2006 (13 individuals in total) along an underwater slope at Sveta Marina (East coast of the Istrian Peninsula, Croatia) ranging from a depth of 1.8 to 38.5 m. Specimens of approx. the same size were collected in special Kautex sampling vials by self-contained underwater breathing apparatus (SCUBA) diving. In order to avoid damage of the sponge tissue, the substrate to which sponges were attached was removed together with the sponges.

During transport in ambient seawater in cooling boxes, contact of samples with air was avoided. Approximately 5 cm³ sponge tissue was cut off from each individual and

frozen (-20 °C) immediately after transfer. Cutting of sponge tissue with a scalpel and immediate freezing do not affect isoxazoline alkaloid content (Thoms et al. 2006). The frozen sponge tissue was then lyophilised, ground with a mortar and extracted exhaustively over night with methanol (50 ml per 100 mg sponge tissue). After centrifugation 1.5 ml of the extract were transferred into 2 ml reaction tubes. Methanol was evaporated via vacuum centrifugation. The dried samples were redissolved in 450 µl HPLC methanol and directly submitted to HPLC analysis.

HPLC analysis of sponge alkaloids

Extracts were analysed using HPLC, routine detection was at 254 and 280 nm. The standard solvent system as described in Table I.3 was used for compound separation. Identification of substances was based on their online-UV spectra and on direct comparison with the previously isolated standards. All compounds were quantified by HPLC using calibration curves obtained for the respective isolated substances (calibration curves can be found in the appendix).

Quantification of alkaloids

Since alkaloid concentrations were calculated on a weight (in µmol per g dry weight) and not on a volume basis, data do not directly take into account any skeletal density changes. However, measurement of the volume (recorded as replacement of water in ml) and dry weight (in g) of ten pieces of varying size cut from different *Aplysina* individuals revealed a linear correlation between volume and dry weight (Figure II.1, $R^2 = 0.981$). These data show that differences in skeletal density, if present, have a negligible impact on the dry weight of samples. Dry weight thus appears to be a suitable reference value to present alkaloid contents in *Aplysina*.

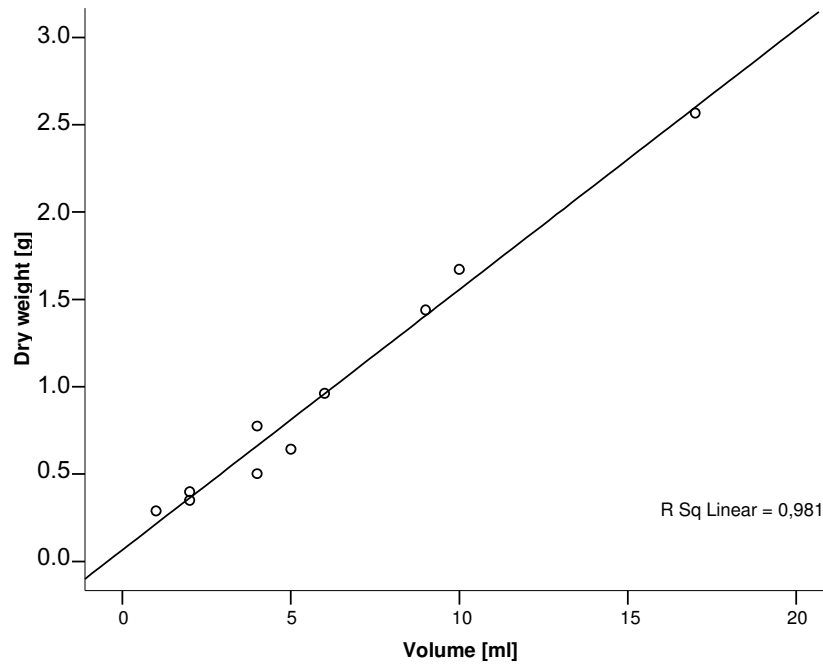


Figure II.1. Correlation of the volume (recorded as replacement of water in ml) and dry weight (in g) of ten *Aplysina* pieces of varying size.

Assessment of environmental parameters

All parameters were measured in the Adriatic Sea close to Sveta marina in the vicinity of Rovinj (Croatia) in July 2006 by the working group of Prof. Brümmer, University of Stuttgart. Temperature, conductivity, pH and oxygen were gauged by a multi-parameter probe (MPP 350, WTW GmbH, Weilheim, Germany) provided with a 25 m cable from the surface down to 25 m depth in 1 m steps. Light (photosynthetically active radiation, PAR) was quantified from the surface down to a depth of 15 m in steps of 5 m with a quantum sensor connected to a microvolt integrator (Delta-T Devices Ltd, Cambridge, England). For water tightness the testing probe was deposited in a waterproof box (Lexan Utility Box, GSI, USA). Measuring fault caused by the Plexiglas plate was eliminated by raising a factor ($f = 1.3636$) under a defined light source. Current velocities were gathered at depths of 5 and 15 m using tracer droplets, which were injected with a syringe in front of a black benchmark. Time was taken with a waterproof microchronometer.

Transplantation of *Aplysina* sponges to different depths

Aplysina sponges involved in the transplantation experiment consisted of 20 individuals of similar size originating from two depth regimes: “Shallow” samples were collected in a depth range of 1-4 m, and “deep” samples originated depths from 14-39 m. All sponges were either sampled in the vicinity of Rovinj, Croatia, in the Limski Kanal or from the underwater slope in Sveta Marina. Whole specimens were attached to a grid by using cable ties and transplanted to a depth of 10 m in the Limski Kanal in April 2006. Different cable tie colour codes allowed recognition of individual samples. Approx. 5 cm³ sponge tissue was cut off from each individual and directly frozen (to prevent the bioconversion of isoxazoline alkaloids) for HPLC analysis at the beginning of the experiment in April (t_0), after four months in August 2006 (t_1) and after twelve months in April 2007 (t_2). Crude extracts were prepared by lyophilising sponge tissue and extraction with methanol as described above. Analysis of alkaloid patterns was achieved by HPLC.

Transplantation of three Mediterranean sponges to different light conditions

In order to test for the influence of light on alkaloid contents and patterns, individuals of three different Mediterranean sponge species were investigated: *Aplysina aerophoba*, *Dysidea avara*, and *Agelas oroides*. All sponges involved in this experiment originated from different locations close to Rovinj, Croatia and were sampled in April 2006. *A. aerophoba* was sampled from depths of 5 to 6 m close to an island called “The two sisters”. Since the two other species commonly dwell in deeper habitats, *D. avara* originated depths of 13-17 m in the Limski Kanal, and *A. oroides* was collected along an underwater slope close to Sveta marina in depths of 13-27 m. All sponge individuals were cut into two pieces. One fragment was allowed to grow in situ under natural illumination, the other one was artificially shaded by a basket covered with black plastic foil, thereby causing a complete erasement of photosynthetically active radiance (PAR). Sponges were attached to a grid by using cable ties and maintained at a depth of 6 m in the Limski Kanal starting in April 2006. Different cable tie colour codes allowed recognition of individual samples. Approx. 5 cm³ sponge tissue was cut off from each individual and directly frozen for HPLC analysis at the beginning of the experiment in April 2006 (t_0), after four months in August 2006 (t_1) and, in case of *A. aerophoba*, after twelve months in April 2007 (t_2). For *D. avara* and *A. oroides*, material was not

sufficient for a second sampling in April 2007 (t_2). Crude extracts of all ten *A. aerophoba* sponges (= 20 clones) and seven *A. oroides* individuals (= 14 clones) were prepared as described before for the *Aplysina* depth profile and transplantation experiment. Extracts of the ten *D. avara* individuals (= 20 clones) were prepared in a similar way, except for one difference: instead of 1.5 ml of the extract 6 ml were dried and redissolved in 410 μ l instead of 450 μ l HPLC methanol prior to HPLC analysis since otherwise metabolite concentration was too low for reliable detection.

Data analysis

For all data analyses, SPSS v. 13.0 for Windows was used. The Spearman rank correlation was employed in order to test for a correlation between secondary metabolite content and depth. Secondary metabolite contents of *A. aerophoba* samples involved in the transplantation experiments were analysed using a 2-way repeated measures analysis of variance (ANOVAR). If normal distribution and homogeneity of variances of the data analysed could not be assumed, the Friedman test (for repeated measures) was employed. As sample size was too low for *D. avara* and *A. oroides*, no statistics were computed. Means are shown \pm standard deviation (SD). In bar graphs error bars depict standard deviations.

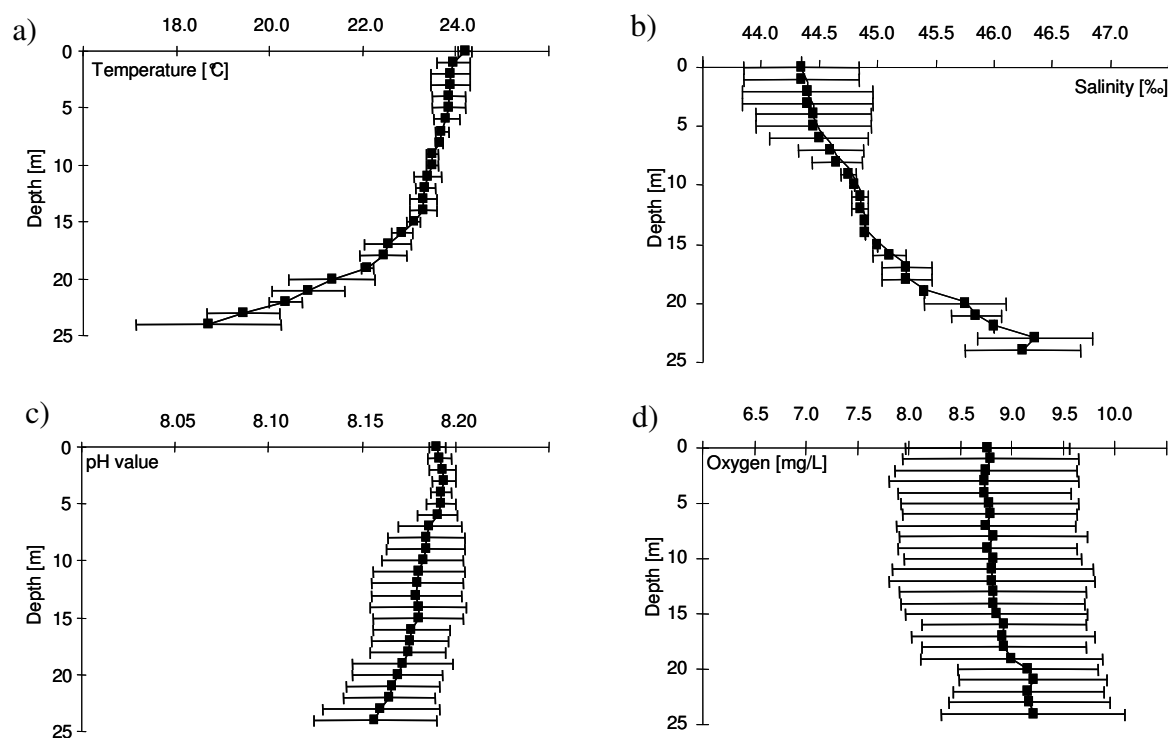
Results

Aplysina depth profile

The following paragraphs summarise the results obtained on the alkaloid profile of *Aplysina* sponges sampled along an underwater slope from 1 to almost 40 m.

Investigated environmental parameters

In order to assess differing physical and chemical factors along the investigated depth gradient, several environmental parameters were measured in the Adriatic Sea close to Sveta marina in the vicinity of Rovinj (Croatia) in July 2006 at depths ranging from 0 to 25 m. Data were kindly provided by the working group of Prof. Brümmer, University of Stuttgart. Figure II.2 a shows a temperature decrease from 24 °C at the surface to 18 °C at a depth of 25 m, and a concomitant increase of salinity (Figure II.2 b) from 44.4 to 46.3 ‰. In contrast, pH and amount of oxygen remained stable over the measured depth gradient (Figure II.2 c and d). On the other hand, light (photosynthetically active radiation, PAR) decreased dramatically from 100 % at the surface to less than 20 % at a depth of 15 m (Figure II.2 e). Water current velocity was reduced from a speed of 1.6 cm/sec at a depth of 5 m to 0.8 cm/sec at 15 m depth (Figure II.2 f).



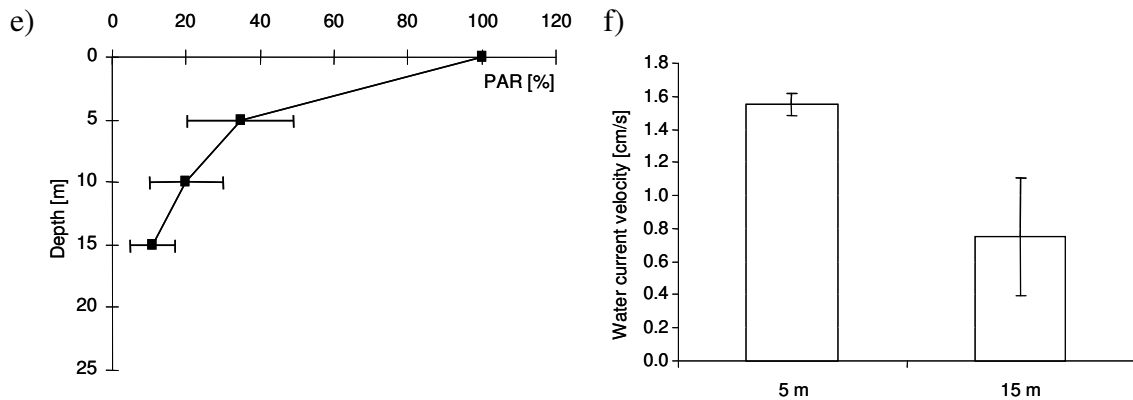


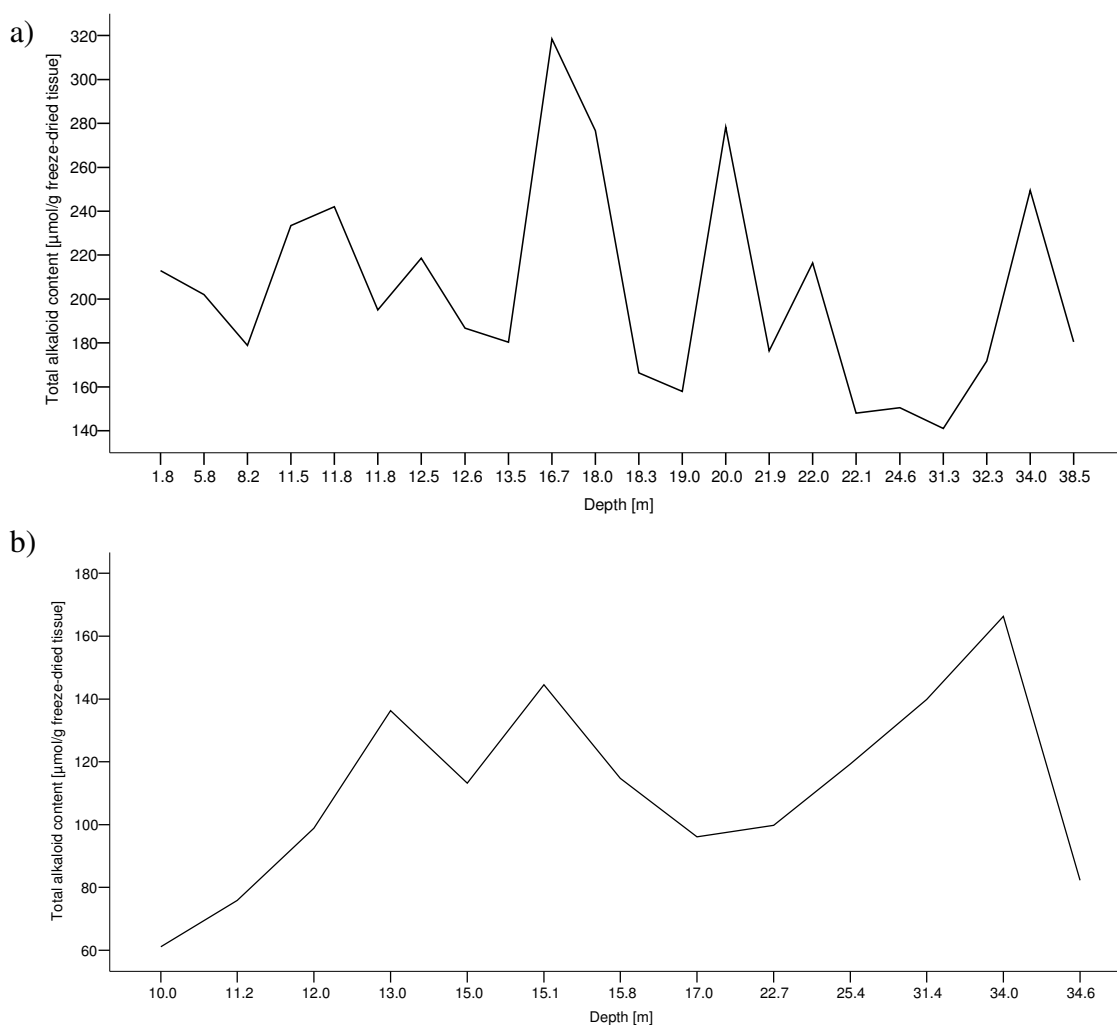
Figure II.2. Environmental parameters measured in the Adriatic Sea in depths of 0 to 25 m close to Rovinj, Croatia in July 2006: a) temperature, b) salinity, c) pH value, d) oxygen content, e) light (photosynthetically active radiation, PAR) down to 15 m, f) current velocity in 5 and 15 m depth. Error bars depict standard deviation (SD).

Alkaloid variation along depth profile

Total amounts of bromoisoxazoline alkaloids (in μmol per g lyophilised tissue) and alkaloid patterns (sum of bromoisoxazoline alkaloids set at 100 %) were determined for *Aplysina* sponges sampled along an underwater slope (1.8–38.5 m) in Sveta Marina, Croatia in April and August 2006. Changing depth regimes had no apparent influence on total alkaloid amounts (Figure II.3, Spearman correlation, II.3 a April 2006: $N = 22$, $r_s = -0.333$, $P = 0.230$; II.3 b August 2006: $N = 13$, $r_s = 0.429$, $P = 0.144$). Instead, large variations in alkaloid contents were observed for individual sponges irrespective of changing depth. Alkaloid patterns that are depicted in Figure II.3 proved to be far more homogenous for sponges originating from either of the two different depth regimes (from 1.8 to 11.8 m vs. a depth of 11.8 to 38.5 m).

Thus, in both series of samples taken along the depth gradient, two distinctly different types of alkaloid patterns were detected: samples originating from less than 11.8 m ($N = 5$) feature the *A. aerophoba* chemotype and are characterised by aerophobin-2 (2) and isofistularin-3 (3) as major constituents (Figure II.3 c, d). In contrast, sponges collected at 11.8 m or below ($N = 17$) contain aplysinamisin-1 (1) and aerothionin (4) as dominant bromoisoxazoline alkaloids and thus resemble the *A. cavernicola* chemotype (Figure II.3 c, d). For sponges collected in April 2006, alkaloid patterns were significantly correlated with depth (Figure II.3 c, Spearman correlation, $N = 22$, aplysinamisin-1 (1): $r_s = 0.525$, $P = 0.012$; aerophobin-2 (2): $r_s = -0.620$, $P = 0.002$; isofistularin-3 (3): $r_s = -0.566$, $P = 0.006$; aerothionin (4): $r_s = 0.669$,

$P = 0.001$). Sponges collected in August showed likewise a homogenous alkaloid pattern that resembled alkaloid patterns detected in the first series of experiments (April 2006) even though for this series of samples no significant correlation of alkaloid patterns with depth existed (Figure II.3 d, Spearman correlation, $N = 13$, aplysinamisin-1 (1): $r_s = 0.286$, $P = 0.344$; aerophobin-2 (2): $r_s = -0.390$, $P = 0.188$; isofistularin-3 (3): $r_s = -0.126$, $P = 0.681$; arothionin (4): $r_s = 0.335$, $P = 0.144$). The single specimen collected at a depth of 10 m exhibited the typical *A. aerophoba* alkaloid pattern, whereas all samples taken from a depth below 10 m featured the *A. cavernicola* chemotype instead. The fact that only one *A. aerophoba* like individual had been included in the second set of experiments (August 2006) explains the lack of a significant correlation between alkaloid pattern and depth in this data set when compared to the collections from April 2006.



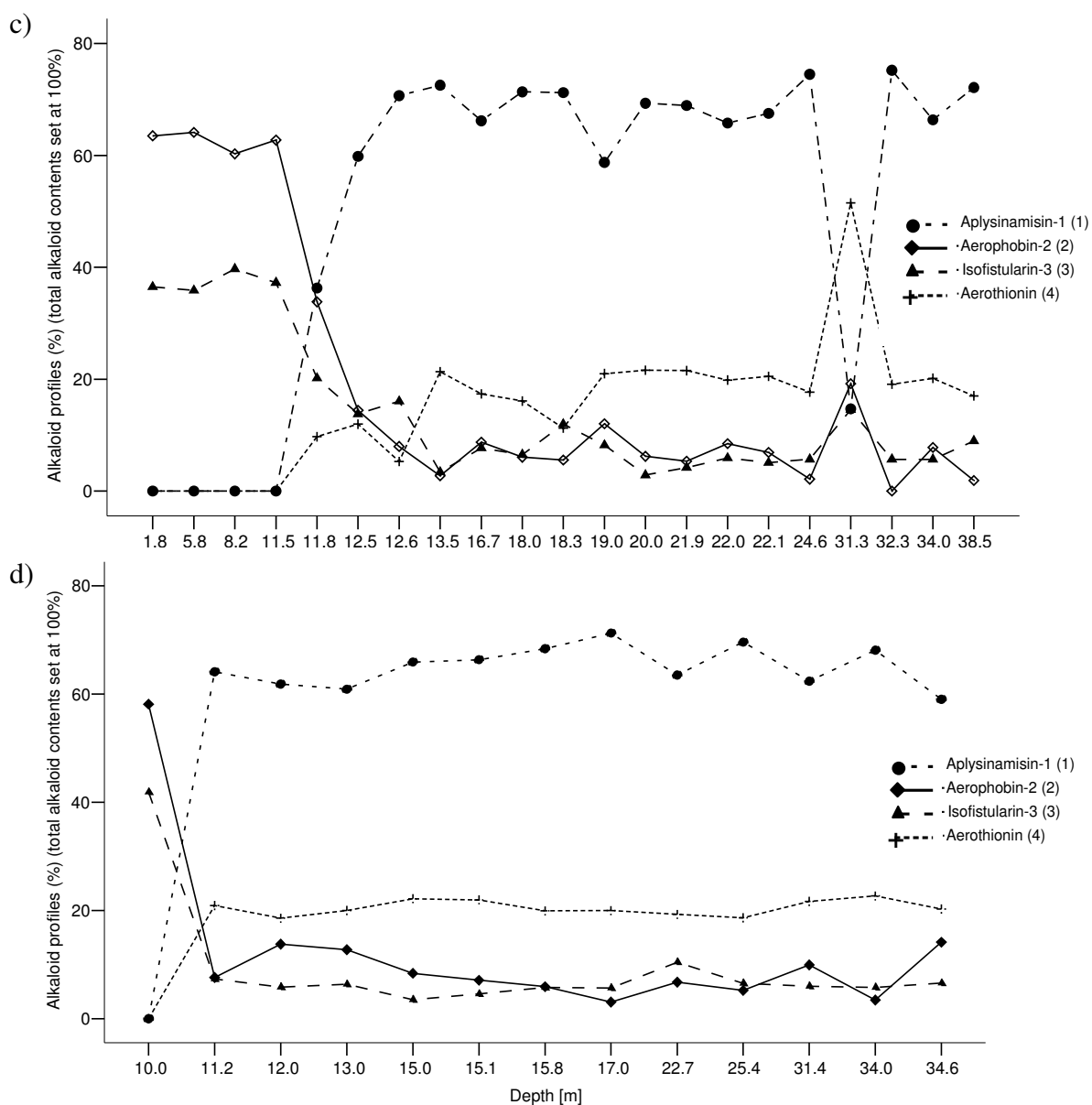


Figure II.3. a), b) Total alkaloid amounts (in $\mu\text{mol/g}$ freeze-dried sponge tissue) in *Aplysina* individuals sampled along an underwater slope ranging from 1.8 to 38.5 m of sponges collected a) in April 2006 (N = 22) or b) in August 2006 (N = 13). c), d) Relative amounts (in %) of aplysinamisin-1 (1), aerophobin-2 (2), isofistularin-3 (3) and aerothionin (4) in sponges collected c) in April 2006 (N = 22) or d) in August 2006 (N = 13). Neither the *A. aerophoba* pigment uranidine (7) nor the *A. cavernicola* pigment 3,4-dihydroxyquinoline-2-carboxylic acid (8) were detectable.

Uranidine (7) which is characteristic for *A. aerophoba* could not be detected in any of the sponges analysed due to its known chemical lability (Cimino et al. 1984). The pigment 3,4-hydroxyquinoline-2-carboxylic acid (8) that is typical for *A. cavernicola* (Thoms et al. 2003a, 2004) was likewise not observed although it is chemically far more stable than uranidine (7). Instead, all sponge samples collected in this study irrespective of the depth they originated developed a black or blue colouration when exposed to air which is typical for polymerisation products of uranidine (7) (Cimino et al. 1984).

Transplantation of *Aplysina* sponges to different depths

Amongst both the shallow as well as the deep samples there was one single individual which displayed an alkaloid pattern just in between the *A. aerophoba* and *A. cavernicola* chemotype, with aplysinamisin-1 (1) as major compound, but no traces of aerothionin (4). Since this alkaloid pattern appeared to occur in a very minor number of *Aplysina* sponges (two out of 20) and was thus not comparable to either the *A. aerophoba* or *A. cavernicola* chemotype, these two individuals have been excluded from figures and statistical analyses, yielding a sampling size of nine individuals in both the shallow and the deep sample set.

Shallow samples

Aplysina samples that originated from shallow depths (1-4 m) showed an alkaloid pattern characteristic for *A. aerophoba*, with aerophobin-2 (2) and isofistularin-3 (3) as major compounds, except for one individual which displayed an alkaloid pattern just in between the *A. aerophoba* and *A. cavernicola* chemotype.

Since all nine individuals were lost after one year (t_2), only the data of the samples taken at the beginning (t_0) and four months after the start of the experiment (t_1) could be compared. Absolute alkaloid amounts did not change significantly during the course of the experiment (Figure II.4 a, paired t-test, d.f. = 8, $t = -1.855$, $P = 0.101$). Although alkaloid patterns changed significantly during the course of the experiment on a quantitative scale (Figure II.4 b, paired t-test, d.f. = 8, aerophobin-2 (2): $t = 2.931$, $P = 0.019$; isofistularin-3 (3): $t = -2.931$, $P = 0.019$), it becomes apparent that these were only minor changes. Aerophobin-2 (2) remained as the major compound, and the only other alkaloid detectable via HPLC was isofistularin-3 (3). Neither was one of these compounds lost or reduced in a significant manner, nor did new compounds (such as aplysinamisin-1 (1) or aerothionin (4)) arise in detectable amounts.

Deep samples

Deep samples (originating 14-39 m) were divided with respect to their alkaloid pattern. Again, the alkaloid pattern of one single individual could not be assigned to either of the two chemotypes *A. aerophoba* or *A. cavernicola* and was thus excluded from analyses.

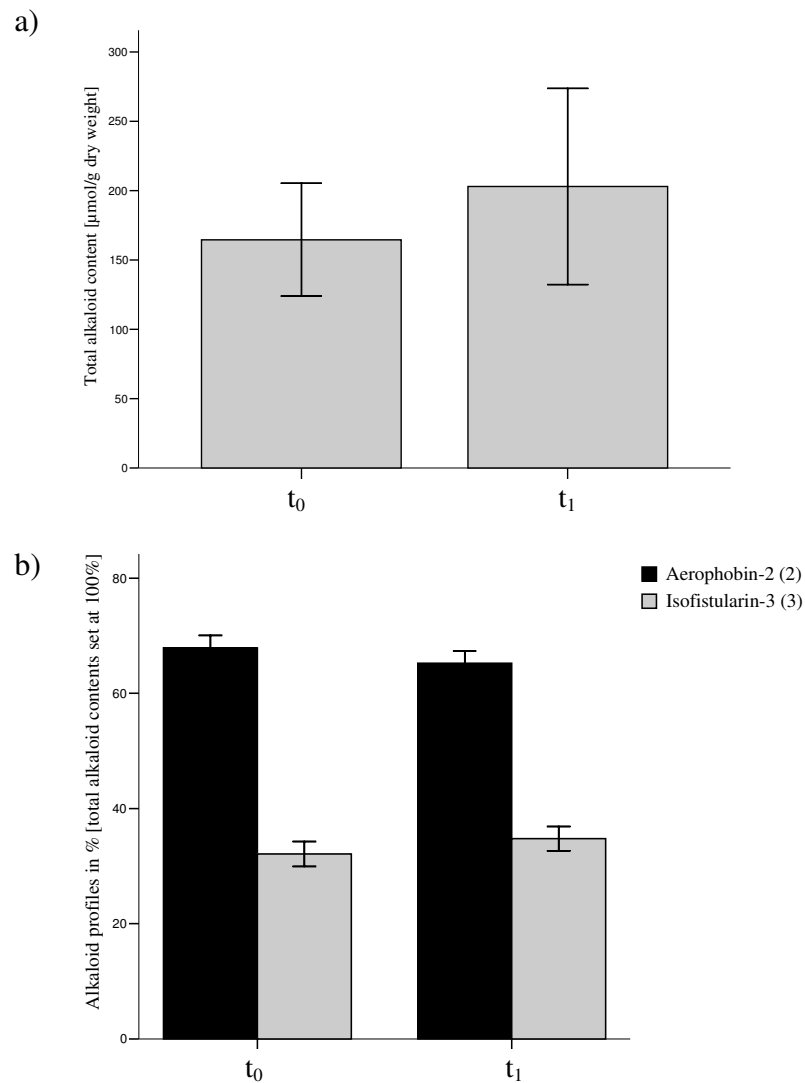


Figure II.4. a) Total alkaloid amounts (in $\mu\text{mol/g}$ freeze-dried sponge tissue) of sponges originating from sites from 1-4 m in the Limski Kanal before transplantation to 10 m depth (t_0) and after four months (t_1) following transplantation. b) Alkaloid patterns (relative amounts in %) of aerophobin-2 (2) and isofistularin-3 (3). Bars are shown \pm SD.

Five individuals exhibited the same pattern as the shallow samples, i.e. the *A. aerophoba* chemotype. Of these, one individual was lost four months after transplantation. For the remaining four individuals, absolute alkaloid amounts did not change significantly during the course of the experiment (paired t-test, d.f. = 3, $t = 2.083$, $P = 0.129$, Figure II.5 a). The same applies to alkaloid patterns, which remained unchanged during the course of the experiment (paired t-test, d.f. = 3, Aerophobin-2 (2): $t = 2.861$, $P = 0.065$; Isofistularin-3 (3): $t = -2.861$, $P = 0.065$, Figure II.5 b).

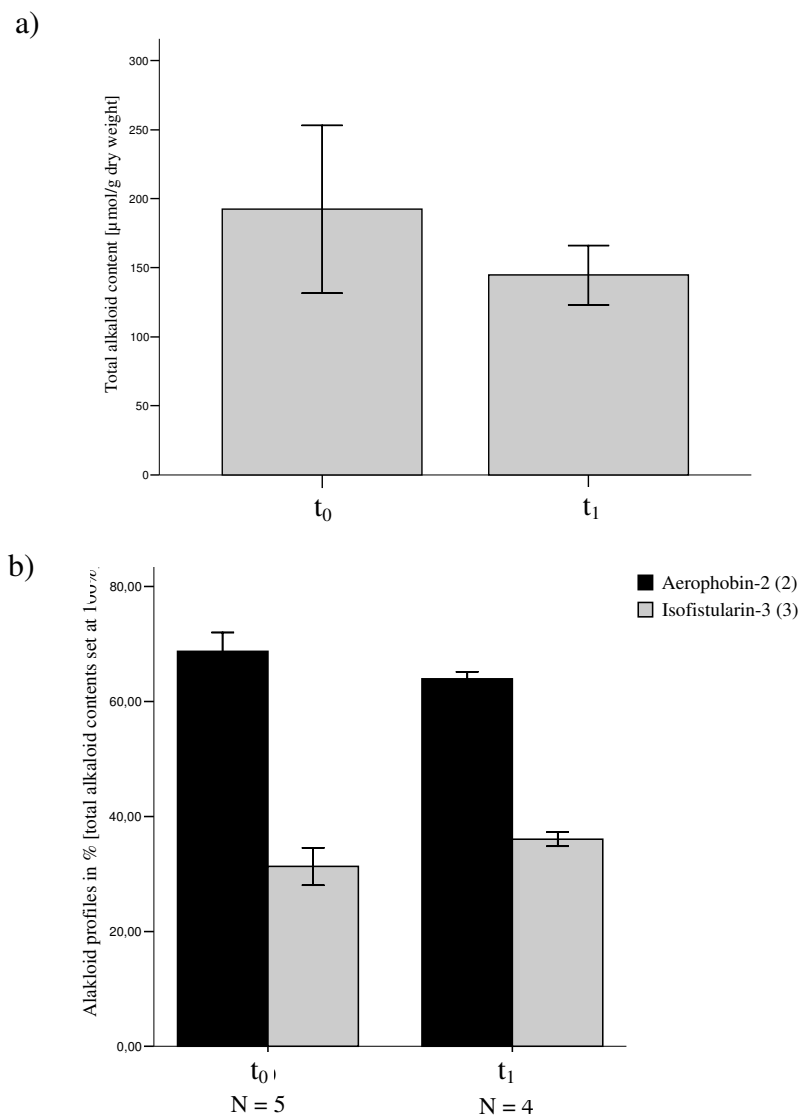


Figure II.5. a) Total alkaloid amounts (in $\mu\text{mol/g}$ freeze-dried sponge tissue) of sponges exhibiting the *A. aerophoba* chemotype originating from sites below 14 m in the Limski Kanal before transplantation to 10 m depth (t_0) and after four months (t_1) following transplantation. b) Alkaloid patterns (relative amounts in %) of aerophobin-2 (2) and isofistularin-3 (3). Bars are shown \pm SD.

Four individuals collected in depths from 31.3 to 38.5 m featured *A. cavernicola* like alkaloid patterns with aerothionin (4) and aplysinamisin-1 (1) as major bromoisoxazoline alkaloids. Total alkaloid amounts in $\mu\text{mol/g}$ freeze dried sponge tissue at the beginning of the experiment (t_0), after four months (t_1) and after twelve months (t_2) following transplantation to a depth of 10 m did not differ significantly (Figure II.6 a, Friedman test, d.f. = 2, $\chi^2 = 4.667$, $P = 0.097$) even though compared to the t_0 samples, t_1 and t_2 samples showed an increase of total alkaloids from 120.2 ± 42.8 $\mu\text{mol/g}$ dry weight to 175.6 ± 81.5 $\mu\text{mol/g}$ (t_1) and 405.5 ± 333.4 $\mu\text{mol/g}$ (t_2) dry

weight, respectively. Alkaloid patterns (total alkaloid contents set at 100 %) remained stable and unaffected by transplantation during the whole length of the experiment (Figure II.6 b, ANOVA with time as the within-subject factor and compound (aerophobin-2 (2), aplysinamisin-1 (1), isofistularin-3 (3) and arothionin (4)) as the between-subject factor: d.f. = 3, $F = 0.316$, $P = 0.813$). Of four individuals transplanted in April 2006, three individuals still remained alive in April 2007 (Figure II.6 b).

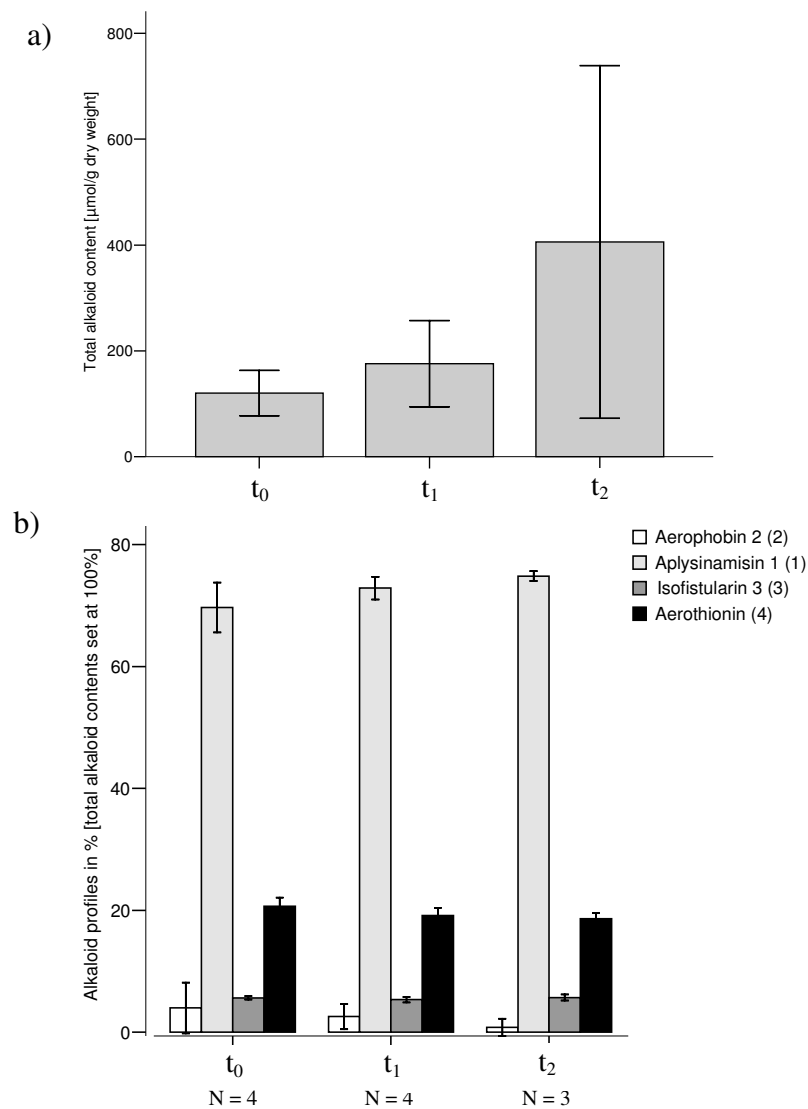


Figure II.6. a) Total alkaloid amounts (in $\mu\text{mol/g}$ freeze-dried sponge tissue) of sponges originating from sites below 30 m at the Sveta Marina underwater slope before transplantation to 10 m depth (t_0), after four months (t_1) or after 12 months following transplantation (t_2). b) Alkaloid patterns (relative amounts in %) of aplysinamisin-1 (1), aerophobin-2 (2), isofistularin-3 (3) and arothionin (4). Bars are shown \pm SD.

Transplantation of three Mediterranean sponges to different light conditions

Aplysina aerophoba

Sponges from a depth of 5-6 m were chosen to investigate the influence of light on alkaloid amounts and patterns. Clones resulting from sponges that were cut into half were subjected to different light conditions: natural illumination and artificial shading. All sponges involved in this experiment except for one individual showed an alkaloid profile characteristic for *A. aerophoba* with aerophobin-2 (2) and isofistularin-3 (3) as major constituents. In contrast to the other sponges, one individual exhibited aplysinamisin-1 (1) as major compound, but did not contain any aerothionin (4), thus representing a chemotype which could not unambiguously be assigned to either *A. aerophoba* or *A. cavernicola*. Since it is thus not comparable to the majority of sponges involved in this experiment, it was not included in figures and statistical analyses.

During the course of the experiment, total alkaloid amounts in $\mu\text{mol/g}$ lyophilised sponge tissue of clonal transplants maintained under natural illumination decreased by more than half from $208.7 \pm 33.6 \mu\text{mol/g}$ (t_0 , onset of experiment) to $178.4 \pm 21.2 \mu\text{mol/g}$ after four months (t_1) and to $77.0 \pm 35.7 \mu\text{mol/g}$ after twelve months (t_2) (Figure II.7 a). The same was true for clones maintained under artificial shading, where alkaloid amounts were reduced to $185.2 \pm 38.9 \mu\text{mol/g}$ after four months (t_1) and to $61.4 \pm 31.5 \mu\text{mol/g}$ after twelve months (t_2) II.7 a). Clones maintained under natural light conditions (“light” t_1 and t_2) had significantly lower absolute alkaloid contents than t_0 samples (Friedman test, d.f. = 2, $\chi^2 = 8.000$, $P = 0.018$), and artificially shaded (“dark” t_1 and t_2) clones tended likewise to have lower absolute alkaloid levels (Friedman test, d.f. = 2, $\chi^2 = 9.000$, $P = 0.050$; significance level Bonferroni corrected to $P = 0.025$).

All clonal explants showed an alkaloid pattern characteristic for *A. aerophoba* at the onset of the experiment. Neither aerothionin (4) nor aplysinamisin-1 (1) were detected in any of these sponges. During the course of the experiment alkaloid patterns did not change significantly (Figure II.7 b, ANOVAR with time as the within-subject factor and treatment (“light” for natural illumination or “dark” for artificial shading) as the between-subject factor: d.f. = 1, aerophobin-1 (2): $F = 0.578$, $P = 0.476$; aerophobin-2 (2): $F = 0.025$, $P = 0.875$; isofistularin-3 (3): $F = 0.376$, $P = 0.562$). From the 18 clones that were recruited for the experiment in April 2006 (t_0), seven survived in the artificially shaded and six in the naturally illuminated treatment until August 2006 (t_1). This sample size further decreased until April 2007 (t_2) to four clones in each of the two

treatments (Figure II.7 b). In t_0 and t_1 samples isofistularin-3 (3) represented the major alkaloid and dominated over aerophobin-2 (2) in both treatments. t_2 samples showed a reversed ratio with aerophobin-2 (2) as major alkaloid in specimens maintained under natural light conditions as well as in those kept under artificial shading. The single individual that could not be assigned to either the *A. aerophoba* or the *A. cavernicola* chemotype was affected by transplantation in a way similar to that of the *A. aerophoba* chemotypes: Total alkaloid amount was similar for t_0 and t_1 samples, but decreased to approx. one half after one year (t_0 : 203.2 $\mu\text{mol/g}$, t_1 : 185.6 $\mu\text{mol/g}$, t_2 : 96.78 $\mu\text{mol/g}$). Alkaloid pattern did not change in a major way.

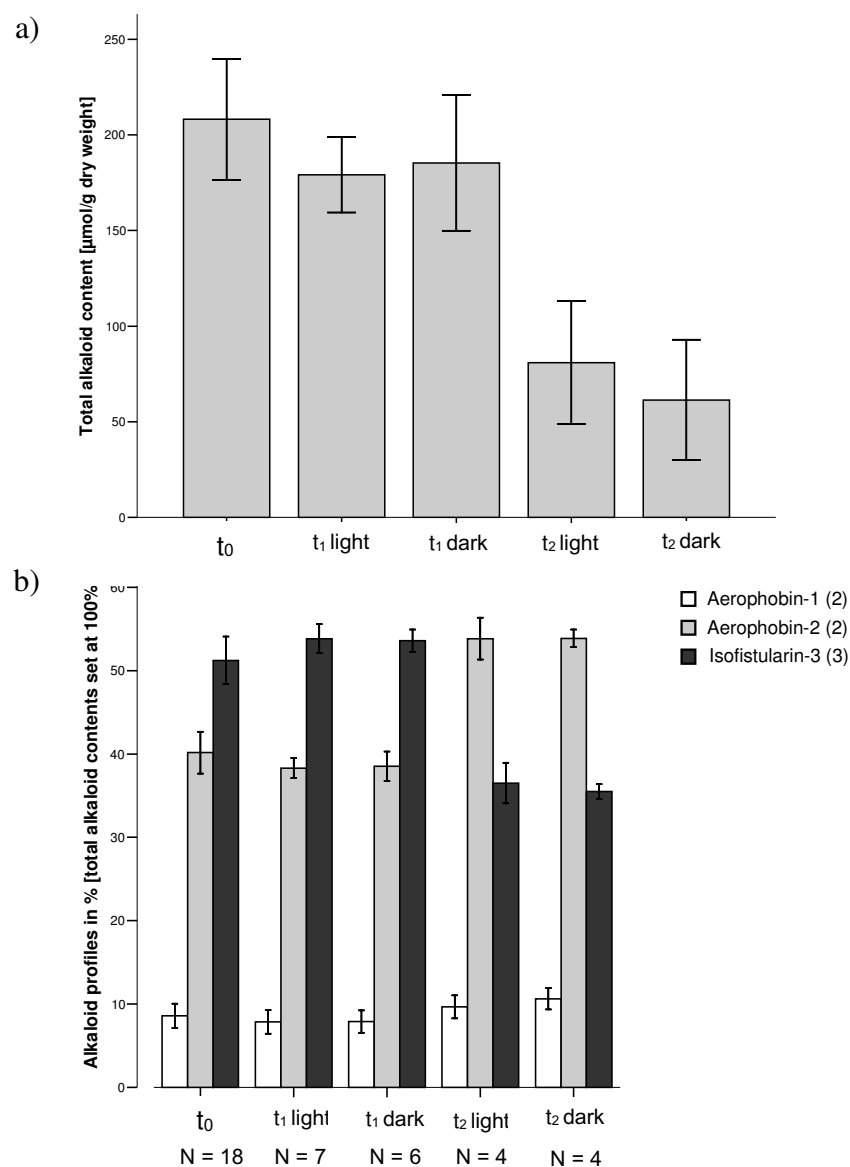


Figure II.7. a) Total alkaloid amounts (in $\mu\text{mol/g}$ freeze-dried sponge tissue) of clonal transplants maintained under natural light conditions or subjected to artificial shading before transplantation (t_0), after four months (t_1) and after 12 months following transplantation (t_2). b) Alkaloid patterns (relative amounts in %) of aerophobin-1 (2), aerophobin-2 (2) and isofistularin-3 (3). Bars are shown \pm standard deviation.

Dysidea avara

From the 20 clonal explants, eight survived under artificially shaded conditions after four months. In contrast, only one clone was left in the control treatment under natural illumination. All surviving explants showed a slightly decreased total content of avarol (9) and avarone (10) after four months (t_1) when compared to t_0 samples, although this was not significant (Figure II.8, paired t-test, d.f. = 7, $t = 1.710$, $P = 0.131$). Relative amounts of these two compounds remained stable as well (Figure II.8; paired t-test, d.f. = 7, avarol (9): $t = 1.922$, $P = 0.096$; avarone (10): $t = -1.922$, $P = 0.096$).

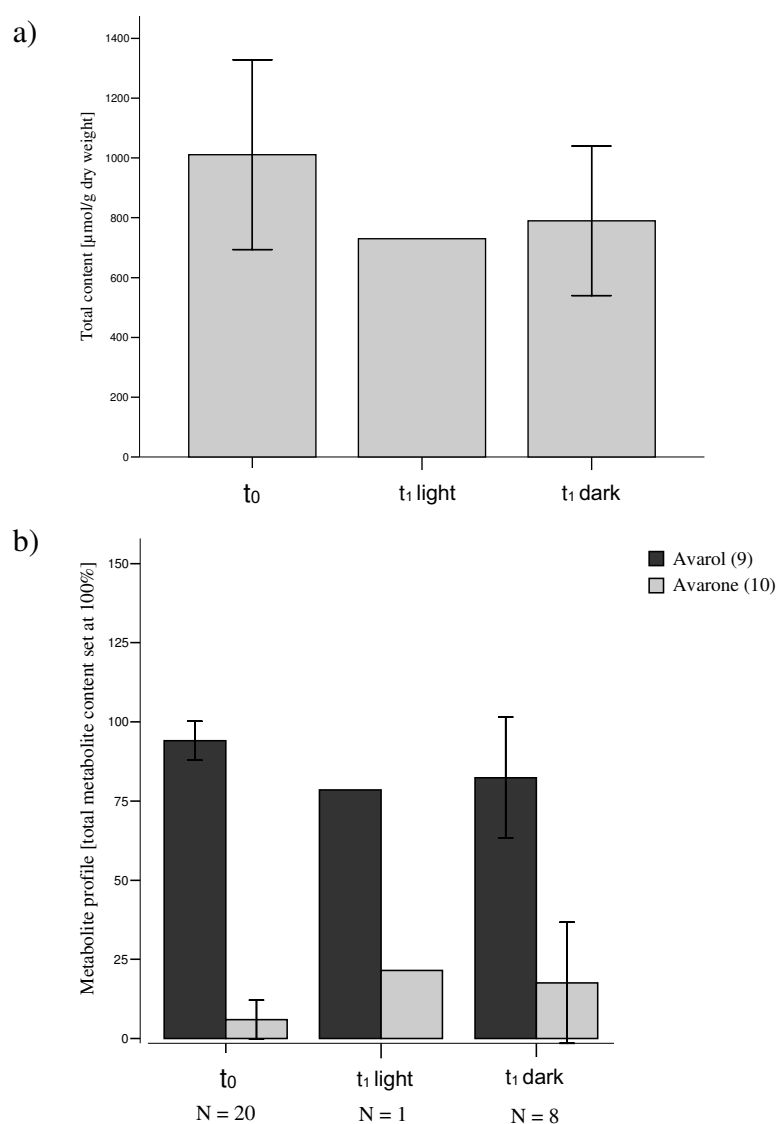


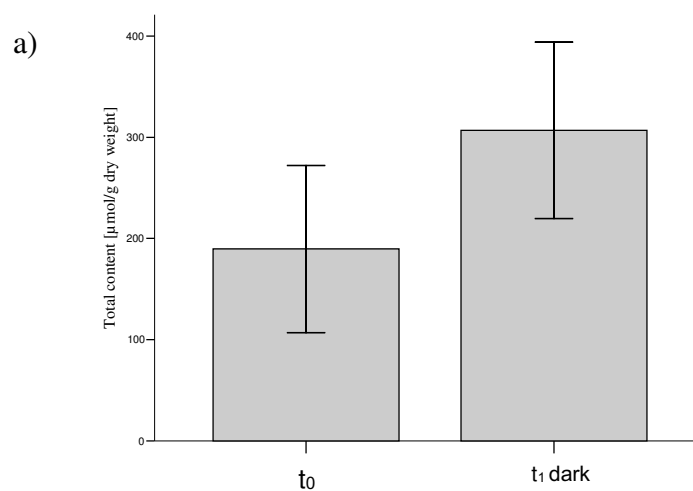
Figure II.8. a) Total metabolite amounts (in $\mu\text{mol/g}$ freeze-dried sponge tissue) of clonal transplants maintained under natural light conditions or subjected to artificial shading before transplantation (t_0) and after four months (t_1) following transplantation. b) Metabolite patterns (relative amounts in %) of avarol (9) and avarone (10). Bars are shown \pm standard deviation.

The finding that except for one individual all *Dysidea* sponges died under natural illumination conditions in 6 m depths can be explained by the fact that *D. avara* is commonly found in deeper habitats (> 15 m), and is obviously unable to cope with increased levels of sunlight as present in shallow depths such as 5-6 m.

Agelas oroides

Of the 14 *A. oroides* clones transplanted in April 2006, four were still found alive after four months under artificially shaded conditions, but not a single one survived under natural illumination. Like *D. avara*, *A. oroides* prefers deeper habitats and thus appears unable to adapt to light conditions prevailing in shallow depths of 5-6 m.

For two of the surviving individuals, no secondary metabolites were detectable, further limiting sample size of viable explants to two clones. These showed a slightly increased total content of the major metabolites oroidin (11) and 4,5-dibromo-1*H*-pyrrol-2-carboxylic acid (12) after four months (t_1) when compared to t_0 samples (Figure II.9). Relative amounts of these two compounds appeared to remain stable (Figure II.9). However, no statistics could be computed due to the small sample size in this experiment.



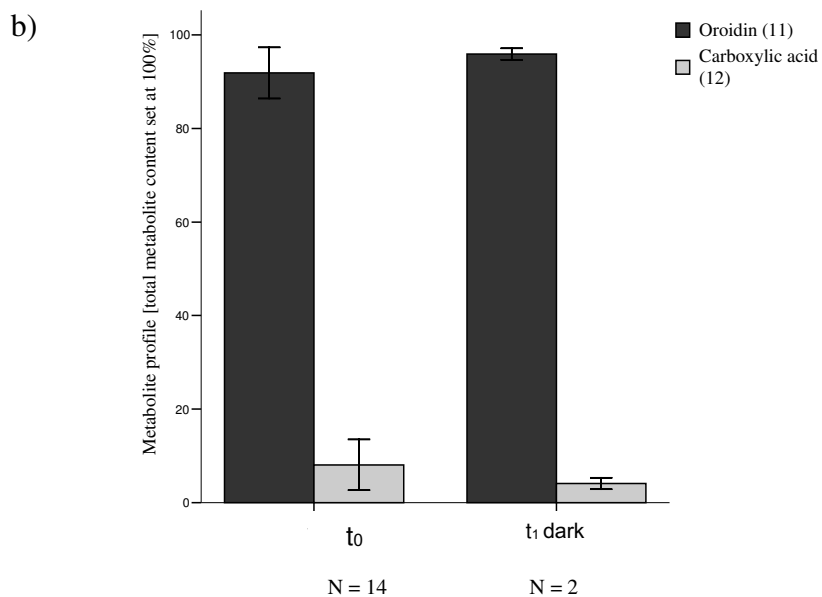


Figure II.9. a) Total metabolite amounts (in $\mu\text{mol/g}$ freeze-dried sponge tissue) of clonal transplants maintained under natural light conditions or subjected to artificial shading before transplantation (t_0) and after four months (t_1) following transplantation. b) Metabolite patterns (relative amounts in %) of oroidin (11) and 4,5-dibromo-1*H*-pyrrol-2-carboxylic acid (12, carboxylic acid). Bars are shown \pm standard deviation.

Part III:

Stress-induced biotransformation in *Aplysina* sponges

Methods

In the following chapter, all materials and methods employed in experiments aimed at characterising and purifying the isoxazoline cleaving enzyme in *Aplysina* sponges are assembled.

General materials and methods

This chapter summarises chemicals, materials and standard techniques which cannot be assigned to a particular experiment, but were commonly involved in most approaches.

Chemicals and materials

Eppendorf pipettes 2/20/100/200/1000	Eppendorf
Eppendorf tubes (0.5, 1.5, 2.0 ml)	Eppendorf
Falcon tubes (15 and 50 ml)	Sarstedt
Multiwell plates	Greiner
Round filters 595 Ø 90 mm/200 mm	Schleicher & Schuell
HPLC methanol	VWR
HPLC acetonitrile	VWR

Water employed for biochemical experiments was cleaned via ion exchange prior to usage (NANOpure, Barnstead or Milli-Q reagent water system, Millipore) and will be referred to as ultrapure water in the following.

Chemicals and materials used for the preparation of buffers and solutions, protein purification, quantification and SDS gel electrophoresis are summarised in Table III.1 and Table III.2.

Table III.1. Chemicals used as ingredients of buffers and solutions, for SDS PAGE and Western blots.

Company	Description
Merck	Ethylendiamintetraacetate (EDTA)
Roth	Trichloroacetic acid
	Rotiphorese [®] Gel 30 (30 % acrylamide, 0.8 % bisacrylamide)
	N, N, N', N'-Tetramethylethyldiamin (TEMED)
	Coomassie Brilliant Blue R-250
	Bovine serum albumin (BSA)
	Ammonium sulfate hydrate
	Glycine p.a.
	SDS ultra pure
Sigma Aldrich	Ammonium peroxide sulfate (APS)
	Bromophenol blue
	Dimethylsulfoxid (DMSO)
	β-mercaptoethanol
	Tris(hydroxymethyl)-aminoethan (TRIS)
	Gel filtration molecular weight marker (MW-GF1000 kit)
Anatrace	FOS-Choline [®] -12 Anagrade
	Sodium cholate
Glycon Bioch. GmbH	n-dodecyl-β-D-maltopyranoside (DDM)
GE Healthcare	ECL Advance [™] Western Blotting Detection Kit
	Low molecular weight calibration kit for SDS electrophoresis (30 to 97 kDa)
Fermentas	PageRuler [™] prestained protein ladder (10 to 170 kDa)
Dianova	Peroxidase-conjugated Streptavidin
	Biotin-SP-conjugated AffiniPure goat Anti-mouse IgG (H+L)
Pierce	ProFound [™] Label Transfer Sulfo-SBED protein:protein interaction reagent
	Coomassie Plus – The Better Bradford [™] Assay Kit
Acros Organics	2-Aminoimidazole hemisulfate, 98+%
VWR	Tri-sodium citrate
	Sodium hydrogen carbonate
	Ethanol abs.
	Sodium carbonate anhydrous, p.a.
Riedel-deHaen	Citric acid monohydrate, p.a.
	Hydrochloric acid (37 %)
	Bromophenol blue
J.T. Baker	Sodium chloride
	Sodium hydroxide (1 mol/l)
AppliChem	Phosphoric acid (85 %)
Serva Electrophoresis GmbH	Polyoxyethylensorbitanmonolaurat (Tween 20)

Table III.2. Materials used for protein purification, SDS-PAGE and Western blot.

Company	Description
BioRad	Mini Protean 3 electrophoresis kit PolyPrep column 10 ml (porous 30 μ M polyethylene bed support) Blot Absorbent Filter Paper (extra thick)
Roth	Roti [®] -PVDF (Membrane for Western Blots)
Millipore	Amicon Ultra-15 centrifugal devices, PLGC Ultracel-PL Membrane, 10 kDa
GE Healthcare	NHS activated sepharose 4 fast flow HiTrap [™] Q FF (ion exchange column) HiTrap [™] SP FF (ion exchange column) Superdex 200 10/300 GL (gel filtration column)

Equipment

Ultrasonic bath Sonorex RK 510H	Bandelin
Heating bath B-490	Büchi
Heating block UBD	Grant
UV lamp and TLC detection table	Camag
Digital scales 2354/TE1502S/ Analytical scale MC1	Sartorius
-86 °C freezer	Forma Scientific
Digital pH-meter 420 Aplus	Orion
Heating-plate/magnetic stirrer Combi Mag	IKA
Vibrax VXR Basic (shaker)	IKA
Roll incubator RM5	CAT
Vortex VF2	IKA
Centrifuge Biofuge pico	Heraeus
Centrifuge Megafuge 1.0 R	Heraeus
Centrifuge 5417R	Eppendorf
Ultracentrifuge Sorvall Discovery, rotor Ti60	Beckmann
Ultracentrifuge Airfuge	Beckmann
Cooling cabinet UniChromat 1500-Duo	UniEquip GmbH
Cooling cabinet Minicoldlab 2023	Pharmacia Biosystems
Plate reader FLUOstar OPTIMA	BMG Labtech
Trans-Blot [®] SD semi-dry electrophoresis transfer cell	BioRad
PowerPac HC [™]	BioRad
ChemiGenius ² BioImaging System	Syngene
Äkta [™] FPLC [™] -system	Amersham Biosciences

Buffers and solutions

Table III.3 summarises buffers and solutions commonly employed in several approaches as described below.

Table III.3. Description of buffers and solutions.

Purpose	Buffer	Ingredients	Final conc.	pH / remarks
Activity assay	Citrate	0.5 M Na citrate; diluted 1:10 (water)	0.5 M	pH 5.8 (set with 0.5 M citric acid); stored at 4 °C
Cell disruption	Citrate	0.5 M Na citrate; diluted 1:10 (water)	0.5 M	pH 5.8 (set with 0.5 M citric acid); stored at 4 °C
Washing of membranes	Sodium carbonate	EDTA 0.1 M Na ₂ CO ₃	5 mM 0.1 M	pH 11.5 prepared fresh
Coupling of NHS activated materials to aerophobin-2 (2)	Sodium hydrogen carbonate	NaHCO ₃ NaCl	0.2 M 0.5 M	Ph 8.3 (set with NaOH 1 mol/l); prepared fresh
	Citrate	0.5 M Na citrate; diluted 1:10 (water)	0.5 M	pH 4.5 (set with 0.5 M citric acid); stored at 4 °C
	Tris-HCl	Tris	0.1 M	pH 8.5 (set with HCl 37 %)
Affinity chromatography	Tris-HCl	Tris NaCl	0.1 M 0.1 M	pH 8.3 (set with HCl 37 %)

Standard proceduresActivity assay

In order to detect and quantify activity of the isoxazoline cleaving enzyme in samples, a standardised activity assay was employed. Aerophobin-2 (2) served as enzyme substrate. The respective protein sample was added to an Eppendorf tube, and filled with 50 mM citrate buffer, pH 5.8 to reach a final volume of 45 µl. pH of all protein samples was adjusted to pH 5-6 prior to the activity assay. Volumes of protein solutions added to the assay varied depending on the protein concentration of the respective sample as measured in the Bradford assay (see below). 5 µl of a substrate solution of aerophobin-2 (2) in a mixture of ultrapure water/MeOH (7/3, 10 mg/ml ≈ 20 mM) were added to the lid of the Eppendorf tube containing the protein sample, yielding a 1.98 µM final concentration of aerophobin-2 (2) in assays. After brief centrifugation up to 8000 rpm (Biofuge pico, Heraeus) and thorough mixing of all components, samples were incubated for 10 min at 50 °C. After incubation, 50 µl HPLC methanol were added to 50 µl final assay volume, and samples submitted to HPLC

analysis. Injection volume was 40 μ l. Detailed pipetting schemes will be given for each single experiment. In general, substrate controls (5 μ l substrate plus 45 μ l buffer) and a control for the respective protein sample (protein sample plus buffer, without substrate) were included in all assays. In some preliminary experiments, assay conditions differed from those described above, and will be specified for the respective experiment in the following.

Two analytical HPLC systems were employed, one purchased from Waters and the other from Dionex (see below). If the product aerophysinin-1 (1) was detectable, the respective sample was considered as active. Activity was quantified as % of product emerging, calculated as the amount of product in the investigated sample (in nmol) divided by the maximum amount of product possible as found in samples where aerophobin-2 (2) was transformed completely into the product aerophysinin-1 (1) (= 38.8 ± 1.4 nmol, averaged for N = 5 samples).

Analytical HPLC

Analytical HPLC systems consisting of an HPLC coupled to a photo diode array detector (UV-Vis) was employed for identification and quantification of product and substrate in assays. Two HPLC systems were used for compound separation:

- 1.) An isocratic solvent system consisting of 23 % acetonitrile and 77 % water, thus allowing for a good separation within 7 min per sample with a flow rate of 2 ml/min. Routine detection was at 254 and 280 nm. Samples consisted of 50 μ l assay volume mixed with 50 μ l HPLC methanol. Injection volume was 40 μ l.

Pumps	Waters 510
Autosampler	Waters 717plus
Column oven	Säulenofen K3, Techlab
Column	Eurospher 100-C18, 5 μ m, 125 x 4 mM i.d., Knauer
Detector	Waters 996 Photodiode array detector
Software	Millenium 32

- 2.) A gradient consisting of a solvent system of methanol/NANOpur water as depicted in Table III.2 allowed for a good separation within 17 min per sample with a flow rate of 1 ml/min. Routine detection was at 254 and 280 nm. Samples consisted of 50 μ l assay volume mixed with 50 μ l HPLC methanol. Injection volume was 40 μ l.

For both HPLC systems, calibration curves of the product aerophysinin-1 (1) and substrate aerophobin-2 (2) were established for quantification of these compounds in samples as described before (Part II Methods).

Table III.4. Gradient employed for HPLC. Flow rate: 1 ml/min.

Time (min)	0.02% phosphoric acid, pH 2 (%)	Methanol (%)
0	90	10
2	90	10
11	55	45
12	0	100
14	0	100
15	90	10
17	90	10

Pump	P 580, Dionex
Autosampler	ASI-100, Dionex
Column oven	STH 585, Dionex
Column	Eurospher 100-C18, 5 µm, 125 x 4 mM i.d., Knauer
Detector	UVD 340 S, Dionex
Software	Chromeleon V6.3

Protein quantification

Protein concentrations were measured by means of the Bradford assay (Bradford 1976). The Bradford assay is a colorimetric protein assay based on the fact that the previously red form of the Coomassie reagent stabilises into Coomassie blue by the binding of protein. The bound dye has an absorption maximum at 595 nm, which can be detected photometrically. The increase of absorbance at 595 nm is proportional to the amount of bound dye, and thus to protein concentration present in the sample. A protein standard, usually BSA, is used to establish calibration curves for protein quantification. The Bradford reagent was prepared as follows:

- Bradford stock solution: 70 mg Coomassie Brilliant Blue
 solve in 50 ml ethanol p.A.
 add 100 ml phosphoric acid (85 %)
 fill up with ultrapure water to a final volume of 100 ml
 store at 4 °C, protect from light
- Ready-to-use solution: mix stock solution with water (1:5)
 Store at 4 °C protect from light over night
 Filter diluted solution

For calibration curves, different volumes of a BSA standard (100 µg/ml) were mixed with water or buffer to a final volume of 100 µl (Table III.5) in disposable cuvettes. In

order to correct for pipetting errors, these samples were prepared in duplicate. 1 ml Bradford ready-to-use solution was added and mixed properly with each sample. After an incubation time of 5 min at room temperature, absorbance was measured at 595 nm.

Table III.5. Pipetting scheme for BSA standard.

BSA (μl)	Buffer (μl)
0	100
5	95
10	90
30	70
50	50
100	0

For determining protein concentration in samples, three dilutions were prepared in disposable cuvettes (final volume 100 μ l). The respective buffer in which the protein sample was stored served as blank sample. To each dilution, 1 ml of Bradford solution was added and samples mixed thoroughly. After 5 min incubation, absorption was measured at 595 nm. Protein dilutions were adjusted to give absorptions between 0.100 and 1.000, since the Bradford assay is linear only within this range.

For samples of little volume and low protein concentration, a more sensitive Bradford setup was chosen employing the Coomassie Plus Bradford assay kit (Pierce). Both the different solutions of the protein sample and the BSA standard (in duplicate) were prepared in 96-well microplate. Total sample volume was 10 μ l, to which 300 μ l of the Coomassie Plus reagent were added and mixed with a plate shaker for 30 s. Incubation was for 10 min at room temperature. After incubation, absorbance was measured at 595 nm with a plate reader.

SDS polyacrylamide gel electrophoresis (SDS PAGE)

After each purification step, protein fractions that showed activity in the activity assay and neighbouring fractions were submitted to SDS polyacrylamide gel electrophoresis (SDS PAGE) where proteins were separated according to their size. SDS gels thus revealed the complexity of protein fractions as represented by band patterns in the gel, and gave an estimate about the purity of the obtained fractions. In addition, SDS gels were used to monitor differences in the band patterns of active versus those of inactive fractions. Table III.6 shows the composition of gels and buffers used for SDS PAGE. By adding SDS electrical charge of proteins is neutralised and, as a consequence, spatial structure is denatured. SDS is a negatively charged detergent which attaches to the aliphatic end of protein molecules. Neighbouring negatively

charged ends push off each other, thus leading to a complete linearisation of protein molecules if not stabilised by disulfide bonds. The latter can be cleaved by adding reducing agents such as β -mercaptoethanol to the sample buffer.

Protein amounts loaded onto the gel depended on the experiments and will be described in detail for the distinct approaches. Generally, a total volume of 15 μ l was applied for each sample, consisting of 3 μ l of 5x sample buffer (Table III.6) and respective volumes of protein solution and ultrapure water if necessary to reach the final volume of 15 μ l.

Table III.6. Gels and buffers used for SDS PAGE.

Description	Components	Volume	Remarks
Stacking gel (4 %)	Ultrapure water	6.1 ml	Add APS and TEMED shortly before pouring the gel; Volume for 4 gels
	0.5 M Tris-HCl, pH 6.8	2.5 ml	
	10 % (w/v) SDS solution	0.1 ml	
	30 % Acrylamide/Bis solution	1.3 ml	
	10 % (w/v) APS solution	0.05 ml	
	TEMED	0.01 ml	
Separating gel (10 %)	Ultrapure water	4.06 ml	Add APS and TEMED shortly before pouring the gel; Volume for 2 gels
	1.5 M Tris-HCl, pH 8.8	2.5 ml	
	10 % (w/v) SDS solution	0.1 ml	
	30 % Acrylamide/Bis solution	3.3 ml	
	10 % (w/v) APS solution	0.05 ml	
	TEMED	0.05 ml	
Separating gel (6 %)	Ultrapure water	5.4 ml	Add APS and TEMED shortly before pouring the gel; Volume for 2 gels
	1.5 M Tris-HCl, pH 8.8	2.5 ml	
	10 % (w/v) SDS solution	0.1 ml	
	30 % Acrylamide/Bis solution	2.0 ml	
	10 % (w/v) APS solution	0.05 ml	
	TEMED	0.05 ml	
Sample buffer (5x)	Ultrapure water	2.75 ml	Add 50 μ l β -mercaptoethanol to 950 μ l sample buffer prior to usage
	0.5 M Tris-HCl, pH 6.8	1.25 ml	
	Glycerol	2.5 ml	
	10 % (w/v) SDS solution	2.0 ml	
	0.5 % (w/v) bromophenol blue	1.0 ml	
10x SDS buffer (1 l)	Tris base	30.3 g	pH 8.3; dilute 1:10 (water) prior to usage
	Glycin	144.0 g	
	SDS	10.0 g	
	Ultrapure water	Ad 1000 ml	
Fixing solution	30 % ethanol	300 ml	
	2 % (w/v) phosphoric acid	24 ml	
	Ultrapure water	676 ml	
Staining solution	0.02 % coomassie brilliant blue	100 mg	
	2 % (w/v) phosphoric acid	12 ml (85 %)	
	5 % aluminium sulfate (Al ₂ (SO ₄) ₃ x (H ₂ O) _x , x = 14-18)	25 g	
	10 % ethanol	50 ml	
	Ultrapure water	438 ml	

On each gel, a protein marker consisting of a protein ladder either ranging from 30 to 97 kDa or from 10 to 170 kDa was applied next to the samples analysed. Depending on the protein sample and problem investigated, gels of different polyacrylamide percentages were prepared as given in Table III.6. After mixing sample buffer and protein solution, proteins were denatured for 30 min in a water bath at 37 °C. The gel was run at 120 V until marker bands reached the separating gel, then voltage was set to 150 V. Electrophoresis was stopped shortly before marker bands reached the end of the gel. After electrophoresis, gels were washed with ultrapure water for 3 x 10 min, and incubated in the fixing solution for 30 min. Staining was done over night, and slight background staining removed by repeatedly washing the gel with ultrapure water. Subsequently gels were scanned for documentation, kept humid and stored in plastic foils in the fridge.

TCA precipitation

Low protein concentrations of fractions obtained after diverse purification steps necessitated protein precipitation by trichloroacetic acid (100 % w/v) prior to separating proteins via SDS-PAGE. Therefore, one volume of TCA was added to four volumes of protein sample, e.g. 250 µl TCA were added to 1 ml protein sample, and incubated for 10 min at 4 °C. Subsequently, the whitish, fluffy solution was centrifuged for 5 min at 13000 rpm. After removal of the supernatant, the pellet was washed twice with cold acetone (1/5 of the original protein sample volume, e.g. 200 µl acetone for protein sample of 1 ml volume). Following the last centrifugation step, pellets were dried for 5 min at 95 °C in a heating block to drive off remaining acetone. Pellets were resuspended in ultrapure water (12 µl) and 5 x sample buffer (3 µl), and processed as described above for SDS PAGE. If the (normally blue) sample buffer turned yellow after resuspension of the pellet, 0.5 M Tris was added until the colour of the sample buffer switched to blue again, indicating that an alkaline pH was reached.

Isolation of the substrate aerophobin-2 (2) from *Aplysina aerophoba*

The great number of experiments aiming at the purification of the isoxazoline cleaving enzyme required large amounts of the substrate aerophobin-2 (2). In order to obtain ample amounts of this compound, lyophilised *A. aerophoba* sponge tissue was exhaustively extracted with methanol. Sponges used for the isolation of compounds were collected in Rovinj, Croatia in April 2005. Samples were transported and stored

frozen, lyophilised and ground with a mortar prior to exhaustive extraction in methanol. The dry extract was solved in methanol and loaded in portions to silica gel, stirred until dryness, and taken to complete dryness in the desiccator. The dry sample was then submitted to vacuum liquid chromatography (VLC), i.e. a silica gel column (9 x 10 cm) with a solvent system consisting of hexane/ethyl acetate and dichloromethane/methanol which is shown in Table III.7. Two of the VLC fractions yielded pure compounds, aerophysinin-1 (1) and isofistularin-3 (3). Further separation of a fraction containing aerophobin-2 (2) was achieved by a sephadex column (5.0 x 65 cm) with methanol (100 %) as solvent (Figure III.1).

Table III.7. Solvent system applied for vacuum liquid chromatography.

Fraction	Hexane (%)	Ethyl acetate (%)
1	100	0
2	75	25
3	50	50
4	25	75
5	0	100
Fraction	Dichloromethane (%)	Methanol (%)
6	100	0
7	75	25
8	50	50
9	25	75
10	0	100

Fractions were collected with a fraction collector, and approx. 20 µl of each fraction were spotted on TLC (silica gel, solvent system: ethyl acetate/methanol/ultrapure water/acetic acid 100/13.5/9/1) in order to identify and combine similar fractions. TLC detection was under a UV lamp at 254 nm. Combined fractions were dried via rotary evaporation, and redissolved in HPLC methanol. Identification of compounds was achieved by comparing their online-UV spectra with the respective spectra stored in the HPLC database, and by determining their molecular weight via HPLC-MS. This isolation procedure yielded aerophobin-2 (2) in large amounts (> 1.5 g), although slightly contaminated by aerophobin-1 (2) and aplysinamisin-2.

Purification of the isoxazoline cleaving enzyme

Several attempts were undertaken in order to purify the isoxazoline cleaving enzyme of *A. aerophoba*, including ultracentrifugation, ion exchange, gel filtration and affinity

chromatography, and labelling of the enzyme with the substrate aerophobin-2 (2) attached to a biotin label.

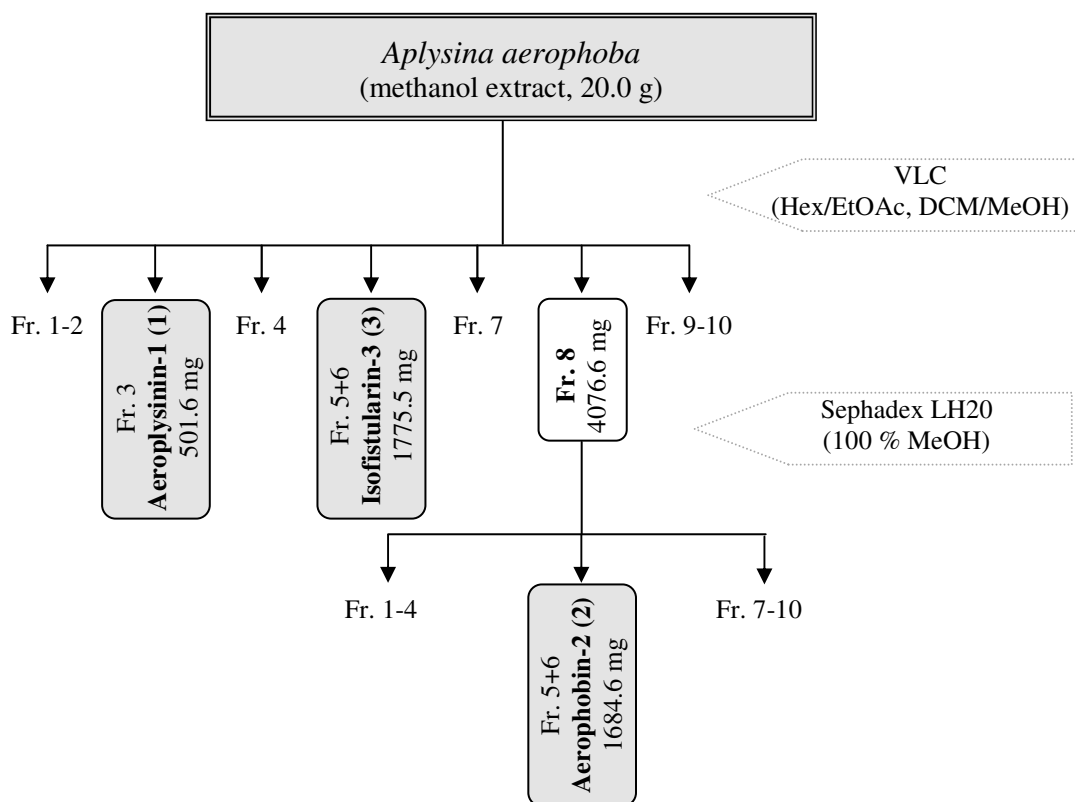


Figure III.1. Isolation scheme for the substrate aerophobin-2 (2) from *Aplysina aerophoba* extract.

Origin of sponge material

The sponge material involved in purification of the isoxazoline cleaving enzyme was exclusively derived from *A. aerophoba* collected in Rovinj, Croatia. For preliminary experiments, pooled samples collected in May 2005 were used. After establishing purification protocols via ultracentrifugation, ion exchange and gel filtration columns, a fresh sample set was collected in April 2008 and kindly provided by Prof. F. Brümmer (University of Stuttgart). The latter consisted of 5 - 8 large *A. aerophoba* individuals growing on a big rock in close vicinity to each other at a depth of approx. 7 m. Sponge samples were lyophilised, cleaned from attached organisms (such as bryozoans, little crustaceans etc.) and sediment, and ground in a mortar. Approx. 560 g freeze dried sponge powder could be obtained and were stored dry at -80 °C. This sample represented the sponge material for all subsequent analyses and purification attempts.

Differential centrifugation

Prior to purification, sponge cells were solubilised for 45 min in an ultrasonic bath cooled by ice. Per 2.5 g lyophilised sponge material, 20 ml of a 50 mM citrate buffer (containing 5 mM EDTA, pH 5.8) were added into a 50 ml falcon tube. Commonly 8 x 2.5 g were prepared per approach, yielding a total of 20 g sponge tissue. After incubation in the ultrasonic bath, samples were centrifuged for 20 min at 800 x g, 4 °C in order to remove cell nuclei, unsolubilised cells and cell debris. The supernatant was transferred into vials suited for ultracentrifugation, the pellet washed with another 5 ml citrate buffer (containing 5 mM EDTA, pH 5.8) and centrifuged at 800 x g, 4 °C for 15 min. The supernatant was added to the ultracentrifugation tubes already containing the supernatants of the first centrifugation step. The two fractions obtained this way will be referred to as P1 (for pellet) and S1 (for supernatant) in the following. 200 µl of S1 were stored for bioactivity assays and SDS PAGE. P1 was resuspended in 20 ml citrate buffer. S1 was ultracentrifuged (Sorvall Discovery, rotor Ti60, Beckmann) at 10000 x g, 4 °C for 30 min for removal of cell organells. The pellet (P2) was dispensed in 2 ml citrate buffer per falcon tube, adding to a total volume of 16 ml. The supernatant (S2) was transferred into new vials after 200 µl were stored for bioactivity assays and SDS PAGE. In the last centrifugation step, S2 was centrifuged for 1.5 h at 100000 x g, 4 °C, yielding the membrane fraction P3 and soluble cell ingredients in fthe supernatant S3. P3 was dissolved in 0.75 ml citrate buffer per falcon tube, adding to a total volume of 6 ml. Figure III.2 illustrates the process of differential centrifugation.

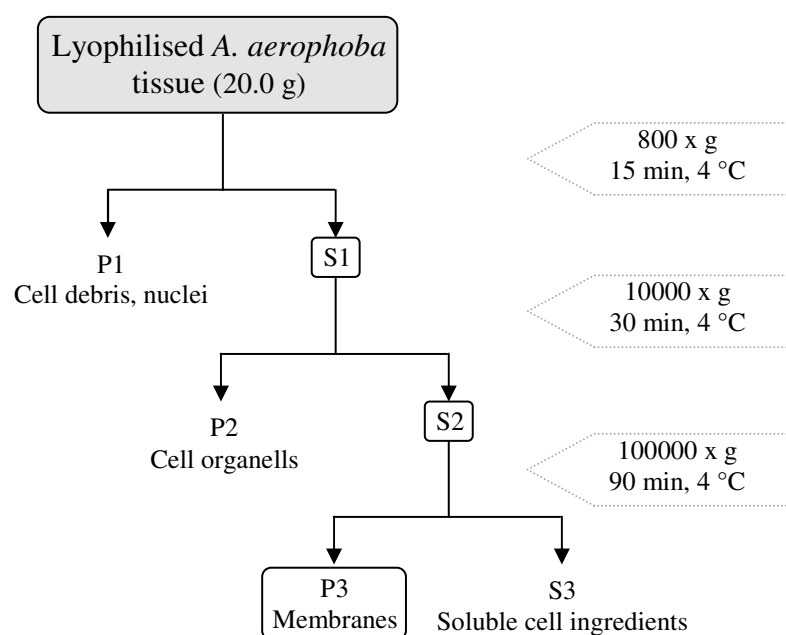


Figure III.2. Scheme for differential centrifugation.

Protein concentration of each fraction was determined via the Bradford assay. For determining activity, a volume corresponding to 5 µg of protein was added to 5 µl of substrate and filled to a final assay volume of 50 µl with citrate buffer in order to employ equal amounts of protein for each fraction in the assay. Quantification of substrate and product was achieved by HPLC. Complexity of protein patterns was checked via 10 % SDS-PAGE (5 µl sample + 3 µl 5 x sample buffer + 7 µl ultrapure water).

Washing membranes with sodium carbonate

Since major activity was found in the membrane fraction P3 emerging from ultracentrifugation, the question arose whether the protein catalysing the biotransformation of isoxazoline alkaloids is an integral membrane protein or attached to the surface of membranes. In order to shed light on this issue, membranes were washed with ice cold sodium carbonate buffer (Na₂CO₃, pH 11.5) after a protocol by (Fujiki et al. 1982). At this strongly alkaline pH, both proteins and membranes are negatively charged and repel each other, thus leading the non-integral proteins to be stripped off the membrane. In addition, membrane vesicles are opened under a strongly alkaline milieu, releasing intravesicular proteins. However, conformation of integral membrane proteins is preserved due to the stabilising effects of the membrane. After a centrifugation step, it is therefore possible to obtain non-integral and vesicular proteins in the supernatant, and integral membrane proteins in the pellet. Tracking the activity of the thus obtained fractions then allows for identifying the protein in question as either being an integral or a non-integral protein.

50 µl P3 (protein concentration: 1.5 mg/ml) were diluted 1:10 with Na₂CO₃ (pH 11.5) to a final volume of 500 µl and incubated on ice for 30 min. After centrifugation at 100000 x g, 4 °C, the supernatant was transferred into a new vial and the pellet resuspended in 60 µl citrate buffer (pH 5.8). pH of the supernatant was adjusted to pH 5 - 6 with 0.5 M citric acid. Activity of both fractions was checked via the activity assay, where a sample of untreated P3 (diluted 1:10 with citrate buffer) served as reference. 16 µl of the respective fraction were diluted with 16 µl citrate buffer and 8 µl of an aerophobin-2 (2) solution (20 mg/ml). Incubation was at 50 °C for 30 min. To the total assay volume of 40 µl, another 40 µl of HPLC MeOH were added, and substrate as well as product quantified via HPLC. Injection volume was 40 µl.

Solubilisation of cell membranes

Since the attempt to wash off the protein in question from membranes identified it as an integral membrane protein, the necessity arose to solubilise it for further purification. Detergents are amphiphilic molecules which attach with their hydrophobic ends to the hydrophobic parts of protein molecules (e.g. trans-membrane areas) and thus partly displace phospholipids. When an adequate number of amphiphilic molecules has attached, the membrane proteins are solubilised as complexes of detergent, phospholipids and protein. When solubilising a membrane protein, there are two important things that must be avoided, (1) that the protein aggregates (and is not solubilised), and (2) that the protein is denatured. Since every protein requires different conditions for being solubilised in its native form (in terms of the detergent used, detergent concentration, pH, buffer etc.) it was necessary to test different detergents and conditions for solubilisation in order to obtain an optimal result. The functionality of the protein after treatment with different detergents was controlled in the activity assay.

Screening of detergents

For a first screening, four different detergents were employed: Tween 20, sodium cholate, FOS-choline 12 and n-dodecyl- β -D-maltopyranoside (DDM). Detergents are either non-ionic, anionic, cationic or zwitterionic. Each detergent is characterised by the critical micelle concentration (CMC), defining the minimal detergent concentration at which micelles can still be formed. Upon reaching CMC, any further addition of detergent will increase the number of micelles. Thus, CMC is a critical value when calculating the amount of detergent used for solubilisation of membrane proteins.

10 μ l (sodium cholate: 20 μ l) of a 10 % (w/v) detergent solution were added to 100 μ l of P3 obtained by ultracentrifugation as described above (in citrate buffer, pH 5.8). Table III.8 gives an overview over the detergents and concentrations employed. Samples were incubated on ice for 1h, and mixed thoroughly every 15 min. After subsequent centrifugation at 100000 x g, 4 °C, the supernatant was removed and the pellet resuspended in 120 μ l citrate buffer (pH 5.8). Both pellet and supernatant were checked for protein functionality in the activity assay. 16 μ l of each fraction were mixed with 16 μ l citrate buffer (pH 5.8) and 8 μ l substrate solution (aerophobin-2 (2), 20 mg/ml), and incubated for 20 min at 50 °C. Respective controls with enzyme and buffer but no substrate were included. Substrate and product amounts were quantified via HPLC (Dionex).

Table III.8. Detergents tested to solubilise P3.

Detergent	Description	CMC (%)	End conc. (%)
Tween 20	Non-ionic	0.007	1
Sodium cholate	Anionic	0.410	2
FOS-choline 12	Zwitterionic	0.047	1
DDM	Non-ionic	0.009	1

Assessment of optimal solubilisation and storage conditions

Since membranes treated with FOS-choline 12 retained most of their activity when compared to the other detergents tested, further experiments should help to identify the optimal FOS-choline 12 concentration for solubilisation. Two aspects were crucial in this context, (1) solubilisation efficiency and (2) storage of samples. The aim was thus to find a detergent concentration where an ample amount of membrane protein is solubilised and activity is retained even if samples are frozen and thawed for further processing. Therefore, a 10 % (w/v) stock solution of FOS-choline 12 was prepared, added to the membrane fraction P3 obtained by ultracentrifugation, and filled up with citrate buffer (pH 5.8) to reach a final volume of 100 μ l as described in Table III.9.

Table III.9. Detergent concentrations tested to solubilise the membranes in ultracentrifugation fraction P3.

P3 (μl)	FOS 10 % (μl)	Citrate buffer (μl)	End conc. FOS (%)
80	5.0	15.0	0.50
80	7.5	12.5	0.75
80	10.0	10.0	1.00
80	12.5	7.5	1.25

All samples were incubated on ice and mixed thoroughly every 15 min. After centrifugation at 100000 x g, the pellet was resuspended in 120 μ l citrate buffer pH 5.8 and both pellet and supernatant checked for activity in the activity assay. Fractions were diluted 1:10, of which 2 μ l were mixed with 43 μ l citrate buffer (pH 5.8) and 5 μ l substrate solution (aerophobin-2 (2), 10 mg/ml), then incubated for 10 min at 50 °C. Respective controls with enzyme and buffer but no substrate were included. Substrate and product amounts were quantified via HPLC. In order to assess the effect of detergent concentration on protein functionality under different storage conditions, activity of the samples described in Table III.9 was measured again after one day and after seven days, respectively. Storage conditions included 4 °C (fridge) and -20 °C. For samples stored for seven days, one aliquot stayed frozen over seven days without thawing, another aliquot was subjected to freezing and thawing once every day (i.e. 6 x in total). Table III.10 shows the setup of the storage experiment.

Table III.10. Testing the influence of detergent concentration in combination with storage conditions on protein functionality.

End conc. FOS (%)	Time (days)	Storage (°C)
0.50	1	+4
	1	-20
	7	+4
	7	-20
	7	-20*
0.75	1	+4
	1	-20
	7	+4
	7	-20
	7	-20*
1.00	1	+4
	1	-20
	7	+4
	7	-20
	7	-20*
1.25	1	+4
	1	-20
	7	+4
	7	-20
	7	-20*

*repeated freezing and thawing cycles

In addition, different concentrations of NaCl were tested in combination with the two detergent concentrations found to be best suited for solubilising and subsequent storage, i.e. a final concentration of 0.75 and 1.00 % FOS-choline 12. Therefore, a 10 % (w/v) stock solution of FOS-choline 12 and a 2.5 M stock solution of NaCl were prepared, respective amounts added to the membrane fraction P3 obtained by ultracentrifugation, and filled up with citrate buffer (pH 5.8) to reach a final volume of 100 µl. Table III.11 shows the pipetting scheme for this experiment.

Table III.11. Testing the influence of different NaCl concentrations on protein functionality.

End conc. FOS (%)	End conc. NaCl (mM)	P3 (µl)	FOS 10 % (µl)	NaCl 2.5M (µl)	Citrate buffer (µl)
0.75	100	80	7.5	4.0	8.5
	150	80	7.5	6.0	6.5
	200	80	7.5	8.0	4.4
	250	80	7.5	10.0	2.5
1.0	100	80	10.0	4.0	6.0
	150	80	10.0	6.0	4.0
	200	80	10.0	8.0	2.0
	250	80	10.0	10.0	-

All samples were incubated on ice and mixed thoroughly every 15 min. After centrifugation at 100000 x g, the pellet was resuspended in 120 µl citrate buffer (pH 5.8) and both pellet and supernatant checked for activity in the activity assay as described above for testing different detergent concentrations. In addition, different storage conditions were tested as summarised by Table III.12.

Table III.12. Experimental setup for testing the influence of different NaCl concentrations and storage conditions on activity. Solubilisation was achieved with end concentrations of 0.75 and 1.00 % FOS, respectively.

End conc. FOS (%)	End conc. NaCl (mM)	Time (days)	Storage conditions (°C)
0.75 / 1.00	100	1	+4
		1	-20
		7	+4
		7	-20
	150	7	-20*
		1	+4
		1	-20
		7	+4
	200	7	-20
		7	-20*
		1	+4
		1	-20
	250	7	+4
		7	-20
		7	+4
		7	-20
		7	-20*

* repeated freezing and thawing cycles

Standard protocol for solubilisation

Based on the results of the detergent screening, a standard protocol for solubilisation of the ultracentrifugation membrane fraction (P3) emerged. A detergent concentration of 0.75 % FOS-choline 12 in combination with a final concentration of 100 mM NaCl proved to give optimal solubilisation results. Since ultracentrifugation results were perfectly reproducible in terms of activity as well as protein concentration (1.9 ± 0.2 mg/ml, N = 3, measured via Bradford assay), solubilisation was always performed after the following, standardised scheme: 6 ml P3 obtained from ultracentrifugation were thawed slowly on ice and mixed with 46.8 mg NaCl and 2 ml of a 3 % (w/v) FOS-choline 12 stock solution to give end concentrations of 0.75 % FOS-choline 12 and 100 mM NaCl. The sample was mixed thoroughly and incubated for 1 h on ice.

Mixing was repeated every 15 min. Subsequent centrifugation at 100000 x g, 4 °C yielded the solubilised membranes in the supernatant. Since loss of protein activity during each freezing and thawing event could not be avoided, solubilisation was performed directly prior to each purification step. In each approach, protein concentration as well as activity of solubilised membranes (referred to as P3 Sol in the following) was assessed.

Ion exchange chromatography

Ion exchange chromatography was employed to purify the isoxazoline cleaving enzyme in the solubilised membrane fraction. Proteins have various functional groups with different charges adding up to a net charge which depends on pH, thus enabling ion exchange chromatography. Proteins can be separated according to their net charge by adjusting pH or ionic concentration of the mobile phase. The stationary phase surface displays ionic functional groups that interact with analyte ions of opposite charge, i.e. a negatively charged protein will bind to a positively charged stationary phase, and vice versa. Elution can be achieved by changing pH or ionic strength of the mobile phase. In the latter case, ions from the mobile phase interact with the immobilised ions in preference over those in the stationary phase, thus allowing the protein to elute.

Chromatography media involved in the purification of the isoxazoline cleaving enzyme included HiTrap IEX columns prepacked with Q Sepharose™ Fast Flow (strong anion) and SP Sepharose™ Fast Flow (strong cation, both purchased from GE Healthcare). The following Äkta-FPLC® system was employed for purification of the solubilised membrane fraction (P3 Sol) at 4 °C:

Pump	P-900, Amersham Biosciences
Autosampler	Frac-920, Amersham Biosciences
Detector	UV-900, Amersham Biosciences
Cooling cabinet	Unichromat 1500-Duo, UniEquip GmbH
Software	Unicorn

HiTrap columns were washed with 10 medium volumes ultrapure water (= 10 ml) and equilibrated with buffer A (see below) for at least 30 column volumes with a flow rate of 1 ml/min. Buffer A: HiTrap Q FF: 50 mM citrate buffer pH 5.8

HiTrap SP FF: 100 mM citrate buffer pH 4.0

Buffer B: HiTrap Q FF: 50 mM citrate buffer pH 5.8, 1 M NaCl

HiTrap SP FF: 100 mM citrate buffer pH 4.0. 1 M NaCl

All buffers generally contained 2.5 x CMC FOS-choline 12 to keep proteins in solution, i.e. 117.5 mg FOS-choline 12 per 100 ml buffer. 8 ml of the sample P3 Sol were applied via a 50 ml SuperLoop injection device. After washing off protein not bound to the column, elution of proteins was achieved with a gradient of buffer A and B as given in Table III.13. Detection was via a UV-detector at 280 nm. The first four fractions of 5 ml volumes were collected in 15 ml plastic tubes, the subsequent fractions (1 and 2 ml, respectively, Table III.13) in 2 ml Eppendorf tubes with a fraction collector. After usage, columns were excessively washed with buffer B and stored at 4 °C.

Table III.13. Gradient employed for FPLC. Flow rate: 1 ml/min.

Volume (ml)	Buffer A (%)	Buffer B (%)	Fraction size (ml)
0.0	100	0	2
10.5	70	30	2
71.5	0	100	1
82.5	0	100	2

Fractions were checked for activity in the activity assay directly after purification. For fractions 1-4, 2 µl protein solution was added to 43 µl buffer and incubated with 5 µl substrate solution (aerophobin-2 (2) 10 mg/ml) for 10 min at 50 °C. The 50 µl assay volume was mixed with 50 µl HPLC MeOH for HPLC analysis. Of the later fractions, 25-45 µl protein solution were employed in the activity assay, depending on protein concentration as measured in the Bradford assay.

However, since purification over HiTrap SP FF afforded to use a mobile phase with pH 4, no activity could be detected in any of the fractions in the activity assay, even after setting the pH of samples to 5.8 prior to the activity assay. Due to this reason, this approach was not established for further purification attempts. Ion exchange purification over the strong anion exchange column HiTrap Q FF yielded good and reproducible results with clear activity in a range of fractions, therefore used as standard purification protocol.

Gel filtration

Gel filtration or size exclusion chromatography separates molecules according to their size, or more accurately their hydrodynamic diameter. Smaller molecules are able to enter the pores of the media and, therefore, take longer to elute, whereas larger molecules are excluded from the pores and elute faster.

Since active ion exchange fractions proved to be quite complex on SDS PAGE, gel filtration was used as a second purification step following ion exchange chromatography. For this purpose, a Superdex 200 10/300 gel filtration column (GE Healthcare) was employed on the same Äkta-FPLC[®] system as described for ion exchange chromatography. The column was equilibrated with 10 medium volumes of the respective buffer used (see below) at a flow rate of 0.3 ml/min at 4 °C over night prior to usage. In order to protect the column from collapse, an upper pressure limit of 1.5 MPa was programmed. After several preliminary trials with 50 mM citrate buffer, pH 5.8, 2.5 x CMC FOS-choline 12 either without NaCl, with 100 mM or 1 M NaCl, the buffer with 100 mM NaCl proved to serve best as mobile phase. The most active ion exchange fraction was chosen and 500 µl were applied to the gel filtration column with a 1 ml syringe (Injekt[®]-F, Braun) via a 500 µl injection loop. Flow rate was 0.5 ml/min, and detection with a UV detector at 280 nm. Fractions of 0.5 ml volume were collected with a fraction collector. After usage, columns were washed excessively with buffer and ultrapure water and stored in 20 % ethanol at 4 °C. Fractions obtained from gel filtration were tested in the activity assay with 45 µl of each fraction incubated with 5 µl substrate solution (aerophobin-2 (2) 10 mg/ml) for 10 min at 50 °C. The 50 µl assay volume was mixed with 50 µl HPLC MeOH for HPLC analysis. Protein concentration was determined by the Bradford assay, and complexity of fractions monitored via SDS PAGE.

Calibration of the gel filtration column with size standards

Gel filtration can give good estimates of the size of eluted proteins if the column used is calibrated with size standards. Molecular weight determinations of unknown proteins are made by comparing the ratio of V_e/V_0 for the protein in question to the V_e/V_0 of protein standards of known molecular weight, where V_e is the elution volume and V_0 is the void volume. The void volume of a given column is based on the volume of effluent required for the elution of a large molecule such as Blue Dextran (molecular weight approx. 2000 kDa). A calibration curve can then be obtained by plotting the logarithms of the known molecular weights of protein standards versus their respective V_e/V_0 values.

This was done to gather information on the size of the protein(s) eluted in the active gel filtration fractions. All standards were taken from the MW-GF 1000 Kit (Sigma Aldrich, MW range 29-700 kDa) and elution volumes were determined according to the

manufacturer's instructions. Blue Dextran was used to determine the column void volume. A 50 mM phosphate buffer containing 100 mM NaCl and 0.1 mM EDTA served as mobile phase. Flow rate was 0.5 ml/min. Injection volume was 500 μ l via a 500 μ l injection loop, identical to that used for the application of the protein sample. Table III.14 shows the details for the size standards applied to the Superdex 200 column.

Table III.14. Size standards used to establish a calibration curve for the Superdex 200 column.

Standard	Size (kDa)	Conc. (mg/ml)
Thyrogobulin	669	1.6
Apoferritin	443	5.0
Alcohol dehydrogenase	150	1.0
BSA	66	2.0

For the calibration curve, the logarithms of molecular weight were plotted versus V_e/V_0 for each respective protein standard. V_e of the unknown target protein was determined and V_e/V_0 calculated. Its molecular weight could then be derived from the standard curve.

Increasing concentration of samples with low protein content

In several approaches, protein concentration of gel filtration fractions was low and no activity was detectable in the activity assay. In these cases it was therefore attempted to increase protein concentration in these samples by centrifugation in Amicon Ultra-15 centrifugal devices (Millipore, exclusion 10 kDa) at 6000 rpm, 4 °C until a the desired sample volume was reached. As control, a sample of known activity was diluted appropriately and activity checked before and after concentration in relation to the original, undiluted sample. Activity of concentrated fractions was checked by the activity assay.

Affinity chromatography

Since one of the substrates of the isoxazoline cleaving enzyme, aerophobin-2 (2), possesses a free NH_2 -group it appeared feasible to immobilise it at an N-hydroxy-succinimide activated sepharose (NHS) matrix. However, before attempting to immobilise aerophobin-2 (2), it was crucial to find conditions where the enzyme is inactive, but can regain activity when conditions are rendered optimal again. If the isoxazoline cleaving enzyme is still active when applied to an affinity column with immobilised aerophobin-2 (2), the enzyme would cleave the substrate instead of binding

to the column, and purification would not be achieved. Due to this reason, conditions needed to be found where the enzyme is inactive, but can still bind to the substrate. Furthermore, activity should be regained when conditions are rendered optimal again (i.e. pH 5.8, 50 °C) to track the enzyme in fractions obtained from affinity chromatography.

Determination of suitable conditions for affinity chromatography

Factors tested to find such conditions included pH, temperature, and NaCl concentration. In all approaches, one of the first, highly active fractions of the ion exchange chromatography containing proteins that did not bind to the column material was employed for testing.

Temperature

In a first attempt, it was tested whether incubation of the protein sample at 4 °C would already suffice to reduce isoxazoline cleaving enzyme activity. Therefore, 5 µl protein sample were mixed with 40 µl 50 mM citrate buffer (pH 5.8) and 5 µl substrate solution (aerophobin-2 (2) 10 mg/ml), and incubated at 4 °C for different time ranges: 10, 20, 30, 60, 120, 180, 300 min, and over night. After the respective times, the 50 µl assay volume was mixed with 50 µl HPLC MeOH for HPLC analysis.

pH

As temperature did not appear to be a suitable means to inactivate the isoxazoline cleaving enzyme, pH was considered as further possibility to achieve this goal. In order to get a first idea about the influence of different pH values on enzyme activity within the temperature optimum of the enzyme, buffers from pH 8.5 to 12.0 were prepared in 0.5 steps. Since the pKs value of citrate buffer is 4.8 making it unsuitable for buffering at higher pH values, a 0.1 M Tris-HCl buffer was employed. A volume of 5 µl protein sample was mixed with 40 µl 0.1 M Tris-HCl buffer of respective pH and 5 µl substrate solution (aerophobin-2 (2) 10 mg/ml), and incubated at 50 °C for 10 min. A sample incubated with buffer of pH 5.8 served as positive control. After incubation, the 50 µl assay volume was mixed with 50 µl HPLC MeOH for HPLC analysis. Since buffers of a particular pH were mixed with a total of 10 µl protein sample and substrate solution in assays, end pH was changed as depicted in Table III.15. For each pH, a respective substrate control was prepared to check the stability of the substrate under these conditions.

Table III.15. pH values tested in assays.

pH of buffer	pH in assay
8.5	6.0
9.0	6.5
9.5	7.0
10.0	7.5
10.5	8.0
11.0	8.5
11.5	9.0
12.0	9.5

Based on this first investigation of the influence of different pH values on enzyme activity, three pH values were chosen to test for the influence of a combination of incubation temperature and time. In this setup, a volume of 10 μ l protein sample was mixed with 80 μ l 0.1 M Tris-HCl buffer of respective pH and 10 μ l substrate solution (aerophobin-2 (2) 10 mg/ml), and incubated at different temperatures for different time ranges as described by Table III.16.

Table III.16. Testing the influence of different pH values in combination with temperature and incubation time on enzyme activity.

pH in assay	Temperature ($^{\circ}$ C)	Incubation (min)	
8.0	4	10	
	4	30	
	4	60	
	4	360	
	RT [*]	10	
	RT [*]	30	
	RT [*]	60	
	RT [*]	360	
	8.5	4	10
		4	30
		4	60
		4	360
RT [*]		10	
RT [*]		30	
RT [*]		60	
RT [*]		360	
9.0		4	10
		4	30
		4	60
		4	360
	RT [*]	10	
	RT [*]	30	
	RT [*]	60	
	RT [*]	360	

*RT = room temperature

After incubation, samples were aliquoted into 2 x 50 μ l. One aliquot was directly mixed with 50 μ l HPLC MeOH for HPLC analysis. The pH of the other aliquot was set to approx. pH 5.8 with 3.7 % HCl (checked with 0.5 pH paper) and incubated at 50 °C for 10 min. A sample in buffer of pH 5.8 was incubated in parallel as positive control. For each pH, a substrate control was included.

NaCl concentration

After it was confirmed that the enzyme could be inactivated at certain pH values and activity regained afterwards by changing pH and incubation temperature to optimal conditions, attempts were made to optimise restored activity by adding different concentrations of NaCl to the assays. For this purpose, stock solutions of 1 M, 2.5 M and 5 M NaCl were prepared. In this setup, a volume of 10 μ l protein sample was mixed with 70 μ l 0.1 M Tris-HCl buffer of respective pH, 10 μ l NaCl stock solution and 10 μ l substrate solution (aerophobin-2 (2) 10 mg/ml). In samples where no NaCl was added, a volume of 10 μ l protein sample was mixed with 80 μ l 0.1 M Tris-HCl buffer of respective pH, and 10 μ l substrate solution. Incubation was at different temperatures for 3 h, as depicted in Table III.17.

Table III.17. Testing the influence of different pH values in combination with temperature and NaCl concentrations on enzyme activity.

pH in assay	Temperature (°C)	NaCl final conc. (mM)
8.5	4	0
	4	100
	4	250
	4	500
	RT*	0
	RT*	100
	RT*	250
	RT*	500
9.0	4	0
	4	100
	4	250
	4	500
	RT*	0
	RT*	100
	RT*	250
	RT*	500

*RT = room temperature

After incubation, samples were aliquoted into 2 x 50 μ l. One aliquot was directly mixed with 50 μ l HPLC MeOH for HPLC analysis. The pH of the other aliquot was set to approx. pH 5.8 with 3.7 % HCl (checked with 0.5 pH paper) and incubated at 50 °C

for 10 min in order to check for the regeneration of enzyme activity. A sample in buffer of pH 5.8 was incubated in parallel as positive control. For each pH, a substrate control was included.

Immobilisation of the substrate on an agarose matrix

As aerophobin-2 (2) possesses a free NH_2 -group it appeared feasible to immobilise it at an N-hydroxy-succinimide activated sepharose (NHS) with a 14 atom spacer arm (= 6-aminocaproic acid), a material particularly suited to immobilise ligands with primary amine groups. In principle, the succinimide group is split off the matrix upon nucleophilic attack, and a stable amide bond is formed between the ligand and the matrix, thus immobilising the ligand (Figure III.3).

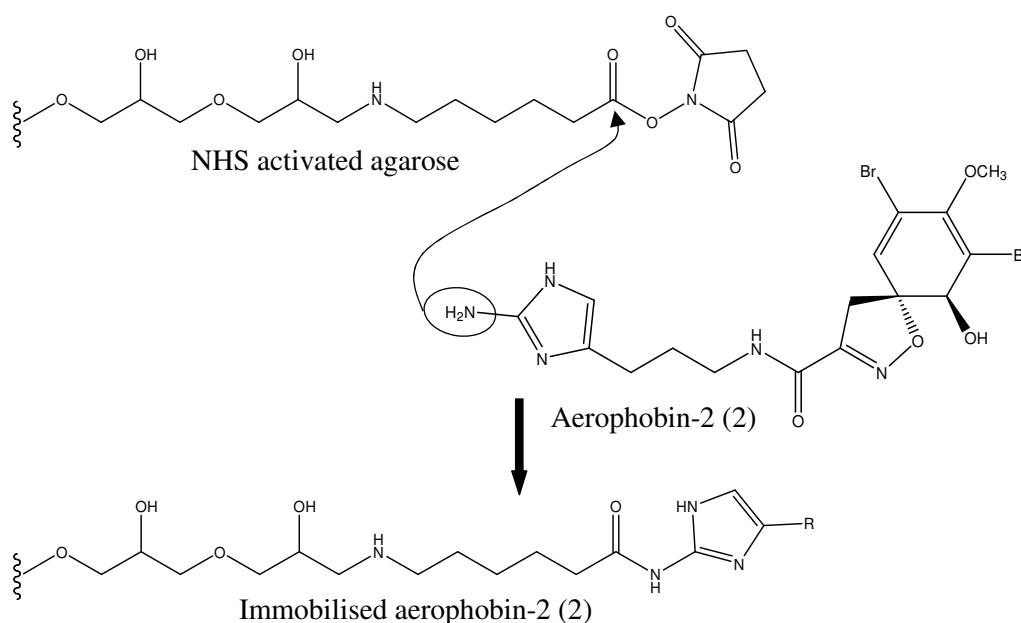


Figure III.3. Principle of immobilising aerophobin-2 (2) at an NHS activated sepharose matrix.

In general, coupling of aerophobin-2 (2) to the NHS activated matrix was performed according to the manufacturer's instructions. However, since pH, temperature and ligand concentration potentially represent important factors affecting coupling efficiency, different coupling conditions were tested on a small scale in a preliminary trial. For this purpose, 2 ml NHS activated agarose (supplied as suspension in isopropanol by the manufacturer) were washed twice with 7 ml cold 1 mM HCl per wash. The NHS activated material was then filled into Eppendorf tubes (1.5 ml) in aliquots of 100 μl . Two coupling solutions (CS) were prepared consisting of aerophobin-2 (2) a) 10 mg/ml and b) 20 mg/ml solved in a 1/1 mixture of MeOH and 0.2 M NaHCO_3 0.5 M NaCl pH 8.3. Of this coupling solution, 50 μl were added to the

activated matrix, and pH adjusted to the desired value with NaOH (1 mol/l). After thorough mixing, 10 μ l of each sample were removed, mixed with 90 μ l HPLC MeOH and centrifuged 5 min at 13000 rpm for HPLC analysis (= PRE incubation sample). The remaining part of samples was incubated at room temperature for 4 h. Table III.18 shows the experimental setup. After incubation, again 10 μ l of samples were mixed with 90 μ l HPLC MeOH, centrifuged 5 min at 13000 rpm and submitted to HPLC analysis (= AFTER incubation sample). HPLC injection volume was 20 μ l. Photometric measurement (which would have been more convenient) was not feasible for determining coupling efficiency because the absorption maximum of free NHS groups split off from the matrix (λ_{max} (MeOH) 230 nm) was completely overlapped by one of the aerophobin-2 (2) absorption maxima. The NHS groups could also not be quantified via HPLC because they were directly washed off the column and no conditions were found where it bound to the RP18 column material. Therefore the amount of aerophobin-2 (2) was determined in both the PRE and the AFTER incubation sample via HPLC. Since the matrix with immobilised aerophobin-2 (2) could easily be removed by centrifugation prior to HPLC analysis, the decrease in the amount of aerophobin-2 (2) in the AFTER sample relative to the aerophobin-2 (2) concentration in the PRE sample served to determine coupling efficiency.

Table III.18. Testing coupling efficiency between aerophobin-2 (2) and NHS activated agarose under different conditions.

Temperature ($^{\circ}$ C)	pH	Conc. CS* (mg/ml)
RT**	9	10
		20
	10	10
		20
	11	10
		20
12	10	
	20	
50 $^{\circ}$ C	9	10
		20
	10	10
		20
	11	10
		20
12	10	
	20	

*CS = coupling solution, aerophobin-2 (2) in a 1/1 mixture of MeOH/0.2 M NaHCO₃ 0.5 M NaCl pH 8.3

**RT = room temperature

After determining optimal coupling conditions, a standard protocol for the immobilisation of aerophobin-2 (2) on the NHS activated agarose matrix was established as follows:

3 ml of a coupling solution consisting of aerophobin-2 (2) (20 mg/ml) dissolved in a 1/1 mixture of MeOH/0.2 M NaHCO₃ 0.5 M NaCl pH 8.3 was prepared. 6 ml of the NHS activated matrix were washed with 10 - 15 medium volumes cold 1 mM HCl. NHS material and coupling solution were mixed, and pH adjusted to pH 10 with NaOH (1 mol/l). An aliquot of 10 µl was mixed with 90 µl HPLC MeOH and centrifuged for determining coupling efficiency (PRE incubation sample). The CS/NHS mixture was incubated at room temperature for 4 h. After incubation, another 10 µl of the sample were mixed with 90 µl HPLC MeOH and centrifuged for HPLC analysis (AFTER incubation sample). For blocking of non-reacted NHS groups, two medium volumes of a 0.1 M Tris-HCl buffer pH 8.5 were added and samples incubated at room temperature for 1.5 h. After blocking, the material was transferred into PolyPrep columns (10 ml, BioRad). The medium was washed with 3 x 1 medium volume of a low (50 mM citrate buffer pH 4.5) and a high pH buffer (0.1 M Tris-HCl pH 8.5) to complete the preparation of the column material employed for affinity chromatography. The material was stored at approx. 4 °C in the fridge. If the material needed to be retained for an extended time (> 2 days), it was stored in 20 % ethanol. However, since the impact of long-term storage on performance in terms of protein binding was not assessed, the material was generally prepared shortly before usage, i.e. at maximum of one or two days in advance.

Affinity chromatography

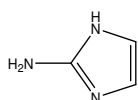
Standard protocol

For affinity chromatography, 3 ml of the prepared column material were transferred into a PolyPrep column (10 ml, BioRad). The complete process of affinity chromatography was performed at 4 °C in a cooling cabinet. Close attention was paid to set the correct pH of all buffers and solutions employed. The column material was washed with 3 medium volumes ultrapure water if stored in ethanol. Otherwise, it was directly equilibrated with 10 x 1 medium volume equilibration buffer (0.1 M Tris-HCl, 0.1 M NaCl, 2.5 x CMC FOS-choline 12, pH 8.3), i.e. 3 ml buffer were applied, the column fell dry, and then the next 3 ml were applied. After equilibration, the dry column was closed. 4 ml of solubilised membranes (P3 Sol) were mixed with

equilibration buffer 1/1 to give a total volume of 8 ml. pH of the mixture was adjusted to pH 8.3 with NaOH (1 mol/l) gauged by a pH meter. This mixture was subsequently applied to the column, thoroughly mixed with the column material, and incubated for 30 min. Mixing was repeated every 10 min. After incubation, the column was opened again and the protein solution collected in a 15 ml falcon tube. The material was then washed with 10 - 12 medium volumes of equilibration buffer, and fractions of 2 ml were collected in Eppendorf tubes. Due to its structural similarity to aerophobin-2 (2) with regard to the aminoimidazole ring, the commercially available 2-aminoimidazole was employed for elution (Figure III.4). For this purpose, a 0.3 M 2-aminoimidazole solution solved in equilibration buffer (pH 8.3) was prepared. Elution was achieved with 5 medium volumes, and factions of 1 ml were collected in Eppendorf tubes. Following elution, the column was excessively cleaned with 5 medium volumes equilibration buffer containing 15 x CMC FOS-choline 12 to remove all proteins still attached to the medium. The column was eventually cleaned with 4 medium volumes ultrapure water and stored in 20 % ethanol in the fridge.

All fractions obtained were checked for protein functionality in the activity assay. For the first fractions obtained from washing after sample application, a volume of 5 μ l protein sample was mixed with 40 μ l 50 mM citrate buffer pH 5.8, and 5 μ l substrate solution (aerophobin-2 (2) 10 mg/ml). For the last washing fractions and the fractions derived from elution, 45 μ l protein sample were mixed with 5 μ l substrate solution. For all protein samples employed in the activity assay, pH was adjusted to approx. pH 5.8 with HCl (3.7 %). Incubation was at 50 °C for 10 min. The 50 μ l assay volume were mixed with 50 μ l HPLC MeOH for subsequent HPLC analysis. Protein concentration of fractions was determined via the Bradford assay. Complexity of fractions was assessed by SDS PAGE after TCA protein precipitation.

2-Aminoimidazole



Aerophobin-2 (2)

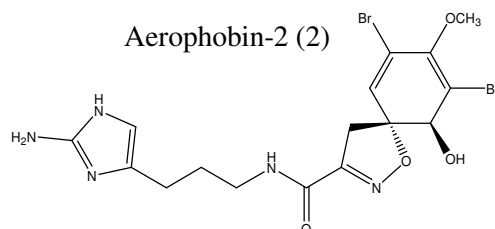


Figure III.4. Structures of 2-aminoimidazole and the substrate aerophobin-2 (2).

Elution with aerophobin-2 (2)

In the standard protocol usually employed for affinity chromatography, the commercially available 2-aminoimidazole was used for elution in order to avoid expending large amounts of aerophobin-2 (2) which needs to be isolated from *A. aerophoba* extract with some effort if required. However, to make sure that band patterns in SDS PAGE were similar for elution with 2-aminoimidazole and aerophobin-2 (2), two affinity columns containing 3 ml aliquots of the same column material were run in parallel. For both, the affinity chromatography standard protocol was applied as described above. However, instead of 2-aminoimidazole, elution was achieved with three medium volumes of a 10 mM aerophobin-2 (2) solution (solved in equilibration buffer containing 5 % DMSO) for one of these columns. After elution with aerophobin-2 (2), another 5 medium volumes of the standard 2-aminoimidazole solution were applied for a second elution to ensure the elution of all proteins bound to the column.

In the activity assay, controls were included for all fractions eluted with aerophobin-2 (2) in order to correct for higher aerophobin-2 (2) amounts present in the assay when compared to the elution with 2-aminoimidazole.

Re-use of old columns

Due to the amount of aerophobin-2 (2) used to prepare the affinity chromatography column material and the time effort for coupling, it was attempted to reuse old affinity columns stored in 20 % ethanol in the fridge. However, results were poor in terms of protein binding and reproducibility. Therefore, the affinity chromatography medium was prepared anew for each purification approach.

Labelling of the isoxazoline cleaving enzyme and detection via Western blot

Unfortunately, band patterns of affinity chromatography fractions were still complex on SDS PAGE, thus hampering unambiguous identification of bands correlated to the isoxazoline cleaving enzyme. In order to solve this problem, it was attempted to find a commercially available reagent carrying a label that can be coupled to the substrate aerophobin-2 (2) which can then bind the protein. Sulfo-SBED (Pierce) represents such a trifunctional label transfer reagent, it is activated by an NHS group which allows coupling of the reagent to the substrate aerophobin-2 (2). It further carries a biotin label and a crosslink function facilitating to achieve a strong bound to the protein once “captured” by the substrate. Figure III.5 illustrates the structure of the label transfer reagent, and the desired product.

Labelling the substrate

For coupling of the substrate aerophobin-2 (2) to the label transfer reagent the same conditions applied as employed for the immobilisation of the substrate at the NHS activated sepharose matrix. However, since the label transfer reagent Sulfo-SBED carries a photoactivated crosslink function, all steps described in the following were performed under reduced light conditions, and all vials were protected from light by wrapping them with aluminium foil to avoid photoactivation.

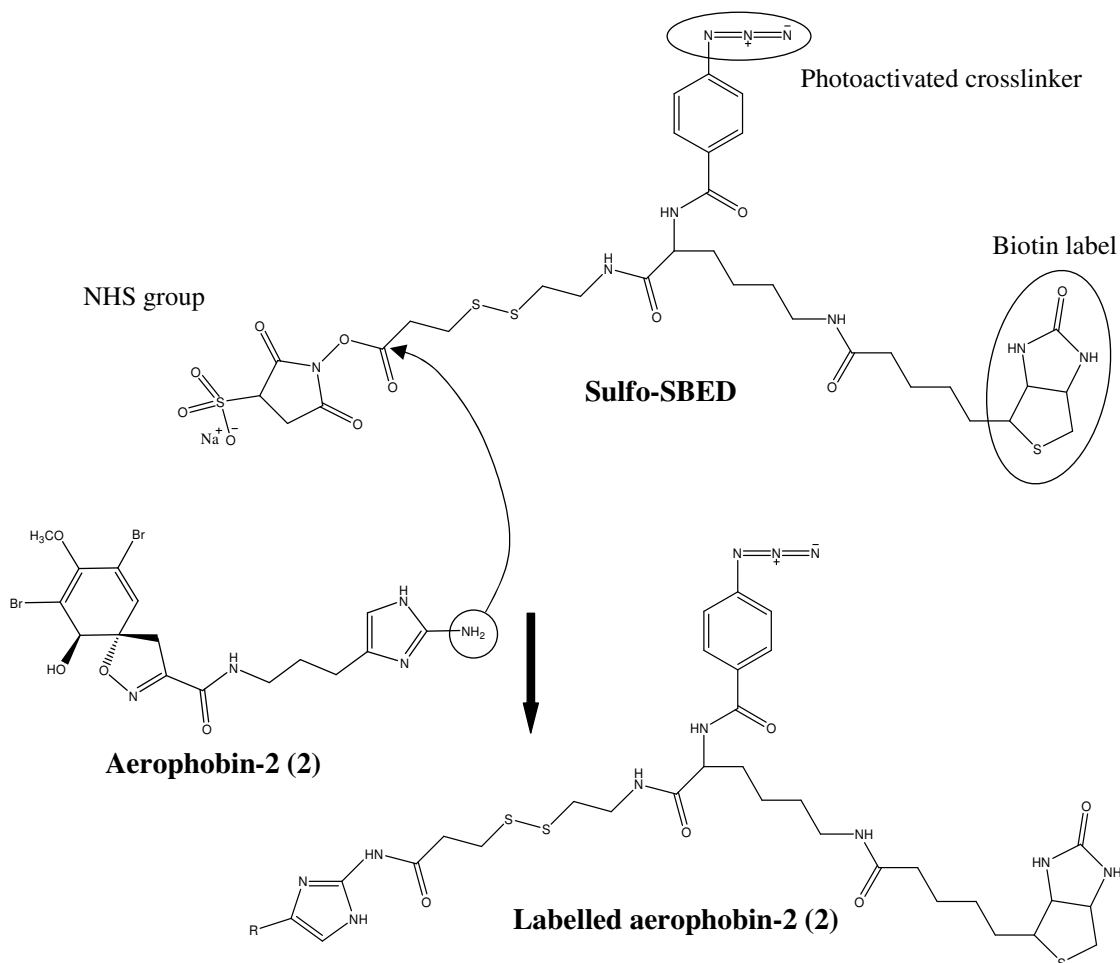


Figure III.5. Structure of the label transfer reagent Sulfo-SBED and the desired product after coupling of the substrate aerophobin-2 (2).

A 10 mg/ml solution of aerophobin-2 (2) was prepared in a 1/1 mixture of MeOH/0.2 M NaHCO₃ 0.5 M NaCl pH 8.3. Of this substrate solution, two aliquots of 28.8 μ l were pipetted into 1.5 ml eppendorf tubes wrapped with aluminium foil. 1 mg Sulfo-SBED solved in 25 μ l DMSO was added to one aliquot (LABEL) to give a twofold molar excess of Sulfo SBED over aerophobin-2 (2), while 25 μ l DMSO were

mixed with the second aliquot (BLANK). Both samples were mixed thoroughly. A volume of 2.5 μl of each solution was mixed with 47.5 μl HPLC MeOH and 0.66 μl 1 M Tris-HCl to block NHS groups for HPLC analysis (LABEL PRE and BLANK PRE). The remaining sample was incubated at room temperature in the dark for 30 min. After incubation, another aliquot of 2.5 μl was removed for HPLC analysis as described above (LABEL AFTER and BLANK AFTER). In addition, PRE and AFTER samples were analysed via LC-MS to confirm successful attachment of aerophobin-2 (2) to the Sulfo SBED label transfer reagent. A volume of 0.65 μl 1 M Tris-HCl was added to the remaining sample and incubated for 1 h at room temperature in the dark to block non-reacted NHS groups. Samples were finally frozen at $-80\text{ }^{\circ}\text{C}$ until usage.

Crosslinking the labelled substrate with the bound protein

For labelling, the most active fraction obtained from affinity chromatography was chosen. As for affinity chromatography, pH was crucial for the success of labelling, therefore pH of the protein solution employed was carefully checked prior to labelling (pH 8.3). To a protein sample volume equalling 11.54 μg protein 6 μl labelled aerophobin-2 (2) solution were added in a 1.5 ml eppendorf tube wrapped with aluminium foil. The sample was incubated for 1 h at $4\text{ }^{\circ}\text{C}$. After incubation, the tube was unwrapped, opened and positioned on ice under a UV lamp (6 W, 366 nm, distance to sample 5 cm) for 15 min. Subsequently samples were frozen at $-20\text{ }^{\circ}\text{C}$. Detection of the labelled protein(s) was achieved by Western blot as described below.

In addition, most active fractions derived from ion exchange chromatography were incubated with the labelled substrate. To a protein sample volume equalling 11.54 μg protein 6 μl labelled aerophobin-2 (2) solution were added in a 1.5 ml eppendorf tube wrapped with aluminium foil. In parallel, another aliquot of the same sample equalling 11.54 μg protein was added to 6 μl of a 1:10 diluted label solution. Samples were incubated for 1 h at $4\text{ }^{\circ}\text{C}$. After incubation, the tube was unwrapped, opened and positioned on ice under a UV lamp (6 W, 366 nm, distance to sample 5 cm) for 15 min. Subsequently samples were frozen at $-20\text{ }^{\circ}\text{C}$ prior to detection via Western blot.

Competition between labelled versus unlabelled aerophobin-2 (2)

In order to assess the specificity of labelling, an experiment was undertaken to outcompete the labelled aerophobin-2 (2) with the unlabelled substrate. To achieve this, 11.54 μg protein in a volume of 39 μl and 6 μl labelled aerophobin-2 (2) solution were added in a 1.5 ml eppendorf tube wrapped with aluminium foil. Another 5 μl of a

solution of respective concentration of unlabelled aerophobin-2 (2) (in 0.1 M Tris-HCl, 0.1 M NaCl, 2.5 x CMC FOS-choline 12 containing 5 % DMSO) was added after the scheme given in Table III.19.

Table III.19. Competition between labelled and unlabelled aerophobin-2 (2).

Protein (μg)	End conc. labelled aerophobin-2 (μM)	End conc. unlabelled aerophobin-2 (μM)	Ratio unlabelled / labelled aerophobin-2 (2)
11.54	0.00828	0.0000000	0
11.54	0.00828	0.0000828	1/10
11.54	0.00828	0.0008280	1
11.54	0.00828	0.0828000	100
11.54	0.00828	8.2800000	10000

Samples were incubated for 1 h at 4 °C. After incubation, tubes were unwrapped, opened and positioned on ice under a UV lamp (6 W, 366 nm, distance to sample 5 cm) for 15 min. Subsequently, samples were frozen at -20 °C. Detection of the labelled protein(s) was achieved by Western blot as described below.

Detection via Western blot

Protein samples that were crosslinked with labelled aerophobin-2 (2) and thus carried a biotin moiety were visualised by Western blot. Western blot is a technique to transfer proteins to a membrane, typically polyvinylidene difluoride (PVDF) or nitrocellulose with non-specific protein binding properties, where they are detected using antibodies specific to the target protein.

Buffers and solutions used for blotting

Table III.20 gives details of the buffers and solutions employed for Western blots and subsequent detection.

Blotting

In general, labelled proteins were separated by SDS PAGE as described above and subsequently transferred from the gel into the PVDF membrane by electroblotting using a semi-dry system (Figure III.6). Thereby the organisation of bands in the gel is maintained on the membrane. Six filter papers were cut into pieces approx. matching the size of the SDS gel and soaked in blot buffer (Table III.20). Three of these were applied as the bottommost layer of the “sandwich”.

Table III.20. Buffers and solutions used for Western blots.

Description	Purpose	Ingredients	End conc./ volume	Remarks
Blot buffer (10 x)	Blotting	10 x SDS MeOH Ultrapure water	100 ml 200 ml 700 ml	Dilute 1/10 with ultrapure water before usage
Ponceau	Staining	Ponceau S Acetic acid	0.02 % (w/v) 5 % (v/v)	
TBS (10 x)	Washing membranes	Tris-HCl, pH 8.0 NaCl	200 mM 2.5 M	Dilute 1/10 with ultrapure water before usage
TBS-T (10 x)	Washing membranes	Tris-HCl, pH 8.0 NaCl Tween 20	200 mM 2.5 M 1 % (v/v)	Dilute 1/10 with ultrapure water before usage
5 % BSA	Blocking	BSA 1 x TBS-T	0.5 g 10 ml	
3 % BSA	Detection	BSA 1 x TBS-T	0.3 g 10 ml	Add 1 μ l HRP* for a 0.01 μ g/ml solution
Stripping buffer	Stripping	Glycine SDS Tween 20 Ultrapure water	15 g 1 g 10 ml Ad 1 l	Set pH to 2.2 with HCl

* HRP = streptavidin conjugated horse radish peroxidase

The PVDF membrane was likewise cut to the right size and activated in MeOH (approx. 1 min) before it was positioned onto the filter papers. After the SDS gel was positioned on the membrane, another three filter papers concluded the upper layer of the sandwich, and blotting was performed for 1 h at 0.1 A (per gel, i.e. 0.2 A for two gels etc.). As positive control for blotting, a biotinylated goat-anti mouse antibody was applied to one lane of the SDS gel in parallel to the investigated samples.

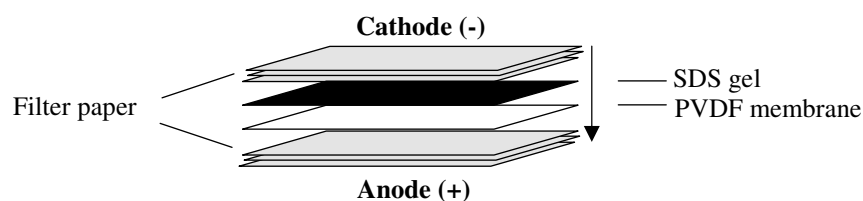


Figure III.6. Setup of the semi-dry blotting system.

Staining

Ponceau S is a rapid and reversible staining method for visualising proteins on the membrane after blotting by producing reddish pink stained bands. However, Ponceau S is less sensitive than Coomassie staining, thus only suited for the detection of highly concentrated protein samples. For staining, membranes were incubated in a 0.2 % (w/v) Ponceau S solution for 5-10 min under gentle agitation. After washing with water to wash off background colouration, the bands on the membrane were documented by scanning or by taking a picture on a detection Table (Syngene). Prior to blocking, membranes were washed with TBS-T buffer (Table III.20) for 5 min.

Blocking

As PVDF membranes are chosen for blotting due to their non-specific protein binding properties, interactions between the membrane and the antibody used for detection must be avoided. Therefore, membranes were incubated in a 5 % (w/v) BSA solution in TBS-T buffer under gentle agitation for 40 min to block non-specific binding. During this process, BSA attaches to the membrane surface which is not occupied by the target proteins transferred to the membrane during blotting, thereby reducing background noise during subsequent detection. After blocking, membranes were washed in TBS-T buffer for 5 min under gentle agitation.

Detection

For detection in general, the membrane is incubated with an antibody linked to a reporter enzyme which, when exposed to an appropriate substrate, drives a colourimetric reaction. This is usually achieved in two steps: In the first step, the membrane is probed with the primary antibody. Subsequently, membranes are incubated with a secondary antibody directed at a species-specific portion of the primary antibody. Most commonly, a horseradish peroxidase-linked secondary antibody is used in conjunction with a chemiluminescent agent, and the reaction product shows luminescence in proportion to protein amount.

However, the “probing” of proteins using a primary antibody (first step) was rendered unnecessary for the samples of this study since the target protein was already labelled and crosslinked with the aerophobin-2 (2) carrying a biotin moiety. Thus, only the second detection step was performed. Therefore, membranes were incubated in a 3 % BSA solution with 0.10-0.02 µg/ml (exact concentration was adjusted to protein concentration for each sample) streptavidin conjugated horse radish peroxidase (HRP)

for 1 h under gentle agitation (Table III.20). After subsequent washing (4 x 5 min in TBS-T buffer), the membrane was placed on a detection table (Syngene) and incubated with the ECL Advance™ Western Blotting Detection Kit (GE Healthcare) following the manufacturer's instructions. Pictures were taken at exposure times of 1 s, 5 s, 10 s, 20 s, 30 s, 60 s and 120 s with the GeneSnap software to visualise labelled protein bands.

Stripping membranes for reprobng

In some cases, i.e. to adjust the concentration of HRP in the detection solution, detection was repeated. In this context, HRP from the first detection needed to be stripped off the membrane by the following treatment: The membrane was incubated in stripping buffer (Table III.20) for 2 x 10 min, in TBS buffer for 2 x 10 min, in TBS-T buffer for 5 min, in MeOH (to reactivate the membrane) for 1 min, and another 5 min in TBS-T buffer under gentle agitation. Blocking and detection could then be repeated (with adjusted HRP concentration) as described above.

Trypsin digestion and mass analysis of the isoxazoline cleaving enzyme

Bands clearly labelled in the Western blot which could be unequivocally identified on SDS PAGE were cut out of gels and submitted to trypsin digestion and subsequent mass analysis at the BMFZ (Biologisch-Medizinisches Forschungszentrum, HHU Düsseldorf). All works described subsequently were conducted by the coworkers of the BMFZ. Table III.21 shows the chemicals used by the BMFZ.

Table III.21. Chemicals used for washing, digestion and elution of proteins.

Company	Description
Merck	Acetonitrile, HPLC grade
Fluka	Ammonium bicarbonate, p.a. Formic acid, p.a.
Promega	Trypsin V511A, Sigma proteomics grade T6567

Washing of proteins

Target proteins were cut out of the gel, carved into pieces of approx. 1 mm³ and transferred into 0.5 ml eppendorf tubes. Special attention was paid to avoid contamination with keratin. In order to wash off the Coomassie stain, gel pieces were washed with a destaining solution. Afterwards, 100 µl of a 1/1 mixture of 25 mM ammonium bicarbonate/acetonitrile were added and samples incubated for 10 min unter gentle agitation. The fluid was then carefully removed and transferred into a separate

Eppendorf tube. Another 100 µl of the 25 mM ammonium bicarbonate/acetonitrile mixture were added to the gel pieces and samples incubated for 30 min under gentle agitation. Again, the fluid was collected in a separate tube. This step was repeated for another two times. In a last step, gel pieces were washed with 100 % acetonitrile for 30 min, thus completely dehydrating the gel. After removal and collection of the washing solution, gel pieces were dried completely via vacuum centrifugation.

Digestion of proteins

Dry gel pieces were rehydrated in 1 volume trypsin solution (0.1 µg/µl in cold 25 mM ammonium bicarbonate buffer pH 8) for 30 min. To avoid drying of the gel pieces during digestion, samples were covered with 25 mM ammonium bicarbonate buffer, and incubated for 12 - 16 h at 37 °C.

Elution of digested proteins from the gel

After digestion of proteins in the gel pieces, samples were centrifuged and the supernatant transferred into new tubes. Two volumes of water were added to the gel pieces, samples incubated for 5 min on a shaker, 5 min in the ultrasonic bath, centrifuged again and the supernatant collected in a new tube. Subsequently, gel pieces were washed with an elution solution (50 % acetonitrile, 5 % formic acid, 45 % water) and incubated for 30 min. This procedure was repeated twice before one volume of 100 % acetonitrile was used to dehydrate gel pieces, thereby removing all remaining peptides. These samples were incubated under gentle agitation for 30 min, centrifuged and the supernatant collected in new tubes. The collected eluted peptides were dried via vacuum centrifugation and stored at -20 °C.

Mass analysis

Peptides obtained after trypsin digestion were analysed either by MALDI-TOF (self constructed) or ESI-QqTOF (Hybrid mass spectrometer, QSTAR XL, Applied Biosystems). Particularly sensible protein separation was provided by Nano-HPLC (Ultimate, Dionex) which can be coupled to both mass spectrometers both on- and offline. Amino acid sequences homologous to those obtained were searched for in different protein databases (EMBL via WU Blast2, Mascot by the BMFZ) in order to shed light on the identity and type of the purified protein.

Results

This chapter summarises the outcome of experiments aiming at the purification and characterisation of the isoxazoline cleaving enzyme of the sponge *Aplysina aerophoba* collected in the Mediterranean Sea (Rovinj, Croatia).

Differential centrifugation

In order to achieve a first separation of the proteins contained in solubilised sponge cells, differential centrifugation was applied. The activity assay served to track the isoxazoline cleaving enzyme in fractions. For sake of comparability, volumes equalling a protein amount of 5 μg were employed to determine the activity of each fraction. In the first centrifugation step separating cell debris, unsolubilised cells and cell nuclei, most activity was found in the supernatant (S1, 39 %, Figure III.7). After the second centrifugation step removing cell organelles, most of the product aeroplysinin-1 (1) was detected in the supernatant (S2, 71 %, Figure III.7). The third centrifugation step yielded soluble cell ingredients in the supernatant (S3) and membranes in the pellet (P3).

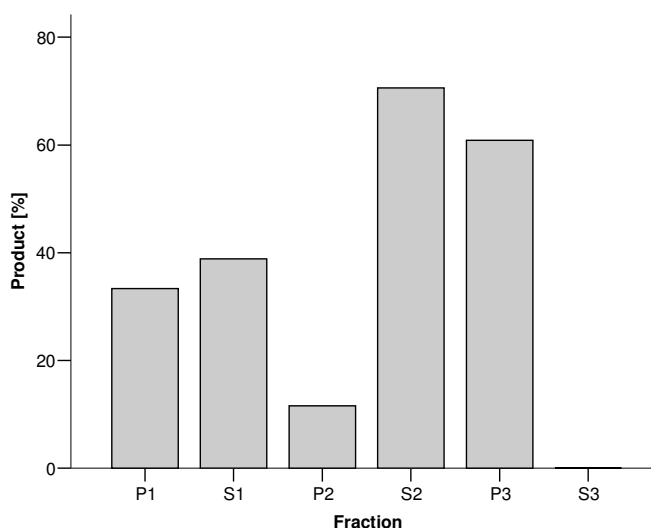


Figure III.7. Relative amount of the product aeroplysinin-1 (1) (in %, calculated as nmol aeroplysinin-1 in respective sample divided by nmol aeroplysinin-1 in control sample where aerophobin-2 was completely transformed into aeroplysinin-1) detected via the activity assay in fractions derived from differential centrifugation, i.e. pellet (P1) and supernatant (S1) of the first, Pellet (P2) and supernatant (S2) of the second, and pellet (P3) and supernatant (S3) of the third centrifugation step. Activity assay: 5 μl substrate solution (aerophobin-2 (2), 19.8 μM), 5 μg protein (volume depended on protein concentration of each fraction), filled up to a final assay volume of 50 μl with 50 mM citrate buffer, pH 5.8.

Monitoring activity of these fractions unambiguously showed that the isoxazoline cleaving enzyme is located in the membrane fraction (P3, Figure III.7), since activity was exclusively found in P3 (61 %) in contrast to the supernatant where no product (aeropylsinin-1 (1)) was detectable (Figure III.7).

Protein concentration of each fraction obtained was determined by the Bradford assay. Table III.22 gives an overview over protein concentrations and total protein yield of each fraction. Comparison of several differential centrifugation attempts following the same protocol showed that protein concentration of the membrane fraction P3 was well reproducible ($1.9 \text{ mg/ml} \pm 0.2$, $N = 3$). However, it needs to be emphasised that measurement of protein concentration of P3 membrane fractions by the Bradford assay cannot be accurate since the membrane proteins are not solubilised. Reliable values for protein concentration were obtained after solubilisation of membranes which will be described in a separate chapter (see below).

Table III.22. Protein concentrations and total amounts of fractions derived from differential centrifugation.

Fraction	Protein conc. (mg/ml)*	Total volume (ml)	Total protein content (mg)
P1	2.2	16.0	34.9
S1	3.1	200.0	625.6
P2	1.2	16.0	18.5
S2	2.9	207.9	608.5
P3	1.9	6.0	11.7
S3	2.7	212.7	578.3

* Protein concentration measured in triplicate in different dilutions.

Of all fractions, 5 μl were applied to a 10 % SDS polyacrylamide gel to monitor their band patterns. Not unexpectedly, band patterns were very complex (Figure III.8). One band of a large protein barely entering the separating gel appeared to be exclusively found in S1, S2 and especially P3.

Washing membranes with sodium carbonate

As differential centrifugation could unambiguously show that the isoxazoline cleaving enzyme is located in the membrane fraction (P3), the question arose whether it is an integral or a non-integral membrane protein. Washing membranes with ice cold sodium carbonate buffer, pH 11.5, should shed light on this issue.

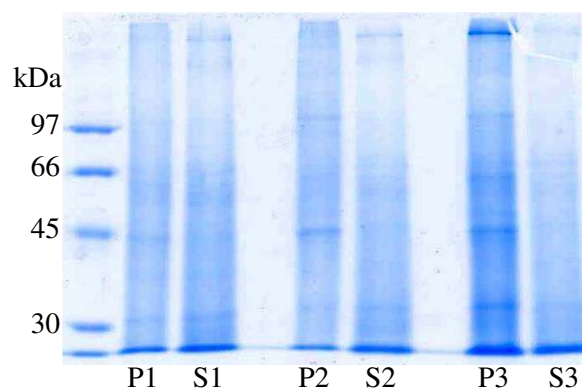


Figure III.8. SDS PAGE (10 %) of differential centrifugation fractions, i.e. pellet (P1) and supernatant (S1) of the first, pellet (P2) and supernatant (S2) of the second, and pellet (P3) and supernatant (S3) of the third centrifugation step. 5 μ l of each fraction were applied to the gel.

The strongly alkaline pH causes a negative charge of both proteins and membranes, thus repelling each other and causing the non-integral proteins to be stripped off the membrane. After a centrifugation step, non-integral and vesicular proteins are obtained in the supernatant, whereas integral membrane proteins accumulate in the pellet. As for differential centrifugation, the isoxazoline cleaving enzyme was identified by employment of both pellet and supernatant in the activity assay.

Figure III.9 shows the relative amount of the product aeroplysinin-1 (1) emerging in the activity assay for the supernatant and pellet obtained after washing membranes with sodium carbonate buffer. The activity of untreated membranes as control was set as 100 %. While aeroplysinin-1 (1) was clearly detectable in the pellet (56 %), this was not the case for the supernatant where the product was not detectable at all.

The reduced activity of the pellet when compared to the control can be explained by the harsh treatment at pH 11.5. It is even surprising that after this treatment, over 50 % of the activity could be regenerated. However, it could undoubtedly be inferred that the isoxazoline cleaving enzyme is an integral membrane protein.

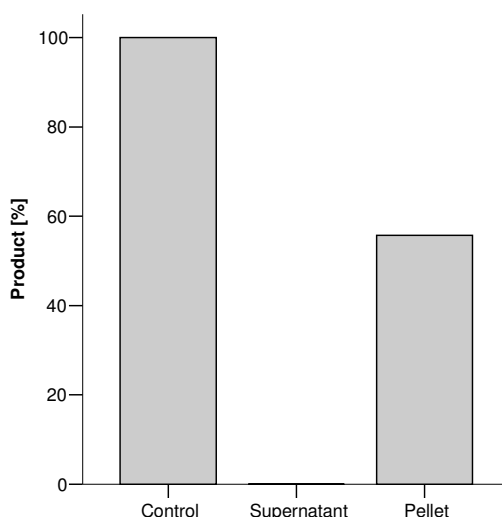


Figure III.9. Relative amount of the product aeropylsinin-1 (1) (in %) detected in pellet and supernatant derived after incubation of the membrane fraction P3 with ice cold sodium carbonate buffer of pH 11.5 and subsequent centrifugation at 100000 x g. Untreated membranes (P3) served as positive control, whose relative amount of product was set as 100 %. Activity assay: 8 μ l substrate solution (aerophobin-2 (2), 39.6 μ M), 16 μ l protein solution (adjusted to pH 5.8), filled up to a final assay volume of 40 μ l with 50 mM citrate buffer, pH 5.8.

Solubilisation of cell membranes

The finding that the isoxazoline cleaving enzyme is an integral membrane protein necessitated the screening of different detergents to solubilise membranes for further processing. The aim was to find optimal solubilisation conditions in terms of protein functionality, yield of solubilised protein and storage.

Screening of different detergents

In a first screening, different types of detergents were tested to identify the most suitable one for solubilisation of the isoxazoline cleaving enzyme. Therefore, the non-ionic detergents Tween 20 and n-dodecyl- β -D-maltopyranoside (DDM), the anionic detergent sodium cholate and the zwitterionic detergent FOS-choline 12 were employed. Membranes obtained by ultracentrifugation (P3) were incubated with these detergents for 1 h on ice and centrifuged subsequently for 1 h at 100000 x g. Functionality of the target protein was tested by quantification of the product of both supernatant and pellet in the activity assay. Untreated membranes (P3) served as positive control. Figure III.10 reveals that differences after treatment with various detergents were not large. However, FOS-choline 12 gave a slightly better result than

the other detergents with 96 % activity in the pellet and 100 % activity in the supernatant. The anionic detergent sodium cholate showed a comparable result, although activity was lower (supernatant: 93 %, pellet: 92 %). The non-ionic detergents Tween 20 (supernatant: 83 %, sellet: 93 %) and DDM (supernatant: 90 %, pellet: 95 %) yielded higher activity in the pellet, indicating that solubilisation, at least at the concentration tested, was slightly less efficient as for the zwitterionic detergent FOS-choline 12. As a consequence, FOS-choline 12 was chosen as detergent for solubilisation of membranes in all further attempts to purify the isoxazoline cleaving enzyme.

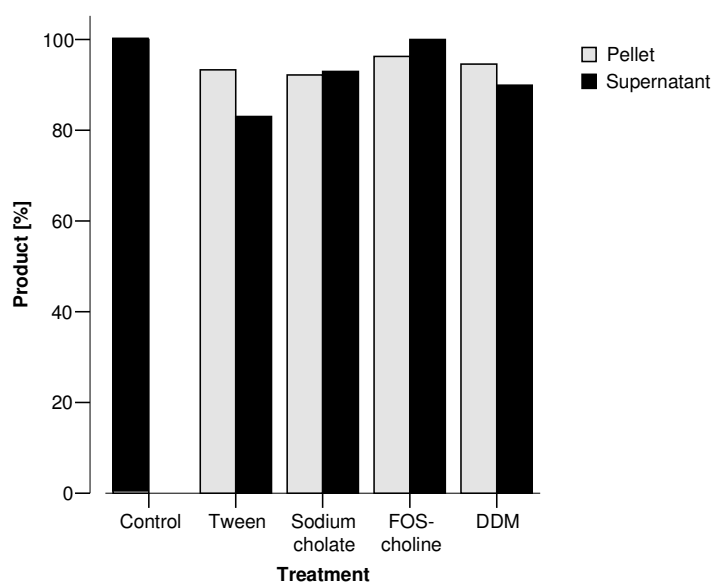


Figure III.10. Relative amount of the product aeropylsinin-1 (1) (in %) detected in pellet and supernatant derived after incubation of the membrane fraction P3 with different detergents and subsequent centrifugation at 100000 x g. Untreated membranes (P3) served as positive control, whose relative amount of product was set as 100 %. Activity assay: 8 μ l substrate solution (aerophobin-2 (2), 39.6 μ M), 16 μ l protein solution, filled up to a final assay volume of 40 μ l with 50 mM citrate buffer, pH 5.8.

Optimal solubilisation and storage conditions

Two aspects were crucial when attempting to find optimal solubilisation conditions for the membrane fraction P3, (1) solubilisation efficiency and (2) storage of samples. Since membranes treated with FOS-choline 12 proved to retain most of their activity when compared to other detergents, further experiments were aimed at finding optimal conditions for solubilisation with this detergent.

In a first approach, the optimal detergent concentration should be determined, thus membranes were incubated with final concentrations of 0.50, 0.75, 1.00 and 1.25 %

FOS-choline 12 for 1 h on ice. After centrifugation, activity of both supernatant and resuspended pellet was assessed as given in Figure III.11. It became obvious that a final concentration of FOS-choline 12 of 0.75 % yielded best results with respect to solubilisation efficiency (major activity in the supernatant) and functionality of the isoxazoline cleaving enzyme (Figure III.11).

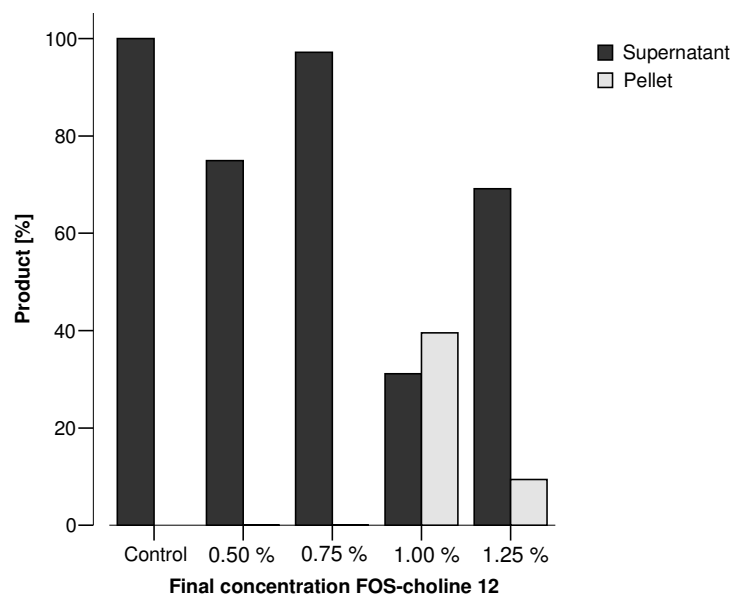


Figure III.11. Relative amount of the product aeropylsinin-1 (1) (in %) detected in pellet and supernatant derived after incubation of the membrane fraction P3 with different detergent concentrations and subsequent centrifugation at 100000 x g. Untreated membranes (P3) served as positive control, whose relative amount of product was set as 100 %. Activity assay: 5 μ l substrate solution (aerophobin-2 (2), 19.8 μ M), 2 μ l protein solution (diluted 1:10), filled up to a final assay volume of 50 μ l with 50 mM citrate buffer, pH 5.8.

In a further experiment, the influence of different detergent concentrations was tested in combination with storage conditions. Therefore, membranes were incubated with final concentrations of 0.50, 0.75, 1.00 and 1.25 % FOS-choline 12 for 1 h on ice, centrifuged (1 h, 100000 x g) and submitted to the following treatment. One aliquot of each sample was directly investigated via the activity assay. Another aliquot was stored in the fridge and activity checked after one day and after seven days, respectively. The remaining sample was divided into three aliquots. One of these was thawed after one day, the second after seven days and activity determined in the activity assay. The third aliquot was thawed and frozen once per day over a period of seven days (in total six freezing and thawing cycles), and activity assessed after these seven days. Untreated membranes served as positive control, activity of these was set as 100 %. Figure III.12 shows the outcome of this experiment. A detergent concentration of 0.75 % showed best

results for a storage over night, with storage at $-20\text{ }^{\circ}\text{C}$ yielding better activity (81 %, 16 % less in comparison to the sample where activity was determined directly without storage) when compared to the sample stored at $4\text{ }^{\circ}\text{C}$ (51 %, Figure III.12 a). Likewise, a final concentration of 0.75 % FOS-choline 12 proved to yield best results after seven days at $-20\text{ }^{\circ}\text{C}$ (64 %, 33 % less in comparison to the sample where activity was determined directly without storage, Figure III.12 b). Storage at $4\text{ }^{\circ}\text{C}$ and repeated freezing and thawing cycles had a detrimental effect on enzyme activity.

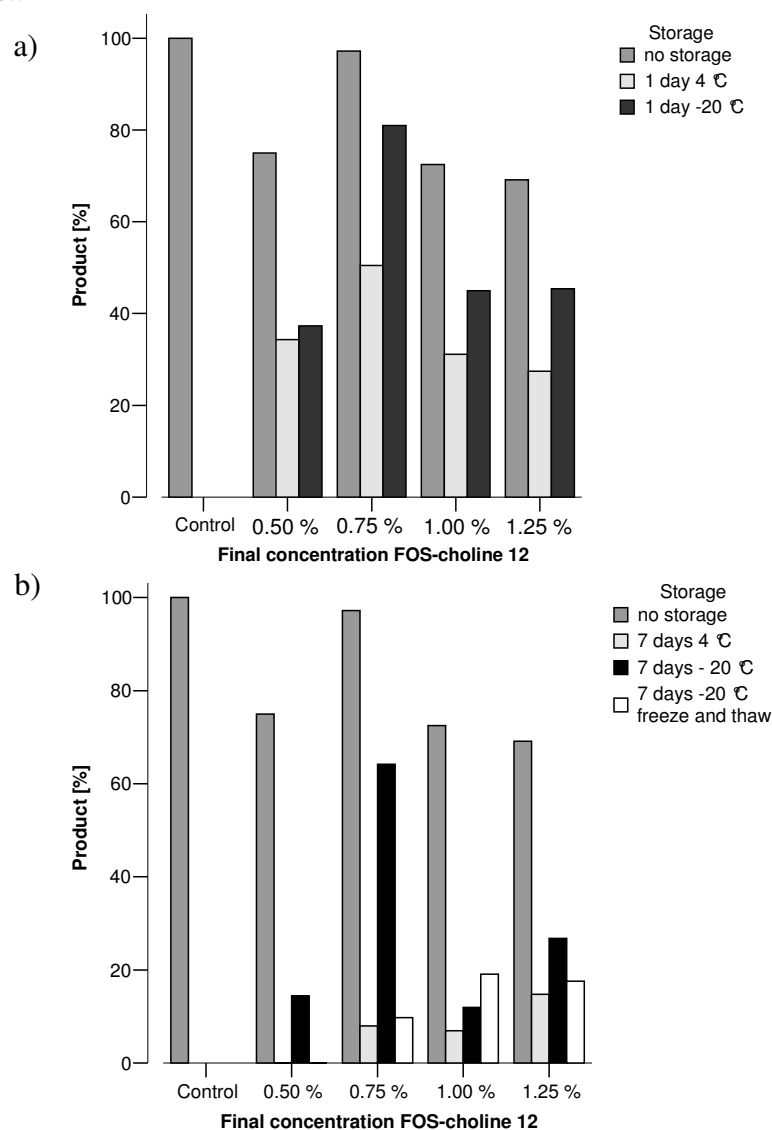


Figure III.12. Relative amount of the product aerophysinin-1 (1) (in %) detected in the supernatant derived after incubation of the membrane fraction P3 with different detergent concentrations and subsequent centrifugation at $100000 \times g$. Samples were a) stored for one day either at $4\text{ }^{\circ}\text{C}$ or at $-20\text{ }^{\circ}\text{C}$, or b) stored for seven days at $4\text{ }^{\circ}\text{C}$ or at $-20\text{ }^{\circ}\text{C}$, where samples either stayed frozen or were subjected to repeated freezing- and thawing cycles. Untreated membranes (P3) served as positive control, whose relative amount of product was set as 100 %. Activity assay: $5\text{ }\mu\text{l}$ substrate solution (aerophobin-2 (2), $19.8\text{ }\mu\text{M}$), $2\text{ }\mu\text{l}$ protein solution (diluted 1:10), filled up to a final assay volume of $50\text{ }\mu\text{l}$ with 50 mM citrate buffer, pH 5.8.

In order to further improve solubilisation and storage conditions in terms of enzyme activity, the influence of different concentrations of NaCl was tested in combination with a final FOS-choline 12 concentration of 0.75 % which proved to be best suited in former experiments as described above. Membranes obtained from ultracentrifugation (P3) were incubated with final concentrations of 0, 100, and 200 mM NaCl and a final detergent concentration of 0.75 % for 1 h on ice, centrifuged (1 h, 100000 x g) and submitted to the following treatment. One aliquot of each sample was directly investigated via the activity assay. Another aliquot was stored in the fridge and activity checked after one day and after seven days, respectively. The remaining sample was divided into three aliquots, of which one was thawed after one day and activity determined in the activity assay, the second after seven days, and the third one repeatedly thawed and frozen (in total six freezing and thawing cycles). Untreated membranes served as positive control, activity of these was set as 100 %.

As demonstrated by Figure III.13 a, most activity was obtained if solubilisation was performed under addition of 200 mM NaCl (63 % when compared to untreated membranes). However, for storage over night (Figure III.13 a) as well as for seven days (Figure III.13 b), a concentration of 100 mM yielded best results, with 58 % and 53 % activity, respectively, when compared to untreated membranes. Loss of activity in samples stored at -20 °C for one and for seven days added up to 5 % and 10 %, respectively, when compared to the sample where activity was determined directly without storage (Figure III.13 b). For storage at 4 °C, activity was lost almost completely after seven days (Figure III.13 b). Likewise, repeated freezing and thawing cycles were disadvantageous in terms of activity (Figure III.13 b). In summary, solubilisation could be optimised by adding a final concentration of 100 mM NaCl to samples, thereby reducing losses after storage of samples at least at -20 °C.

In conclusion, a standard protocol emerged based on these results. Membranes obtained from ultracentrifugation were solubilised with final concentrations of 0.75 % FOS-choline 12 and 100 mM NaCl by incubation on ice for 1 h and thorough mixing every 15 min. After centrifugation for 1 h at 100000 x g (4 °C), solubilised membranes were gathered in the supernatant, which could then be employed for various purification procedures. Protein concentration of solubilised membranes was 8.4 ± 0.6 mg/ml (N = 6, total yield for 20 g lyophilised sponge tissue: 67.2 mg protein). In general, solubilisation was performed shortly before each purification attempt to avoid freezing and thawing. Activity assays and all experiments relying on good activity of fractions

(e.g. crosslinking of the aerophobin-2 (2)-binding protein with labeled substrate) were directly performed after the respective purification step. Afterwards, samples were frozen at $-20\text{ }^{\circ}\text{C}$ for further processing (e.g. SDS PAGE or quantification of protein concentration in the Bradford assay).

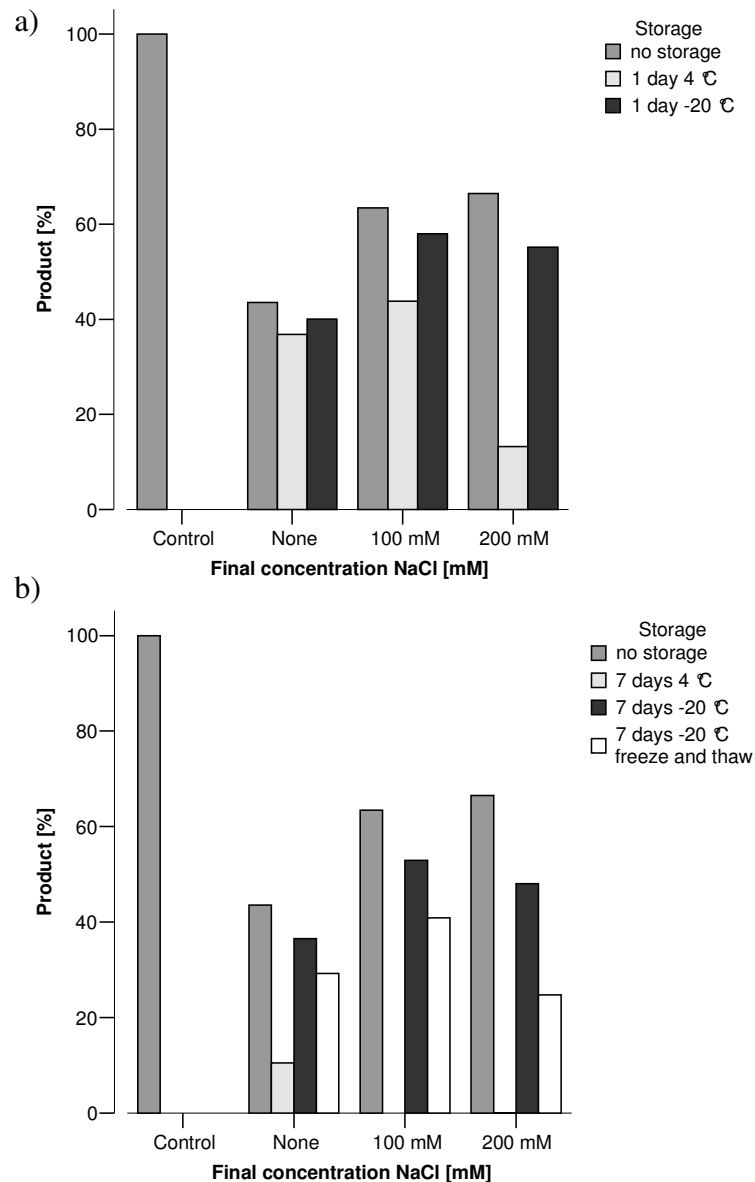


Figure III.13. Relative amount of the product aerophysinin-1 (1) (in %) detected in the supernatant derived after incubation of the membrane fraction P3 with different NaCl concentrations and subsequent centrifugation at $100000 \times g$ (final FOS-choline 12 concentration = 0.75 %). Samples were a) stored for one day either at $4\text{ }^{\circ}\text{C}$ or at $-20\text{ }^{\circ}\text{C}$, or b) stored for seven days at $4\text{ }^{\circ}\text{C}$ or at $-20\text{ }^{\circ}\text{C}$, where samples either stayed frozen or were subjected to repeated freezing- and thawing cycles. Untreated membranes (P3) served as positive control, whose relative amount of product was set as 100 %. Activity assay: $5\text{ }\mu\text{l}$ substrate solution (aerophobin-2 (2), $19.8\text{ }\mu\text{M}$), $2\text{ }\mu\text{l}$ protein solution (diluted 1:10), filled up to a final assay volume of $50\text{ }\mu\text{l}$ with 50 mM citrate buffer, pH 5.8.

Ion exchange chromatography

Solubilised membranes were purified via ion exchange chromatography involving 1 ml columns prepacked with strong anion exchange (HiTrap Q FF, GE Healthcare) and strong cation exchange (HiTrap SP FF, GE Healthcare) material, respectively. Solubilisation was done just prior to the application of solubilised membranes to the column. The Äkta-FPLC[®] system employed was located in a cooling cabinet to keep temperature at 4 °C. 8 ml of solubilised membranes (= 67.2 mg protein) were applied to the column. A gradient of buffer A (50 mM citrate buffer, pH 5.8, 2.5 x CMC FOS-choline 12) and B (buffer A plus 1 M NaCl) served as mobile phase. Proteins eluted from the column were detected at 280 nm. Figure III.14 depicts the chromatogram obtained for the purification of solubilised membranes over the anion exchange column HiTrap Q FF.

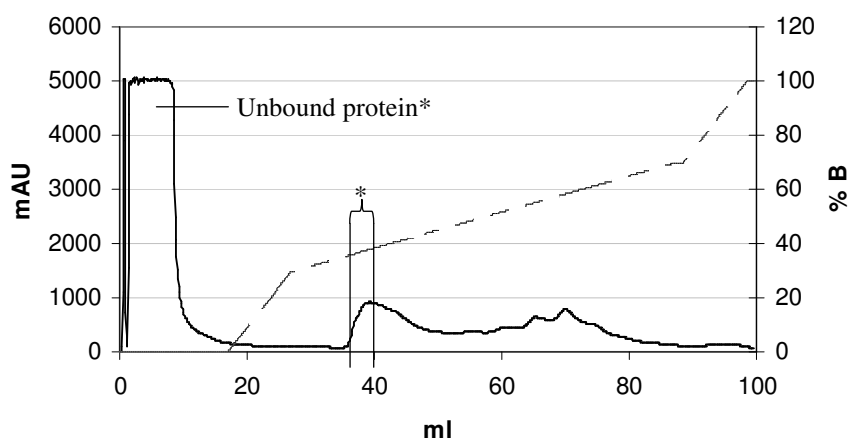


Figure III.14. Chromatogram obtained for the purification of solubilised membranes over an anion exchange column (HiTrap Q FF, detection at 280 nm, solid line). A gradient of buffer A (50 mM citrate buffer, pH 5.8, 2.5 x CMC FOS-choline 12) and B (buffer A plus 1 M NaCl) served as mobile phase (% B represented by the dashed line). Most active fractions (> 90 % activity) are marked by asterisks.

Table III.23 summarises activity and protein concentration for the active fractions. In the first four fractions, proteins that did not bind to the column were obtained. These fractions proved to be highly active in the activity assay. However, activity was also clearly detected in fractions with proteins eluted from the column at approx. 350 mM NaCl. Specific activity was highest for fractions 23 and 24 (approx. 11 % per μg protein), and lowest for the unbound protein collected in the first fractions (3 % per μg protein, Table III. 23).

Table III.23. Protein concentrations ($\mu\text{g/ml}$), activity (%) and specific activity (% activity per μg protein) of most active fractions derived from ion exchange chromatography over a HiTrap Q FF column.

Fraction	Protein conc. ($\mu\text{g/ml}$)	Activity (%)	Protein in assay (μg)	Specific activity (%)
1	2027.1	12.3	4.1	3.0
21	343.8	91.8	15.5	5.9
22	214.6	93.7	9.7	9.7
23	200.0	99.7	9.0	11.1
24	175.0	91.0	7.9	11.6
25	202.1	90.3	9.1	9.9

To monitor the purity of active fractions and band patterns of highly active versus less active fractions, samples were applied to 10 % SDS PAGE. Since protein concentrations were comparably low, proteins were precipitated with 100 % TCA. Precipitation volumes were calculated according to protein concentration of each fraction in order to guarantee comparable amounts of protein applied to the gel. Figure III.15 shows the SDS PAGE prepared for the fractions obtained by anion exchange chromatography. Complexity of band patterns hampered the identification of bands that might correlate to activity of fractions.

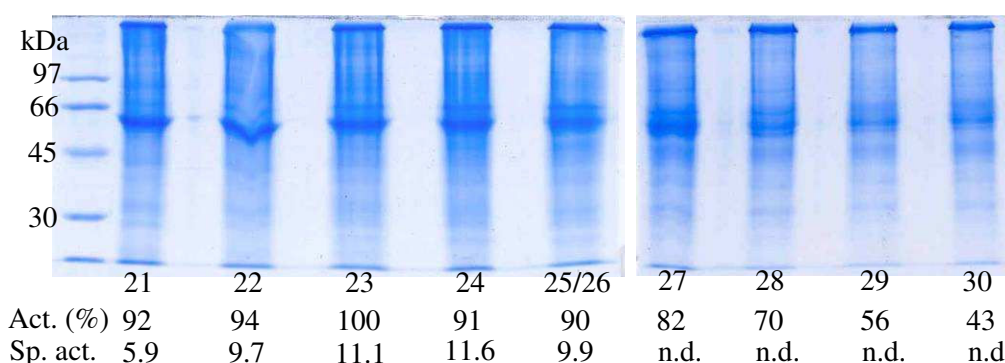


Figure III.15. SDS PAGE (10 %) of fractions obtained from anion exchange chromatography. “Act.” represents the activity in %, “Sp. act.” the specific activity in % per μg protein (just given for the most active fractions, n.d. = not determined). Proteins in all fractions were precipitated with 100 % TCA to yield approx. 50 μg protein applied to the gel.

As an alternative to purification over anion exchange material, a strong cation exchanger, HiTrap SP FF, was employed. However, no activity could be detected in any of the fractions obtained from the latter. This might possibly be attributed to the necessity to use a mobile phase of pH 4.0, probably rendering conditions too harsh for the isoxazoline cleaving enzyme. Cation exchange chromatography was thus not pursued any further.

After usage, columns were stained violet-black by polymerisation products of the sponge pigment urandine (5). However, reuse of old HiTrap Q FF columns showed that the accumulation of pigment did not interfere with purification, at least not upon second usage. In order to exclude that the proteins obtained in the first fractions of ion exchange chromatography did not bind to the column due to an overload of the column, this fraction was reappplied to a new column. However, no protein bound to the new material, thereby confirming that the column was not overloaded. In conclusion, purification via HiTrap Q FF columns yielded good results in terms of both activity of the obtained fractions and reproducibility of chromatograms. However, since band patterns were still very complex, ion exchange chromatography could just represent the first of further purification steps.

Gel filtration

Gel filtration was employed as a further purification step following ion exchange chromatography. For this purpose, the most active fraction obtained from ion exchange chromatography was chosen. 500 µl of this fraction were applied to a Superdex 200 10/300 (GE Healthcare) gel filtration column (= 100 µg protein). The Äkta-FPLC[®] system employed was located in a cooling cabinet to keep temperature at 4 °C. A 50 mM citrate buffer, pH 5.8, 2.5 x CMC FOS-choline 12 either without NaCl, 100 mM or 1 M NaCl served as mobile phase. Proteins eluted from the column were detected at 280 nm. In a first approach, buffer without NaCl was employed as mobile phase, but no activity was detected in any of the fractions. Since it was suspected that the isoxazoline cleaving activity might be due to several proteins that were separated by gel filtration, several fractions were combined in different combinations and activity assessed again. However, activity could still not be detected. Increasing protein concentration of fractions via centrifugal devices likewise did not yield activity. Figure III.16 a shows the chromatogram obtained for the purification of ion exchange fractions over the gel filtration column using a mobile phase without NaCl. It was characterised by a large peak of a protein eluting at approx. 18 ml (Figure III.16 a). In contrast, when the mobile phase contained either 100 mM or 1 M NaCl, active fractions were detected. The chromatograms shown in Figure III.16 b and c look almost identical, but differ completely from Figure III.16 a where no NaCl was employed in the mobile phase. When elution was achieved with a buffer containing 100 mM and 1 M NaCl,

respectively, a prominent peak at approx. 10 ml appeared which corresponded to the active fractions (Figure III.16 b and c).

Table III.24 summarises activity of all active fractions, and protein concentration for the most active fraction. No data are shown for gel filtration using a buffer without NaCl since no active fractions were detected. In comparison, a mobile phase with 100 mM NaCl appears more advantageous in terms of both activity and number of active fractions obtained. However, activity was significantly lower when compared to fractions obtained from ion exchange chromatography, which might be due to the reduced amount of protein applied to the gel filtration column (ion exchange ≈ 8 ml x 8 mg/ml = 64 mg; gel filtration ≈ 0.5 ml x 200 μ g/ml = 100 μ g).

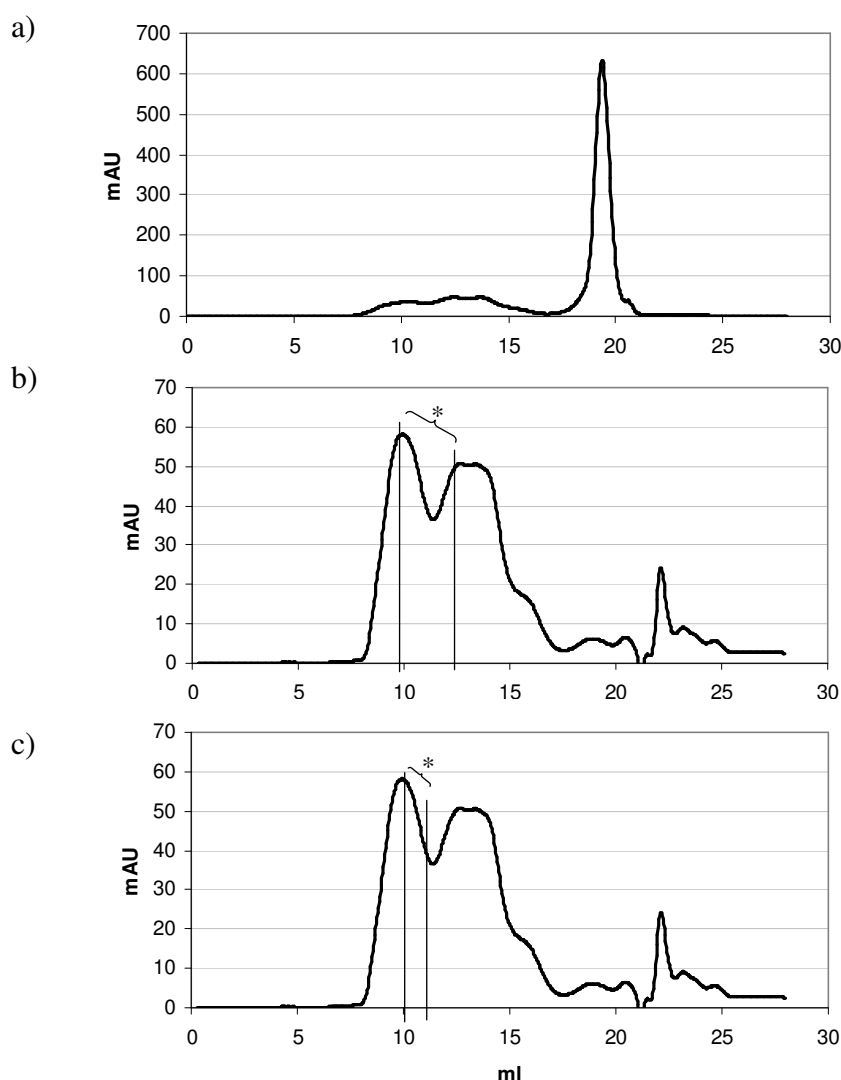


Figure III.16. Chromatograms obtained for the purification of ion exchange fractions over a gel filtration column (Superdex 200, detection at 280 nm). a) Mobile phase without NaCl, b) with 100 mM NaCl, c) with 1 M NaCl. Active fractions (> 2.5 %) are marked by asterisks (*).

When considering protein amounts as given in Table III.24 it becomes obvious that concentrations were too low to be reliably determined via the Bradford assay. Thus, values for specific activity could not be reliably determined.

Table III.24. Protein concentrations ($\mu\text{g/ml}$) and activity (%) of active fractions derived from gel filtration with mobile phases of different NaCl concentrations.

NaCl conc.	Frac-tion	Protein conc. ($\mu\text{g/ml}$)	Activity (%)	Protein in assay (μg)
100 mM	18		4.5	
	19		6.0	
	20		8.4	
	21		8.6	
	22	46.7	9.6	2.1
	23		8.3	
	24		5.0	
1 M	19		2.7	
	20	6.2	3.2	0.3
	21		2.8	

To monitor the purity of active fractions and band patterns of active versus inactive fractions, samples were applied to 10 % SDS PAGE. Since protein concentrations were comparably low, proteins were precipitated with 100 % TCA. Precipitation volumes were calculated according to protein concentration of each fraction in order to load comparable amounts of protein to the gel. Figure III.17 shows the SDS PAGE prepared for the fractions obtained by gel filtration (mobile phase with 100 mM NaCl).

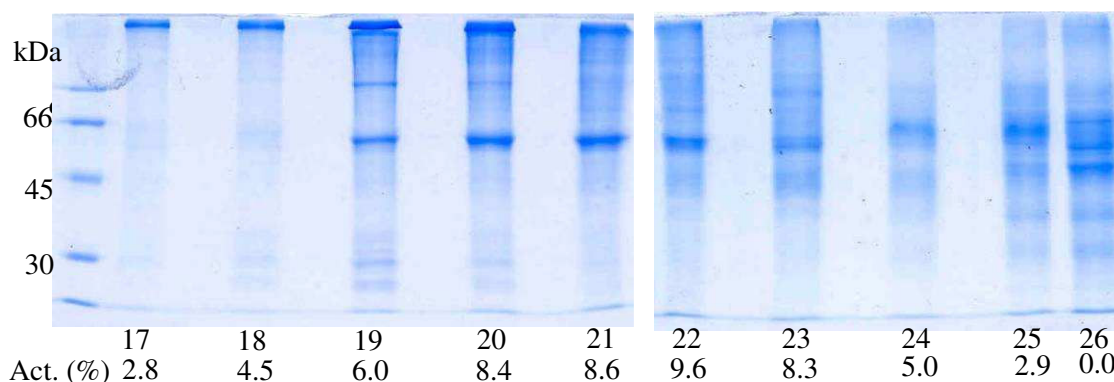


Figure III.17. SDS PAGE (10 %) of fractions obtained from gel filtration with 100 mM NaCl in the mobile phase. "Act." represents the activity in %. Proteins in all fractions were precipitated with 100 % TCA to yield approx. 50 μg protein applied to the gel. However, due to low protein concentrations, measurements of the latter are not accurate.

Gel filtration fractions were still complex on SDS PAGE. Two prominent bands, one of a protein of approx. 60 kDa and the other represented by the band barely entering the separating gel, appeared to be correlated with activity since they were most prominent in the most active fractions (21-23). In conclusion, gel filtration fractions were not of sufficient purity for a characterisation of the isoxazoline cleaving enzyme. However, further purification steps were not attempted due to the low protein yield and activity of fractions. Further fractionation would most probably cause additional loss of activity, thereby rendering the identification of fractions containing the isoxazoline cleaving enzyme impossible. Thus, affinity chromatography was chosen as a completely different approach as described in the next chapter.

Although not providing satisfactory results in terms of purification, gel filtration yielded some further information concerning the size of the isoxazoline cleaving enzyme. In order to get an estimate about the size of the target protein, the Superdex 200 gel filtration column used to purify the most active fractions of ion exchange chromatography was calibrated with size standards. A calibration curve was obtained by plotting the logarithms of the known molecular weights of the size standards versus their respective V_0/V_e values (Figure III.18). V_e is the elution volume of the respective protein, and V_0 the void volume of the column as determined by a large protein, in this case blue dextran (2000 kDa). Determination of the elution volume of the isoxazoline cleaving enzyme (10.5 ml, inferred by identification of active fractions) allowed for the calculation of the molecular weight of this protein, which was estimated as ≈ 540 kDa.

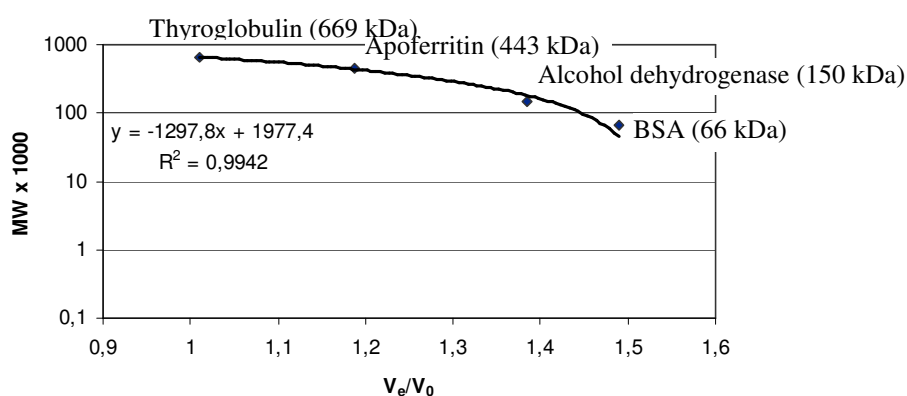


Figure III.18. Calibration curve obtained by plotting logarithms of molecular weights of size standards versus their respective V_0/V_e values, where V_e is the elution volume of the respective protein, and V_0 the void volume of the column as determined by blue dextran (2000 kDa).

Affinity chromatography

The fact that one of the substrates of the isoxazoline cleaving enzyme, aerophobin-2 (2) possesses a primary amine group led to an attempt to immobilise the substrate on an agarose matrix for affinity chromatography. N-hydroxy-succinimide activated sepharose (NHS) is a material particularly suited for this purpose. However, before considering affinity chromatography as a means to purify the isoxazoline cleaving enzyme, it was crucial to find conditions where the enzyme is inactive (and thus does not cleave the substrate, aerophobin-2 (2)), but can still bind the substrate. Furthermore, activity should be reconstituted when conditions are optimal for enzyme activity in order to identify active fractions. Several factors were tested to achieve this aim: temperature, pH and NaCl concentration.

Determination of optimal conditions for affinity chromatography

For testing the influence of temperature on enzyme activity, 5 μ l of a substrate solution (19.8 μ M) were incubated with 5 μ l of solubilised membranes in 40 μ l 50 mM citrate buffer, pH 5.8 at 4 °C for different time intervals (10-360 min). In summary, the substrate was completely transformed into the product aeroplysinin-1 (1) even after an incubation time of 10 min, thus excluding temperature as a single factor to inactivate the enzyme. The next parameter assessed was pH. Therefore, a first screening was achieved by incubating 5 μ l substrate solution (19.8 μ M) with 5 μ l solubilised membranes in 40 μ l at the temperature optimum of the isoxazoline cleaving enzyme at 50 °C for 10 min. Since citrate buffer is not suited for alkaline pH, 0.1 M Tris-HCl buffer of respective pH was prepared. A sample incubated with buffer of pH 5.8 served as positive control.

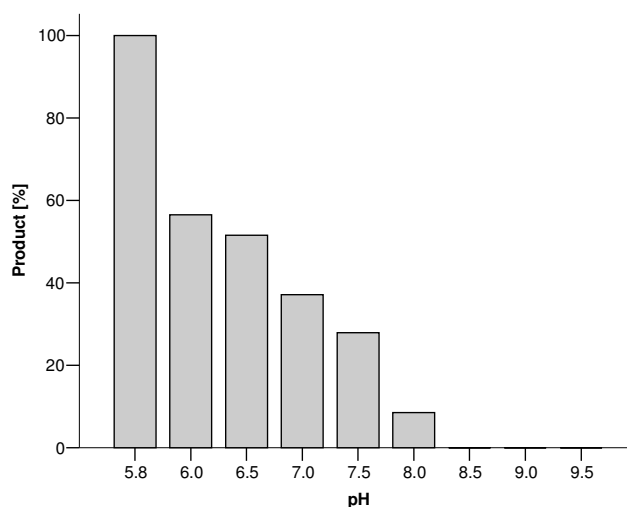


Figure III.19. Product yield (%) after incubation of substrate and enzyme at 50 °C at different pH values.

Figure III.19 shows that enzyme activity decreases with increasing pH. Activity was lost completely at pH 8.5. Therefore, in a further experiment, the influence on product yield after incubation of enzyme and substrate at pH 8.0, 8.5 and 9.0 was tested in combination with temperature. It became evident that a pH of 9.0 is too drastic for the isoxazoline cleaving enzyme, since no activity could be regained when conditions were rendered optimal for enzyme activity again (pH 5.8, 50 °C) (Figure III.20).

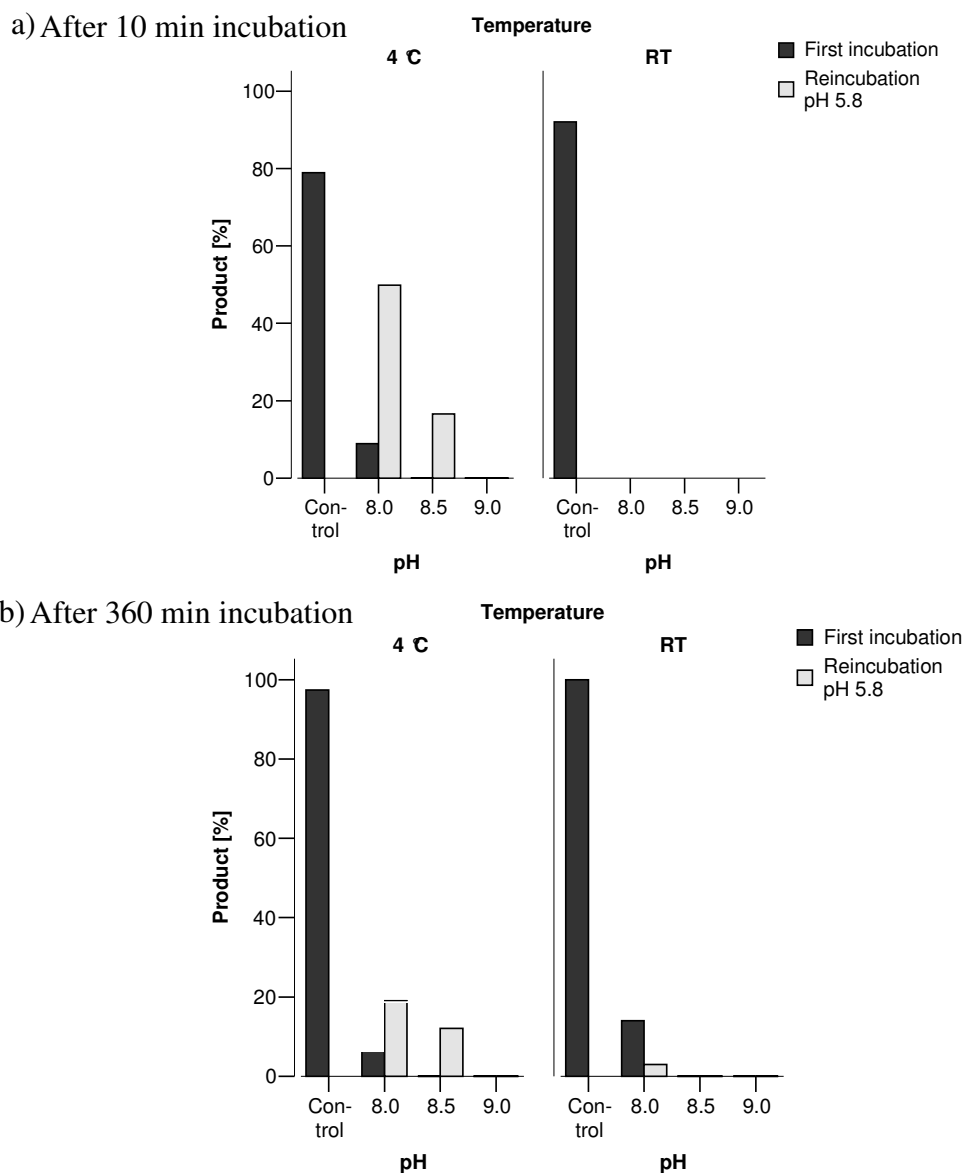


Figure III.20. Relative product yield (in %) after incubation of enzyme and substrate at pH 8.0, 8.5 and 9.0 was determined in combination with different temperatures (4 °C and room temperature(RT)), a) after 10 min incubation and b) after 360 min. One aliquot of these samples was directly submitted to HPLC (first incubation), for another aliquot pH was set to 5.8, followed by incubation for 10 min at 50 °C (reincubation). A sample incubated in parallel at pH 5.8 was included as positive control.

After 10 min incubation at room temperature, no activity could be detected for any pH value (Figure III.20 a), whereas samples incubated at 4 °C at pH 8.0 still showed reduced activity (14 %, Figure III.20). For both pH 8.0 as well as pH 8.5, activity could be restored (51 % and 18 % product, respectively).

However, running an affinity column commonly takes several hours, thus the results obtained for incubation times of 360 min are more relevant (Figure III.20 b). After this incubation time, activity was detected in samples incubated at room temperature at pH 8.0 (59 %), but when incubated at 50 °C for 10 min at pH 5.8, activity decreased to 25 %, indicating that incubation at room temperature has detrimental effects on protein functionality. For samples incubated at 4 °C, some remaining activity was detected in the approach with pH 8.0 (5 %). For both samples at pH 8.0 and 8.5, activity could be regained (18 % and 14 %, respectively) (Figure III.20 b).

In conclusion, a pH of 8.5 appeared most advantageous for affinity chromatography, since no activity was detected at this pH, but 14 % activity could be regained after incubation of samples under optimal conditions.

In an attempt to further optimise and increase restored enzyme activity, different concentrations of NaCl were added to assays. For incubation at room temperature, no significant influence of NaCl on restored activity was observed (Figure III.21 b). For pH 9.0, only the sample with 250 mM NaCl showed little restored activity (9 %). However, for samples incubated at 4 °C at pH 8.5, 46 % of the original activity (compared to the positive control incubated at pH 5.8) were regained when 100 mM NaCl were added (Figure III.21 a).

Based on these results, it was concluded that a buffer of pH 8.3 with 0.1 M NaCl would yield best results for affinity chromatography, which should be conducted at 4 °C. The value of pH 8.3 was chosen instead of pH 8.5 in order to reliably prevent irreversible damage to the protein as is obviously achieved at pH > 8.5. Remaining activity, if present at pH 8.3, was assumed to be minimal as activity at pH 8.0 did not exceed 5 %.

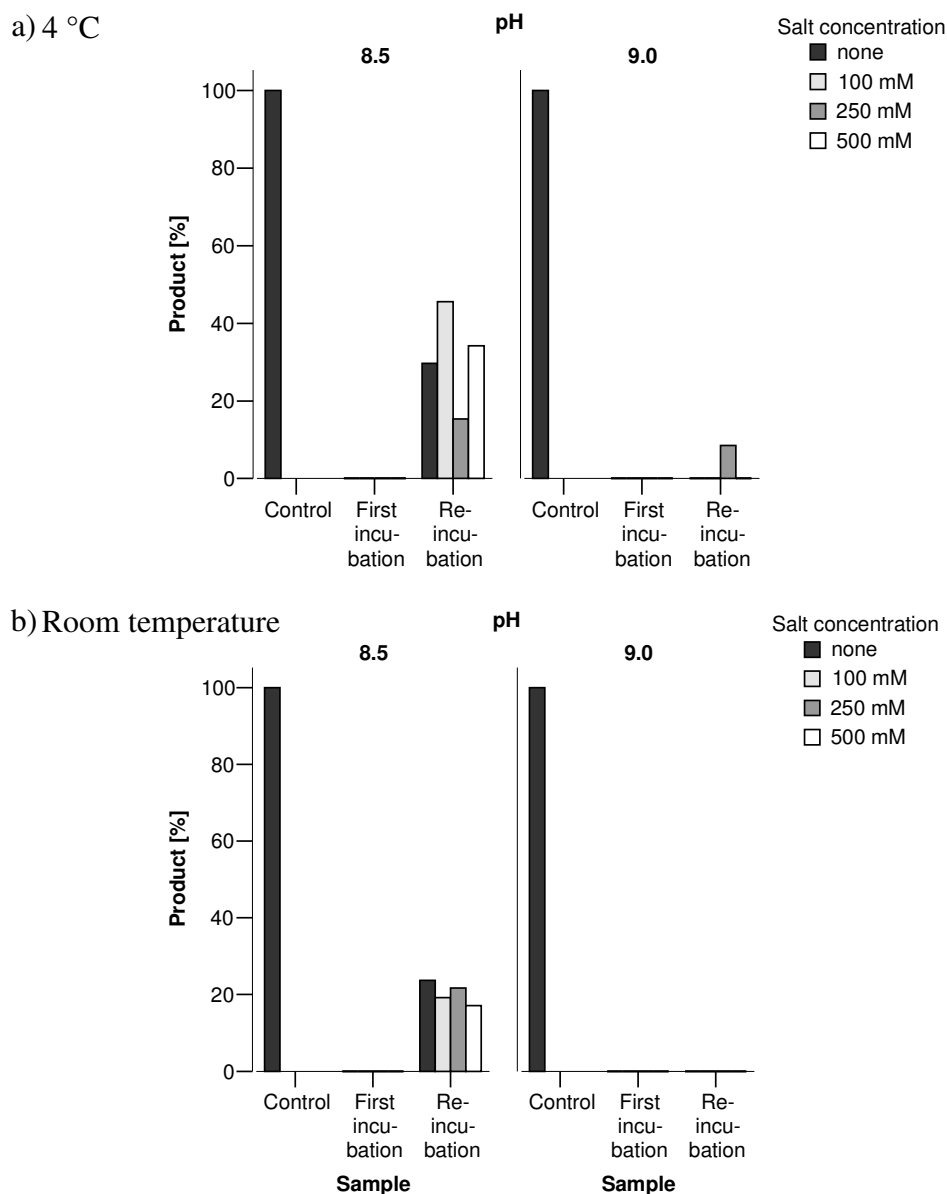


Figure III.21. Relative product yield (in %) after incubation of enzyme and substrate at pH 8.5 and 9.0 for 3 h was determined in combination with different temperatures, a) 4 °C and b) at room temperature (RT). One aliquot of these samples was directly submitted to HPLC (first incubation), for another aliquot pH was set to 5.8, followed by incubation for 10 min at 50 °C (reincubation). A sample incubated in parallel at pH 5.8 was included as positive control.

Immobilisation of the substrate aerophobin-2 (2) on an agarose matrix

In addition to finding optimal conditions for affinity chromatography in terms of pH and temperature, the immobilisation of aerophobin-2 (2) on an NHS activated sepharose matrix was essential. Crucial factors influencing coupling efficiency include pH, temperature, and concentration of the aerophobin-2 (2) solution incubated with the matrix. Therefore, an experiment investigating different combinations of these factors

was performed. Aliquots of NHS activated sepharose were incubated with different concentrations of aerophobin-2 (2) in the coupling solution (CS, 10 and 20 mg/ml), at different pH (pH 9, 10, 11 and 12) and temperatures (room temperature (RT), 50 °C). Coupling efficiency was determined by quantification of aerophobin-2 (2) in the supernatant before and after the coupling reaction via HPLC in order to identify coupling conditions yielding highest coupling efficiency.

Best results were found for an incubation of NHS activated sepharose at room temperature at pH 10 with a coupling solution containing 20 mg/ml aerophobin-2 (2), where coupling efficiency was 28 % (Figure III.22). Interestingly, coupling efficiency was highest for incubations with concentrations of 20 mg/ml aerophobin-2 (2) at pH 9 and 10, but this was reversed for pH 11 and 12, where highest efficiencies were achieved with coupling solutions of 10 mg/ml for both temperatures (Figure III.22). For these samples, efficiencies did not differ significantly (range 22-28 %). Based on these results, it was decided to incubate the NHS activated matrix with a coupling solution of 20 mg/ml aerophobin-2 (2) at pH 10 at room temperature. For approaches involving larger amounts of matrix, coupling efficiency was 25 ± 5 % (N = 3, range: 20-29 %).

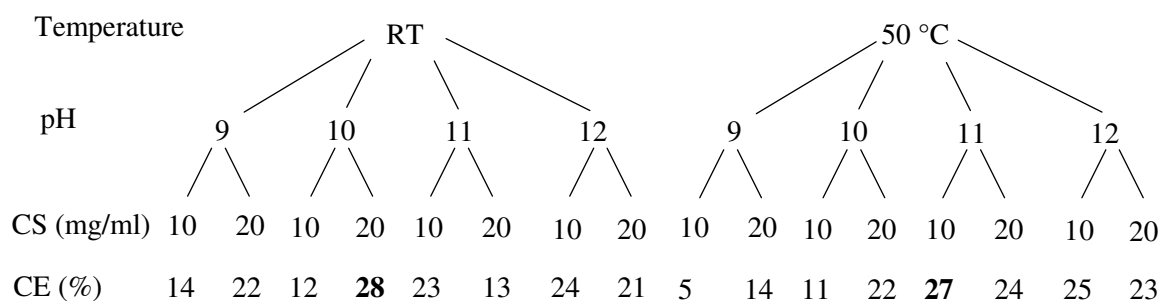


Figure III.22. Coupling efficiency (CE, in %) of aerophobin-2 (2) incubated with NHS activated sepharose at different temperatures (room temperature (RT) and 50 °C), pH values (pH 9, 10, 11, and 12) and concentrations of aerophobin-2 (2) (coupling solution, CS, 10 mg/ml and 20 mg/ml).

Affinity chromatography

Standard protocol

After it was confirmed that aerophobin-2 (2) can be immobilised on an agarose matrix and that conditions exist where the isoxazoline cleaving enzyme is reversibly inactive, purification of solubilised membranes via affinity chromatography was attempted. After the column was equilibrated, 4 ml of solubilised membranes

(concentration: 8.4 ± 0.6 mg/ml, $N = 6$, total amount of protein: 33.6 mg) were incubated with 3 ml matrix providing immobilised aerophobin-2 (2). Subsequently, the protein solution was collected and the column washed with equilibration buffer prior to elution with 2-aminoimidazole. For washing, fractions of 2 ml volume were collected, for elution collected volumes were decreased to 1 ml. For determination of activity, pH was set to 5.5-6.0 for aliquots of each fraction before employment in the activity assay.

Table III.25 summarises activity and protein concentration for the last washing fraction and fractions obtained from elution for a column washed with 12 (Table III.25 a) and 10 (Table III.25 b) medium volumes equilibration buffer prior to elution. In both cases, elution fractions E3 and E4 were most active, also with respect to specific activity. However, overall activity was higher for fractions from the column washed with 10 medium volumes prior to elution, which might be attributed to the higher protein concentration (approx. 40 % more in active fractions than for columns washed with 12 medium volumes, Table III.25).

Table III.25. Protein concentrations ($\mu\text{g/ml}$), activity (%) and specific activity (% per μg protein) of active fractions derived from purification of solubilised membranes via affinity chromatography. The column was washed with a) 12 medium volumes equilibration buffer prior to elution, or b) with 10 medium volumes.

a)	Fraction	Protein conc. ($\mu\text{g/ml}$)	Activity (%)	Protein in assay (μg)	Specific activity (%)
	LW*	24.6	0.0	1.1	0.0
	E1	22.7	0.0	1.0	0.0
	E2	93.5	0.8	4.2	0.2
	E3	372.9	33.1	16.8	2.0
	E4	202.3	19.3	9.1	2.1
	E5	197.9	14.2	8.9	1.6
	E6	104.0	9.1	4.7	1.9

b)	Fraction	Protein conc. ($\mu\text{g/ml}$)	Activity (%)	Protein in assay (μg)	Specific activity (%)
	LW*	29.1	6.1	1.3	4.7
	E1	69.1	4.6	3.1	1.5
	E2	186.9	4.9	8.4	0.6
	E3	116.0	19.8	5.2	3.8
	E4	595.6	53.5	26.8	2.0
	E5	270.9	16.6	12.2	1.4
	E6	99.4	9.5	4.5	2.1

* LW = last fraction obtained from washing of the column

Remaining activity (6.1 %) in the last washing fraction of the column washed with only 10 medium volumes indicated insufficient washing, since activity is obviously due to excess protein not bound to the column. Since prolonged washing of the column is at

the expense of protein functionality, washing with 12 medium volumes appeared to be a good compromise.

For SDS PAGE, proteins in all fractions were precipitated with 100 % TCA to yield approx. 100 µg for application to the gel. Figure III.23 shows the SDS PAGE for fractions of an affinity column and respective activities.

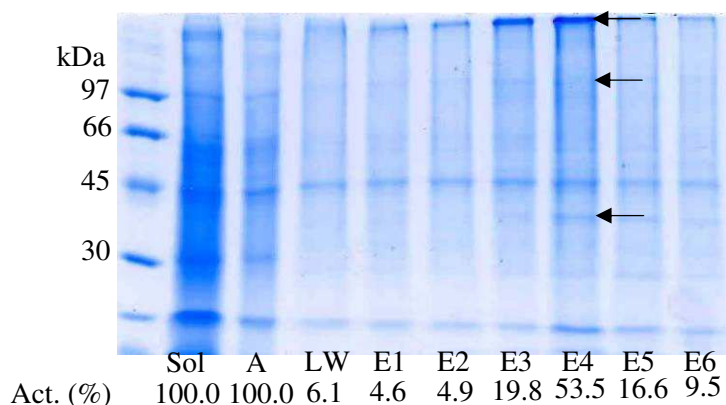


Figure III.23. SDS PAGE (10 %) of fractions obtained from an affinity column washed with 10 medium volumes equilibration buffer prior to elution. “Act.” represents the activity in %. Proteins in all fractions were precipitated with 100 % TCA to yield approx. 100 µg protein applied to the gel. Arrows mark bands that were assumed to be correlated with activity.

The three bands marked by arrows were suspected to be correlated with activity, since they appeared more intense in most active fractions when compared to fractions with less activity (of which equal protein amounts were applied to the gel). The band at 45 kDa was not considered as a candidate since it was already very prominent in the solubilised membranes applied as well as in the last washing fraction, thus making it probable that it represents an artefact from insufficient washing of the column.

Elution with aerophobin-2 (2)

In order to compare elution with 2-aminoimidazole and aerophobin-2 (2) in terms of activity and band patterns in SDS polyacrylamide gels, two affinity columns were run in parallel. An aliquot of the same sample of solubilised membranes was applied to each column containing 3 ml each of the same set of column material. Both columns were treated the same way in terms of washing. The single difference was elution, which was achieved by a 0.3 M 2-aminoimidazole solution as used in the standard protocol, and a 10 mM aerophobin-2 (2) solution, respectively. Table III.26 shows the respective activities and protein concentrations for the most active fractions of both columns.

Protein concentration of fractions eluted with aerophobin-2 (2) could not be determined because the aerophobin-2 (2) solution used for elution interfered strongly when measuring absorption at 595 nm via the Bradford assay, thus leading to non-reproducible results. However, activity of fractions was comparable. The same applies to band patterns showing up in SDS PAGE, which looked identical to the one depicted in Figure III.23.

Table III.26. Protein concentrations ($\mu\text{g/ml}$), activity (%) and specific activity (% per μg protein) of active fractions derived from purification of solubilised membranes via affinity chromatography. Elution with a) 0.3 M 2-aminoimidazole, b) 10 mM aerophobin-2 (2).

Fraction	a) Elution with 2-aminoimidazole		b) Elution with aerophobin-2 (2)	
	Protein conc. ($\mu\text{g/ml}$)	Activity (%)	Protein conc. ($\mu\text{g/ml}$)	Activity (%)
LW*	24.6	0.0	23.1	0.0
E1	22.7	0.0	17.1	0.1
E2	93.5	0.8	27.3	0.0
E3	372.9	33.1	-	29.6
E4	202.3	19.3	-	13.4
E5	197.9	14.2	-	9.0
E6	104.0	9.1	-	5.5

* LW = last fraction obtained from washing the column

Affinity chromatography as a second purification step following ion exchange

Band patterns of fractions obtained from purification of solubilised membranes via affinity chromatography were still complex on SDS PAGE. It was thus attempted to improve purification by using affinity chromatography as a second purification step following ion exchange chromatography. For the sake of comparability, three affinity columns were run in a parallel approach involving aliquots of the same sample of column material with immobilised aerophobin-2 (2). On one of these columns, solubilised membranes were applied as described for the standard protocol. On the other two columns, unbound protein from the first fraction and the three most active fractions of an ion exchange column were applied, respectively.

Table III.27 summarises activity and protein concentration for the fractions obtained after purification of ion exchange fractions over an affinity column. Overall activity was very low, i.e. less than 1/10 when compared to purification of solubilised membranes (2.1 and 1.6 %, respectively, in comparison to approx. 30 %). At the same time, protein amount in active fractions was reduced by just 1/3 when compared to purification of solubilised membranes, which leads to the conclusion that protein functionality suffers from ion exchange as additional purification step.

Table III.27. Protein concentrations ($\mu\text{g/ml}$) and activity (%) of ion exchange fractions, a) unbound protein (first fraction) and b) most active fractions.

Fraction	a) Unbound protein		b) Active fractions	
	Protein conc. ($\mu\text{g/ml}$)	Activity (%)	Protein conc. ($\mu\text{g/ml}$)	Activity (%)
E1	-	0.7	-	0.7
E2	65.6	0.8	11.5	0.8
E3	265.7	2.1	177.7	1.0
E4	205.7	1.9	235.5	1.6
E5	45.8	0.7	92.1	0.7
E6	19.6	0.6	63.3	0.0

For SDS PAGE, proteins of all fractions were precipitated with 100 % TCA to yield approx. 100 μg for application to the gel. Figure III.24 shows the SDS PAGE for fractions obtained by purification of solubilised membranes (Figure III.25 a), unbound protein from ion exchange (Figure III.25 b), and active ion exchange fractions (Figure III.25 c). Of all fractions, approx. 100 μg protein were applied to the gel. Three bands could be identified that were found in all active ion exchange fractions, increasing probability that they were correlated with activity: one for a large protein barely entering the separating gel, one at approx. 125 kDa and a weak one at 60 kDa, which was consistent with active fractions obtained from ion exchange and gel filtration. The band at 45 kDa was not considered as a candidate since it was already very prominent in the solubilised membrane fraction, thus making it probable that it represents an artefact which could not be completely removed from the column by washing.

In conclusion, purification of solubilised membranes via affinity chromatography yielded more satisfying results than employment of ion exchange and gel filtration materials. Activity was clearly detectable, although band patterns on SDS PAGE were still too complex to reliably correlate particular bands with activity. Purity was improved when affinity chromatography was applied as a second purification step following ion exchange chromatography, but was at the cost of activity which was barely detectable in fractions obtained from the affinity column employed as second purification step. For identification of proteins correlated with activity on SDS PAGE, a more reliable method was needed which will be described below.

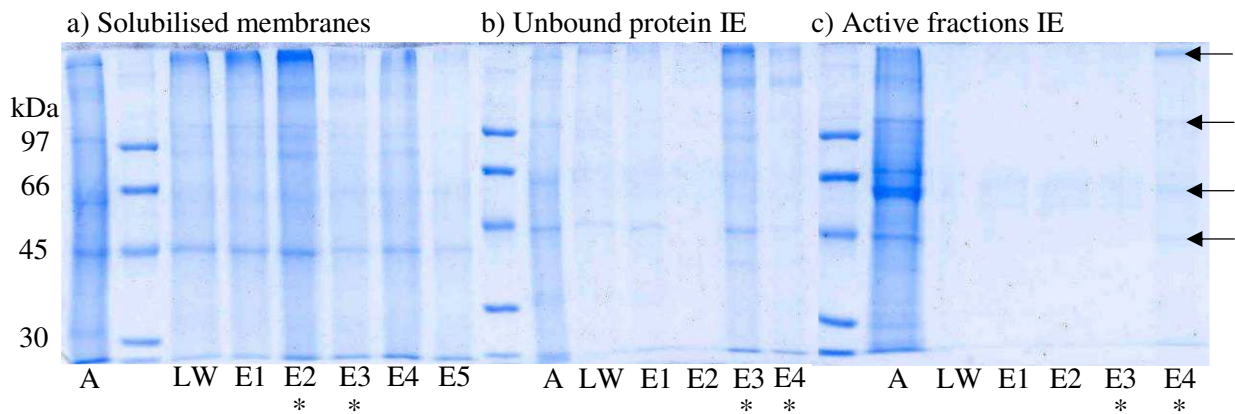


Figure III.24. SDS PAGE (10 %) of fractions obtained from affinity chromatography, purification of a) solubilised membranes, b) unbound protein from ion exchange (IE), c) most active fractions from IE. A = sample applied to the affinity column, LW = last fraction obtained from washing. Most active fractions are marked by asterisks (*). Proteins in all fractions were precipitated with 100 % TCA to yield approx. 100 µg protein applied to the gel. Arrows mark bands that were present in all active fractions.

Labelling of the isoxazoline cleaving enzyme & detection via Western blot

In order to solve the problem of identifying proteins correlated with active fractions on SDS PAGE, a reagent was needed that (1) can be coupled to the substrate aerophobin-2 (2), (2) possesses a crosslinking function to bind the protein after it bound to the substrate, and (3) possesses a label for detection on Western blots. Sulfo SBED is a trifunctional label transfer reagent which combines all these functions, and was thus employed to achieve a more reliable identification of proteins that bind the substrate aerophobin-2 (2).

Labelling the substrate

Aerophobin-2 (2) was coupled to the Sulfo SBED label transfer reagent via an NHS group following the same principle as the immobilisation of aerophobin-2 (2) on an NHS-activated sepharose matrix. Coupling efficiency should be detected via HPLC. However, even though samples were protected from light prior to HPLC analysis, photoactivated crosslinking of Sulfo SBED with aerophobin-2 (2) and other molecules or fragments present in the sample could not be prevented, making quantification of coupled aerophobin-2 (2) impossible. Instead, HPLC-MS was employed to qualitatively confirm successful coupling of aerophobin-2 (2) to the reagent. Figure III.25 shows the LC-MS chromatogram which proves successful coupling by exhibiting the molecular ion peak of Sulfo SBED coupled to aerophobin-2 (2) at m/z 1183 $[M+H]^+$. Further peaks represented NHS groups split off the Sulfo SBED reagent, the reagent itself

lacking the NHS group, aerophobin-2 (2), and various combinations of Sulfo SBED coupled to these molecules or fragments via the crosslinker function (Figure III.25).

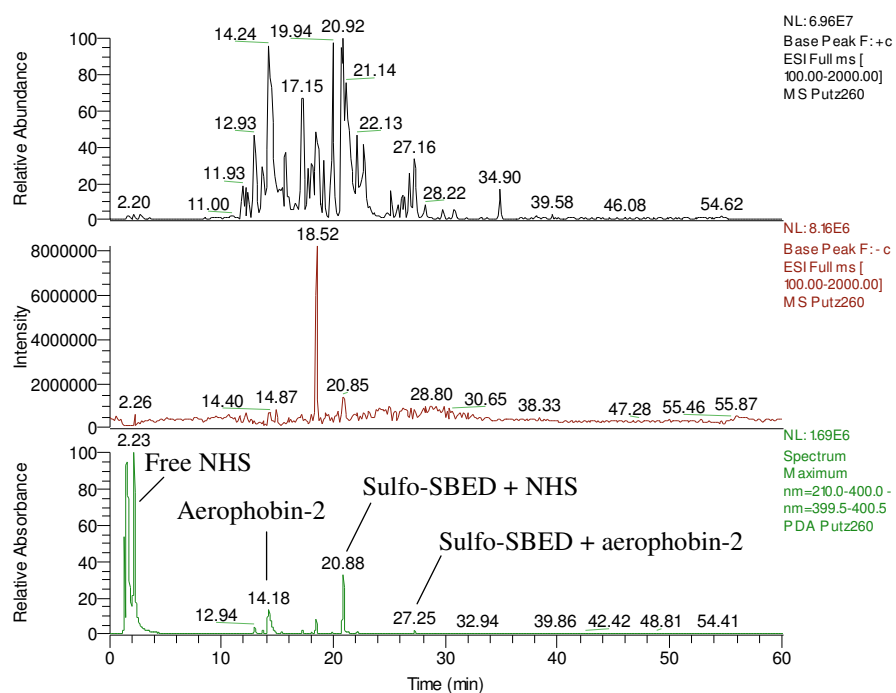


Figure III.25. LC-MS chromatogram for a sample of Sulfo SBED label transfer reagent incubated with aerophobin-2 (2) for 30 min.

Crosslinking the protein with labelled substrate

After successful coupling of aerophobin-2 (2) to the Sulfo SBED label transfer reagent was confirmed, the labelled substrate was incubated with active fractions derived from affinity chromatography. Subsequently, samples were treated with UV light (366 nm) to form a stable bond between the protein “caught” by the substrate and Sulfo SBED. Successfully labelled proteins, i.e. those proteins possessing binding sites for the substrate aerophobin-2 (2), were visualised by Western blot and subsequent detection with streptavidin conjugated horse radish peroxidase (HRP). Despite some background noise caused by excessive label, three labelled bands could be identified, two of them clearly visible (the band of a large protein barely entering the separating gel, and one at 45 kDa), one very weak (at approx. 125 kDa, Figure III.26 a). In order to confirm specificity of labelling, a series of samples with increasing concentrations of unlabelled aerophobin-2 (2) competing with the labelled substrate was prepared. In theory, affinity of the enzyme should be higher towards the unlabelled substrate, thus outcompeting the labelled substrate at increasing concentrations. Practically, this could

be well observed for the band of a large protein barely entering the separating gel that vanished after adding a 10000 fold excess of unlabelled substrate over the labelled substrate (Figure III.26 a). Unfortunately, this was less clear for the other two bands, where band intensity was fluctuating irrespective of concentrations of unlabelled substrate added (Figure III.26 a).

For identification of the labelled bands on SDS PAGE, the best way would be a reversible staining with Ponceau S after blotting proteins on the PVDF membrane. After a picture has been taken, the membrane is washed and staining is removed. By directly overlaying the picture taken of the stained membrane with the picture obtained after detection, an unequivocal identification of labelled bands is achieved. However, due to low protein amounts obtained after affinity purification and low sensitivity of the Ponceau staining when compared to Coomassie, bands could not be visualised on the PVDF membrane by this means. Identification of bands was thus obtained by comparison of the labelled bands detected in Western blots with SDS PAGE, where the marker served as orientation (Figure III.26 b). In addition to the labelled bands, two bands of comparable intensity occurred on SDS PAGE (Figure III.26 b, e.g. the band at approx. 35 kDa), which did not appear on the Western blot (Figure III.26 a), thereby further confirming specificity of labelling.

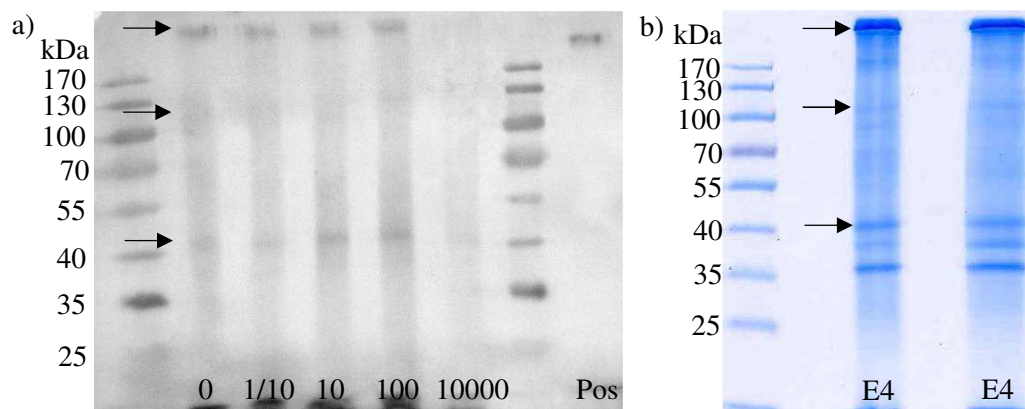


Figure III.26. a) Western blot and b) SDS PAGE (10 %, Coomassie staining) of the most active fraction derived from purification of solubilised membranes via affinity chromatography (E4). For Western blot, this fraction was incubated with substrate attached to Sulfo SBED label transfer reagent and subsequently crosslinked. To prove specificity of labelling increasing concentrations of unlabelled aerophobin-2 (2) were added as competitor for the labelled substrate (0, 1/10, 10, 100, and 10000 fold excess of unlabelled over labelled aerophobin-2 (2)). A biotinylated goat-anti mouse antibody was applied as positive control for successful blotting (Pos).

In order to check whether the band barely entering the separating gel represents one or several proteins which are not separated on a 10 % SDS polyacrylamide gel, a 6 % gel was prepared. All proteins < 70 kDa were let to move out of the gel. Figure III.27 b shows that on the 6 % gel, two sharp bands occurred. Since the size range of commercially available SDS PAGE markers do not exceed 270 kDa, thyroglobulin used for the calibration of the gel filtration column was added to the gel as size standard. Thyroglobulin is a dimer of 669 kDa which decays upon addition of β -mercaptoethanol. To see whether one or both of the bands were labelled a Western blot was prepared in parallel. Unfortunately, background noise was intense. However, in samples treated with β -mercaptoethanol prior to loading the gel, two bands appeared, confirming that both of the bands visible on SDS PAGE were labelled and thus appeared in the Western blot (Figure III.27 a). The reason for the increased background is probably due to the marginal ability of a 6 % SDS PAGE to resolve proteins of this size.

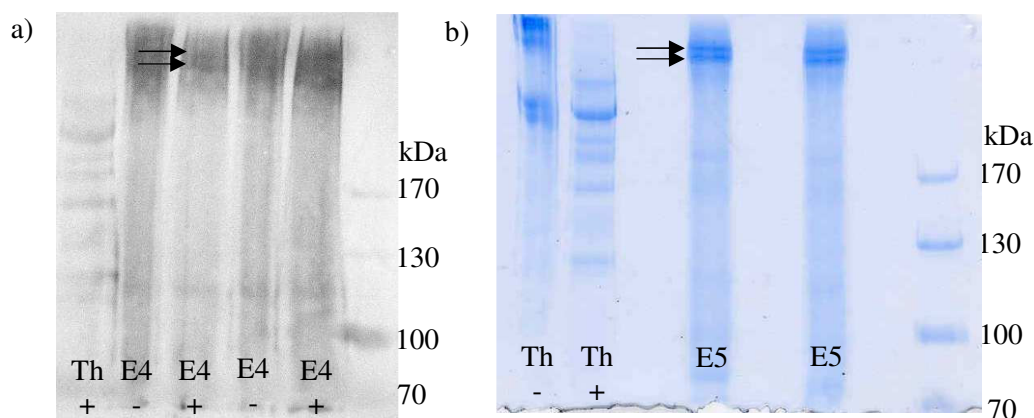


Figure III.27. a) Western blot and b) SDS PAGE (6 %, Coomassie staining) of the most active fractions derived from purification of solubilised membranes via affinity chromatography. For Western blot, fraction E4 was incubated with substrate attached to Sulfo SBED label transfer reagent and subsequently crosslinked. Identical samples were applied in different concentrations. + sample buffer with β -mercaptoethanol, - sample buffer without β -mercaptoethanol, Th: Thyroglobulin, E4, E5: active fractions from affinity chromatography.

In addition, the most active fraction derived from ion exchange chromatography was incubated with labelled aerophobin-2 (2), crosslinked and subsequently analysed via SDS PAGE and Western blot. One band was clearly labelled, which was not clearly recognized in the affinity chromatography fraction (Figure III.28 a). The band appearing at approx. 45 kDa which was clearly labelled in the affinity fraction also appeared in the ion exchange fraction, although less pronounced, it was only detectable in higher concentrations of samples. However, the two very large proteins were not clearly

detectable in the ion exchange fraction (Figure III.28 a and b). When comparing samples incubated with different concentrations of labelled substrate, it becomes evident that adding a 1:10 diluted label solution to the protein sample gives better results with respect to background noise in Western blots.

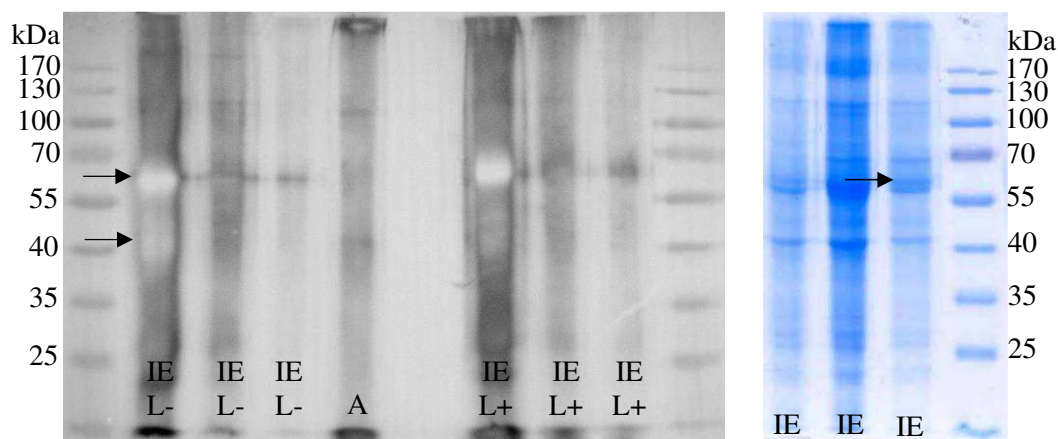


Figure III.28. a) Western blot and b) SDS PAGE (10 %, Coomassie staining) of the most active fraction derived from purification of solubilised membranes via ion exchange chromatography. For Western blot, this fraction was incubated with substrate attached to Sulfo SBED label transfer reagent and subsequently crosslinked (IE). L+: 11.54 μ g protein incubated with 6 μ l labelling solution, L-: 11.54 μ g protein incubated with 6 μ l diluted labelling solution (1:10). Different dilutions of each sample were applied, concentration decreases from left to right. As comparison, a labelled fraction obtained from affinity chromatography was applied (A).

When β -mercaptoethanol was added to the sample buffer, bands of the complex ion exchange fraction were resolved much better on Western blots (Figure III.29 b). It became evident that all bands that were labelled in the most active affinity fraction were also found in the most active ion exchange fraction. However, an additional band of approx. 60 kDa appeared in the ion exchange fraction (Figure III.29 b). The same applies to the first fraction obtained from ion exchange chromatography containing proteins which did not bind to the column material, and which was likewise very active (Figure III.29 a). Thus, the pattern of labelled bands looked identical in the two ion exchange fractions, although the band representing the very large protein barely entering the separating gel was less pronounced in the fraction containing proteins that bound to the ion exchange material (Figure III.29). The fact that, except for the protein of approx. 60 kDa, active affinity and ion exchange fractions showed the same pattern of labelled bands in Western blots further supports their correlation with activity.

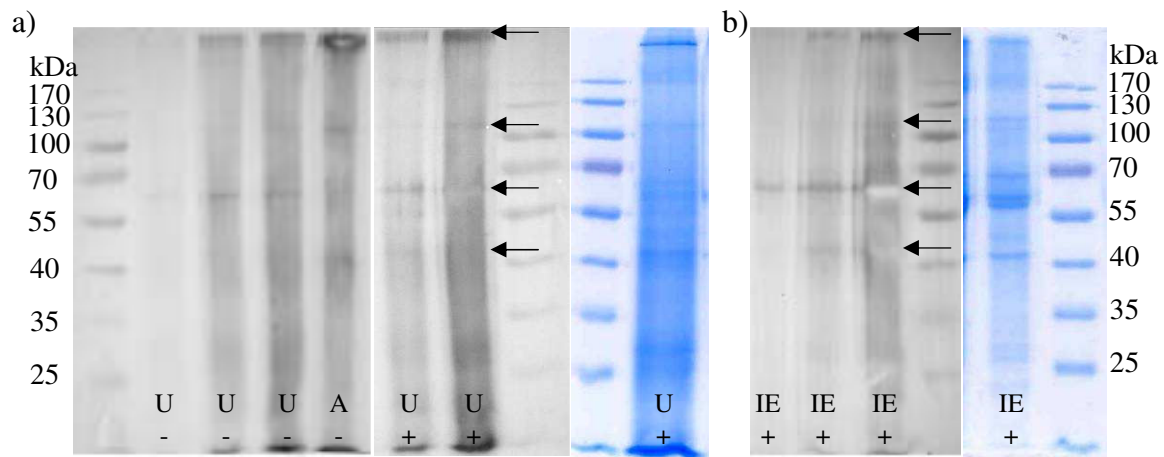


Figure III.29. Western blot and SDS PAGE (10 %, Coomassie staining) of active fractions derived from purification of solubilised membranes via ion exchange chromatography, a) first fraction (unbound protein, U), b) most active fraction (IE, eluted at approx. 350 mM NaCl). + sample buffer with β -mercaptoethanol, - sample buffer without β -mercaptoethanol. For Western blot, fractions were incubated with substrate attached to Sulfo SBED label transfer reagent (11.54 μ g protein incubated with 6 μ l diluted labelling solution (1:10)) and subsequently crosslinked. Different dilutions of each sample were applied, concentration increases from left to right. As comparison, a labelled fraction obtained from affinity chromatography was applied (A).

In summary, labelling and subsequent detection via Western blot could identify five bands in total representing proteins with binding affinity towards the isoxazoline cleaving enzyme aerophobin-2 (2). All five bands (marked by arrows in Figure III.30) were cut out of the gel and submitted to the analytical laboratory at the BMFZ (Biologisch-Medizinisches Forschungszentrum, HHU Düsseldorf) for trypsin digestion and subsequent mass analysis (see below).

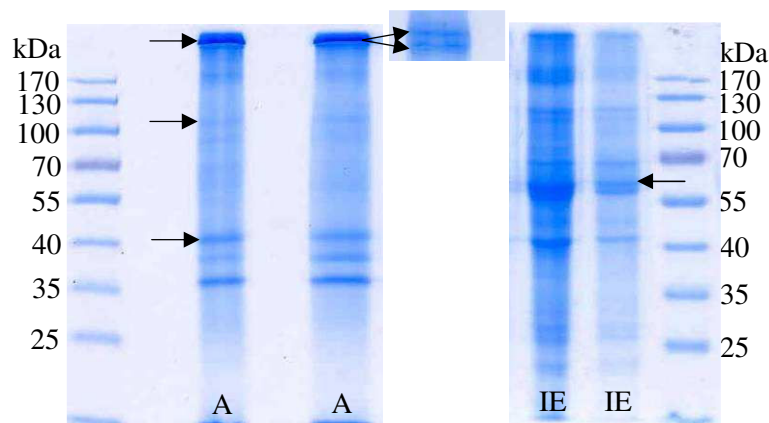


Figure III.30. SDS PAGE (10 %, Coomassie staining) of the most active fractions derived from purification of solubilised membranes via affinity- (A) or ion exchange chromatography (IE). Arrows mark the bands that were cut out of the gel and submitted to the analytical laboratory at the BMFZ (Biologisch-Medizinisches Forschungszentrum, HHU Düsseldorf).

Trypsin digestion and mass analysis of the isoxazoline cleaving enzyme

Peptide sequences were obtained for two of the five proteins analysed. The concentration of the protein of approx. 125 kDa was probably too low to detect any signals. For the two very large proteins, no signals were detected either. Since concentration was ample for both proteins, it is more plausible that the lack of measurable signals was due to insufficient trypsin digestion and, as a consequence, subsequent insufficient elution, or the proteins might not ionise well. However, for both the protein of approx. 45 kDa and the 60 kDa protein obtained in active ion exchange fractions, peptide sequences (Table III.28) could be inferred from MS spectra (Appendix). For the 45 kDa protein, homologous sequences were found from a wide range of eukaryotic species which unequivocally identified this protein as actin by comparison with the sequence similarity search machine of EMBL database (WU Blast2). One of these sequences was described for *Discodermia*, a demosponge of the family Theonellidae (Steenkamp et al. 2006). For the 60 kDa protein, no sequences with significant homologies were found. Table I.28 shows chosen examples of homologous sequences. For all peptide sequences obtained, a list of the best-matching homologous sequences identified by Blast2 can be retained from the Appendix.

Table III.28. Peptide sequences obtained after trypsin digestion and subsequent mass analysis.

Protein (kDa)	Sequence	Amino acids	Homologous sequences*	Identity (%)*
45	VAPEEHPVLLTEAPLNPK	18	Actin-1, <i>Absidia glauca</i>	100
45	DLYANTVLSGGSTMYPGIADR	21	Actin, <i>Botrylloides leachi</i>	100
45	TTGIV(M _{ox} /F)DSGDGVSHTVPI YEGYALPHAILR	30	Actin, <i>Pseudocentrotus depressus</i>	100
60	(EP)LGTSGAETESR or (EP)LGTSGAETEDK	13	Uncharacterized protein, <i>Halobacterium salinarum</i>	72
60	YSQLDELNVV.....	10	-	-
60	...FTVL(LP)AVDGK	11	-	-

*identified by comparison with the sequence similarity search machine of EMBL database (WU-Blast2)

Discussion

The phylum Porifera is a rich source of bioactive secondary metabolites, which represent potentially effective agents or lead structures for the treatment of a wide range of human diseases. Furthermore, since sponges are sessile and lack physical defence structures, these compounds commonly play a crucial role in the chemical defence system by effectively repelling predators, pathogens, fouling organisms and competitors. During the course of evolution, various selecting forces generated quite sophisticated chemical defence systems in the rather basal Metazoan phylum Porifera, which is exemplified by the activated chemical defence exhibited by *Aplysina* sponges.

This thesis focused on three major topics, i.e. (I) the isolation and structure elucidation of bioactive compounds from marine sponges, (II) investigating the influence of environmental factors on secondary metabolite production in three Mediterranean sponge species, and (III) the purification and characterisation of the isoxazoline cleaving enzyme involved in the activated defence of *Aplysina* sponges.

Secondary metabolites from marine sponges

A total of 15 compounds was isolated from eight sponge species collected in the Mediterranean (Croatia and Turkey) and in the Andaman Sea (Thailand). Several isolated compounds exhibited considerable activity in *in vitro* bioassays assessing the antimicrobial and cytotoxic potential of these substances. Isolated substances included alkaloids, terpenes, brominated and phenolic compounds. The sesquiterpenoid avarol (9) and the quinone avarone (10) isolated from *Dysidea avara* are known metabolites of the sponge and were isolated to establish calibration curves for their quantification in sponge raw extracts via HPLC as required for the experiments on chemical ecology. The same applies to the bromopyrrol alkaloids oroidin (11) and 4,5-dibromo-1*H*-pyrrol-2-carboxylic acid (12) isolated from *Agelas oroides*. Therefore, and since these compounds were already described in the introduction of this thesis, they will not be discussed further in more detail.

Bromopyrrole alkaloids isolated from Agelas oroides

In addition to the well known bromopyrrole alkaloids oroidin (11) and 4,5-dibromo-1*H*-pyrrol-2-carboxylic acid (12) two derivatives of the latter were isolated from the Mediterranean sponge *Agelas oroides*, 4,5-dibromo-1*H*-pyrrol-2-carboxylic acid ethyl

ester (13) and 4,5-dibromo-1*H*-pyrrol-2-carbonitrile (14). Both compounds have been previously described (Forenza et al. 1971; Handy et al. 2004; Handy and Zhang 2006). 4,5-dibromo-1*H*-pyrrol-2-carbonitrile (14) is a common metabolite of *Agelas oroides* (Forenza et al. 1971; König et al. 1998). However, no literature was found describing the isolation of 4,5-dibromo-1*H*-pyrrol-2-carboxylic acid ethyl ester (13) from a natural source, literature dealing with this compound focussed on the synthesis of the lamellarin family of natural products (which have a 3,4,5-triarylpyrrol-2-carboxylate at their core) (Handy et al. 2004; Handy and Zhang 2006). Instead, 4,5-dibromo-1*H*-pyrrol-2-carboxylic acid methyl ester was repeatedly isolated from *Agelas oroides* (Forenza et al. 1971; König et al. 1998). Neither the methyl ester nor the carbonitrile (14) were found to have noteworthy biological effects with respect to cytotoxicity, fungicidal, antibacterial, algicidal and antiplasmodial activity (König et al. 1998), which is in line with the results obtained during this thesis.

Prenylated hydroquinones from Sarcotragus muscarum and Ircinia fasciculata

Three prenylated hydroquinones with a variable number of isoprenic units were isolated, hexa- (15) and nonaprenylhydroquinone (17) from the Mediterranean sponge *Sarcotragus muscarum*, and heptaprenylhydroquinone (16) from *Ircinia fasciculata* (both belonging to the family Irciniidae). In addition to all three compounds, their respective quinones and sulfates were previously isolated from *Ircinia* and *Sarcotragus* sponges (Cimino et al. 1972; Venkateswarlu and Venkata Ramy Reddy 1994; Bifulco et al. 1995; De Rosa et al. 1995; Wakimoto et al. 1999). None of the three prenylated hydroquinones isolated during this thesis (15-17) was antimicrobially active. However, all of them exhibited strong cytotoxic activity in the MTT assay involving the mouse lymphoma cells L5178Y. This finding was further corroborated by the inhibitory effects found in the protein kinase assay including kinases involved in signal transduction pathways (cell proliferation, survival, angiogenesis and metastasis). In both assays, the nonaprenylhydroquinone (17) had slightly stronger effects than hexa- (15) and heptaprenylhydroquinones (16). One explanation for this finding could be the higher lipophilicity of nonaprenylhydroquinone (17), thus facilitating its uptake into cells. However, since hexa- (15) was more active than heptaprenylhydroquinone (16), this appears less likely. Interestingly, activity was reversed when cytotoxicity was tested towards H4IIE hepatoma cells, where heptaprenylhydroquinone (16) was more active than the respective hydroquinones with six (15) and nine (17) isoprenic units. In the

TEAC assay, all three compounds showed strong antioxidative potential. The antioxidative properties of prenylated hydroquinones were investigated before by Gil et al. (1995). They found that 2-polyprenyl-1,4-hydroquinones failed to scavenge the superoxide anion generated by the hypoxanthine/xanthine oxidase system. Treatment of human neutrophils with 2-polyprenyl-1,4-hydroquinones did not block the release of superoxide anions. On the other hand, Terencio et al. 1998 reported that 2-prenyl-, 2-diprenyl, 2-triprenyl- and 2-tetraprenyl-1,4-hydroquinone scavenge reactive oxygen species and inhibit 5-lipoxygenase (5-LO) activity in human neutrophils.

All three isolated compounds significantly inhibited NF- κ B signalling in H4IIE cells, a transcription factor involved in a variety of physiological processes. The prenylated hydroquinones did not inhibit the basal activity of this transcription factor, but the amount of activation after stimulation was decreased. Since NF- κ B is commonly discussed as a transcription factor responsible for cell survival, this inhibition may also contribute to the toxic effects of the prenylated hydroquinones. In analogy to this, Terencio et al. (1998) reported that prenylated hydroquinones suppress the production of TNF- α in J774 cells stimulated with lipopolysaccharide.

Further interesting pharmacological activities for polyprenylated hydroquinones are described in the literature. For example, 2-hexaprenylhydroquinone, isolated from the Red Sea sponge *Ircinia* spec, has been shown to be a general inhibitor of retroviral reverse transcriptases (from HIV-1, HIV-2 and murine leukaemia virus) as well as of cellular DNA polymerases (*Escherichia coli* DNA polymerase I, and DNA polymerases alpha and beta) (Loya et al. 1993; Loya et al. 1997). Heptaprenylhydroquinone isolated from the Mediterranean sponge *Ircinia spinosula* showed no effect against human recombinant synovial phospholipase A2, but octaprenylhydroquinone inhibited this enzyme in a concentration-dependent manner (Gil et al. 1995). Octaprenylhydroquinone sulfate slightly affected superoxide generation and showed topical anti-inflammatory activity against the TPA-induced ear inflammation in mice (Gil et al. 1995). Nonaprenylhydroquinone sulfate isolated from the Australian sponge *Sarcotragus* spec inhibited α -1,3-fucosyltransferase (Fuc TVII), a key enzyme in the biosynthesis of selectin ligands (Wakimoto et al. 1999). Moderate to strong antimicrobial effects were found in studies by De Rosa et al. (1994) and Mihopoulos et al. (1999) who investigated structure-activity relationships and demonstrated that both the oxidation of the hydroquinone to the quinone and a hydrogenation of the side-chain double bonds increases the pharmacological potency of these molecules.

In conclusion, prenylated hydroquinones may be useful for the development of new agents in cancer therapy due to (1) their pronounced cytotoxicity, (2) inhibition of NF- κ B-signalling and (3) specific inhibition of EGF-R, therefore disrupting the extracellular signal-regulated kinase (ERK) signalling pathway which is of importance for a potential use in tumour therapy since it functions in cellular proliferation, differentiation, and survival, and since its inappropriate activation is a common occurrence in human cancers.

New brominated ambigol A derivatives from *Sarcotragus muscarum*

Two new brominated ambigol A derivatives (18 and 19) were isolated from the Mediterranean sponge *Sarcotragus muscarum*, which differed from each other by the number of bromine substituents. Both compounds resembled ambigol A, a polychlorinated compound from the terrestrial cyanobacterium *Fischerella ambigua* (Falch et al. 1993). However, compounds 18 and 19 isolated during the course of this thesis were substituted with bromine instead of chlorine atoms, and lacked the single proton in the central ring system present in ambigol A which was replaced by a bromine atom in compounds 18 and 19. Unfortunately, the low yield of isolated compounds 18 and 19 did not allow for measurement of C-C correlations for unequivocal proof of the existence of the central ring system which was derived from high resolution mass spectroscopical data.

Due to the low amounts of compound obtained, bioactivity was not determined for ambigol derivatives 1 (18) and 2 (19). In literature, ambigol A was shown to possess antibacterial, antifungal and molluscicidal effects, and to inhibit the enzymes cyclooxygenase and HIV reverse transcriptase (Falch et al. 1993).

It is interesting, though, to find derivatives of ambigol A produced by terrestrial cyanobacteria in a marine sponge. However, since a wide range of cyanobacteria inhabits marine environments (e.g. as so-called fouling organisms or as symbionts) and sponges are filter-feeders, it appears plausible to find compounds of cyanobacterial origin in the sponge tissue. The fact that ambigol A derivatives were found as minor metabolites in the *Sarcotragus* methanol extract further supports this assumption (approx. 0.001 % of the extracted sponge wet weight in contrast to 0.02 % for the prenylated hydroquinones).

Linear furanosesterterpene from *Ircinia variabilis*

Fasciculatin (20), a linear furanosesterpene was isolated as the major metabolite from the Mediterranean sponge *Ircinia variabilis*. Fasciculatin was first isolated from the Mediterranean sponge *Ircinia fasciculata* (Cafieri et al. 1972), but has later also been found in *Ircinia variabilis* (Alfano et al. 1979; Rifai et al. 2005).

Linear sesterterpenes incorporating furanyl and tetronic acid termini have been shown to possess a wide range of biological activity including antiviral, antibacterial, anti-inflammatory, antitumor, and protein phosphatase inhibitory activity (Choi et al. 2004; Erdogan-Orhan et al. 2004). This corresponds to the results of the antimicrobial assay conducted during this thesis where fasciculatin (20) showed significant activity against *Staphylococcus aureus* and *Streptococcus pyogenes*. However, fasciculatin (20) had almost no cytotoxic effect on mouse lymphoma L5178Y cells, and displayed only weak activity against a range of kinases. In analogy to this, Rifai et al. (2005) found moderate cytotoxicity of fasciculatin (20), and showed that this compound is inactive on human lymphocyte proliferation.

A study investigating the chemical defence of three Mediterranean *Ircinia* species, i.e. *I. spinulosa*, *I. variabilis* and *I. oros*, demonstrated antifeedant and antifouling activity of crude extracts and selected pure compounds such as the furanosesterpenes variabilin and ircinins I and II (Tsoukatou et al. 2002). However, fasciculatin was not among the substances tested, therefore it could be rewarding to test the antifouling and antifeedant potential of fasciculatin in order to identify a potential involvement in the sponge's chemical defence.

Brominated diphenyl ethers obtained from *Dysidea granulosa*

Dysidea granulosa was collected in the Andaman Sea, Thailand. Purification of *Dysidea* extracts yielded two brominated diphenyl ethers, 4,5,6-tribromo-2-(2',4'-dibromophenoxy)phenol (21) and 4,6-dibromo-2-(2',4'-dibromophenoxy)phenol (22) as major metabolites. Both were described previously and are commonly found among the major metabolites of *Dysidea* sponges (Carté and Faulkner 1981; Salvá and Faulkner 1990; Fu and Schmitz 1996).

As a group, polybrominated diphenyl ethers exhibit a wide range of activities in bioassays, including antibacterial and cytotoxic activities (Popov et al. 1999; Agrawal and Bowden 2005). Cytotoxic activity is due to the inhibition of a range of enzymes implicated in tumor development such as inosine monophosphate dehydrogenase,

guanosine monophosphate synthetase and 15-lipoxygenase (Fu et al. 1995). Several brominated diphenyl ethers inhibit the Tie2 kinase supporting angiogenesis essential for tumor growth and survival (Xu et al. 2005), and inhibit microtubule assembly (Liu et al. 2004). Pronounced cytotoxicity was also found for the two brominated diphenyl ethers 21 and 22 isolated during this thesis. Compound 21 differs from compound 22 just by the presence of one additional bromine substituent, but showed an approx. 20 fold increased cytotoxicity towards mouse lymphoma L5178Y cells when compared to compound 22. Likewise, compound 22 selectively displayed strong activity against the protein kinase SAK, which was not found for compound 21. Therefore, it appears plausible to conclude a correlation of the bromination pattern with cytotoxic activity of these compounds. Antimicrobial activities were not found for the two diphenyl ethers (21 and 22) isolated during the course of this thesis, at least not against the strains tested (*Escherichia coli*, *Enterococcus faecalis*, *Staphylococcus aureus*, *Streptococcus pyrogenes*, *Pseudomonas aeruginosa* and *Klebsiella pneumoniae*).

For *Dysidea herbacea*, the polybrominated diphenyl ethers have been reported to be produced by the symbiotic cyanobacterium *Oscillatoria spongelliae* (Unson and Faulkner 1993; Unson et al. 1994). Brominated diphenyl ethers are also known to occur in a wide range of marine organisms such as algae and mussels, although it is often not clear whether these metabolites are produced by host organisms or by their symbionts (Malmvärn et al. 2005). Recently, brominated diphenyl ethers have also been reported in species at higher trophical levels, such as fish, turtles, and marine mammals (Haglund et al. 1997; Vetter et al. 2002), indicating their distribution via the food chain. However, synthetic polybrominated diphenyl ethers are frequently used as flame retardants in polymers, rubber and textiles, thus rendering several of these compounds widespread environmental pollutants (Marsh et al. 2003) which likewise explains their omnipresence in marine as well as terrestrial organisms.

Papuanine, an alkaloid from Haliclona spec

The alkaloid papuanine (23) was derived from *Haliclona spec* sampled in the Andaman Sea, Thailand. This pentacyclic alkaloid was previously isolated from *Haliclona spec* collected in Papua New Guinea by (Baker et al. 1988) and possesses antifungal properties (Baker et al. 1988; Fahy et al. 1988; Barrett et al. 1996; McDermott et al. 1996). In addition to haliclonadamine, papuanine is commonly found among the major metabolites of *Haliclona spec* (Fahy et al. 1988). Haliclonadamine is

identical to papuamine but is epimeric at the point where the diaminopropane portion is attached to one hydrindan unit (McDermott et al. 1996). The $[\alpha]_D^{20}$ value of compound 23 was identical to that published for papuamine by Baker et al. (1988). However, since papuamine and haliclonadamine, respectively, contain more than one chiral center, looking at the optical rotation alone did not allow for confirming the stereochemistry of compound 23.

In this thesis, papuamine (23) showed pronounced cytotoxic activity against mouse lymphoma L5178Y cells (approx. twofold activity of the known cytotoxic compound avarol (9)). Unfortunately, papuamine (23) inhibited a wide range of protein kinases unspecifically, thus reducing the value of this compound as potential anti-cancer agent. Likewise, papuamine (23) proved to possess a strong antimicrobial potential against *E. coli*, *E. faecalis*, *S. aureus*, *S. pyrogenes*, *P. aeruginosa* and *K. pneumoniae*.

Chemical ecology

The production of secondary metabolites is costly in terms of energy and nutrients, thus entailing a trade-off between chemical defence and other physiological processes such as growth (Donaldson et al. 2006). Considerable qualitative as well as quantitative variation found for the secondary metabolites of marine sponges (Paul and Puglisi 2004; Paul et al. 2006; Paul and Ritson-Williams 2008) further indicates a dependence of secondary metabolite production on environmental factors such as light, depth and corresponding threats in terms of predation, fouling, competition for space and resources, and many more. In this thesis it was therefore attempted to shed more light on these issues by investigating the influence of environmental parameters on secondary metabolites of three Mediterranean sponge species. The influence of depth on *Aplysina* isoxazoline alkaloids was investigated along an underwater slope ranging down to a depth of approx. 40 m. Subsequent transplantation experiments were conducted to assess the stability of isoxazoline patterns. The influence of light on secondary metabolites of sponges of the genera *Aplysina*, *Agelas* and *Dysidea* was investigated by subjecting clones of the same individual to different light conditions.

Aplysina

In accordance with previous studies on bromoisoxazoline alkaloids in *A. aerophoba* (Thoms et al. 2006), absolute bromoisoxazoline alkaloid amounts were found to be

highly variable in the investigated *Aplysina* sponges. This is an obstacle for a detailed analysis of environmentally caused changes of alkaloids as large standard deviations are likely to conceal experimentally caused changes among individual sponge specimens. This problem was circumvented by comparing the patterns of sponge alkaloids rather than alkaloid amounts since alkaloid patterns proved to be more homogenous for individual sponges.

Influence of depth

The influence of depth on the composition of bromisoxazoline alkaloids was investigated along a depth gradient ranging from 1.8 to 38.5 m at Sveta Marina, Croatia. At a depth of approximately 12 m, a clear change was observed with regard to the alkaloid patterns of the analysed sponges, independently whether samples were taken in April or in August 2006. Sponges collected at depths above 11.8 m exhibited a bromoisoxazoline alkaloid pattern typical for *A. aerophoba* with aerophobin-2 (2) and isofistularin-3 (3) as major constituents (Cimino et al. 1983; Ciminiello et al. 1997; Thoms et al. 2006). Sponges from deeper sites (below 11.8 m) consistently showed a bromoisoxazoline alkaloid pattern typical for *A. cavernicola* with aerothionin (4) and aplysinamisin-1 (1) as dominating compounds (Ciminiello et al. 1997). The pigment 3,4-hydroxyquinoline-2-carboxylic acid (6) which is characteristic for *A. cavernicola* (Thoms et al. 2003a; Thoms et al. 2004); studies performed in Elba, Italy and Rovinj, Croatia), however, was missing in these latter specimens but appeared to be replaced by the chemically labile *A. aerophoba* pigment uranidine (5) (Cimino et al. 1984). Even though the instability of uranidine (5) proved to be an obstacle to its unequivocal detection by HPLC the fact that all sponge specimens analysed in this study showed blackening at the cut ends which is typical for polymerisation of this pigment (Cimino et al. 1984) is a strong evidence for the presence of uranidine (5) in all analysed sponge samples. Sponges from depths below 12 m therefore resemble *A. cavernicola* with regard to bromoisoxazoline alkaloids but differ clearly from the latter with regard to their pigment. Thus, these latter specimens resembled neither *A. aerophoba* nor *A. cavernicola* but rather hold an intermediate position between the two species.

Transplanting sponges with a bromoisoxazoline alkaloid pattern resembling *A. cavernicola* from a depth below 30 m to a depth of 10 m caused no significant changes of the alkaloid pattern even after an observation period of twelve months, although this result is weakened by the low sample size (three surviving specimens). For *Aplysina*

sponges from shallow sites (1-4 m) transplanted to 10 m likewise no changes were observed. However, this observation is in congruence with an earlier study on *A. cavernicola* at the island of Elba (Italy). Transplantation of sponges from a depth of 40 m to a depth of 15 m caused likewise no changes of the alkaloid pattern over an observation period of three months (Thoms et al. 2003b). These experiments suggest that the bromoisoxazoline alkaloid patterns found in “deep” samples of *Aplysina* sponges from Sveta Marina are obviously fixed rather than being modulated by changes in environmental parameters such as light, temperature or salinity that differ considerably between a depth of 10 m compared to 30 m.

Influence of light

This conclusion is corroborated by the experiment designed to investigate the effect of light on alkaloid accumulation. Clones of *Aplysina* sponges from shallow depths (5-6 m) that exhibited bromoisoxazoline alkaloid patterns resembling *A. aerophoba* were either subjected to ambient light conditions at a depth of 6 m or were shaded by placing them under baskets covered with a black plastic foil. The latter treatment blocks photosynthetically active radiation (PAR). During the observation period of twelve months only a minor change in alkaloid patterns was observed: Isofistularin-3 (3) which constituted the major bromoisoxazoline alkaloid in specimens collected at the beginning of the experiment (t_0) was gradually replaced by aerophobin-2 (2) after one year (t_2) in both treatments. None of the *Aplysina* sponges analysed in this experiment, however, accumulated any detectable amounts of aerothionin (4) or of aplysinamisin-1 (1) that are typical for *Aplysina* sponges below 12 m. In both treatments, total alkaloid amounts decreased during the observation period of twelve months. Variation in parameters such as water temperature or nutrient availability could be among the factors accounting for the decreased alkaloid amounts in 2007 when compared to 2006.

Conclusion

In summary, neither transplantation of *Aplysina* sponges to different depth regimes nor maintenance under differing light conditions affected bromoisoxazoline alkaloid patterns in a significant manner. On the contrary, alkaloid patterns proved to be remarkably stable and unaffected by changing environmental conditions. Since chemical and physical environmental factors that are likely to have an influence on alkaloid composition such as light, temperature or salinity change gradually rather than

abruptly along the analysed depth gradient, an area of co-occurring *A. aerophoba* and *A. cavernicola* like chemotypes would have been expected. Instead a clear boundary between the two well defined chemotypes of sponges (“shallow” and “deep” specimens) was found at a depth of approximately 12 m which at present appears inexplicable.

Since *A. aerophoba* and *A. cavernicola* only differ by a series of phenotypically quite variable characters such as colour, shape and surface texture, sponge taxonomists have debated whether the two taxa should be considered as distinct species, or, due to their different ecological requirements, as ecotypes (Ciminiello et al. 1997). Analysis of the secondary metabolites produced by these two *Aplysina* species seemed to offer further characteristics to cope with this question (Ciminiello et al. 1997), with *A. cavernicola* producing aerothionin (4) and aplysinamisin-1 (1) as major metabolites and the pigment 3,4-hydroxyquinoline-2-carboxylic acid (6), and aerophobin-2 (2) and isofistularin-3 (3) being the major constituents of *A. aerophoba* with the pigment uranidine (5) (Cimino et al. 1983; Ciminiello et al. 1997; Thoms et al. 2006). However, since chemical characteristics distinguishing both *Aplysina* species seem to merge at least with regard to the sponge pigment in our dataset, anew the question arises whether Mediterranean sponges of the genus *Aplysina* represent one species with two different chemotypes. Future studies will have to systematically investigate the correlation between habitat, morphology and secondary metabolites of *Aplysina* sponges from different locations in order to eventually answer the question whether either two distinct *Aplysina* species exist in the Mediterranean, or whether they are different chemo- or ecotypes of one species.

Dysidea avara* and *Agelas oroides

Transplantation of clonal explants of *Dysidea avara* and *Agelas oroides* to either natural illumination or artificially shaded conditions reflected the outcome for the transplantation of *Aplysina* sponges. For both species, transplantation did not affect secondary metabolite patterns in a significant manner. However, the reduced numbers of surviving explants impede the drawing of conclusions for these two species. For *Dysidea avara*, nine of the 20 originally transplanted clones survived after four months, and only two of the 14 originally transplanted *Agelas oroides* clones were still viable. On the one hand, this finding might indicate a detrimental effect of transplantation. On the other hand, it is intriguing that for both species, surviving clones were exclusively found in the artificially shaded treatment (except for one single *Dysidea avara* clone

that survived under natural illumination). In the Limski Kanal, both *Agelas oroides* and *Dysidea avara* were observed to naturally occur in depths below 15 m (personal observation). However, in order to evoke significant differences between the natural illumination and the artificially shaded treatment, it was necessary to transplant sponges to a depth of 5-6 m. This had no influence on *Aplysina* sponges that were found to naturally occur in depth ranges from as low as 1 m down to 40 m. However, the fact that surviving *Agelas* and *Dysidea* explants almost exclusively occurred in the artificially shaded treatment hints at a general incapability of these two species to live in light-exposed habitats.

Related studies

Several studies found spatial and temporal variation of secondary metabolites in sponges, e.g. for the cytotoxic metabolites produced by the New Zealand sponge *Mycale hentscheli* (Page et al. 2005) or salicylilalamide A, a cytotoxic compound found in *Haliclona* spec (Abdo et al. 2007). Several studies investigated the influence of different transplantation procedures and environmental factors on aquaculture success of different sponges (Duckworth et al. 1997; Duckworth and Battershill 2003; Duckworth and Wolff 2007). However, few investigations so far directly addressed the influence of depth on natural products in marine invertebrates by carrying out transplantation experiments. When specimens of *A. cavernicola* were transplanted from a depth of 40 m to depths ranging from 12-15 m no changes in alkaloid patterns were observed over a period of three months (Thoms et al. 2003b). Transplanting specimens of *Dysidea granulosa* from shallow to deep sites did likewise not influence the concentration of polybrominated diphenyl ethers (Becerro and Paul 2004), even though abundance of symbiotic cyanobacteria *Oscillatoria spongelliae* (which are assumed to produce these metabolites) decreased as a result of decreased light exposure. When transplanting colonies of the gorgonian coral *Briareum asbestinum* from shallow to deep habitats and vice versa, (Harvell et al. 1993) failed to discover qualitative changes in briarane- and asbestinane-derived diterpenes. However, there was evidence for quantitative variation as diterpene concentrations increased in colonies moved to deeper habitats compared to those from shallow habitats. Genetically identical individuals of the Great Barrier Reef sponge *Rhopaloeides odorabile* transplanted to shallow sites (5 m) contained higher levels of diterpenes than individuals transplanted to 20 m depth

after an experimental period of one year (Thompson et al. 1987), but diterpene composition did not change qualitatively.

In summary, all these studies show outcomes similar to the results described in this thesis. Absolute contents of secondary metabolites varied considerably, making it difficult to track changes attributed to transplantation. However, no qualitative changes as a consequence of transplantation occurred, indicating that metabolite patterns of individual organisms are fixed rather than modificatory. Since sponges as well as corals are sessile organisms which will not be translocated under natural conditions, it seems plausible that secondary metabolite composition is fixed in adult individuals. It remains open whether environmental factors encountered by the larva upon settlement influence secondary metabolite composition or -concentration.

In summary, secondary metabolite contents and patterns of marine invertebrates are not stable through space and time, but are rather subject to considerable quantitative and/or qualitative variation. These findings therefore emphasize the importance of chemico-ecological studies when analysing the chemical defence of marine organisms.

Stress-induced biotransformation of *Aplysina* alkaloids

Sponges of the genus *Aplysina* are prone to a stress-induced biotransformation reaction where fish deterrent isoxazoline alkaloids (Thoms et al. 2004) are split in a first step giving rise to the nitrile aeroplysinin-1 (5), which might be further cleaved to yield a dienone (6) (Teeyapant and Proksch 1993). This biotransformation occurs very fast, within seconds after the sponge tissue has been injured (Thoms et al. 2006). The antimicrobially active biotransformation products (Weiss et al. 1996) thus prevent the invasion of pathogens into the wounded sponge tissue. Ecologically, this activated defence mechanism represents a sophisticated chemical defence protecting the physically vulnerable, but nevertheless conspicuously coloured *Aplysina* sponges from predation and overgrowth by or infection with fouling organisms.

The cleavage of isoxazoline alkaloids is an unusual chemical reaction showing parallels to the abnormal Beckmann fragmentation known from the field of Organic Chemistry (McCarty 1970) as described in the Introduction chapter. However, the fact that no biochemical pendant of such a reaction is known to date raises questions about the nature of the catalysing enzyme. This thesis therefore aimed at the purification and characterisation of the isoxazoline cleaving enzyme in *Aplysina aerophoba*.

The enzyme substrate, the isoxazoline alkaloids, were found to be localised in specialised spherulous cells which accumulate in the surface of the sponge tissue and around the excurrent channels (Thompson et al. 1983; Turon et al. 2000). Spherulous cells are widely distributed in demosponges, and share one characteristic: they can degenerate and apparently release their cell contents into the intercellular matrix (Donadey and Vacelet 1977). It remains open whether the isoxazoline alkaloids are constantly exuded into the intercellular matrix by degenerating spherulous cells, or whether they are liberated upon tissue wounding. Considering their role as antifeedants against fish (Thoms et al. 2004), however, it would be plausible if they were constantly present in the tissue. Cleavage of isoxazoline alkaloids only occurs upon tissue damage. It therefore appears likely that the isoxazoline cleaving enzyme(s) are brought into contact with their substrates after the sponge tissue has been damaged. If isoxazoline alkaloids are constantly present in the intercellular matrix, they would immediately get into contact with the enzyme(s) after cell compartmentalisation has been disturbed, which is corroborated by the extremely short time of <40 sec in which the biotransformation takes place (Thoms et al. 2006).

Purification of the isoxazoline cleaving enzyme

For the purification of the isoxazoline cleaving enzyme, differential ultracentrifugation provided a suitable first step in the purification procedure. Solubilisation conditions were optimised to yield highest enzyme activity, also after storage at – 20 °C. Solubilised membranes derived from 20 g lyophilised sponges tissue yielded approx. 67 mg protein. Although the enzyme was astonishingly stable in the membrane fraction and insensitive towards freezing and thawing cycles (Grüning 2007), this was not the case for solubilised membranes on which repeated freezing and thawing had a detrimental effect. All purification steps following solubilisation were therefore performed consecutively as far as possible in order to avoid freezing and thawing.

Ion exchange and gel filtration chromatography

Ion exchange chromatography via a strong anion exchange medium (HiTrap QFF) yielded good results in terms of reproducibility and activity of fractions. Interestingly, activity was found in both, fractions of proteins that bound to the column material, and the first fractions of unbound protein. Band patterns of the most active fractions were

complex on SDS PAGE, thus further purification of the most active fraction obtained from ion exchange chromatography was attempted by employing a different separation principle, i.e. gel filtration. However, gel filtration did not provide satisfying results with regard to protein yield (approx. 30 µg per active fraction) and purity as monitored by the band pattern on SDS PAGE. Protein yield could probably be optimised by applying a larger amount of solubilised membranes to the ion exchange column which would increase protein concentration of the most active fractions (at least as long as the column is not overloaded). However, due to the unsatisfying purity of gel filtration fractions when compared to ion exchange fractions this approach was not further pursued.

Affinity chromatography

Since the enzyme substrate aerophobin-2 (2) could successfully be coupled to an NHS activated matrix, and conditions were found where the enzyme could be reversibly inactivated, a purification of solubilised membranes via affinity chromatography was attempted. Affinity chromatography gave satisfying results with respect to activity and protein yield (approx. 300-500 µg in the most active fraction). Band patterns on SDS PAGE of active fractions were less complex than those of the fractions obtained from ion exchange or gel filtration. However, affinity fractions were still not pure enough to reliably correlate specific bands with activity. In order to improve purity, it was attempted to wash affinity columns more extensively prior to elution, but since this was at the cost of protein functionality, this approach was not pursued any longer. In an alternative effort, ion exchange chromatography was added as purification step prior to affinity chromatography. SDS PAGE band patterns showed ample purity, although activity of fractions was extremely low, almost not detectable. The finding that protein yield (approx. 200-300 µg) was comparable to that for affinity fractions obtained after the purification of solubilised membranes indicates a detrimental effect of the long handling on protein functionality. For this reason, bigger approaches involving larger amounts of protein to be purified via ion exchange and subsequent affinity chromatography were not considered as an option.

Identification of proteins with affinity towards aerophobin-2 (2)

In order to reliably identify proteins with affinity towards the substrate of the isoxazoline cleaving enzyme, aerophobin-2 (2), the label transfer reagent Sulfo SBED

served as a suitable tool. Aerophobin-2 (2) could be successfully coupled to the Sulfo SBED reagent carrying a biotin moiety and a crosslinker function. After crosslinking proteins with binding affinity towards aerophobin-2 (2), detection was achieved via Western Blot. In order to confirm specificity of labelling, a competition experiment was performed where unlabelled aerophobin-2 (2) was added as competitor in approaches in increasing concentrations. For the bands representing two large proteins barely entering the separating gel, the signal disappeared with increasing concentrations of unlabelled aerophobin-2 (2), proving specific labelling. Unfortunately, clear results for the other bands of labelled proteins detected in Western Blots were hampered by the fact that band intensity was not reliably reproducible, hinting at the need for optimised Western Blot detection conditions in future approaches to assess quantitative effects. However, the existence of prominent bands clearly visible on SDS PAGE which were absent in Western Blots strongly supported the specificity of labelling.

In total, four proteins that possess affinity for aerophobin-2 (2) could be identified in active affinity chromatography fractions: Two large proteins barely entering the separating gel, one weak band representing a protein of approx. 125 kDa, and one of a protein of approx. 45 kDa. All of these were likewise found in ion exchange fractions (unbound as well as bound protein fractions), plus an additional clear band at approx. 60 kDa which was not clearly detectable in affinity fractions. Apart from the latter, the same aerophobin-2 (2) binding proteins were thus found in active fractions obtained from ion exchange as well as affinity chromatography.

Trypsin digestion and subsequent mass analysis was successful for two of these five proteins. The peptide sequences obtained for the protein represented by the band at approx. 45 kDa were homologous to actin as revealed by sequence similarity searches in protein databases. Homologous sequences were found in a wide range of organisms as diverse as i.e. algae, insects and vertebrates, but also in sponges of the genus *Discodermia* (Steenkamp et al. 2006), which is due to the fact that actin is a highly conserved protein across eukaryotic species (Erickson 2007). However, no homology was found for the sequences obtained for the protein of approx. 60 kDa detected in active ion exchange fractions, indicating a less conserved protein when compared to actin. For the protein band at approx. 125 kDa no signal could be detected, which is most probably due to the low concentration of this protein in SDS gels. Less explicable is the fact that no signal was detectable for the two large proteins barely entering the separating gel, since concentration of these appeared ample for mass analysis. A first

obstacle could be an insufficient trypsin digestion, which might be due to a low number of trypsin cutting sites, or an incomplete denaturation of proteins reducing the number of accessible areas of the molecule. If digestion was not successful, proteins are too large to be eluted from the gel, and therefore no signal can be detected in the mass analysis. Another possibility is that elution was not efficient during desalting of the protein fragments via ZipTipC₁₈ tips. Lastly, the investigated proteins could not ionise and therefore no signal would be detectable.

Characterisation of the isoxazoline cleaving enzyme

The purification attempts described above, although not always successful in terms of purity of obtained fractions, gave indications of several characteristics of the isoxazoline cleaving enzyme. Tracking activity in fractions obtained from differential ultracentrifugation and treatment of the membrane fraction with cold sodium carbonate revealed that the isoxazoline cleaving enzyme is an integral membrane protein. The fact that during ion exchange chromatography activity was found in both, first fractions with unbound protein, and fractions of proteins that bound to the column, indicates that the isoxazoline cleaving enzyme is not a single enzyme, but that different proteins or isoforms of the same protein exist. Calibration of a gel filtration column with size standards revealed an approximate size of 540 kDa for the protein(s) in active fractions. Dependent on the buffer employed for elution during gel filtration, chromatograms looked completely different from each other. In approaches where no active fractions were obtained, a significant peak of a small protein (< 60 kDa) occurred which was absent in the approaches yielding active fractions. It therefore appears likely that the loss of activity corresponds to a decay of an enzyme complex. The existence of several different proteins involved in the isoxazoline cleaving activity is further corroborated by the finding that an additional, aerophobin-2 (2) binding protein of approx. 60 kDa appeared in Western Blots of active ion exchange fractions but was not clearly detectable in active affinity fractions. In general, membrane proteins often function within large complexes (Alberts et al. 1997), thus further supporting this assumption.

One of the aerophobin-2 (2) binding proteins could be identified as actin, a globular, approx. 42 kDa protein. Actin is one of the most conserved proteins across eukaryotic species which is attributed to its acquisition of mechanisms for assembly dynamics and interactions with multiple motor and binding proteins, thus contributing to the constraint on actin evolution (Erickson 2007). Determination of the atomic structure of actin in its

monomeric form (Kabsch et al. 1990) has provided the basis to the understanding of this protein (Ayscough and Drubin 1996). A key feature of actin is its ability to bind and hydrolyse ATP. The transition from ATP-actin to ADP-bound actin provokes a conformational change which is central to the dynamic turnover of actin filaments. A plethora of actin-binding proteins regulate the assembly and disassembly of actin filaments, and their organisation into networks (Rybakin and Clemen 2005). The actin cytoskeleton is involved in the generation and maintenance of cell morphology and polarity, in endocytosis and intracellular trafficking, in contractility, motility, cell division and even in apoptosis and ageing (Gourlay and Ayscough 2005; Smythe and Ayscough 2006). Among a complex set of proteins attached to the undersurfaces of cell membranes, actin is responsible for stabilising membranes by regulating the topography and mobility of the different transmembrane proteins. This submembranous network, often referred to as membrane skeleton, is composed of filaments of actin, actin-binding proteins such as spectrin, and connecting proteins that link the stabilising infrastructure to the overlaying membrane (Marchesi 1985). Since the isoxzoline cleaving enzyme(s) are integral membrane proteins, the fact that one of the aerophobin-2 (2) binding proteins in *A. aerophoba* is an actin can be explained by its role in the stabilisation of membrane proteins within cell membranes. It therefore seems plausible that an aerophobin-2 (2) binding protein located in the cell membrane is connected with the actin cytoskeleton.

No significant homologies were found for the peptide sequences obtained from the 60 kDa protein in active ion exchange fractions. This is probably due to the fact that in protein databases, only a limited amount of protein sequences is available from sponges. For the genus *Aplysina*, no protein sequences or cDNA database is published so far, therefore hampering the identification of peptide sequences if not highly conserved as in the case of actin.

Conclusion and perspectives

In summary, a combination of differential ultracentrifugation and further purification of the solubilised membrane fraction via affinity chromatography or, alternatively, ion exchange chromatography yielded active fractions of ample purity to allow for the identification of aerophobin-2 (2) binding proteins by specific labelling. Comparison with protein databases identified one of these proteins of approx 45 kDa as actin. For the 60 kDa protein, no homologous peptide sequences were found, therefore its identity

remained unclear. Based on the findings acquired during purification steps, it became evident that the cleavage of isoxazoline alkaloids is accomplished by several proteins. Whether these are functional on an individual basis or act synergistically remains open. When considering the size of proteins of approx. 540 kDa determined in active gel filtration fractions, and the loss of activity accompanied by the appearance of a significant peak of small proteins (< 60 kDa), the existence of an enzyme complex appears likely.

Based upon the peptide sequences obtained, degenerated primers could be designed in order to amplify according DNA fragments which could then be sequenced. In future approaches to further characterise the isoxazoline cleaving enzyme(s), it would be extremely beneficial to obtain a cDNA database for *Aplysina*, although the isolation of *Aplysina* mRNA might be a challenging task (Prof. Hentschel, University of Würzburg, pers. comm.).

It is important to emphasize, however, that in addition to the proteins identified in this thesis, further proteins involved in catalysing the cleavage of isoxazoline alkaloids might exist which do not possess affinity for aerophobin-2 (2) or an accessible binding site and were thus not detected in the described experiments.

Summary

This thesis focussed on three major topics, (I) the isolation and structure elucidation of bioactive metabolites from marine sponges, (II) investigating the influence of environmental factors on secondary metabolite production in three Mediterranean sponge species, and (III) purification and characterisation of the isoxazoline cleaving enzyme involved in the activated defence of *Aplysina* sponges.

Isolation of natural compounds from marine sponges

Since sponges are sessile organisms that usually lack physical means of protection, they commonly invest in chemical defence mechanisms against predators. The phylum Porifera is therefore a rich source of bioactive secondary metabolites, representing potential agents or lead structures for the treatment of a wide range of human diseases. During the course of this thesis, a total of 15 compounds was isolated from eight sponge species collected in the Mediterranean and Andaman Sea, among those 13 known and two new compounds. Isolated substances included alkaloids, terpenes, brominated and phenolic compounds. *In vitro* bioassays exhibited considerable antimicrobial and/or cytotoxic potential of several of these substances.

Chemical ecology of Mediterranean sponges

Total amounts and patterns of bromoisoxazoline alkaloids of *Aplysina* sponges from Croatia (Mediterranean Sea) were analysed along an underwater slope ranging from 1.8 to 38.5 m. Total amounts of alkaloids varied greatly from sample to sample and showed no correlation with depth. In contrast, striking differences of alkaloid patterns were found between sponges from shallow sites (1.8-11.8 m) and those collected from deeper sites (11.8-38.5 m). Sponges from shallow depths consistently exhibited alkaloid patterns typical for *Aplysina aerophoba* with aerophobin-2 and isofistularin-3 as main constituents. Sponges from deeper sites (below 11.8 m) resembled *Aplysina cavernicola* with aerothionin and aplysinamisin-1 as major compounds. The typical *A. cavernicola* pigment 3,4-dihydroxyquinoline-2-carboxylic acid, however, could not be detected in the latter sponges but was replaced by the *A. aerophoba* pigment uranidine which appeared to be present in all sponge samples analysed. In transplantation experiments, alkaloid patterns were found to be stable over a period of 12 months and unaffected by this change in depth.

In a further experiment, clones of three different sponges, i.e. *Aplysina*, *Dysidea avara* and *Agelas oroides* were either kept *in situ* under natural light conditions or artificially shaded by excluding photosynthetically active radiation in shallow depths of 5-6 m. Secondary metabolite patterns remained unaffected over an observation period of 12 months for *Aplysina* sponges. For *D. avara* and *A. oroides*, the number of viable clones remaining after four months did not allow for conclusions other than a detrimental effect of intense light on these two species. In summary, metabolite patterns in *Aplysina* sponges proved to be remarkably stable and unaffected by changing light conditions or depth.

Stress induced biotransformation in *Aplysina* sponges

Activated defence systems rely on preformed protoxins which are transformed into actual defence metabolites after disturbance of cellular compartmentalisation. In the marine environment, a striking example for this can be found in sponges of the genus *Aplysina*. Upon tissue wounding, fish-deterring bromoisoxazoline alkaloids such as aerophobin-2 are enzymatically cleaved, giving rise to the nitrile aeroplysinin-1, which may be further metabolised into a dienone. Both biotransformation products, the nitrile and the dienone, display pronounced antibiotic activity against a range of marine microorganisms. Since no biochemical equivalent to this unusual biotransformation is known to date, this thesis aimed at the purification and characterisation of the isoxazoline cleaving enzyme. Purification of lyophilised sponge cells via differential centrifugation, ion exchange and affinity chromatography yielded enzymatically active fractions that catalysed cleavage of the isoxazoline alkaloid aerophobin-2 *in vitro* giving rise to aeroplysinin-1. Specific labelling with the biotin-labelled substrate aerophobin-2 and subsequent detection via Western Blot led to the identification of five protein bands with affinity for aerophobin-2 in SDS gels. In-gel trypsin digestion and subsequent mass analysis identified one of these proteins as actin. Another peptide sequence was obtained for a protein of approx. 60 kDa, for which no homologous sequences could be found. In summary, the isoxazoline cleaving enzyme proved to be an integral membrane protein which is most likely held in position by the actin cytoskeleton. It was further revealed that the isoxazoline enzyme is not a single protein, but most probably an enzyme complex.

Zusammenfassung

Die vorliegende Arbeit beschäftigt sich schwerpunktmäßig mit drei Themen, (I) der Isolierung und Strukturaufklärung von bioaktiven Substanzen aus marinen Schwämmen, (II) der Untersuchung des Einflusses von Umweltfaktoren auf die Sekundärmetabolit-Produktion in drei Schwammarten aus dem Mittelmeer, und (III) der Aufreinigung und Charakterisierung des Isoxazolin-spaltenden Enzyms in Schwämmen der Gattung *Aplysina*.

Isolierung von Naturstoffen aus marinen Schwämmen

Aufgrund ihrer sessilen Lebensweise und des Fehlens von physischen Verteidigungsmechanismen investieren Schwämme häufig in eine chemische Abwehr gegen Fraßfeinde. Aus diesem Grund ist der Stamm Porifera als reiche Quelle bioaktiver Substanzen bekannt, die potentielle Mittel oder Leitstrukturen für die Behandlung einer Bandbreite von menschlichen Krankheiten darstellen. Im Verlauf dieser Arbeit wurden 15 Substanzen aus acht Schwammarten isoliert, die aus dem Mittelmeer und dem Andamanischen Meer stammen, von denen 13 Substanzen bereits bekannte und zwei neue Naturstoffe darstellen. Bei den isolierten Stoffen handelte es sich um Alkaloide, Terpene, bromierte und phenolische Verbindungen. In *in vitro* Assays wurde eine ausgeprägte antimikrobielle und/oder cytotoxische Aktivität für einige dieser Substanzen festgestellt.

Chemische Ökologie Mediterraner Schwämme

Die Absolutgehalte und Zusammensetzung von bromierten Isoxazolinalkaloiden in Schwämmen der Gattung *Aplysina* aus Kroatien (Mittelmeer) wurden entlang eines Unterwasser-Steilhangs (1,8-38,5 m) untersucht. Die Absolutgehalte schwankten stark zwischen den einzelnen Proben und zeigten keine Korrelation zur Tiefe, in der die entsprechenden Proben gesammelt wurden. Im Gegensatz dazu fanden sich klare Unterschiede in der Alkaloidzusammensetzung. Schwämme, die in flachen Bereichen (1,8-11,8 m) gesammelt wurden, enthielten Aerophobin-2 und Isofistularin-3, die typischen Hauptmetabolite von *A. aerophoba*. Schwämme, die aus tiefen Bereichen stammten (11,8-38,5 m) zeigten jedoch ein für die Geschwisterart *Aplysina cavernicola* typisches Alkaloidmuster, mit Aerothionin und Aplysinamisin-1 als Hauptkomponenten. Das für *A. cavernicola* typische Pigment 3,4-dihydroxychinolin-2-carboxylsäure konnte in diesen Schwämmen jedoch nicht gefunden werden, stattdessen

schien das *A. aerophoba* Pigment Uranidin in allen analysierten Proben vorhanden zu sein. In Transplantationsversuchen zeigte sich, dass sich die Alkaloidzusammensetzung auch 12 Monate nach Verpflanzung in andere Tiefen nicht verändert.

In einem weiteren Experiment wurden Klone dreier verschiedener Schwammarten (*Aplysina*, *Dysidea avara* und *Agelas oroides*) in 5-6 m Tiefe *in situ* entweder in natürliche Lichtbedingungen verpflanzt oder künstlich abgedunkelt, indem photosynthetisch aktive Strahlung eliminiert wurde. Für die *Aplysina* Schwämme blieb die Sekundärmetabolitzusammensetzung auch bei diesem Transplantationsversuch über einen Zeitraum von 12 Monaten erstaunlich stabil. Bei *D. avara* und *A. oroides* ließ die geringe Menge an auswertbaren Proben nach 4 Monaten keine Schlüsse zu, außer daß die intensive Lichteinstrahlung in 5-6 m Tiefe offenbar tödlich für die nicht-abgedunkelten Klone war. Zusammenfassend blieb die Sekundärmetabolitzusammensetzung der untersuchten *Aplysina*-Schwämme erstaunlich stabil, und änderte sich weder unter Einfluß verschiedener Tiefen noch Lichtbedingungen.

Stressinduzierte Biotransformation in *Aplysina* Schwämmen

Aktivierte Verteidigungssysteme beruhen auf Protoxinen, die nach Zerstörung der Zellkompartimentalisierung in den entsprechenden Verteidigungsstoff umgewandelt werden. Im marinen Habitat stellen Schwämme der Gattung *Aplysina* ein bemerkenswertes Beispiel für solch eine aktivierte Abwehr dar. Wird das Gewebe des Schwammes verletzt, werden die fraßhemmenden Isoxazolin-Alkaloide wie z.B. Aerophobin-2 enzymatisch gespalten, wobei das Nitril Aeroplysinin-1 entsteht, das weiter in ein Dienon metabolisiert werden kann. Beide Biotransformations-Produkte besitzen antimikrobielle Aktivität gegen eine Bandbreite von marinen Mikroorganismen. Da bis heute kein biochemisches Äquivalent zu einer solchen Reaktion bekannt ist, hatte diese Arbeit die Aufreinigung und Charakterisierung des Isoxazolin-spaltenden Enzyms zum Ziel. Die Aufreinigung von gefriergetrockneten, aufgeschlossenen Schwammzellen mittels differenzieller Zentrifugation, Ionenaustausch- und Affinitätschromatographie lieferte enzymatisch aktive Fraktionen, die Aerophobin-2 *in vitro* spalteten. Spezifisches Markieren mit an Biotin gekoppeltem Substrat Aerophobin-2 und anschließender Detektion mittels Western Blot führte zur Identifizierung von fünf Proteinen mit Affinität für Aerophobin-2. Durch In-Gel Trypsinverdau und anschließende Massenanalyse konnte eines dieser Proteine als Actin identifiziert werden. Da für die Peptidsequenzen eines weiteren Proteins keine homologen Sequenzen gefunden wurden, blieb dessen Identität unbekannt.

References

- Abdo D, Motti C, Battershill C, Harvey E (2007) Temperature and spatiotemporal variability of salicylhalamide A in the sponge *Haliclona* sp. *J Chem Ecol* 33: 1635-1645
- Agrawal M, Bowden B (2005) Marine sponge *Dysidea herbacea* revisited: another brominated diphenyl ether. *Mar Drugs* 3: 9-14
- Alberts B, Bray D, Lewis J, Raff M, Roberts K, Watson J (1997) 10.2 Membranproteine. In: Jaenicke L (ed) *Molekularbiologie der Zelle*. VCH, Weinheim, Germany, pp 586
- Alfano G, Cimino G, De Stefano S (1979) Palinurin, a new linear sesterpene from a marine sponge. *Experientia* 35: 1136-1137
- Alves M, Sartoratto A, Trigo J (2007) Scopolamine in *Burgmansia suaveolens* (Solanaceae): Defense, allocation, costs, and induced response. *J Chem Ecol* 33: 297-309
- Assmann M, Lichte E, Pawlik J, Köck M (2000) Chemical defenses of the Caribbean sponges *Agelas wiedenmayeri* and *Agelas conifera*. *Marine Ecology Progress Series* 207: 255-262
- Ayscough K, Drubin D (1996) Actin: General principles from studies in yeast. *Annu Rev Cell Dev Biol* 12: 129-160
- Baker B, Scheuer P, Shoolery J (1988) Papuamine, an antifungal pentacyclic alkaloid from a marine sponge, *Haliclona* sp. *J Am Chem Soc* 110: 965-966
- Bakus G, Targett N, Schulte B (1986) Chemical ecology of marine organisms: an overview. *Journal of Chemical Ecology* 12: 951-987
- Bakus G, Schulte B, Wright M, Green G, Gomez P (1990) Antibiosis and antifouling in marine sponges: laboratory versus field studies. In: Rützler K (ed) *Perspectives in sponge biology*. Smithsonian Institution Press, Washington, pp 102-108
- Barrett A, Boys M, Boehm T (1996) Total synthesis of (+)-Papuamine: an antifungal pentacyclic alkaloid from a marine sponge, *Haliclona* sp. *J Org Chem* 61: 685-699
- Becerro MA, Turon X, Uriz MJ (1995) Natural variation of toxicity in encrusting sponge *Crambe crambe* (Schmidt) in relation to size and environment. *Journal of Chemical Ecology* 21: 1931-1946
- Becerro MA, Paul V (2004) Effects of depth and light on secondary metabolites and cyanobacterial symbionts of the sponge *Dysidea granulosa*. *Marine Ecology Progress Series* 280: 115-128
- Bergmann W, Feeney R (1951) Contribution to the study of marine sponges. 32. The nucleosides of sponges. *Journal of Organic Chemistry* 16: 981-987
- Bezemer T, Wagenaar R, Van Dam N, Van der Putten W, Wäckers F (2004) Above- and below-ground terpenoid aldehyde induction in cotton, *Gossypium herbaceum*, following root and leaf injury. *J Chem Ecol* 30: 53-67
- Bifulco G, Bruno I, Minale L, Riccio R, Debitus C, Bourdy G, Vassas A, Lavayre J (1995) Bioactive polyprenylated sulfates and a novel C31 furanoterpene alcohol sulfate from the marine sponge, *Ircinia* sp. 58: 1444-1449
- Blunt J, Copp B, Hu W, Munro M, Northcote P, Prinsep M (2008) Marine natural products. *Nat Prod Rep* 25: 35-94
- Bradford M (1976) A rapid and sensitive method for the quantitation of microgram quantities of protein utilizing the principle of protein-dye binding. *Anal Biochem* 72: 248-254

- Branch G (1984) Competition between marine organisms: ecological and evolutionary implications. *Oceanogr Marine Biology Annual Reviews* 22: 429-593
- Cafieri F, Fattorusso E, Santacroce C (1972) Fasciculatin, a novel sesterterpene from the sponge *Ircinia fasciculata*. *Tetrahedron* 28: 1579-1583
- Cafieri F, Carnuccio R, Fattorusso E, Tagliatalata-Scafati O, Vallefucio T (1997) Anti-histaminic activity of bromopyrrole alkaloids isolated from Caribbean *Agelas* sponges. *Bioorganic & Medicinal Chemistry* 7: 2283-2288
- Cariello L, Zanetti L, Cuomo V, Vanzanella F (1982) Antimicrobial activity of avarol, a sesquiterpenoid hydroquinone from the marine sponge, *Dysidea avara*: 281-283
- Carté B, Faulkner DJ (1981) Polybrominated diphenyl ethers from *Dysidea herbacea*, *Dysidea chlorea* and *Phyllospongia foliascens*. *Tetrahedron* 37: 2335-2339
- Chanas B, Pawlik J, Lindel T, Fenical W (1996) Chemical defense of the Caribbean sponge *Agelas clathrodes* (Schmidt). *J Exp Mar Biol Ecol* 208: 185-196
- Choi K, Hong J, Lee C-O, Kim D, Sim C, Im K, Jung J (2004) Cytotoxic furanosesterpenes from a marine sponge *Psammocinia* sp. *J Nat Prod* 67: 1186-1189
- Ciminiello P, Costantino V, Fattorusso E, Magno S, Mangoni A (1994a) Chemistry of Verongida Sponges, II. Constituents of the Caribbean sponge *Aplysina fistularis forma fulva*. *J Nat Prod* 57: 705-712
- Ciminiello P, Fattorusso E, Magno S (1994b) Chemistry of Verongida Sponges, III. Constituents of a Caribbean *Verongula* sp. *J Nat Prod* 57: 1564-1569
- Ciminiello P, Fattorusso E, Magno S (1995) Chemistry of Verongida Sponges, IV. Comparison of the secondary metabolite composition of several specimens of *Pseudoceratina crassa*. *J Nat Prod* 58: 689-696
- Ciminiello P, Dell'Aversano C, Fattorusso E, Magno S (1996a) Chemistry of Verongida Sponges - VII Bromocompounds from the Caribbean sponge *Aplysina archeri*. *Tetrahedron* 52: 9863-9868
- Ciminiello P, Fattorusso E, Magno S, Pansini M (1996b) Chemistry of Verongida Sponges - VI. Comparison of the secondary metabolic composition of *Aplysina insularis* and *Aplysina fulva*. *Biochemical Systematics and Ecology* 24: 105-113
- Ciminiello P, Fattorusso E, Forino M, Magno S (1997) Chemistry of Verongida Sponges VIII - Bromocompounds from the Mediterranean sponges *Aplysina aerophoba* and *Aplysina cavernicola*. *Tetrahedron* 53: 6565-6572
- Ciminiello P, Dell'Aversano C, Fattorusso E, Magno S, Pansini M (1999) Chemistry of Verongida Sponges. 9. Secondary metabolite composition of the Caribbean sponge *Aplysina cauliformis*. *J Nat Prod* 62: 590-593
- Ciminiello P, Dell'Aversano C, Fattorusso E, Magno S, Pansini M (2000) Chemistry of Verongida Sponges 10. Secondary metabolite composition of the Caribbean sponge *Verongula gigantea*. *J Nat Prod* 63: 263-266
- Cimino G, De Stefano S, Minale L (1972) Polyprenyl derivatives from the sponge *Ircinia spinulosa*. *Tetrahedron* 28: 1315-1324
- Cimino G, De Rosa S, De Stefano S, Self R, Sodano G (1983) The bromo-compounds of the true sponge *Verongia aerophoba*. *Tetrahedron Letters* 24: 3029-3032
- Cimino G, De Rosa S, De Stefano S, Spinella A, Sodano G (1984) The zochrome of the sponge *Verongia aerophoba* ("Uranidine"). *Tetrahedron Letters* 25: 2925-2928
- Conn E (1979) Cyanide and cyanogenic glycosides. In: Rosenthal G, Janzen D (eds) *Herbivores: their interaction with secondary plant metabolites*. Academic Press, New York, pp 387-412
- Davis A, Targett N, McConnell O, Young C (1989) Epibiosis of marine algae and benthic invertebrates: natural products chemistry and other mechanisms

- inhibiting settlement and overgrowth. In: Scheuer P (ed) Bioorganic Marine Chemistry. Springer-Verlag, Berlin, pp 85-114
- De Rosa S, De Giulio A, Iodice C (1994) Biological effects of prenylated hydroquinones: structure-activity relationship studies in antimicrobial, brine shrimp, and fish lethality assays. *Journal of Natural Products* 57: 1711-1716
- De Rosa S, Crispino A, De Giulio A, Iodice C, Milone A (1995) Sulfated polyprenylhydroquinones from the sponge *Ircinia spinulosa*. *Journal of Natural Products* 58: 1450-1454
- Debitus C, Guella G, Mancini I, Waikedre J, Guemas J, Nicolas J, Pietra F (1998) Quinolones from a bacterium and tyrosine metabolites from its host sponge, *Suberea creba* from the Coral Sea. *Journal of Marine Biotechnology* 6: 136-141
- DeBusk L, Chen Y, Nishishita T, Chen J, Thomas J, Lin P (2003) Tie2 receptor tyrosine kinase, a major mediator of tumor necrosis factor alpha-induced angiogenesis in rheumatoid arthritis. *Arthritis Rheum* 48: 2461-2471
- Dehm S, Senger M, Bonham K (2001) SRC transcriptional activation in a subset of human colon cancer cell lines. *FEBS Letters* 487: 367-371
- Donadey C, Vacelet J (1977) Les cellules à inclusions de l'éponge *Pleraplysilla spinifera* (Schulze) (Démospogones, Dendrocératides). *Archs Zool exp gén* 118: 273-284
- Donaldson J, Kruger E, Lindroth R (2006) Competition - and resource-mediated tradeoffs between growth and defensive chemistry in trembling aspen (*Populus tremuloides*). *New Phytologist* 169: 561-570
- Duckworth A, Battershill C, Bergquist P (1997) Influence of explant procedures and environmental factors on culture success of three sponges. *Aquaculture* 156: 251-267
- Duckworth A, Battershill C (2003) Sponge aquaculture for the production of biologically active metabolites: the influence of farming protocols and environment. *Aquaculture* 221: 311-329
- Duckworth A, Wolff C (2007) Bath sponge aquaculture in Torres Strait, Australia: Effect of explant size, farming method and the environment on culture success. *Aquaculture* 271: 188-195
- Ebel R, Brenzinger M, Kunze A, Gross H, Proksch P (1997) Wound activation of protoxins in marine sponge *Aplysina aerophoba*. *Journal of Chemical Ecology* 23: 1451-1462
- Ebel R (1998) Wundinduzierte Biotransformation bromierter Alkaloide in Schwämmen der Gattung *Aplysina*: Biochemische Charakterisierung und ökologische Bedeutung, Würzburg
- Encarnación-Dimayuga E, Ramírez M, Luna-Herrera J (2003) Aerothionin, a bromotyrosine derivative with antimycobacterial activity from the marine sponge *Aplysina gerardogreeni* (Demospongia). *Pharmaceutical Biology* 41: 384-387
- Erdogan-Orhan I, Sener B, De Rosa S, Perez-Bas J, Lozach O, Leost M, Rakhilin S, Meijer L (2004) Polyprenyl-hydroquinones and -furans from three marine sponges inhibit the cell cycle regulating phosphatase CDC25A. *Natural Product Research* 18: 1-9
- Erickson H (2007) Evolution of the cytoskeleton. *BioEssays* 29.7: 668-677
- Fahy E, Molinski T, Harper M, Sullivan B, Faulkner DJ (1988) Haliclondiamine, an antimicrobial alkaloid from the sponge *Haliclona* sp. *Tetrahedron Lett.* 29: 3427-3428

- Falch B, König G, Wright A, Sticher O (1993) Ambigol A and B: new biologically active polychlorinated aromatic compounds from the terrestrial blue-green alga *Fischerella ambigua*. *J Org Chem* 58: 6570-6575
- Fattorusso E, Tagliatalata-Scafati O (2000) Two novel pyrrole-imidazole alkaloids from the Mediterranean sponge *Agelas oroides*. *Tetrahedron Letters* 41: 9917-9922
- Fendert T (2000) Charakterisierung der enzymatischen Abwehrreaktion in Schwämmen der Gattung *Aplysina* und Isolierung von Bromotyrosinalkaloiden aus *Aplysina insularis*. Mathematisch-naturwissenschaftliche Fakultät, Würzburg
- Forenza S, Minale L, Riccio R (1971) New bromo-pyrrole derivatives from the sponge *Agelas oroides*. *Chemical Communications*: 1129-1130
- Friedrich A, Fischer I, Proksch P, Hacker J, Hentschel U (2001) Temporal variation of the microbial community associated with the mediterranean sponge *Aplysina aerophoba*. *FEMS Microbiology Ecology* 38: 105-113
- Fu X, Schmitz F, Govindan M, Abbas S, Hanson K, Horton P, Crews P, Laney M, Schatzmann R (1995) Enzyme inhibitors: new and known polybrominated phenols and diphenyl ethers from four Indo-Pacific *Dysidea* sponges. *J Nat Prod* 58: 1384-1391
- Fu X, Schmitz F (1996) New brominated diphenyl ether from an unidentified species of *Dysidea* sponge. ¹³C NMR data for some brominated diphenyl ethers. *Journal of Natural Products* 59: 1102-1103
- Fujiki Y, Hubbard A, Fowler S, Lazarow P (1982) Isolation of intracellular membranes by means of sodium carbonate treatment: application to endoplasmatic reticulum. *The Journal of Cell Biology* 93: 97-102
- Fusetani N (2004) Biofouling and Antifouling. *Nat. Prod. Rep.* 21: 94-104
- Gallissan M, Vacelet J (1976) Ultrastructure de quelques stades de Lövogenèse de spongiaries du genre *Verongia* (Dictyoceratida). *Annales des Sciences Naturelles Zoologiques (Ser 12)* 18: 381-404
- Garces C, Kurenova E, Golubovska V, Cance W (2006) Vascular endothelial growth factor receptor-3 and focal adhesion kinase bind and suppress apoptosis in breast cancer cells. *Cancer Research* 66: 1446-1454
- Gil B, Sanz M, Terencio M, De Giulio A, De Rosa S, Alcaraz M, Paya M (1995) Effects of marine 2-polyprenyl-1,4-hydroquinones on phospholipase A2 activity and some inflammatory responses. *European Journal of Pharmacology* 285: 281-288
- Gourlay C, Ayscough K (2005) The actin cytoskeleton in ageing and apoptosis. *FEMS Yeast Res* 5: 1193-1198
- Grüning C (2007) Biotransformation von Sekundärmetaboliten in marinen Schwämmen. Bachelor. Institut für Pharmazeutische Biologie und Biotechnologie, Düsseldorf
- Haglund P, Zook D, Buser H, Hu J (1997) Identification and quantification of polybrominated diphenyl ethers and methoxy-polybrominated diphenyl ethers in Baltic biota. *Environ Sci Technol* 31: 3281-3287
- Handy S, Sabatini J, Zhang Y, Vulfova I (2004) Protection of poorly nucleophilic pyrroles. *Tetrahedron Lett* 45: 5057-5060
- Handy S, Zhang Y (2006) Regioselective couplings of dibromopyrrole esters. *Synthesis* 22: 3883-3887
- Harvell C, Fenical W, Roussis V, Ruesink J, Griggs C, Greene C (1993) Local and geographic variation in the defensive chemistry of a West Indian gorgonian coral (*Briareum asbestinum*). *Marine Ecology Progress Series* 93: 165-173
- Heil M, Bostock R (2002) Induced systemic resistance (ISR) against pathogens in the context of induced plant defences. *Annals of Botany* 89: 503-512

- Hofer M, Fecko A, Shen R, Setlur S, Oienta K, Tomlins S, Chinnaiya A, Rubin M (2004) Expression of the platelet-derived growth factor receptor in prostate cancer and treatment implications with tyrosine kinase inhibitors. *Neoplasia* 6: 503-512
- Iseki H, Ko T, Xue X, Seapan A, Townsend CJ (1998) A novel strategy for inhibiting growth of human pancreatic cancer cells by blocking cyclin dependent kinase activity. *J Gastrointest Surg* 2: 36-43
- Izeradjene K, Douglas L, Delaney A, Houghton J (2004) Influence of casein kinase II in tumor necrosis factor-related apoptosis-inducing ligand-induced apoptosis in human rhabdomyosarcoma cells. *Clinical Cancer Research* 10: 6650-6660
- Jackson J (1977) Competition on marine hard substrata: the adaptive significance of solitary and colonial strategies. *The American Naturalist* 111: 743-767
- Jormalainen V, Honkanen T (2004) Variation in natural selection for growth and phlorotannins in the brown alga *Fucus vesiculosus*. *Journal of Evolutionary Biology* 17: 807-820
- Kabsch W, Mannherz H, Suck D, Pai E, Holmes K (1990) Atomic structure of the actin:DNase 1 complex. *Nature* 347: 37-44
- Kalli K, Falowo O, Bale L, Zschunke M, Roche P, Conover C (2002) Functional insulin receptors on human epithelial ovarian carcinoma cells: Implications for IGF-II mitogenic signalling. *Endocrinology* 143: 3259-3267
- Keen N, Taylor S (2004) Aurora-kinase inhibitors as anticancer agents. *Nature Rev Cancers* 4: 927-936
- Kelly S, Jensen P, Henkel T, Fenical W, Pawlik J (2003) Effects of Caribbean sponge extracts on bacterial settlement. *Aquatic Microbial Ecology* 31: 175-182
- Klöppel A, Pfannkuchen M, Putz A, Proksch P, Brümmer F (2008) Ex situ cultivation of *Aplysina* spp. close to in situ conditions: Ecological, biochemical and histological aspects. *Marine Ecology* 29: 259-272
- König G, Wright A, Linden A (1998) Antiplasmodial and cytotoxic metabolites from the Maltese sponge *Agelas oroides*. *Planta Medica* 64: 443-447
- Kusakai G, Suzuki A, Ogura T, Miyamoto S, Ochiai A, Kaminishi M, Esumi H (2004) ARK5 expression on colorectal cancer and its implications for tumor progression. *Am J Pathol* 164: 987-995
- Lee J, Soung Y, Kim S, Park W, Nam S, Kim S, Lee J, Yoo N, Lee S (2005) ERBB2 kinase domain mutation in a gastric cancer metastasis. *APMIS* 113: 683-687
- Li D, Zhu J, Firozi P, Abbruzzese J, Evans D, Cleary K, Fries H, Sen S (2003) Overexpression of oncogenic STK15/BTAK/Aurora A kinase in human pancreatic cancer. *Clinical Cancer Research* 9: 991-997
- Liu H, Namikoshi M, Meguro S, Nagai H, Kobayashi H, Yao X (2004) Isolation and characterization of polybrominated diphenyl ethers as inhibitors of microtubule assembly from the marine sponge *Phyllospongia dendyi* collected at Palau. *Journal of Natural Products* 67: 472-474
- Loya S, Hizi A (1990) The inhibition of human immunodeficiency virus type 1 reverse transcriptase by avarol and avarone derivatives. *FEBS* 269: 131-134
- Loya S, Tal R, Hizi A, Issacs S, Kashman Y, Loya Y (1993) Hexaprenoid hydroquinones, novel inhibitors of the reverse transcriptase of human immunodeficiency virus type 1. *J Nat Prod* 56: 2120-2125
- Loya S, Rudi A, Kashman Y, Hizi A (1997) Mode of inhibition of HIV reverse transcriptase by 2-hexaprenylhydroquinone, a novel general inhibitor of RNA- and DNA-directed DNA polymerases. *Biochem J* 324: 721-727

- Macmillan J, Hudson J, Bull S, Dennis J, Swallow C (2001) Comparative expression of the mitotic regulators SAK and PLK in colorectal cancer. *Annals of Surgical Oncology* 8: 729-740
- Maida M, Carroll A, Coll J (1993) Variability of terpene content in the soft coral *Sinularia flexibilis* (Coelenterata: Octocorallia), and its ecological implications. *Journal of Chemical Ecology* 19: 2285-2296
- Malmvärn A, Marsh G, Kautsky L, Athanasiadou M, Bergmann A, Asplund L (2005) Hydroxylated and methoxylated brominated diphenyl ethers in the red algae *Ceramium tenuicorne* and blue mussels from the Baltic Sea. *Environmental Science and Technology* 39: 2990-2997
- Marak H, Biere A, Van Damme J (2002) Systemic, genotype-specific induction of two herbivore-deterrent iridoid glycosides in *Plantago lanceolata* L. in response to fungal infection by *Diaporthe adunca* (Rob.) Niessel. *J Chem Ecol* 28: 2429-2448
- Marchesi V (1985) Stabilizing infrastructure of cell membranes. *Ann Rev Cell Biol* 1: 531-561
- MarinLit (2007) A marine literature database maintained by the Marine Chemistry Group. University of Canterbury, Christchurch, New Zealand
- Marsh G, Stenutz R, Bergmann A (2003) Synthesis of hydroxylated and methoxylated polybrominated diphenyl ethers - natural products and potential polybrominated diphenyl ether metabolites. *European Journal of Organic Chemistry* 14: 2566-2576
- McCarty C (1970) syn-anti Isomerizations and rearrangements. Interscience Publishers, London
- McDermott T, Mortlock A, Heathcock C (1996) Total syntheses of (-)-Papuamine and (-)-Haloclonadamine. *J Org Chem* 61: 700-709
- Meijer L, Thunissen A, White A, Garnier M, M N, Tsai L, Walter J, Cleverley K, Salinas P, Wu Y, Biernat J, Mandelkow E, Kim S, Pettit G (2000) Inhibition of cyclin-dependent kinases, GSK-3 β and CK1 by hymenialdisine, a marine sponge constituent. *Chemistry and Biology* 7: 51-64
- Menezes D, Peng J, Garrett E, Louie S, Lee S, Wiesmann M, Tang Y, Shepard L, Goldbeck C, Oei Y, Ye H, Aukerman S, Heise C (2005) CHIR-258: A potent inhibitor of FLT3 kinase in experimental tumor xenograft models of human acute myelogenous leukemia. *Clinical Cancer Research* 11: 5281-5291
- Mihopoulos N, Vagias C, Chinou I, Roussakis C, Scoullou M, Harvala C, Roussis V (1999) Antibacterial and cytotoxic natural and synthesized hydroquinones from sponge *Ircinia spinulosa*. *Zeitschrift für Naturforschung C* 54: 417-423
- Minale L, Riccio R, Sodano G (1974) Avarol, a novel sesquiterpenoid hydroquinone with a rearranged drimane skeleton from the sponge *Dysidea avara*. *Tetrahedron Letters* 38: 3401-3404
- Mosmann T (1983) Rapid colorimetric assay for cellular growth and survival: application to proliferation and cytotoxicity assays. *Journal of Immunological Methods* 65: 55-63
- Müller W, Zahn R, Gasić M, Dogović N, Maidhof A, Becker C, Diehl-Seifert B, Eich E (1984) Avarol, a cytostatically active compound from the marine sponge *Dysidea avara*: 47-52
- Murakami Y, Oshima Y, Yasumoto T (1982) Identification of okadaic acid as a toxic component of a marine dinoflagellate *Prorocentrum lima*. *Bull. Jp. Soc. Sci. Fish.* 48: 69-72
- NationalCancerInstitute (2005) Mutations in glioblastoma in multiforme predict response to target therapies. *NCI Cancer Bulletin (online)* 2

- Ortlepp S, Sjögren M, Dahlström M, Weber H, Ebel R, Edrada RA, Thoms C, Schupp P, Bohlin L, Proksch P (2007) Antifouling Activity of Bromotyrosine Derived Sponge Metabolites and Synthetic Analogues. *Mar. Biotechnol.* in press
- Ouyang B, Knauf J, Smith E, Zhang L, Ramsey T, Yusuff N, Batt D, Fagin J (2006) Inhibitors of Raf kinase activity block growth of thyroid cancer cells with RET/PTC or BRAF mutations in vitro and in vivo. *Clinical Cancer Research* 12: 1785-1793
- Page M, West L, Northcote P, Battershill C, Kelly M (2005) Spatial and temporal variability of cytotoxic metabolites in populations of the New Zealand sponge *Mycale hentscheli*. *Journal of Chemical Ecology* 31: 1161-1174
- Pansini M (1997) Effects of light on the morphology, distribution and ecology of some Mediterranean sponges. *Biol Mar Mediterr* 4: 74-80
- Paul V, Van Alstyne K (1988) Chemical defense and chemical variation in some tropical Pacific species of *Halimeda* (Halimedaceae; Chlorophyta). *Coral Reefs* 6: 263-269
- Paul V, Van Alstyne K (1992) Activation of chemical defenses in the tropical green algae *Halimeda* spp. *Journal of Experimental Marine Biology and Ecology* 160: 191-203
- Paul V, Puglisi M (2004) Chemical mediation of interactions among marine organisms. *Nat. Prod. Rep.* 21: 189-209
- Paul V, Puglisi M, Ritson-Williams R (2006) Marine Chemical Ecology. *Natural Product Reports* 23: 153-180
- Paul V, Ritson-Williams R (2008) Marine chemical ecology. *Nat Prod Rep* 25: 662-695
- Pawlik J, Chanas B, Toonen R, Fenical W (1995) Defenses of Caribbean sponges against predatory reef fish. I. Chemical deterrence. *Mar Ecol Prog Ser* 127: 183-194
- Pedras M, Okanga F, Zaharia I, Khan A (2000) Phytoalexins from Crucifers: synthesis, biosynthesis, and biotransformation. *Phytochemistry* 53: 161-176
- Popov A, Stekhova S, Utinka N, Rebachuk N (1999) Antimicrobial and cytotoxic activity of sesquiterpenequinones and brominated diphenyl ethers isolated from marine sponges. *Pharm Chem* 33: 15-16
- Porter J, Targett N (1988) Allelochemical interactions between sponges and corals. *Biological Bulletin* 175: 230-239
- Proksch P, Edrada R, Ebel R (2002) Drugs from the seas - current status and microbiological implications. *Appl Microbiol Biotechnol* 59: 125-134
- Proksch P, Edrada RA, Ebel R (2006) Implications of marine biotechnology on drug discovery. In: Proksch P, Müller W (eds) *Frontiers in Marine Biotechnology*. Horizon Bioscience, Norfolk, pp 1-19
- Putz A, Proksch P (accepted) Chemical defense in marine ecosystems. In: Wink M (ed) *Functions of Plant Secondary Metabolites and their Exploitation in Biotechnology*
- Qiao H, Hung W, Tremblay E, Wojcik J, Gui J, Ho J, Klassen J, Campling B, Elliot B (2002) Constitutive activation of met kinase in non-small-cell lung carcinomas correlates with anchorage-independent cell survival. *J Cell Biochem* 86: 665-677
- Re R, Pellegrini N, Proteggente A, Pannala A, Yang M, Rice-Evans C (1999) Antioxidant activity applying an improved ABTS radical cation decolorization assay. *Free Radic Biol Med* 26: 1231-1237
- Richelle-Maurer E, De Kluijver M, Feio S, Gaudencio S, Gaspar H, Gomez R, Tavares R, Van de Vyver G, Van Soest R (2003) Localization and ecological significance of oroidin and sceptrin in the Caribbean sponge *Agelas conifera*. *Biochemical Systematics and Ecology* 31: 1073-1091

- Riedl R (1983) Fauna und Flora des Mittelmeeres. Verlag Paul Parey, Hamburg
- Rifai S, Fassouane A, Pinho P, Kijoa A, Nazareth N, Sao M, Nascimento J, Herz W (2005) Cytotoxicity and inhibition of lymphocyte proliferation of fasciculatin, a linear furanosesterpene isolated from *Ircinia variabilis* collected from the Atlantic Coast of Morocco. *Marine Drugs* 3: 15-21
- Rybakin V, Clemen C (2005) Coronin proteins as multifunctional regulators of the cytoskeleton and membrane trafficking. *BioEssays* 27.6: 625-632
- Sale P (1991) The Ecology of fishes on coral reefs. Academic Press, San Diego
- Salvá J, Faulkner DJ (1990) A new brominated diphenyl ether from a Philippine *Dysidea* species. *J Nat Prod* 53: 757-760
- Sarma A, Daum T, Müller W (1993) Part II: Biological properties of new metabolites and physiological activities of avarol and related compounds isolated from *Dysidea* sp. Secondary metabolites from sponges. Akademie gemeinnütziger Wissenschaften zu Erfurt, Erfurt, pp 100-158
- Schmitz K, Grabellus F, Callies R, Otterbach F, Wohlschlaeger J, Levkau B, Kimmig R, Schmid K, Baba H (2005) High expression of focal adhesion kinase (p125FAK) in node-negative breast cancer is related to overexpression of HER-2/neu and activated Akt kinase but does not predict outcome. *Breast Cancer Res* 7: R194-R203
- Smythe E, Ayscough K (2006) Actin regulation in endocytosis. *Journal of Cell Science* 119: 4589-4598
- Sourvinos G, Tsatsanis C, Spandidos D (1999) Overexpression of the Tpl-2/Cot oncogene in human breast cancer. *Oncogene* 18: 4968-4973
- Staal S (1987) Molecular cloning of the akt oncogene and its human homologues AKT1 and AKT2: Amplification of AKT1 in a primary human gastric adenocarcinoma. *Proc Natl Acad Sci USA* 84: 5034-5037
- Steenkamp E, Wright J, Baldauf S (2006) The protistan origins of animals and fungi. *Mol Biol Evol* 23: 93-106
- Stierle A, Strobel G, Stierle D (1993) Taxol and taxane production by *Taxomyces andreanae*, an endophytic fungus of Pacific yew. *Science* 260: 214-126
- Tachibana K, Scheuer P, Tsukitani Y, Kikuchi H, Van Engen D, Clardy J (1981) Okadaic acid: a cytotoxic polyether from two marine sponges of the genus *Halichondria*. *J. Am. Chem. Soc.* 103: 2469-2471
- Teeyapant R, Kreis P, Wray V, Witte L, Proksch P (1993a) Brominated secondary compounds from the marine sponge *Verongia aerophoba* and the sponge feeding gastropod *Tylodina perversa*. *Z Naturforsch [C]* 48: 640-644
- Teeyapant R, Proksch P (1993) Biotransformation of brominated compounds in the marine sponge *Verongia aerophoba* - evidence for an induced chemical defense? *Naturwissenschaften* 80: 369-370
- Teeyapant R, Woerdenbag HJ, Kreis P, Hacker J, Wray V, Proksch P (1993b) Antibiotic and cytotoxic activity of brominated compounds from the marine sponge *Verongia aerophoba*. *Z Naturforsch [C]* 48: 939-945
- Teeyapant R (1994) Brominated secondary metabolites of the marine sponge *Verongia aerophoba* Schmidt and the sponge feeding gastropod *Tylodina perversa* Gmelin: Identification, biological activities and biotransformation, Würzburg
- Terencio M, Ferrandiz M, Posadas I, Roig E, De Rosa S, De Giulio A, Payá M, Alcaraz M (1998) Suppression of leukotriene B4 and tumor necrosis factor release in acute inflammatory responses by novel prenylated hydroquinone derivatives. *Naunyn-Schmiedberg's Arch Pharmacol* 357: 565-572

- Thompson J, Barrow K, Faulkner D (1983) Localization of two brominated metabolites, Aerothionin and Homoaerothionin, in spherulous cells of the marine sponge *Aplysina fistularis* (= *Verongia thiona*). *Acta Zoologica* 64: 199-210
- Thompson J, Murphy P, Bergquist P, Evans E (1987) Environmentally induced variation in diterpene composition of the marine sponge *Rhopaloeides odorabile*. *Biochemical Systematics and Ecology* 15: 595-606
- Thoms C, Ebel R, Hentschel U, Proksch P (2003a) Sequestration of dietary alkaloids by the spongivorous marine mollusc *Tylodina perversa*. *Z Naturforsch [C]* 58: 426-432
- Thoms C, Horn M, Wagner M, Hentschel U, Proksch P (2003b) Monitoring microbial diversity and natural product profiles of the sponge *Aplysina cavernicola* following transplantation. *Marine Biology* 142: 685-692
- Thoms C, Wolff M, Padmakumar K, Ebel R, Proksch P (2004) Chemical defense of Mediterranean sponges *Aplysina cavernicola* and *Aplysina aerophoba*. *Z Naturforsch [C]* 59: 113-122
- Thoms C, Ebel R, Proksch P (2006) Activated chemical defense in *Aplysina* sponges revisited. *Journal of Chemical Ecology* 32: 97-123
- Tsoukatou M, Hellio C, Vagias C, Harvala C, Roussis V (2002) Chemical defense and antifouling activity of three Mediterranean sponges of the genus *Ircinia*. *Z Naturforsch [C]* 57c: 161-171
- Turon X, Becerro M, Uriz M (2000) Distribution of brominated compounds within the sponge *Aplysina aerophoba*: coupling of X-ray microanalysis with cryofixation techniques. *Cell Tissue Res* 301: 311-322
- Unson M, Faulkner DJ (1993) Cyanobacterial symbiont biosynthesis of chlorinated metabolites from *Dysidea herbacea* (Porifera). *Experientia* 49: 349-353
- Unson M, Holland N, Faulkner DJ (1994) A brominated secondary metabolite synthesized by the cyanobacterial symbiont of a marine sponge and accumulation of the crystalline metabolite in the sponge tissue. *Marine Biology* 119: 1-11
- Vacelet J (1959) Répartition générale des éponges et systématique des éponges cornées de la région de Marseille et de quelques stations méditerranéennes. *Receuil des travaux de la Station Marine d'Endoume* 16: 39-101
- Venkateswarlu Y, Venkata Ramy Reddy M (1994) Three new heptaprenylhydroquinone derivatives from the sponge *Ircinia fasciculata*. *Journal of Natural Products* 57: 1286-1289
- Vetter W, Stoll E, Garson M, Fahey S, Gaus C, Müller J (2002) Sponge halogenated natural products found at parts-per-million levels in marine mammals. *Environ Toxicol Chem* 21: 2014-2019
- Wajant H, Effenberger F (1996) Hydroxynitrile lyases of higher plants. *Biol. Chem.* 377: 611-617
- Wakimoto T, Maruyama A, Matsunaga S, Fusetani N (1999) Octa- and Nonaprenylhydroquinone sulfates, Inhibitors of *czl*,3-Fucosyltransferase VII, from an Australian Marine Sponge *Sarcotragus* sp. *Bioorganic & Medicinal Chemistry Letters* 9: 727-730
- Walker R, Thompson J, Faulkner D (1985) Exudation of biologically-active metabolites in the sponge *Aplysina fistularis* II. Chemical evidence. *Marine Biology* 88: 27-32
- Weichert W, Schmidt M, Gekeler V, Denkert C, Stephan C, Jung K, Loening S, Dietel M, Kristiansen G (2004) Polo-like kinase 1 is overexpressed in prostate cancer and linked to higher tumor grades. *Prostate* 60: 240-245

- Weinheimer A, Spraggins R (1969) The occurrence of two new prostaglandin derivatives (15-epi-PGA₂ and its acetate methyl ester) in the gorgonian *Plexaura homomalla*. *Chemistry of Coelenterates*. *Tetrahedron Lett* 15: 5185-5188
- Weiss B, Ebel R, Elbrächter M, Kirchner M, Proksch P (1996) Defense metabolites from the marine sponge *Verongia aerophoba*. *Biochemical Systematics and Ecology* 24: 1-12
- Wilkinson C, Vacelet J (1979) Transplantation of marine sponges to different conditions of light and current. *Journal of Experimental Marine Biology and Ecology* 37: 91-104
- Xia G, Kumar S, Masood R, Zu S, Reddy R, Krasnaperov V, Quinn D, Henshal S, Sutherland R, Pinski J, Daneshmand S, Buscarini M, Stein J, Zong C, Broek D, Roy-Burman P, Gill P (2005) EphB4 expression and biological significance in prostate. *Cancer Res* 65: 4623-4632
- Xu Y, Johnson R, Hecht S (2005) Polybrominated diphenyl ethers from a sponge of the *Dysidea* genus that inhibit Tie2 kinase. *Bioorganic & Medicinal Chemistry* 13: 657-659
- Yates J, Peckol P (1993) Effects of nutrient availability and herbivory on polyphenolics in the seaweed *Fucus vesiculosus*. *Ecology* 74: 1757-1766
- Yu Q, Sicinska E, Geng Y, Ahnstrom M, Zagozdou A, Kong Y, Gardner H, Kiyokawa H, Harris L, Stal O, Sicinski P (2006) Requirement for CDK4 kinase function in breast cancer. *Cancer Cell* 9: 23-32
- Zhang X, Yee D (2000) Tyrosine kinase signalling in breast cancer: Insulin-like growth factors and their receptors in breast cancer. *Breast Cancer Res* 2: 170-175

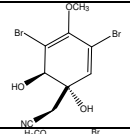
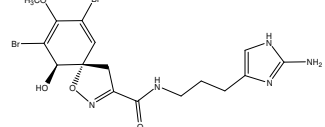
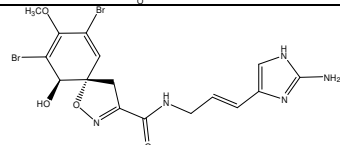
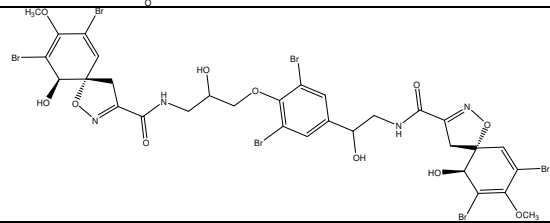
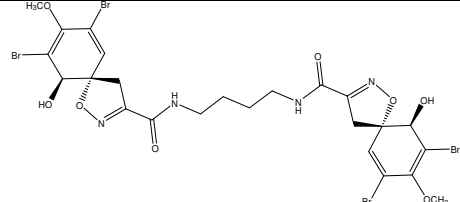
Abbreviations

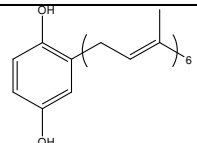
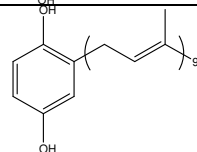
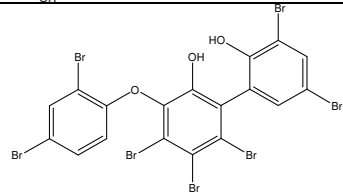
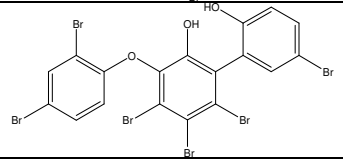
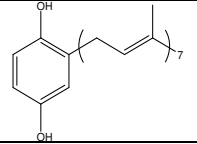
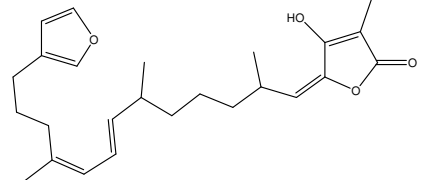
ACN	Acetonitrile
ANOVA	Analysis of variance
APS	Ammonium persulfate
br	Broad
CFU	Colony forming units
COSY	Correlation spectroscopy
d	Doublet
DCM	Dichloromethane
DMSO	Dimethyl sulfoxide
DMSO- <i>d</i> ₆	Deuterated dimethyl sulfoxide
EGMME	Ethylene glycol monomethyl ether
ELISA	Enzyme Linked Immunosorbent Assay
EMBL	European Molecular Biology Laboratory
ESI	Electron spray ionisation
<i>et al.</i>	<i>et alii</i>
EtOAc	Ethyl acetate
FAB	Fast atom bombardment
FPLC	Fast protein liquid chromatography
HHU	Heinrich-Heine-Universität
HMBC	Hetero multinuclear bond coherence
HMQC	Hetero multinuclear quantum coherence
HPLC	High performance liquid chromatography
HPLC-DAD	HPLC with diode array detector
HREI	High resolution electron impact
Hz	Hertz
Da	Dalton
IC	Inhibition concentration
LC	Liquid chromatography
M	Molar
MeOD	Deuterated methanol
MeOH	Methanol
MS	Mass spectrometry

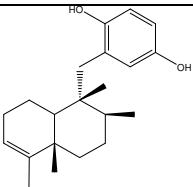
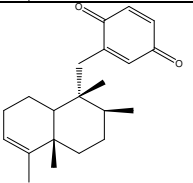
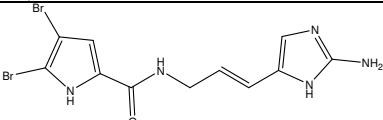
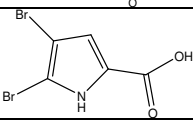
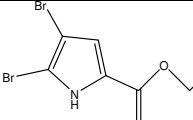
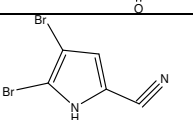
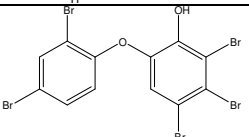
MTT	3-(4,5-Dimethylthiazol-2-yl)-2,5-diphenyltetrazolium bromide
MW	Molecular weight
NaCl	Sodium chloride
NHS	N-hydroxy succinimide
NMR	Nuclear magnetic resonance
PAGE	Polyacrylamide gel electrophoresis
PBS	Phosphate buffered saline
ppm	Parts per million
q	Quartet
RP	Reversed Phase
rpm	Rotations per minute
RT	Retention time
s	Singlet
SD	Standard deviation
SDS	Sodium dodecyl sulphate
t	Triplet
TEMED	N, N, N', N'-tetramethylethylenediamine
TLC	Thin layer chromatography
TMS	Tetramethylsilane
UV	Ultraviolet

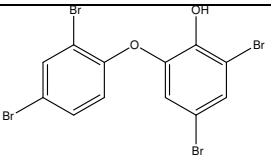
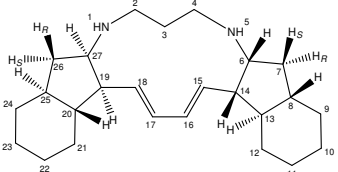
Appendix

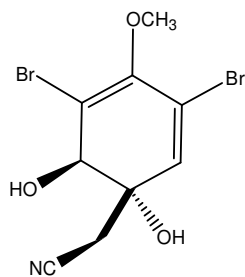
List of isolated compounds

Species	Isolated compounds, amount (mg)	Structure	MW [g/mol]
<i>Aplysina aerophoba</i> , <i>Aplysina cavernicola</i>	Aeroplysin-1 (5), 503.7 mg		339
	Aerophobin-2 (2), 1684.6 mg		505
	Aplysinamis-1 (1), 9.2 mg		503
	Isofistularin-3 (3), 1650.5 mg		1114
	Aerothionin (4), 30.5 mg		818

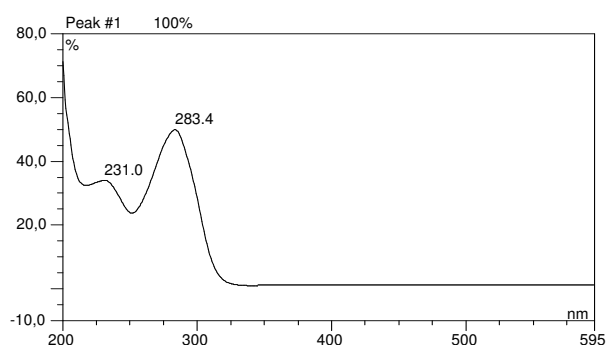
<i>Sarcotragus muscarum</i>	Hexaprenylhydroquinone (15), 76.2 mg		518
	Nonaprenylhydroquinone (17), 18.2 mg		723
	Brominated ambigol derivative 1 (18), 3.4 mg	 Proposed structure	830
	Brominated ambigol derivative 2 (19), 1.7 mg	 Proposed structure	751
<i>Ircinia fasciculata</i>	Heptaprenylhydroquinone (16), 12.6 mg		587
<i>Ircinia variabilis</i>	Fasciculatin (20), 11.1 mg		398

<i>Dysidea avara</i>	Avarol (9), 179.3 mg		314
	Avarone (10), 38.5 mg oxidated from 44.0 mg avarol		312
<i>Agelas oroides</i>	Oroidin (11), 101.6 mg		389
	4,5-dibromo-1H-pyrrol-2-carboxylic acid (12), 106.2 mg		268
	4,5-dibromo-1H-pyrrol-2-carboxylic acid ethyl ester (13), 49.0 mg		296
	4,5-dibromo-1H-pyrrol-2-carbonitrile (14), 3.6 mg		249
<i>Dysidea granulosa</i>	4,5,6-tribromo-2-(2',4'-dibromophenoxy)phenol (21), 86.0 mg		580

	4,6-dibromo-2-(2',4'-dibromophenoxy)phenol (22), 144.3 mg		501
<i>Haliclona spec</i>	Papuamine (23), 22.7 mg	 Proposed structure	368

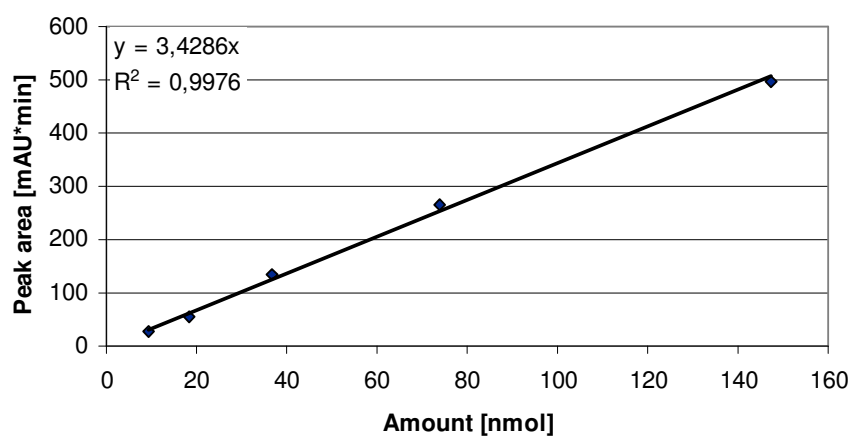
Quantified metabolites: Calibration curves, UV spectra, molecular weightAerplysinin-1 (5) (*Aplysina*)

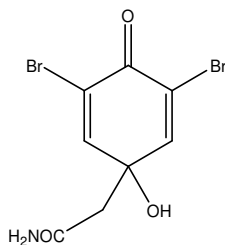
MW: 339 g/mol



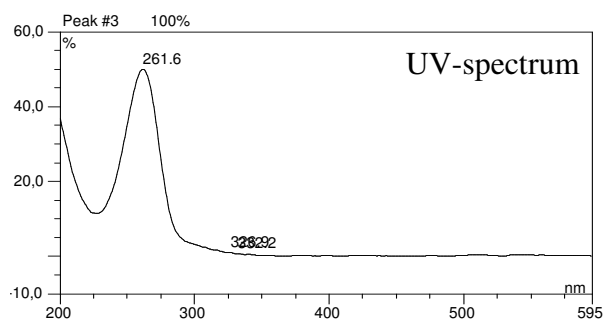
Retention time with HPLC standard gradient: 14.4 min

Calibration curve (at 280 nm)



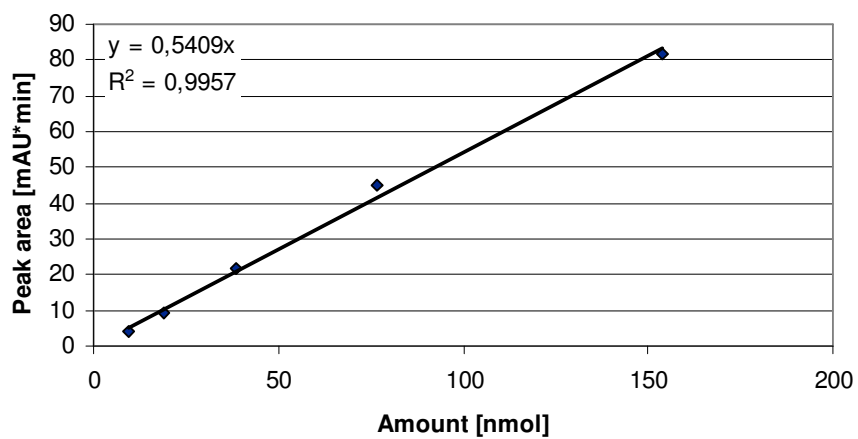
Dienone (6) (*Aplysina*)

MW: 325 g/mol

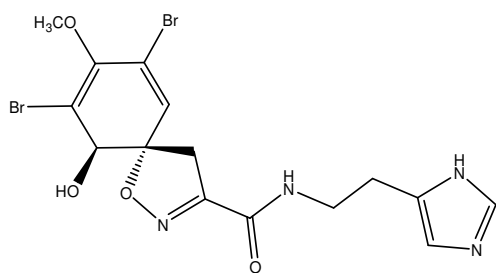


Retention time with HPLC standard gradient: 10.4 min

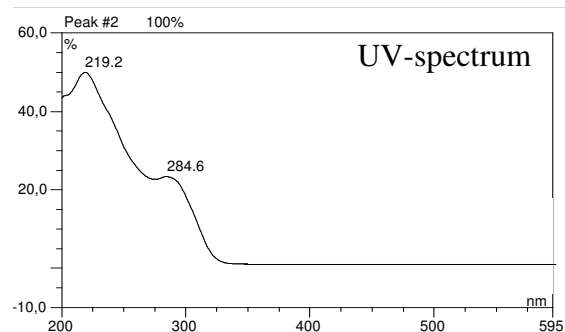
Calibration curve (at 280 nm)



Aerophobin-1 (2) (*Aplysina*)

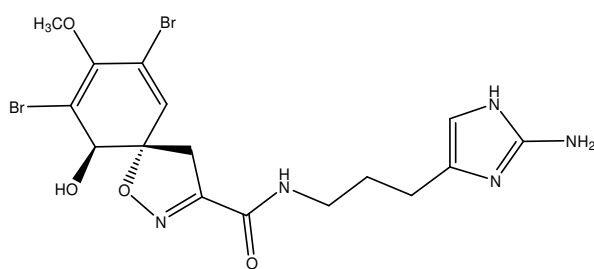


MW: 489 g/mol

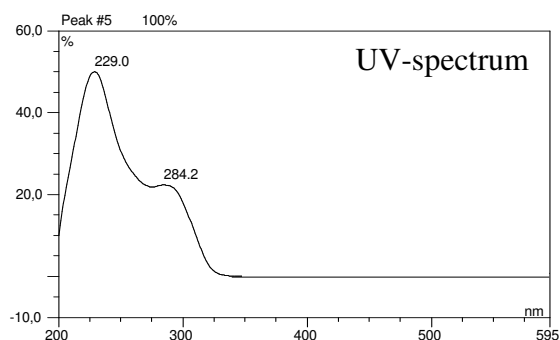


Retention time with HPLC standard gradient: 16.9 min

Aerophobin-2 (2) (*Aplysina*)

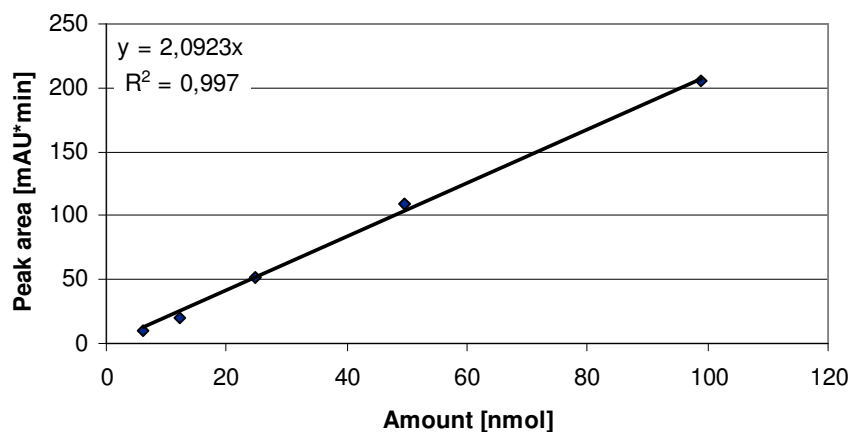


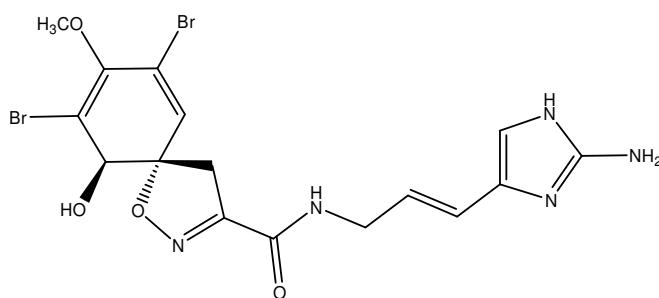
MW: 505 g/mol



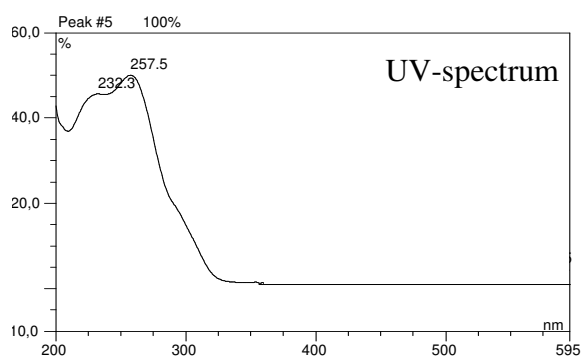
Retention time with HPLC standard gradient: 18.5 min

Calibration curve (at 280 nm)



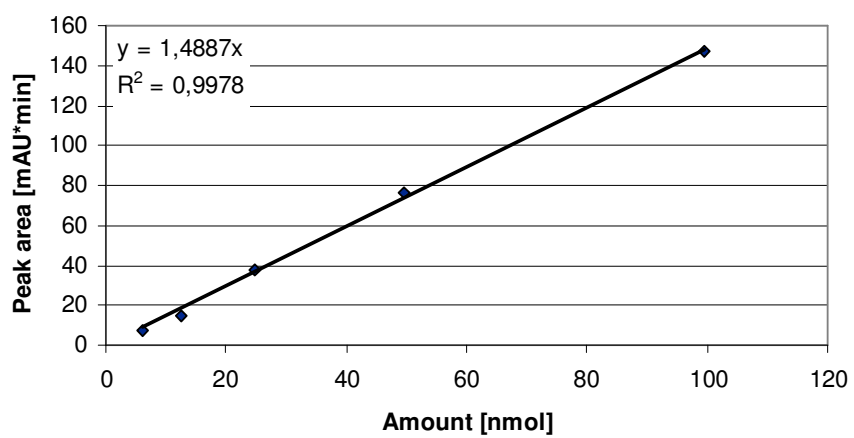
Aplysinamisin-1 (1) (*Aplysina*)

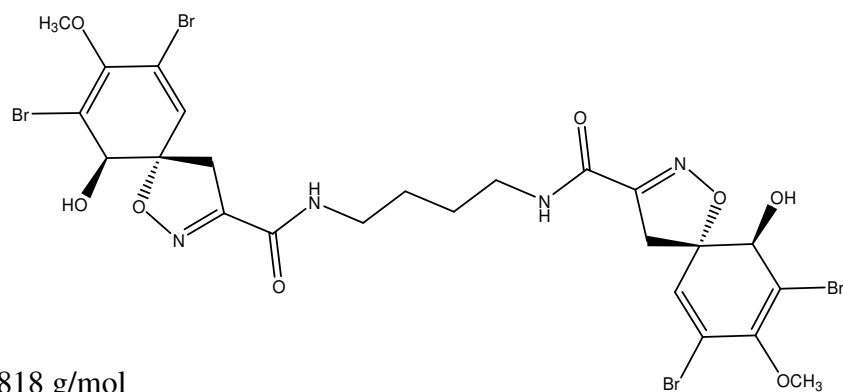
MW: 503 g/mol



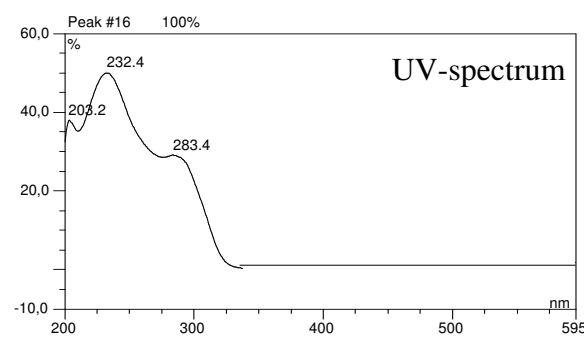
Retention time with HPLC standard gradient: 19.5 min

Calibration curve (at 280 nm)



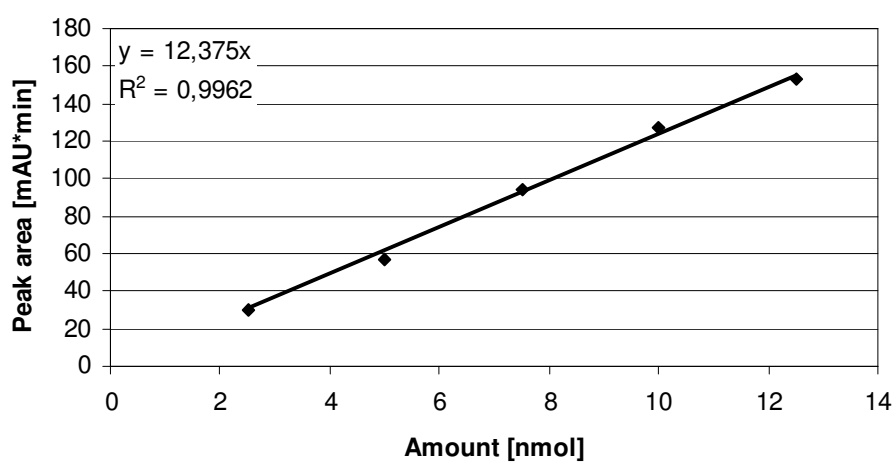
Aerothionin (4) (*Aplysina cavernicola*)

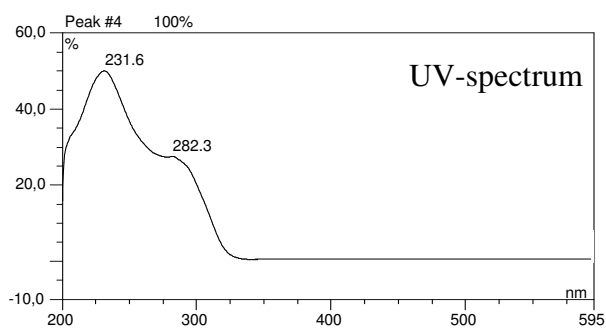
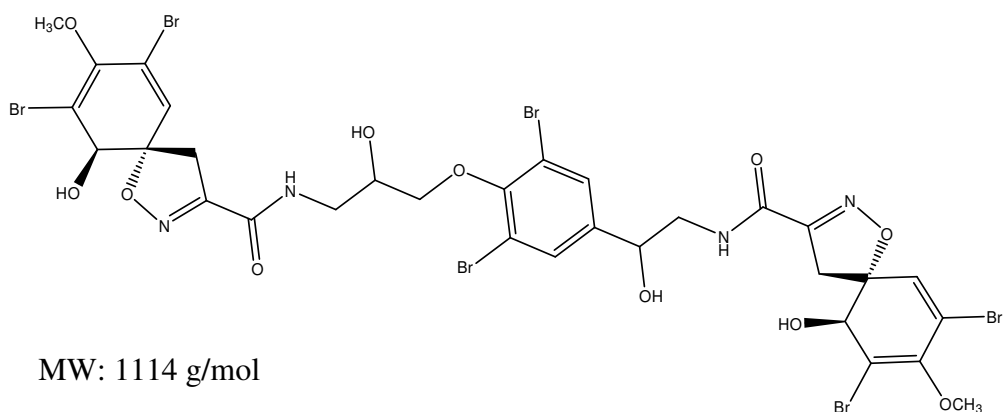
MW: 818 g/mol



Retention time with HPLC standard gradient: 27.0 min

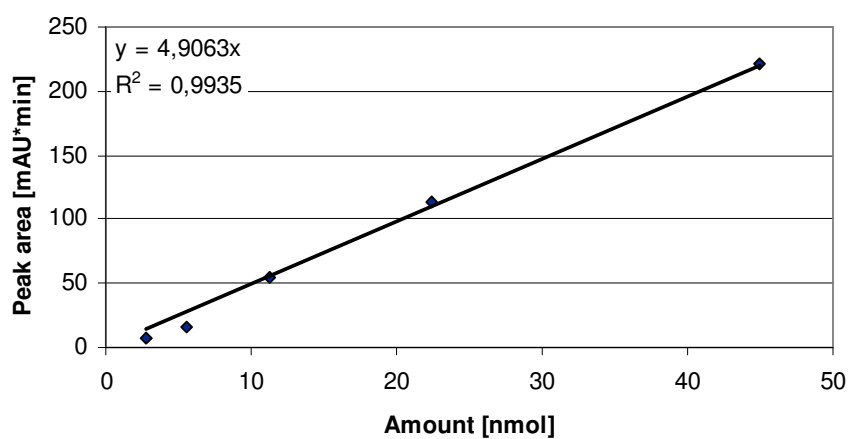
Calibration curve (at 280 nm)

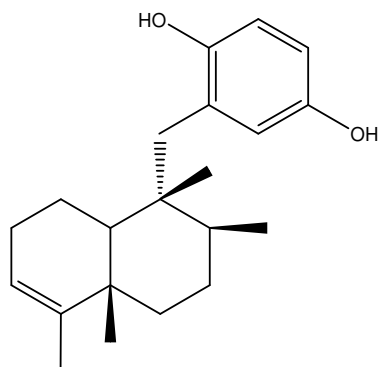


Isofistularin-3 (3) (*Aplysina*)

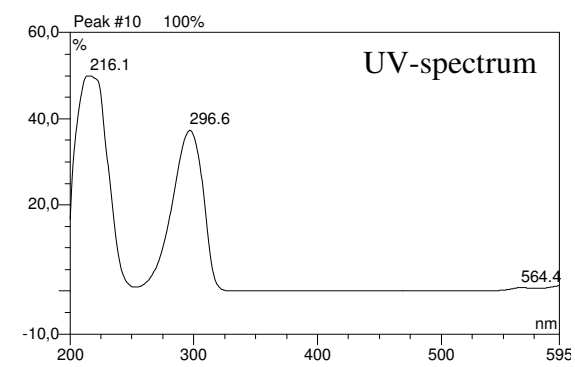
Retention time with HPLC standard gradient: 28.0 min

Calibration curve (at 280 nm)



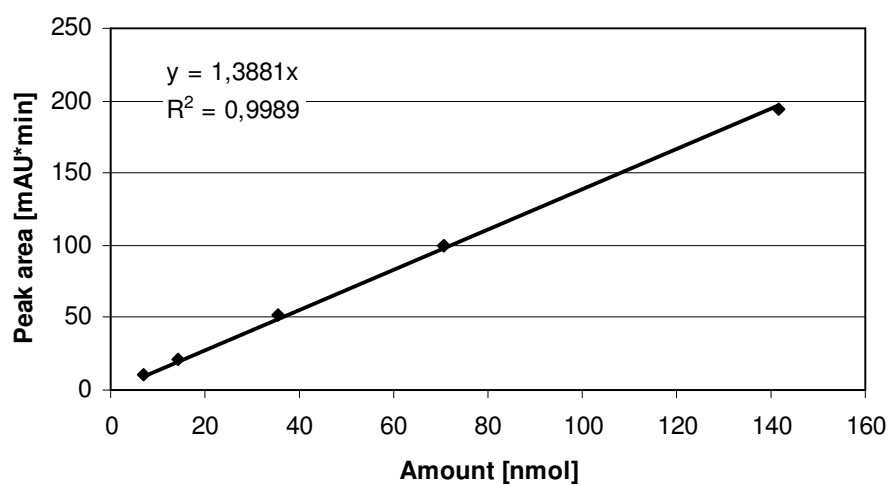
Avarol (9) (*Dysidea avara*)

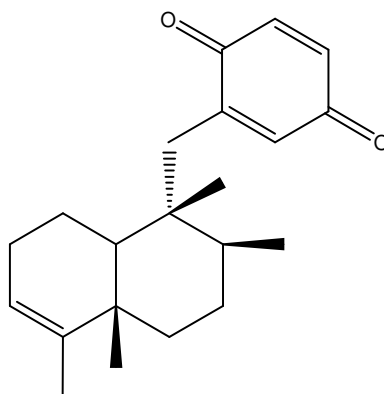
MW: 314 g/mol

 $[\alpha]_D^{20} + 7.5^\circ$ (*c* 0.5, CHCl₃)

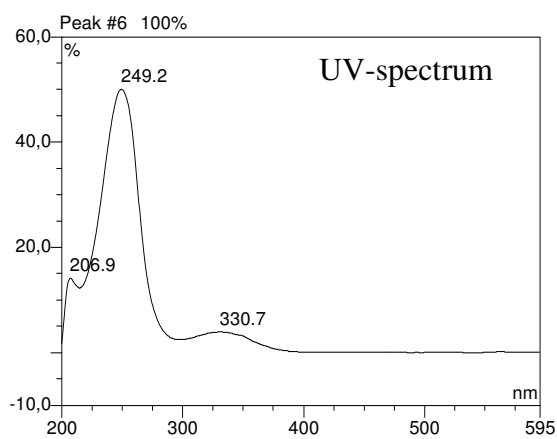
Retention time with HPLC standard gradient: 33.1 min

Calibration curve (at 235 nm)



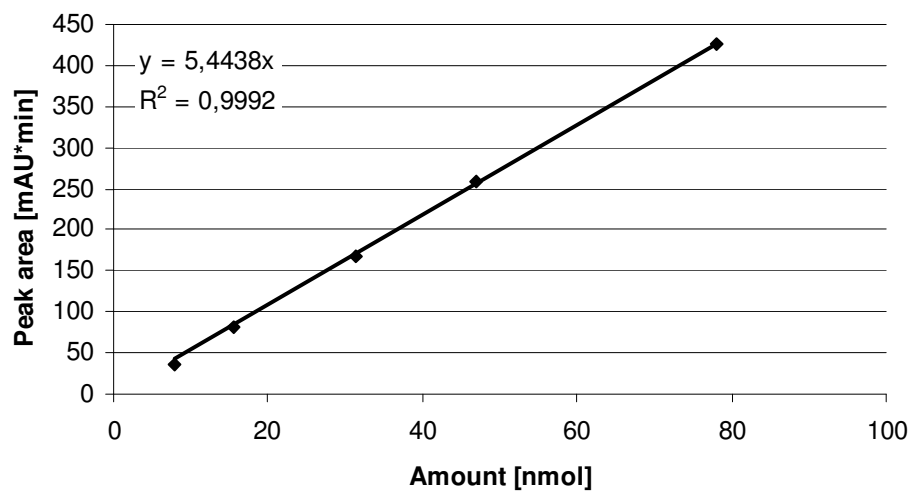
Avarone (10) (*Dysidea avara*)

MW: 312 g/mol

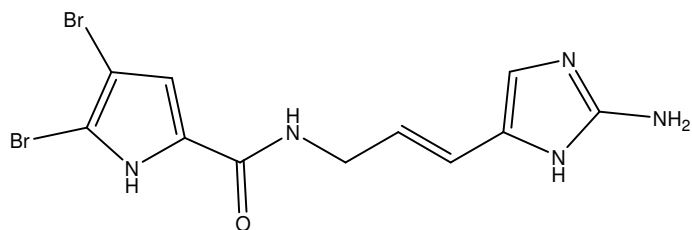


Retention time with HPLC standard gradient: 36.6 min

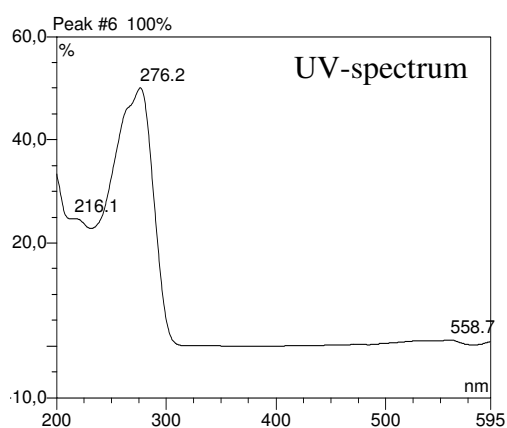
Calibration curve (at 235 nm)



Oroidin (11) (*Agelas oroides*)

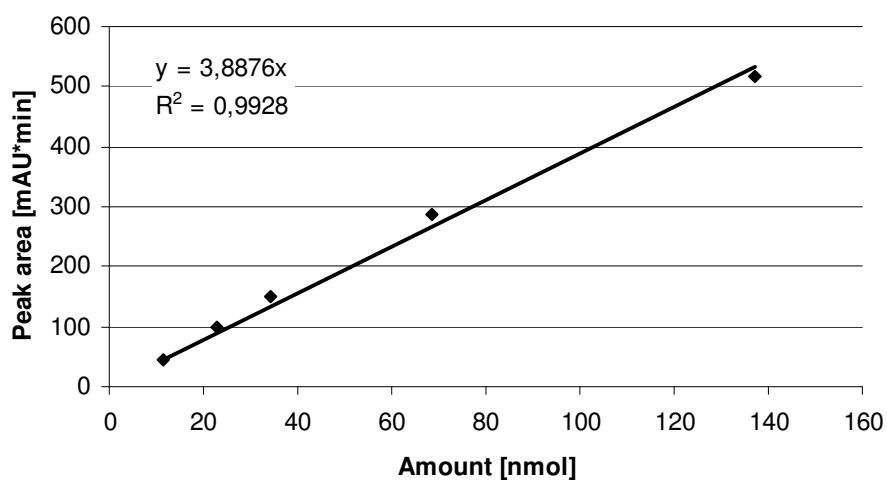


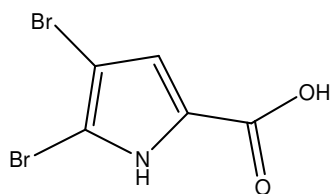
MW: 389 g/mol



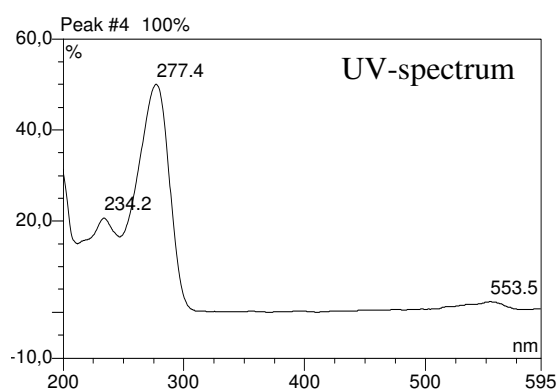
Retention time with HPLC standard gradient: 19.8 min

Calibration curve (at 235 nm)



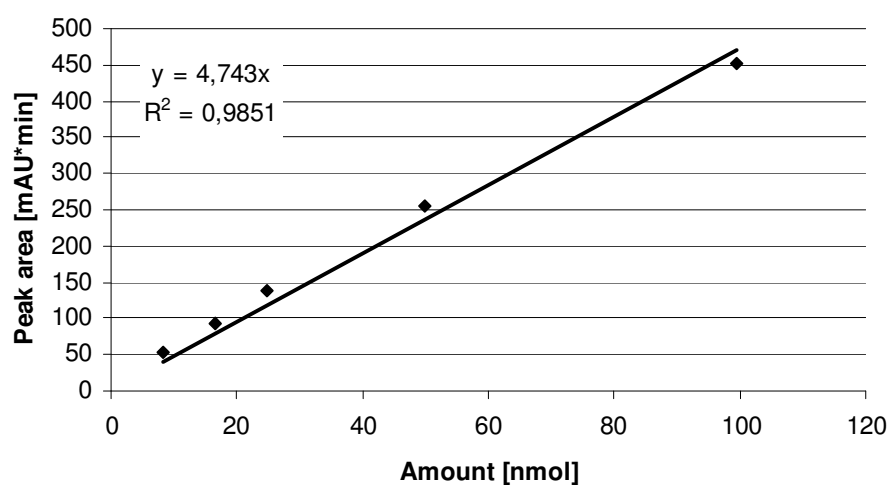
4,5-Dibromo-1H-pyrrol-2-carboxylic acid (12) (*Agelas oroides*)

MW: 268 g/mol

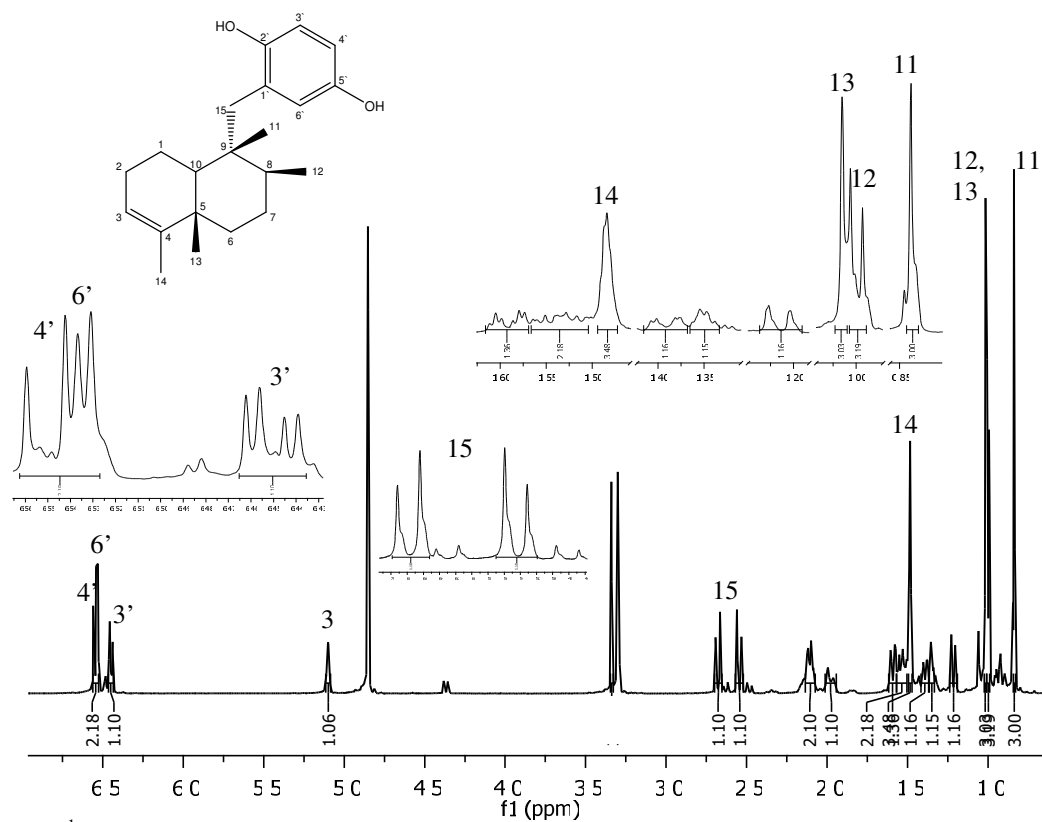
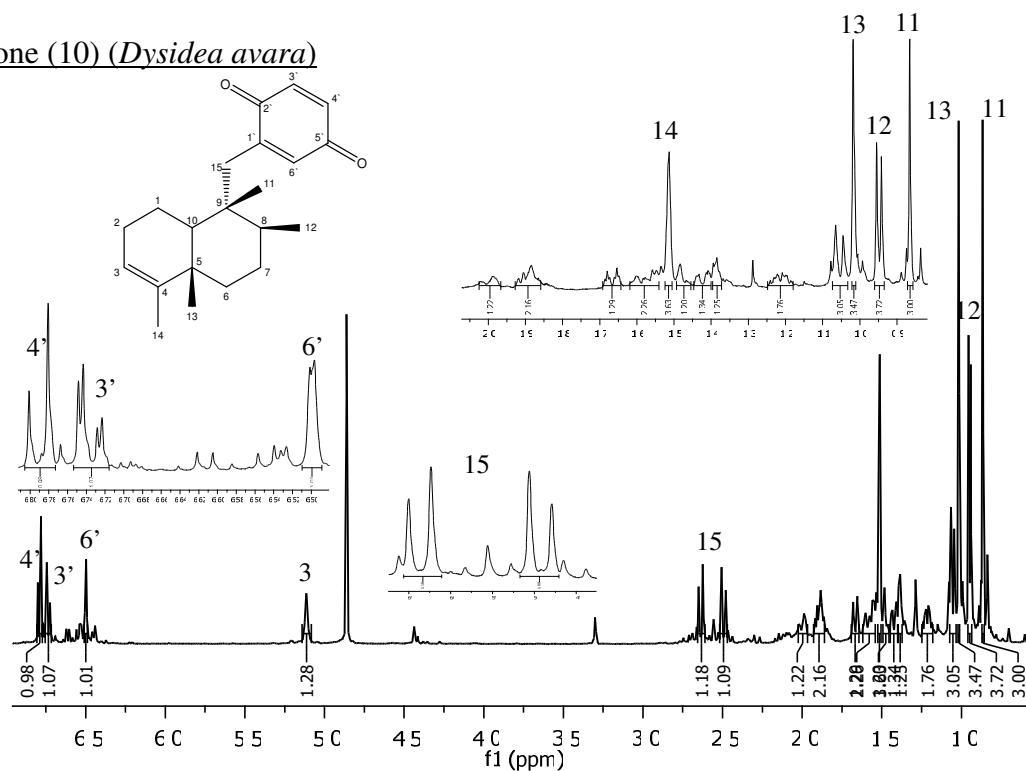


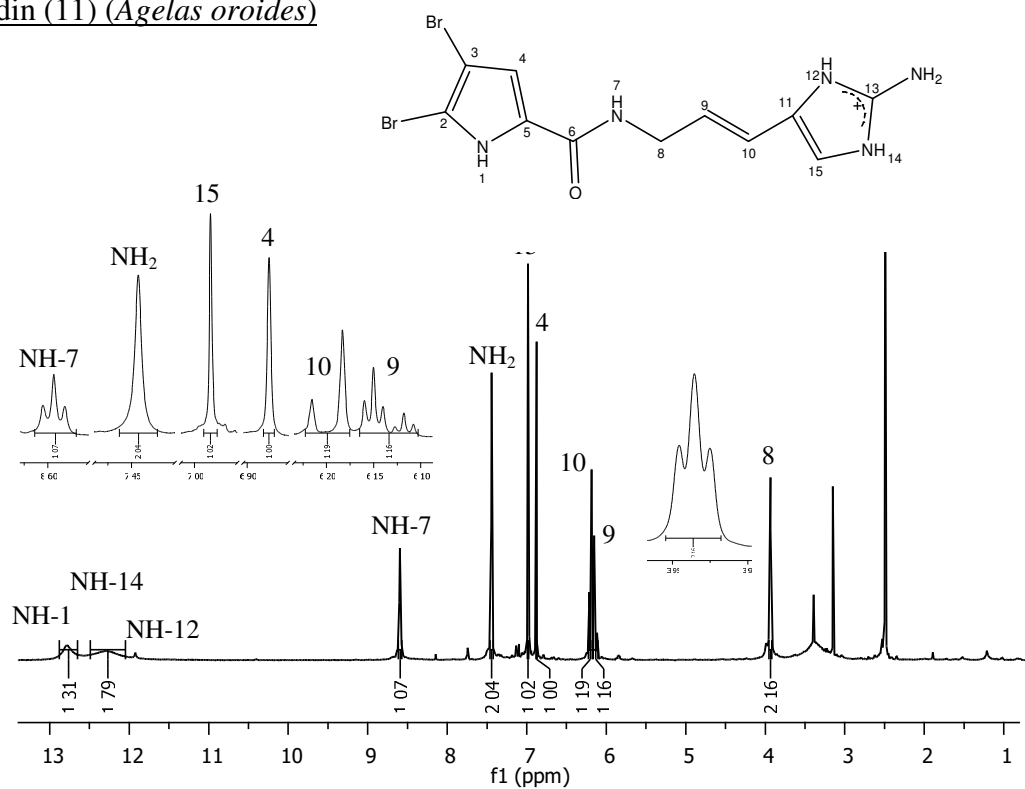
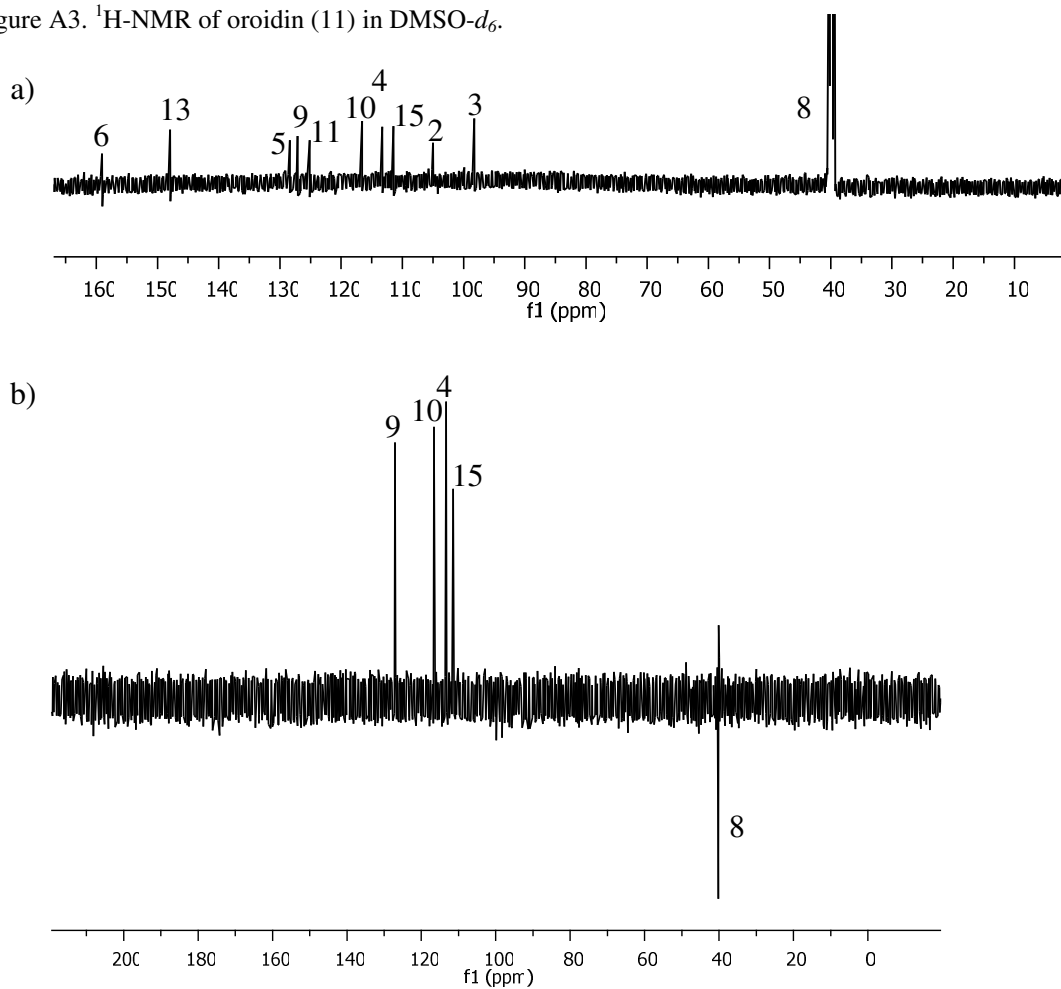
Retention time with HPLC standard gradient: 24.1 min

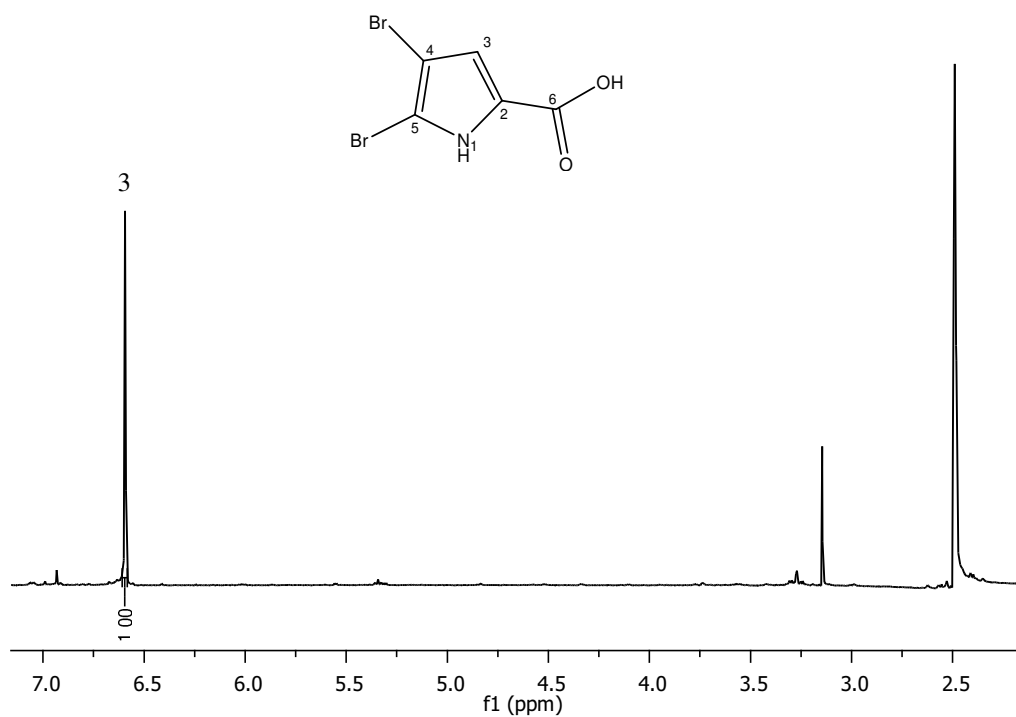
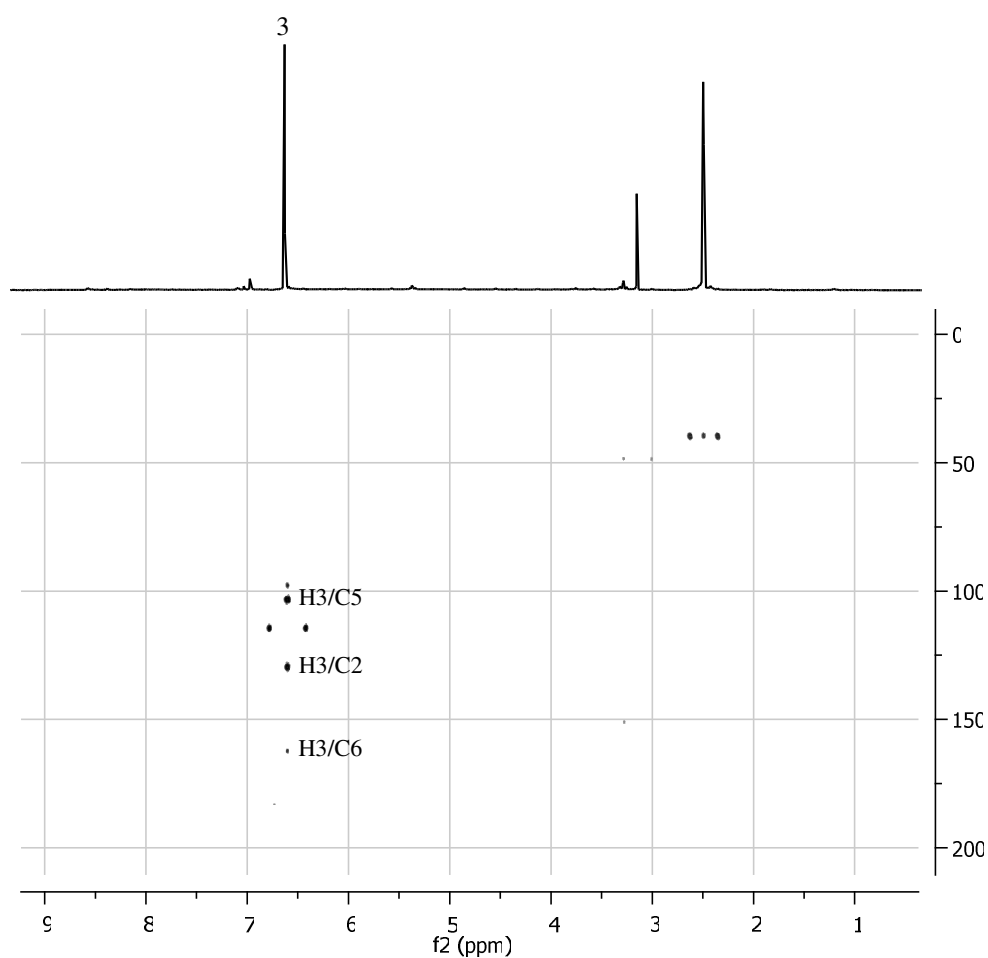
Calibration curve (at 235 nm)

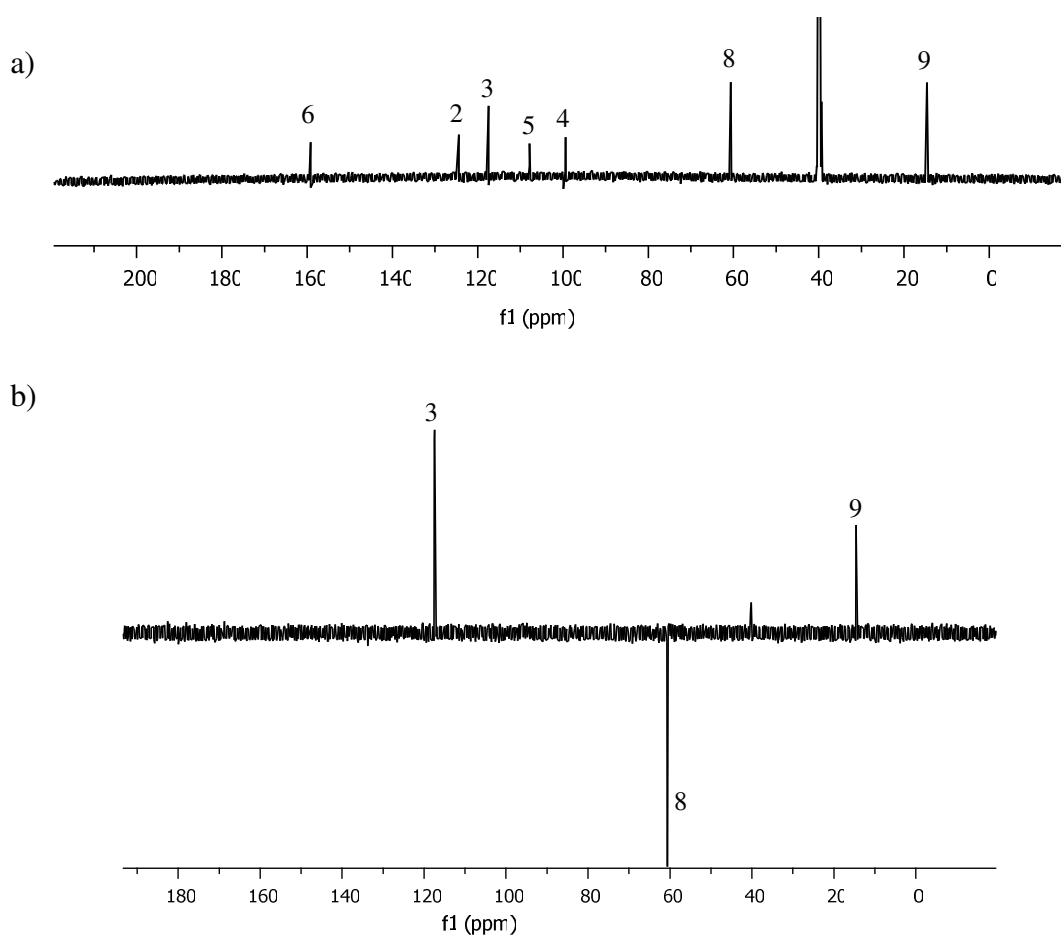
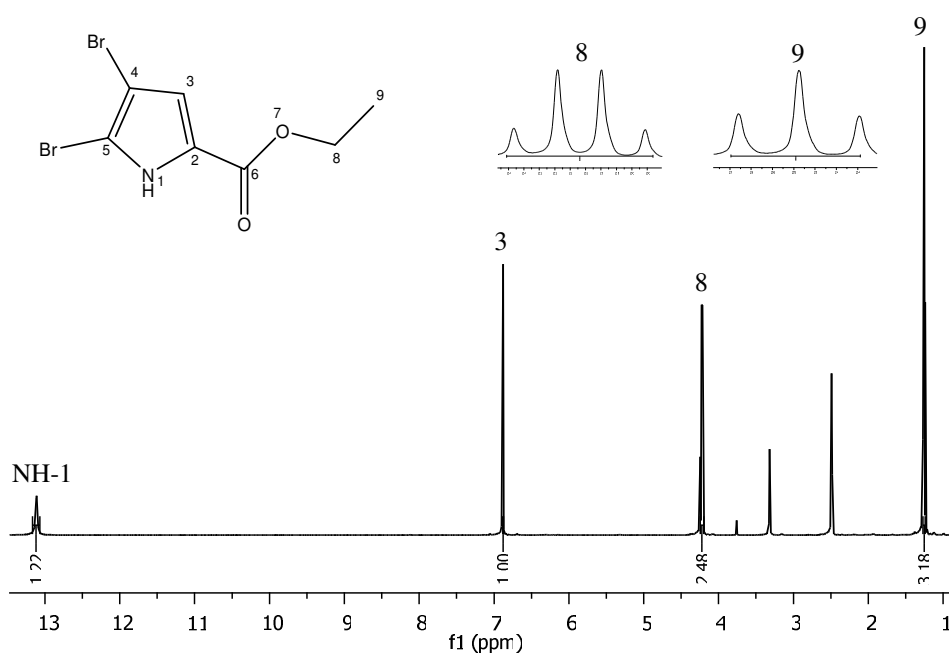


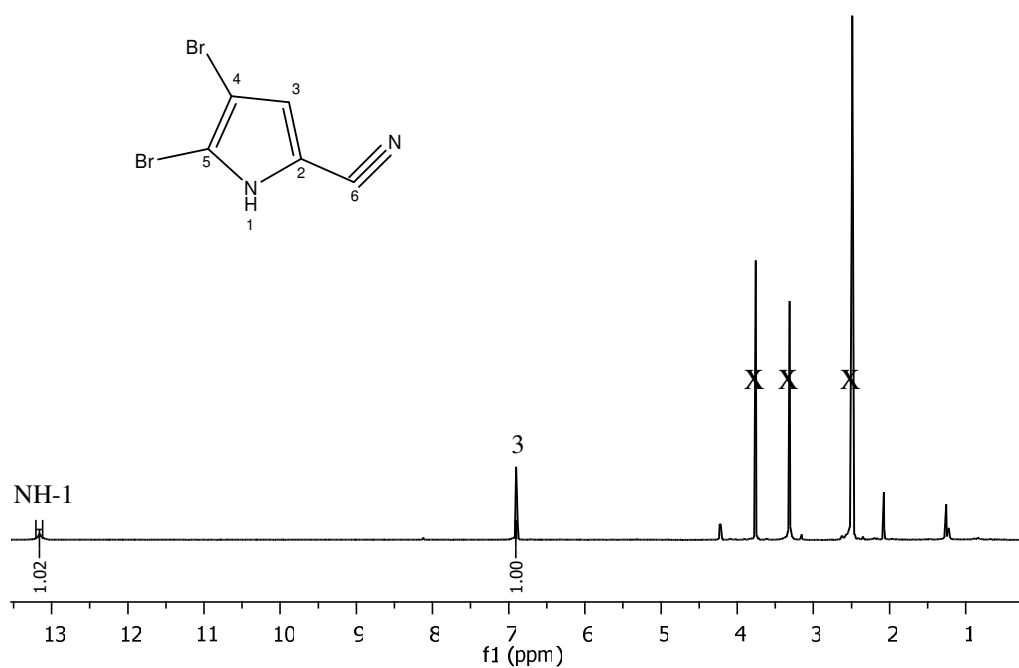
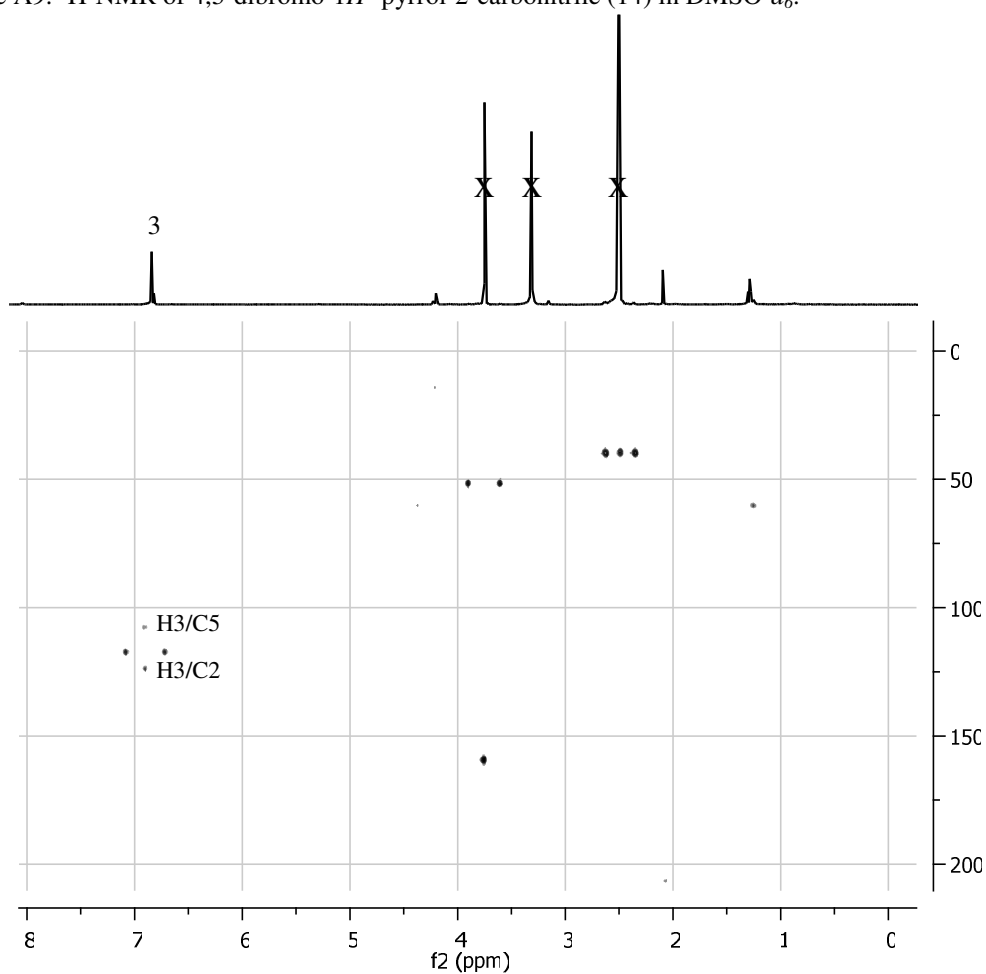
NMR spectra of isolated compounds

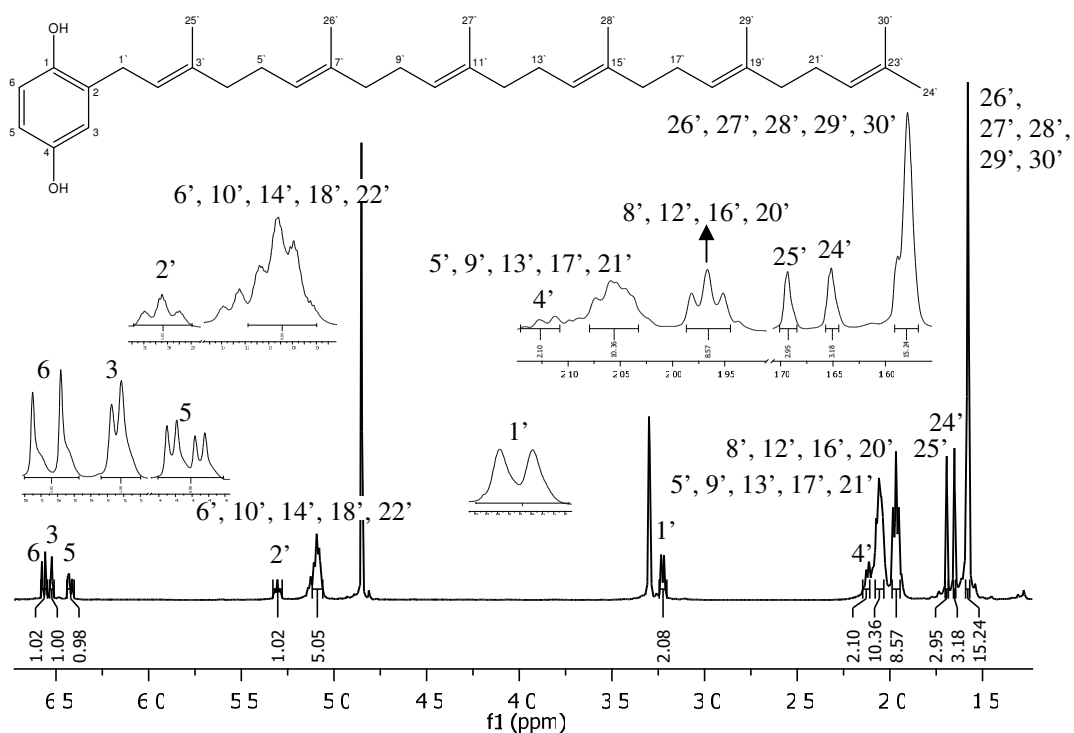
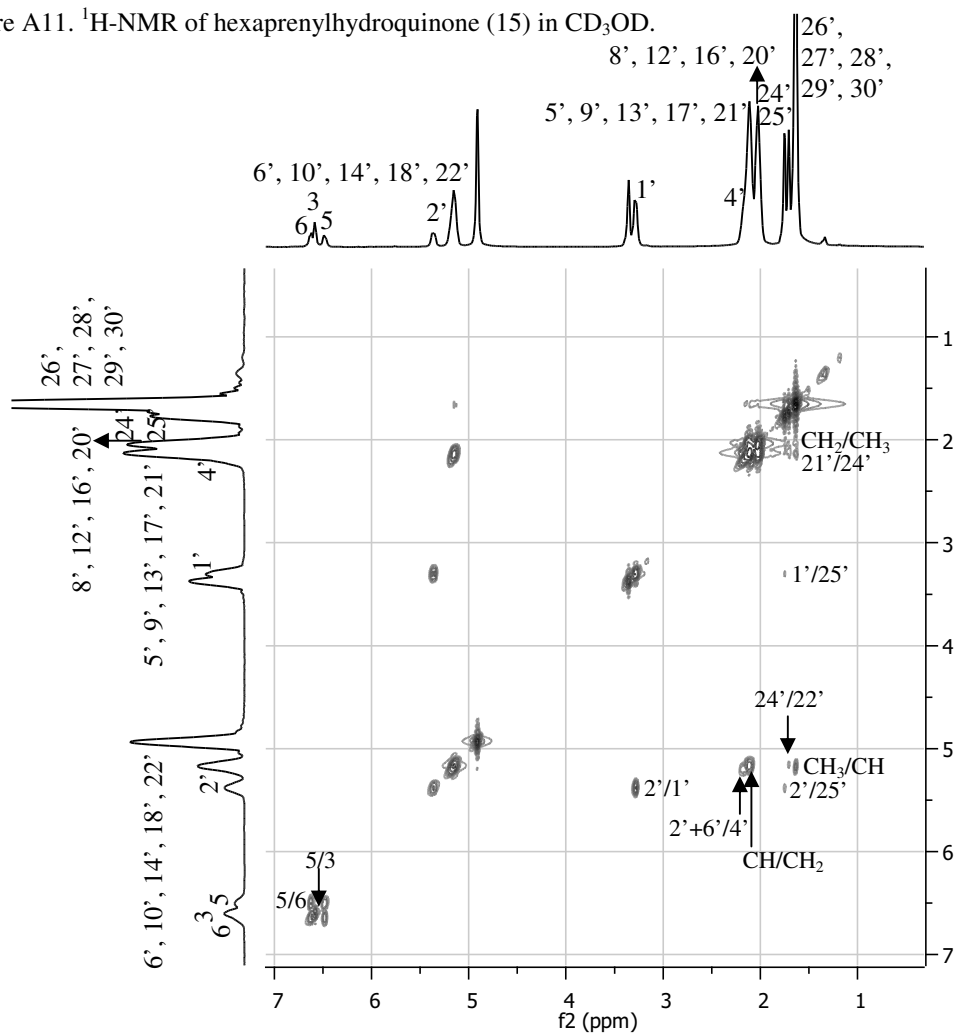
Avarol (9) (*Dysidea avara*)Figure A1. ¹H-NMR of avarol (9) in CD₃OD.Avarone (10) (*Dysidea avara*)Figure A2. ¹H-NMR of avarone (10) in CD₃OD.

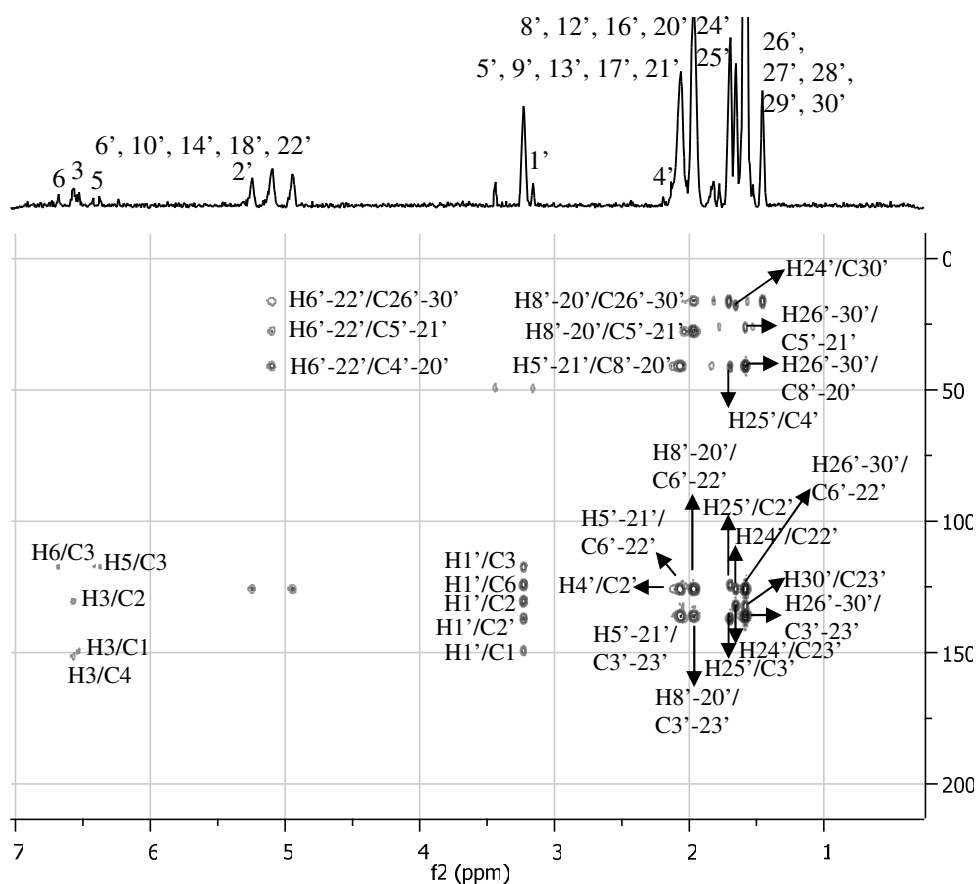
Oroidin (11) (*Agelas oroides*)Figure A3. ¹H-NMR of oroidin (11) in DMSO-*d*₆.Figure A4. a) ¹³C-NMR and b) DEPT of oroidin (11) in DMSO-*d*₆.

4,5-Dibromo-1*H*-pyrrol-2-carboxylic acid (12) (*Agelas oroides*)Figure A5. $^1\text{H-NMR}$ of 4,5-dibromo-1*H*-pyrrol-2-carboxylic acid (12) in $\text{DMSO-}d_6$.Figure A6. HMBC of 4,5-dibromo-1*H*-pyrrol-2-carboxylic acid (12) in $\text{DMSO-}d_6$.

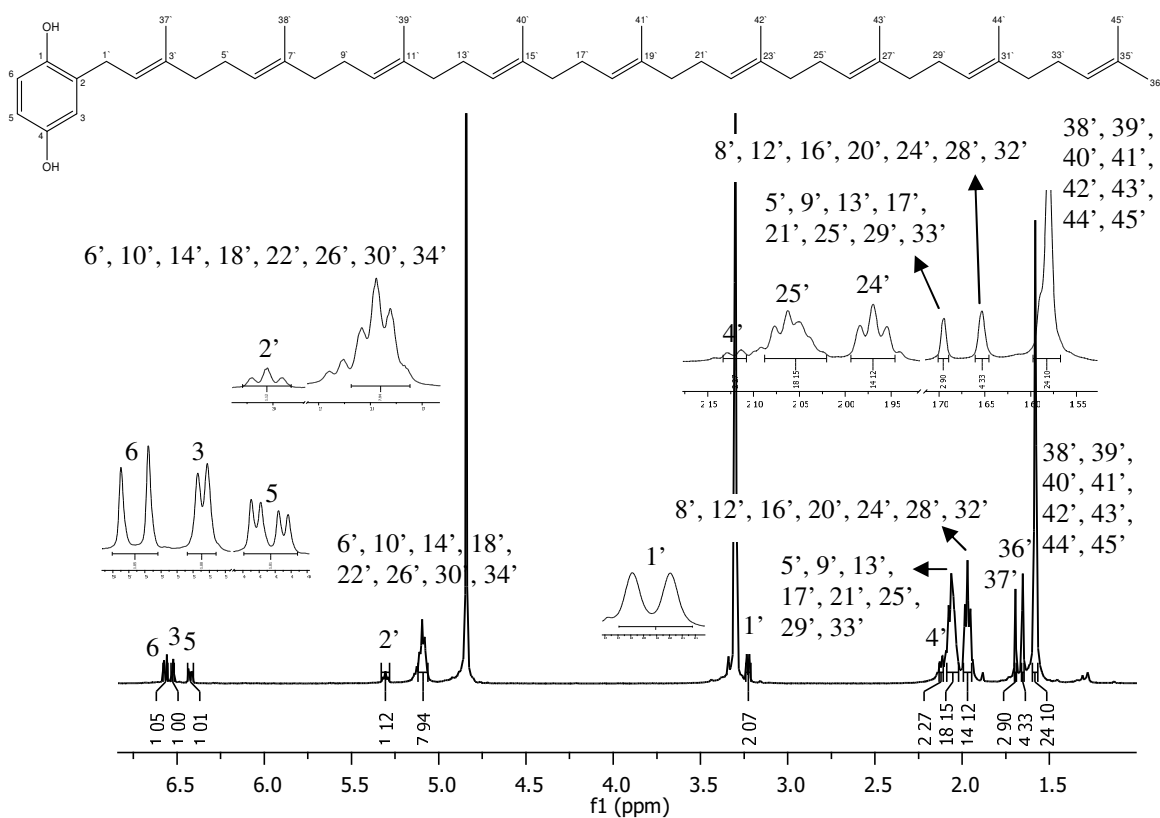
4,5-Dibromo-1*H*-pyrrol-2-carboxylic acid ethyl ester (13) (*Agelas oroides*)

4,5-Dibromo-1H-pyrrol-2-carbonitrile (14) (*Agelas oroides*)Figure A9. ¹H-NMR of 4,5-dibromo-1H-pyrrol-2-carbonitrile (14) in DMSO-*d*₆.Figure A10. HMBC of 4,5-dibromo-1H-pyrrol-2-carbonitrile (14) in DMSO-*d*₆.

Hexaprenylhydroquinone (15) (*Sarcotragus muscarum*)Figure A11. $^1\text{H-NMR}$ of hexaprenylhydroquinone (15) in CD_3OD .Figure A12. H,H-COSY of hexaprenylhydroquinone (15) in CD_3OD .

Figure A13. HMBC of hexaprenylhydroquinone (15) in CD_3OD .

Nonaprenylhydroquinone (17) (*Sarcotragus muscarum*)

Figure A14. ^1H -NMR of nonaprenylhydroquinone (17) in CD_3OD .

Heptaprenylhydroquinone (16) (*Ircinia fasciculata*)

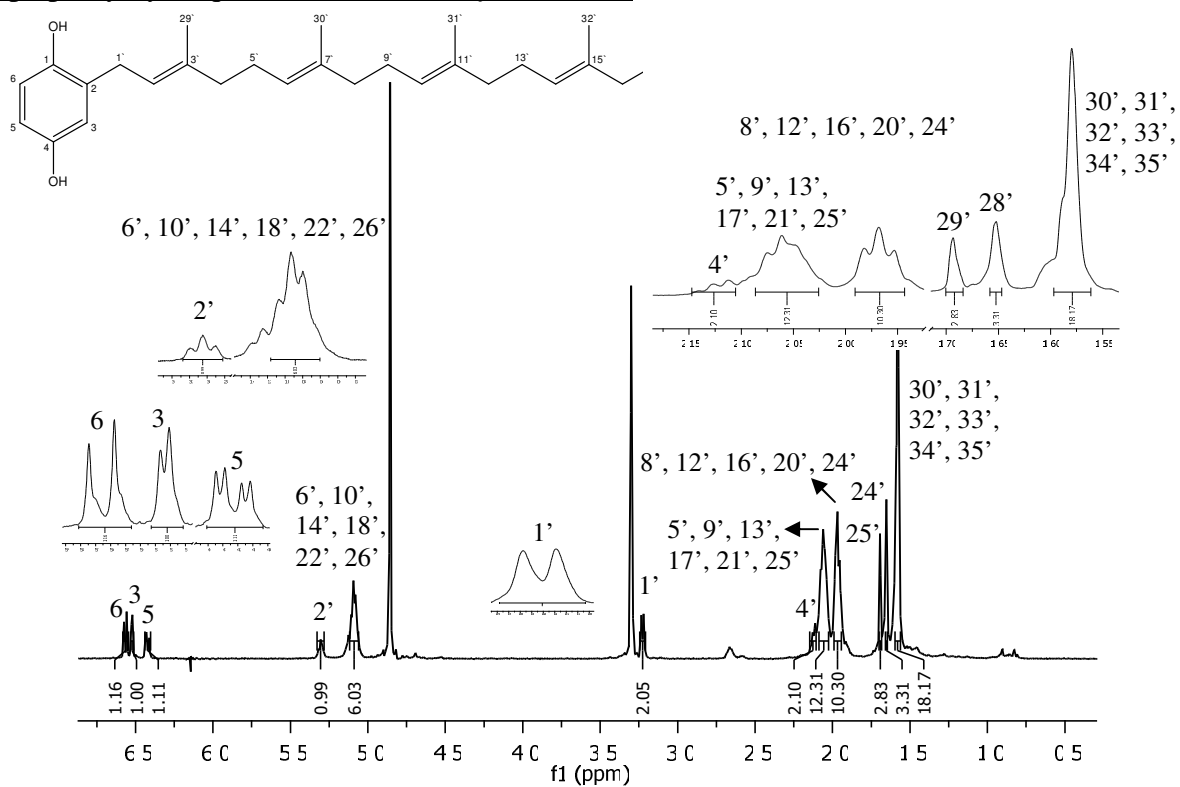


Figure A15. $^1\text{H-NMR}$ of heptaprenylhydroquinone (16) in CD_3OD .

Brominated ambigol A derivative 1 (18) (*Sarcotragus muscarum*)

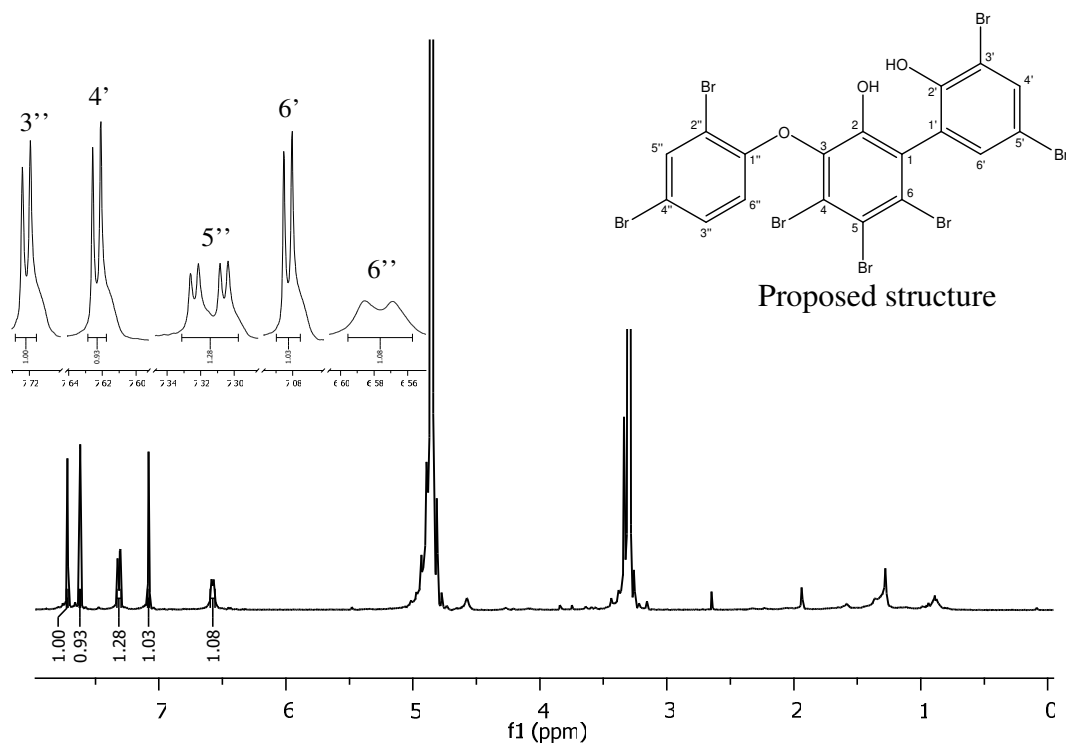
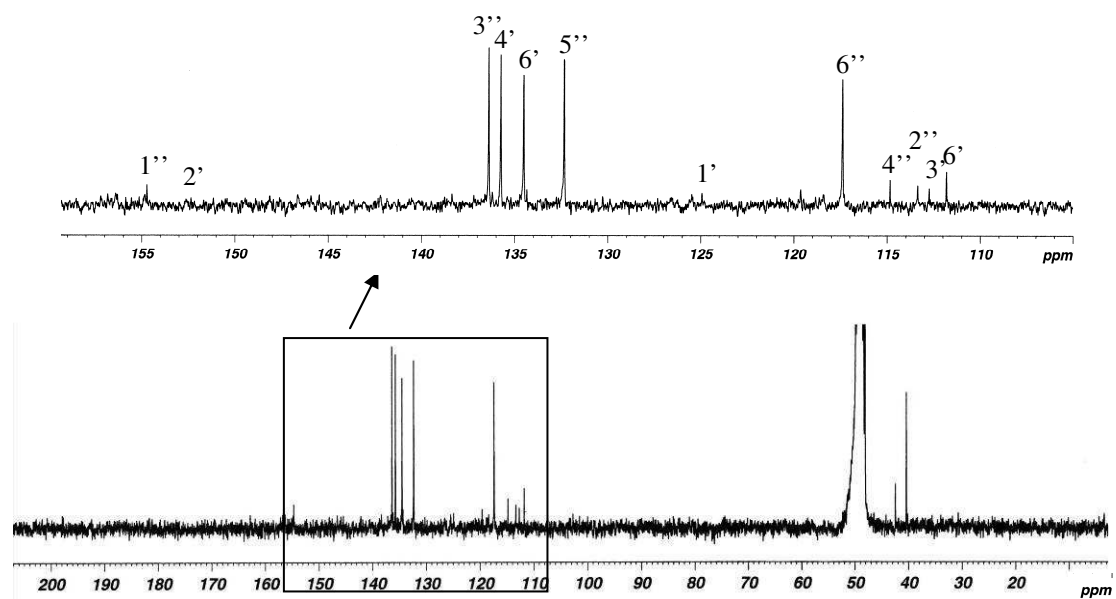
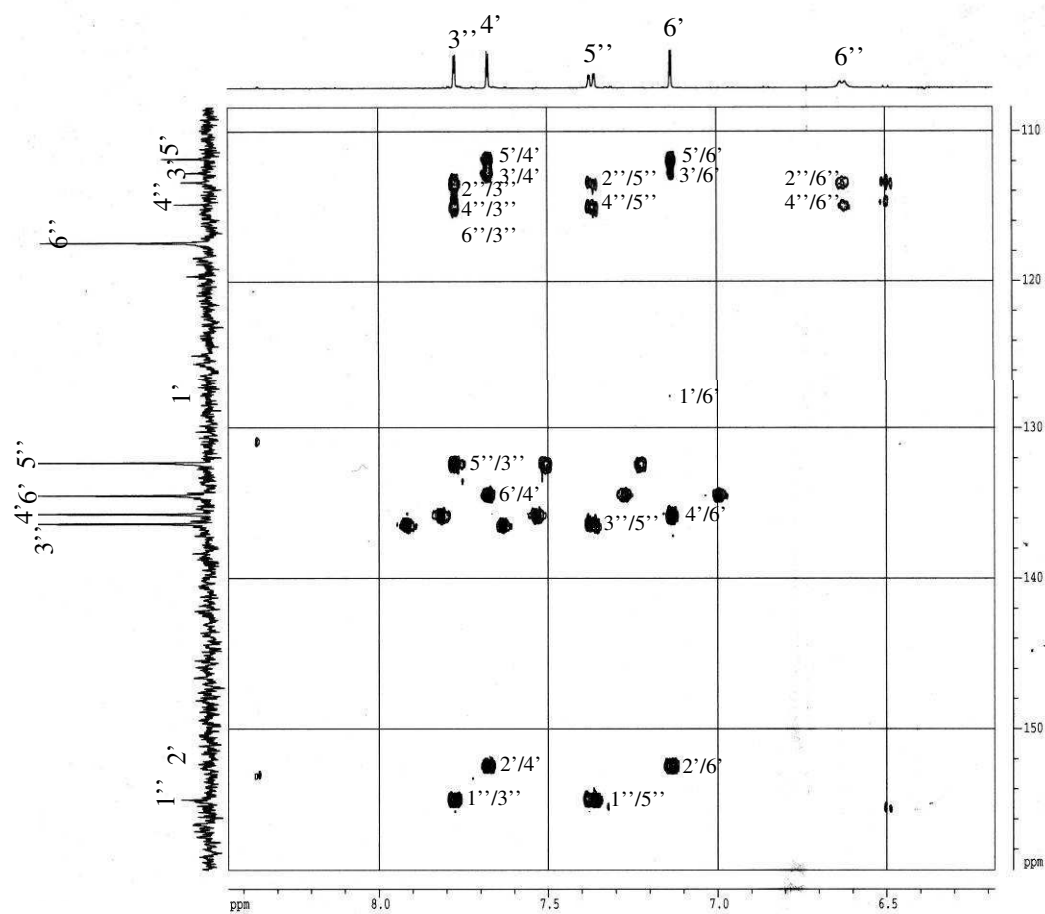
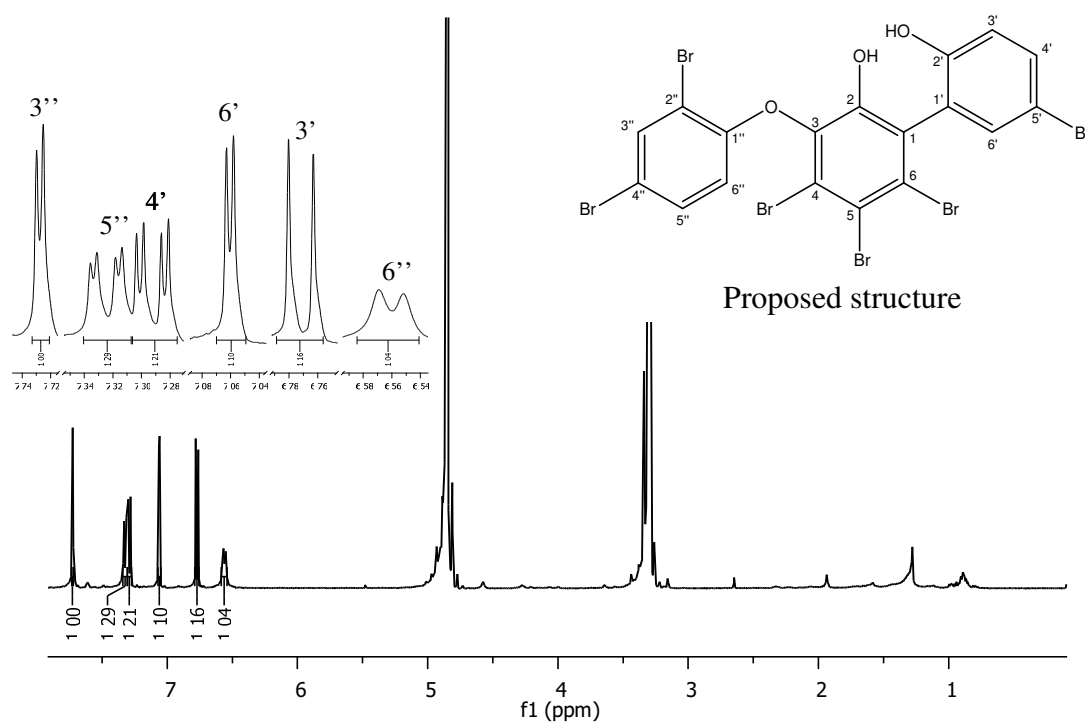
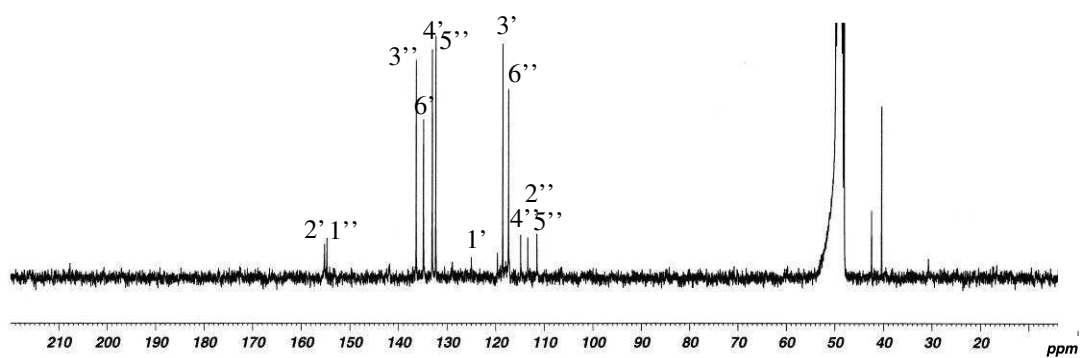
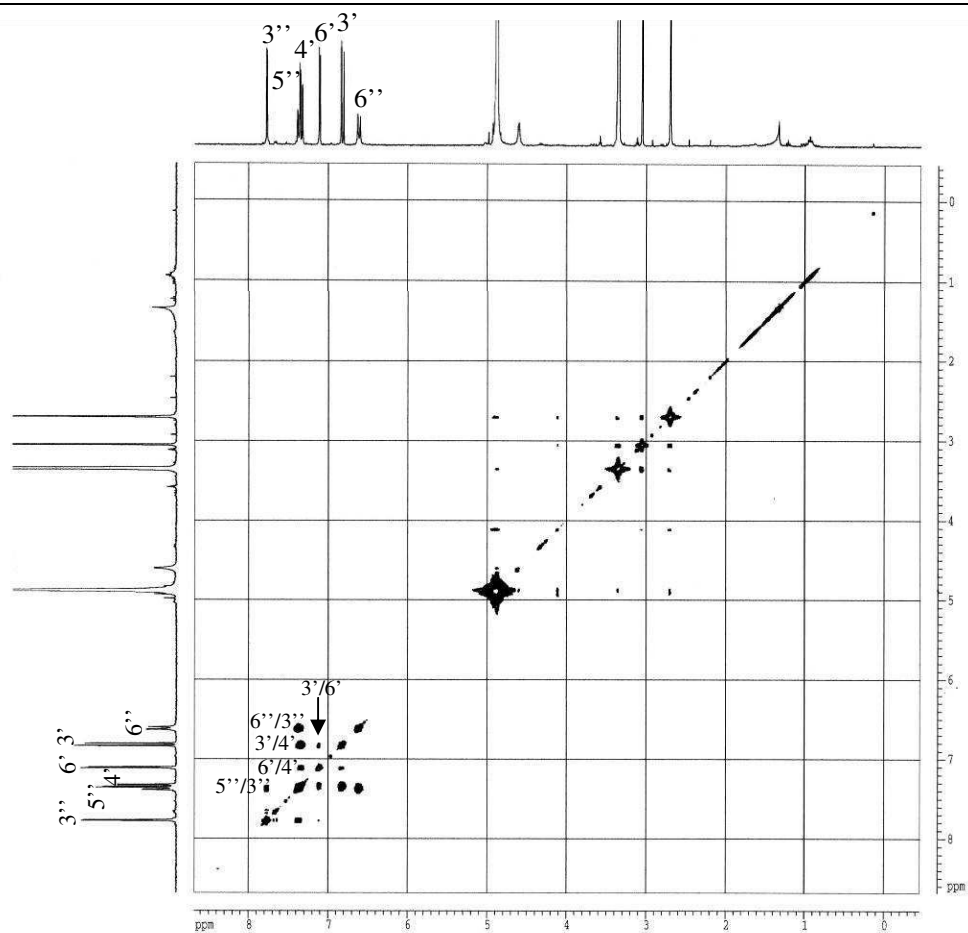
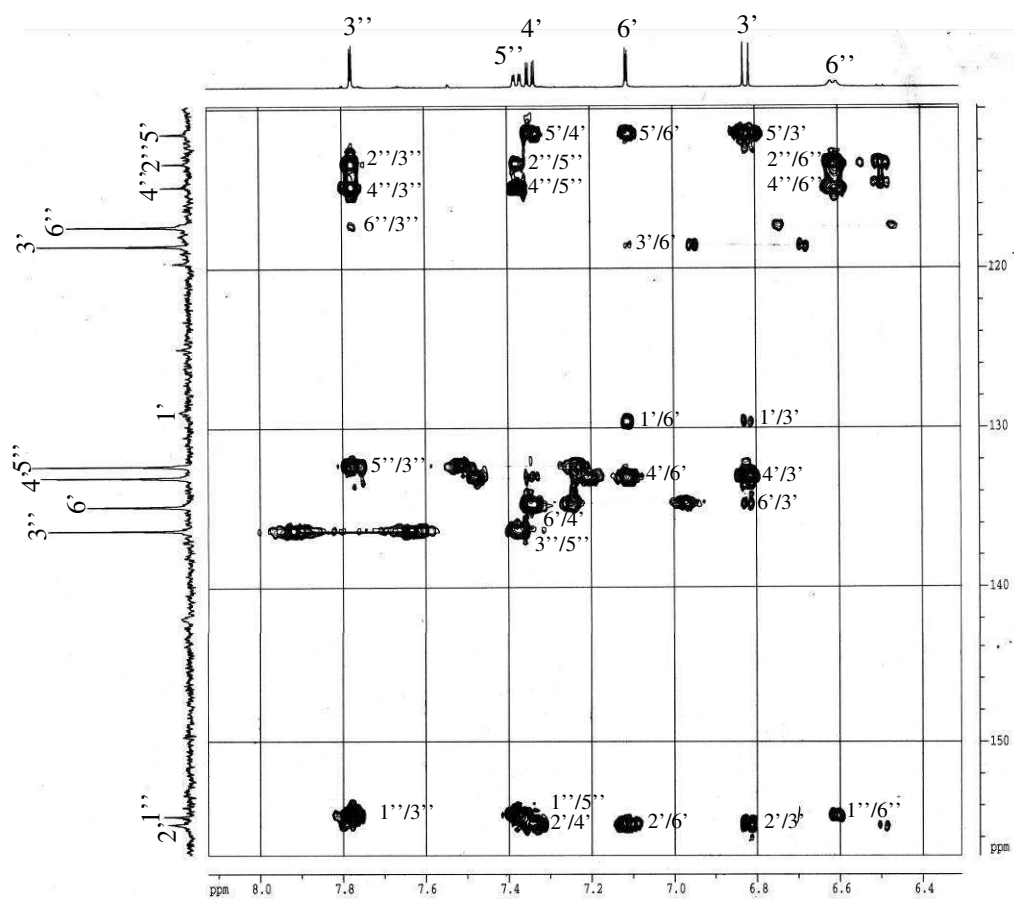
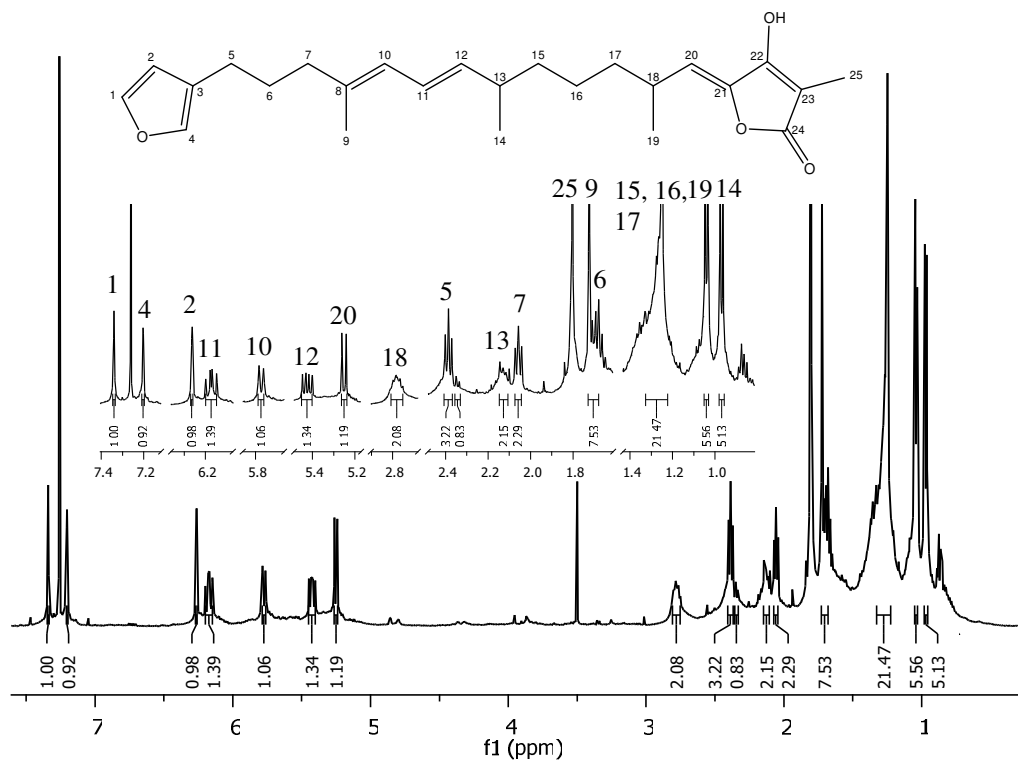
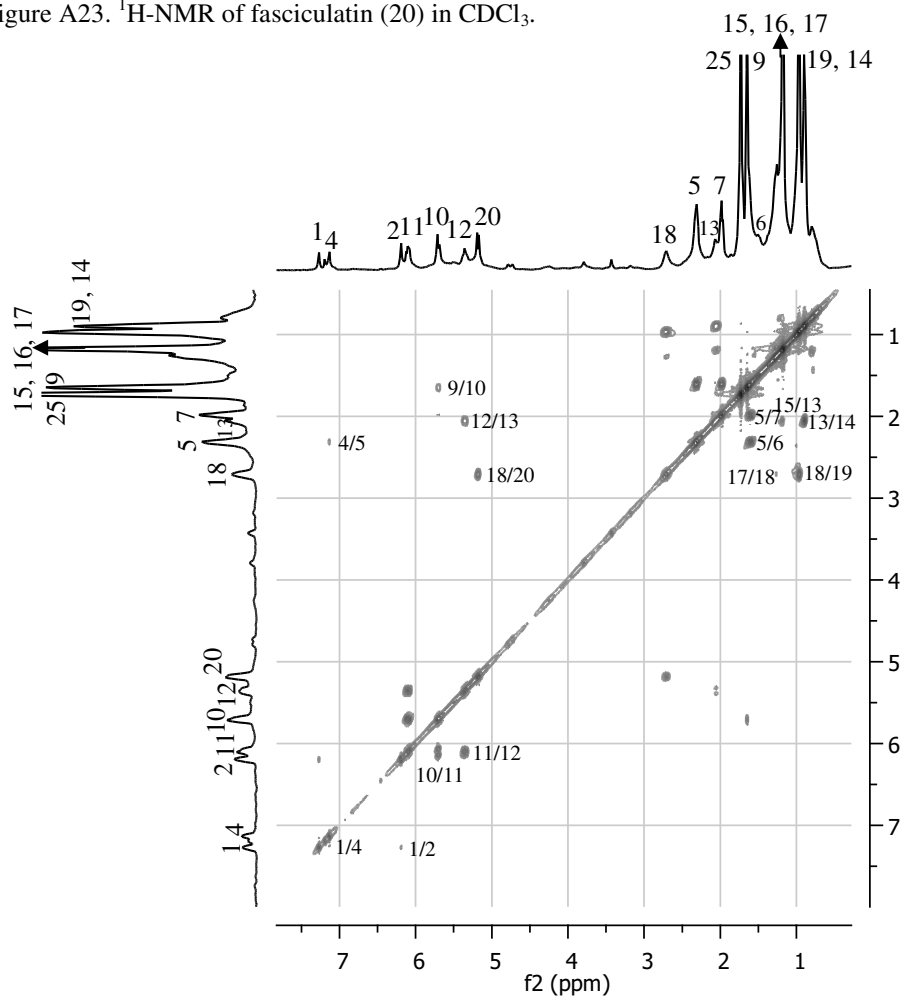


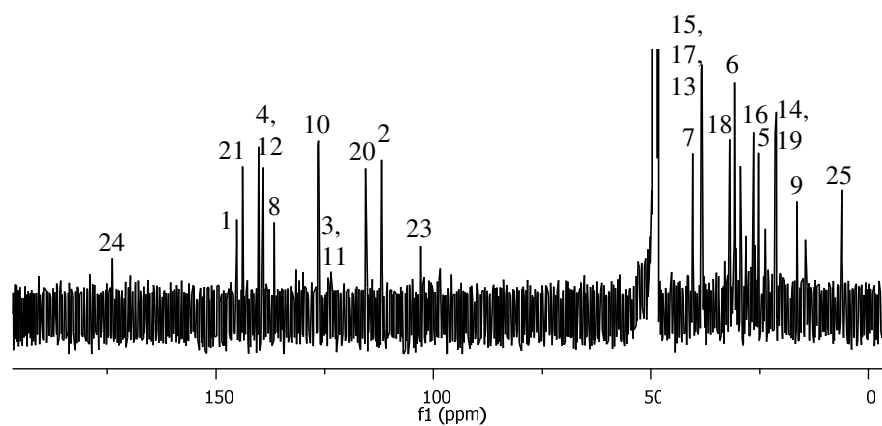
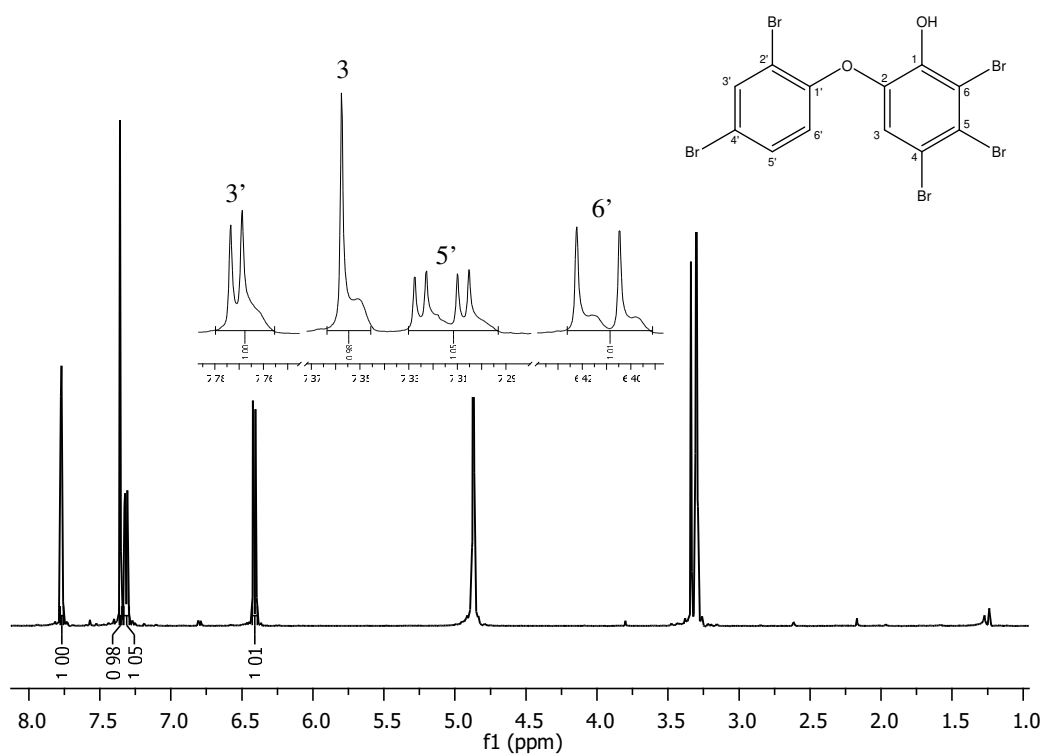
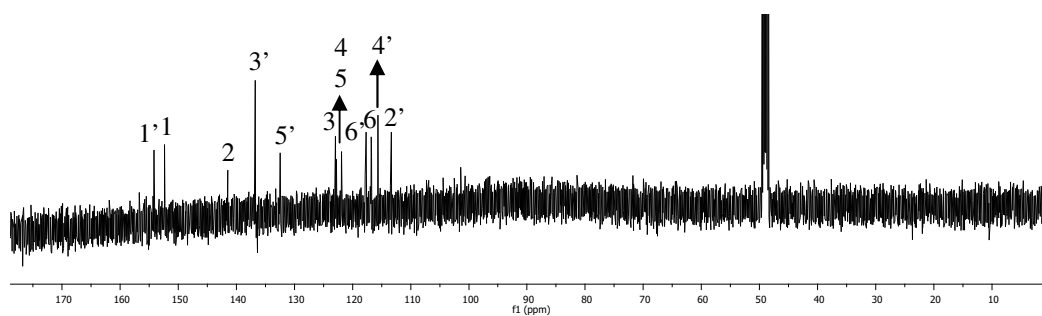
Figure A16. $^1\text{H-NMR}$ of brominated ambigol A derivative 1 (18) in CD_3OD .

Figure A17. ^{13}C -NMR of brominated ambigol A derivative 1 (18) in CD_3OD .Figure A18. HMBC of brominated ambigol A derivative 1 (18) in CD_3OD .

Brominated ambigol A derivative 2 (19) (*Sarcotragus muscarum*)Figure A19. ¹H-NMR of brominated ambigol A derivative 2 (19) in CD₃OD.Figure A20. ¹³C-NMR of brominated ambigol A derivative 2 (19) in CD₃OD.

Figure A21. H,H-COSY of brominated ambigol A derivative 2 (19) in CD₃OD.Figure A22. HMBC of brominated ambigol A derivative 2 (19) in CD₃OD.

Fasciculatin (20) (*Ircinia variabilis*)Figure A23. $^1\text{H-NMR}$ of fasciculatin (20) in CDCl_3 .Figure A24. H,H-COSY of fasciculatin (20) in CDCl_3 .

Figure A25. ^{13}C -NMR of fasciculatin (20) in CDCl_3 .4,5,6-tribromo-2-(2',4'-dibromophenoxy)phenol (21) (*Dysidea granulosa*)Figure A25. ^1H -NMR of 4,5,6-tribromo-2-(2',4'-dibromophenoxy)phenol (21) in CD_3OD .Figure A26. ^{13}C -NMR of 4,5,6-tribromo-2-(2',4'-dibromophenoxy)phenol (21) in CD_3OD .

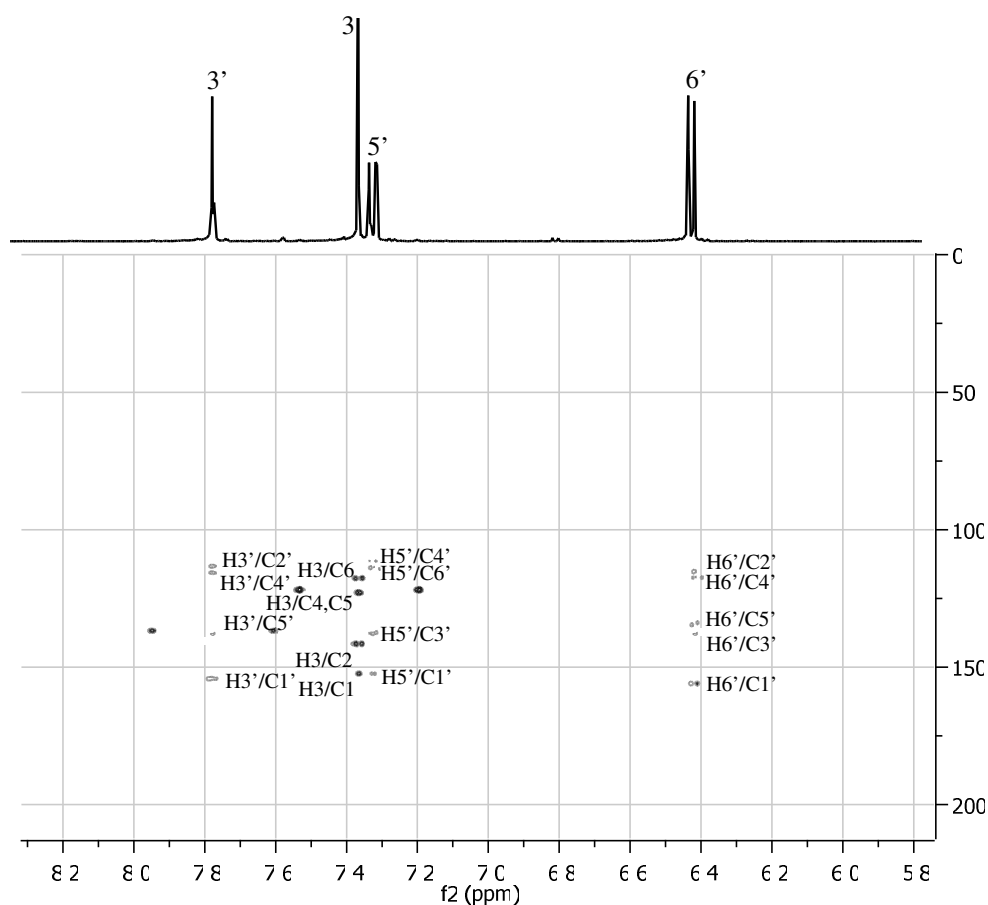


Figure A27. HMBC of 4,5,6-tribromo-2-(2',4'-dibromophenoxy)phenol (21) in CD₃OD.

4,6-Dibromo-2-(2',4'-dibromophenoxy)phenol (22) (*Dysidea granulosa*)

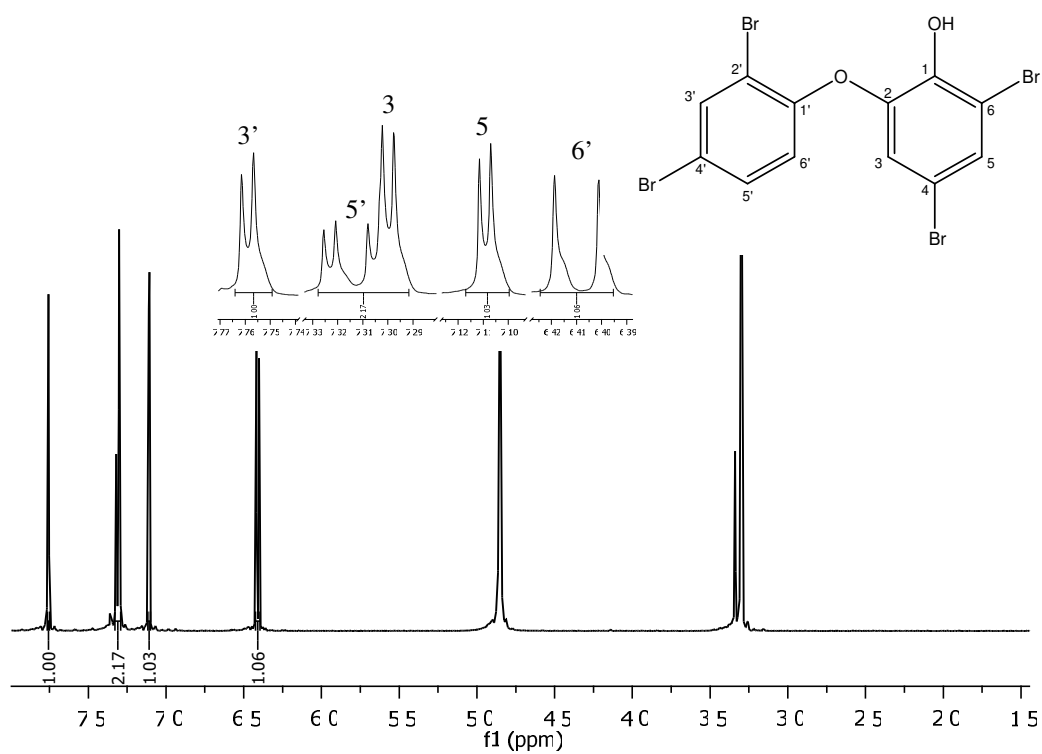
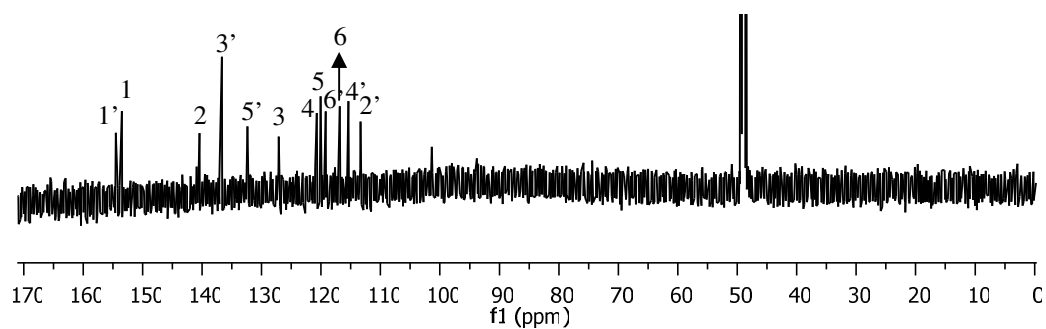
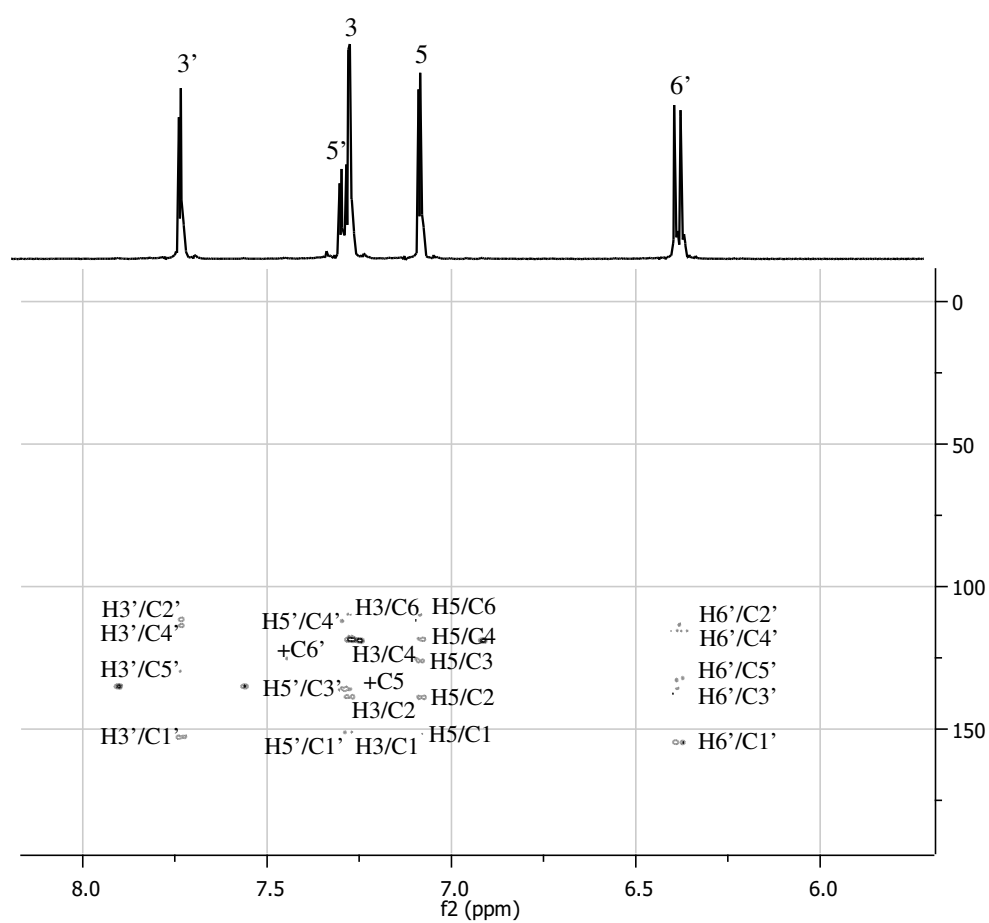
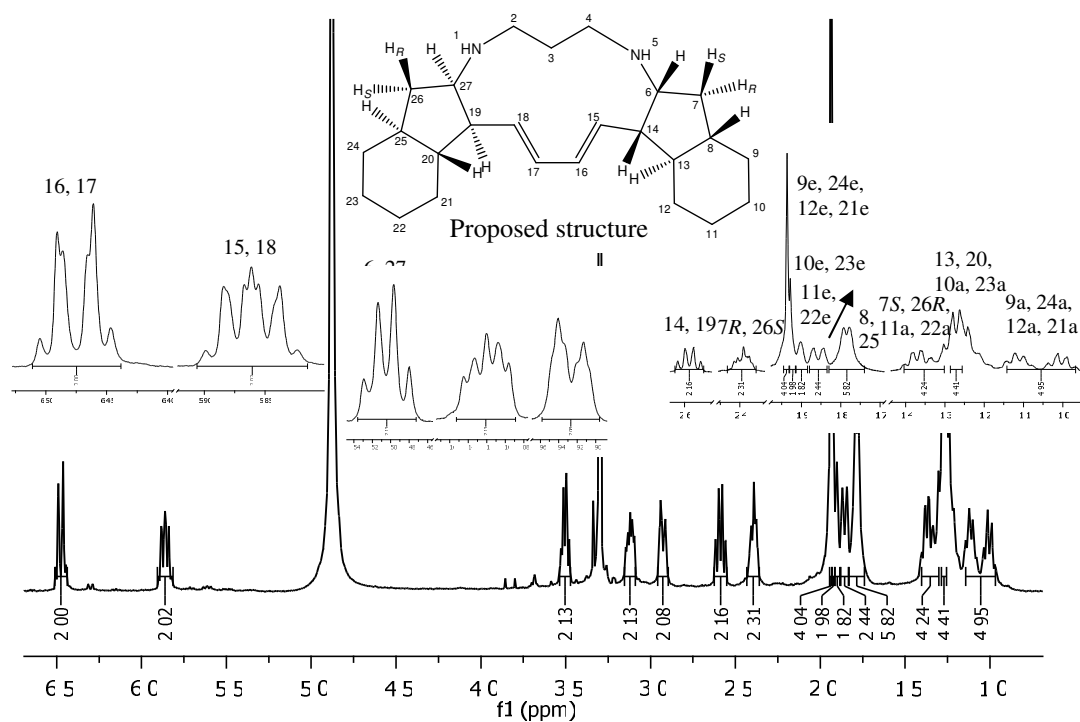
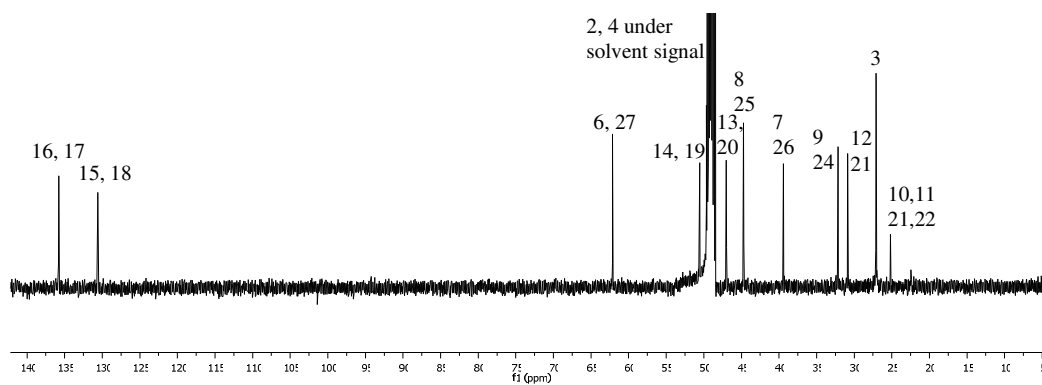


Figure A28. ¹H-NMR of 4,6-dibromo-2-(2',4'-dibromophenoxy)phenol (22) in CD₃OD.

Figure A29. ^{13}C -NMR of 4,6-dibromo-2-(2',4'-dibromophenoxy)phenol (22) in CD_3OD .Figure A30. HMBC of 4,6-dibromo-2-(2',4'-dibromophenoxy)phenol (22) in CD_3OD .

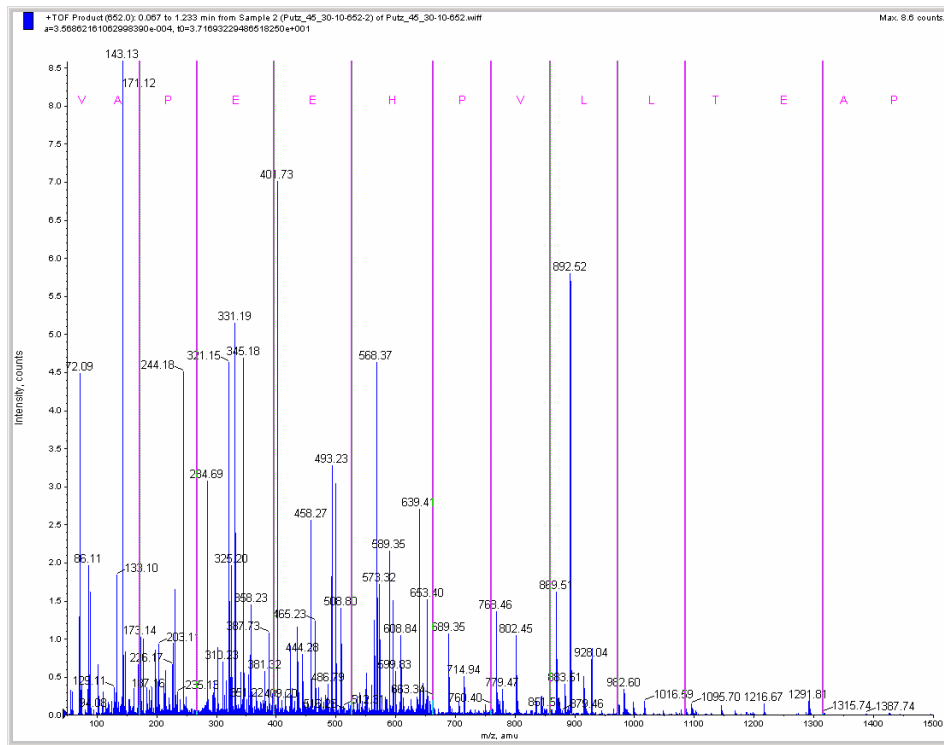
Papouamine (23) (*Haliclona spec*)Figure A31. $^1\text{H-NMR}$ of papouamine (23) in CD_3OD .Figure A32. $^{13}\text{C-NMR}$ of papouamine (23) in CD_3OD .

Supplementary data on *Aplysina* peptide sequences

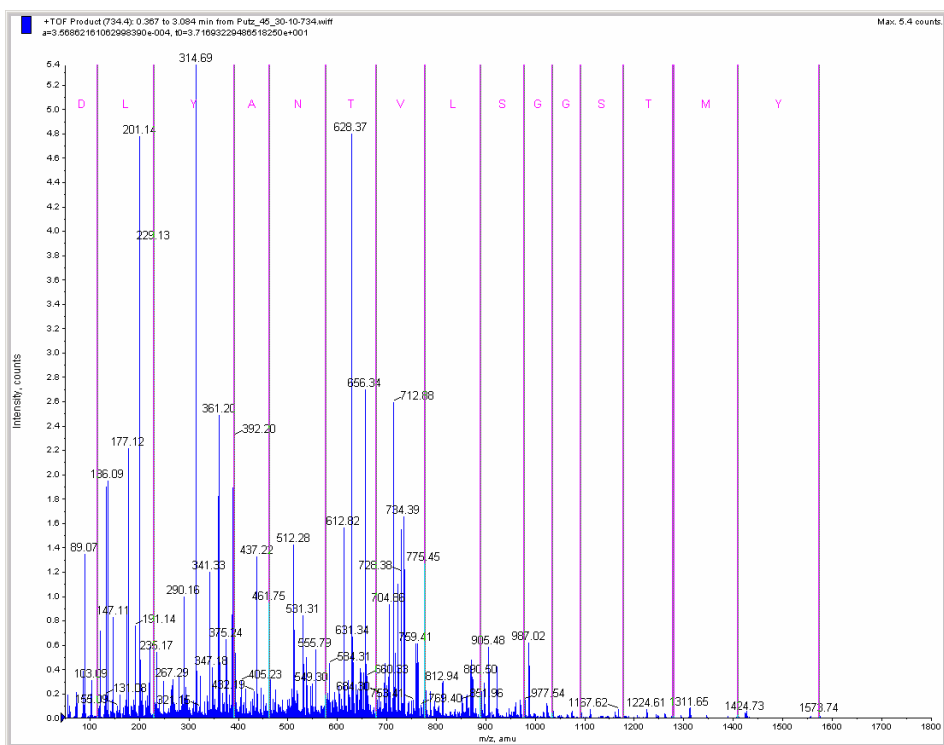
Mass spectra of peptides obtained after trypsin digestion

Actin

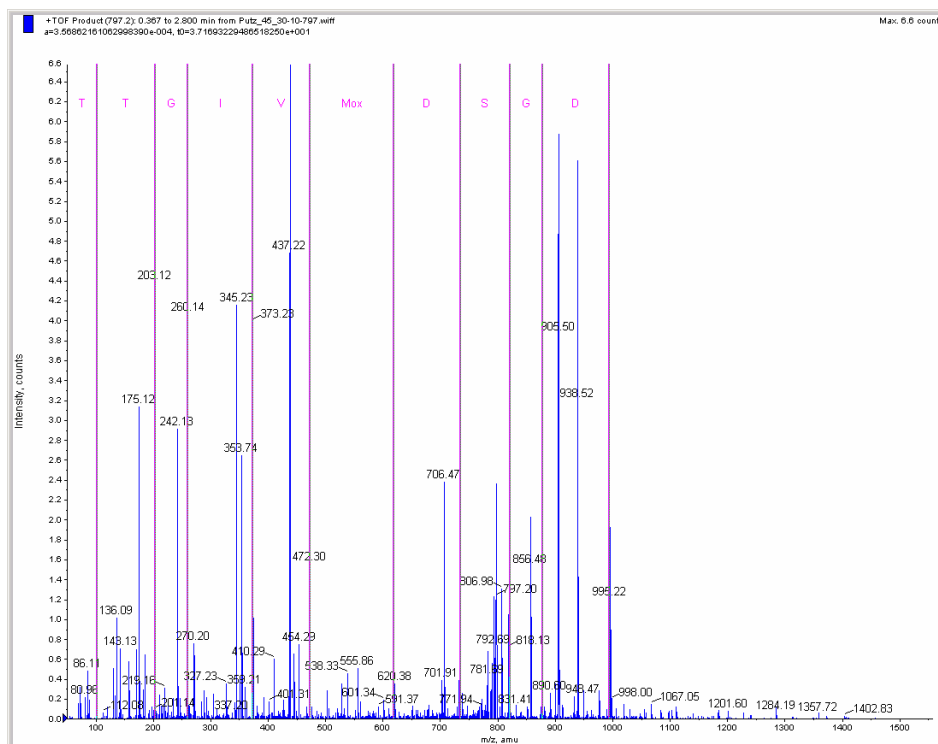
Sequence 1: VAPEEHPVLLTEAPLNPK



Sequence 2: DLYANTVLSGGSTMYPGIADR

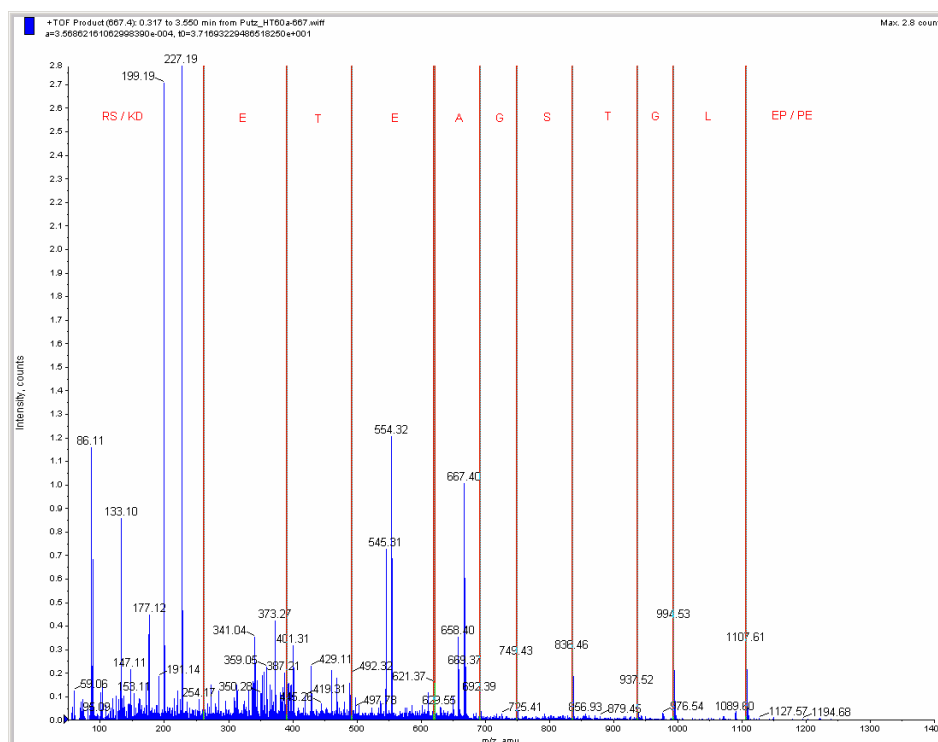


Sequence 3: TTGIVFDSGDGVSH TVPIYEGYALPHAILR

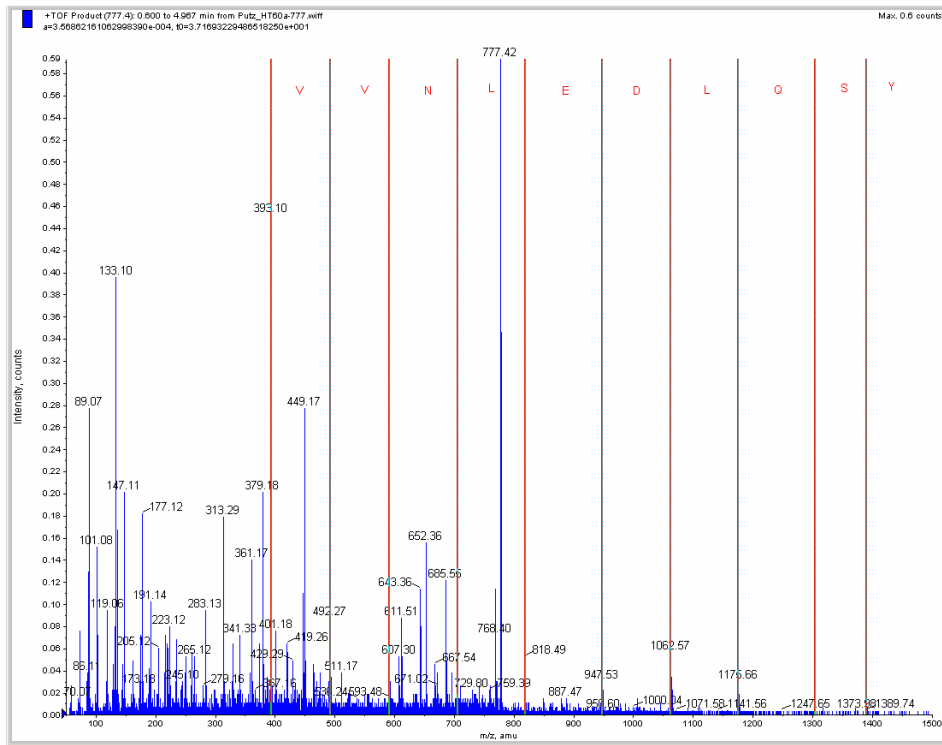


Unknown protein of 60 kDa

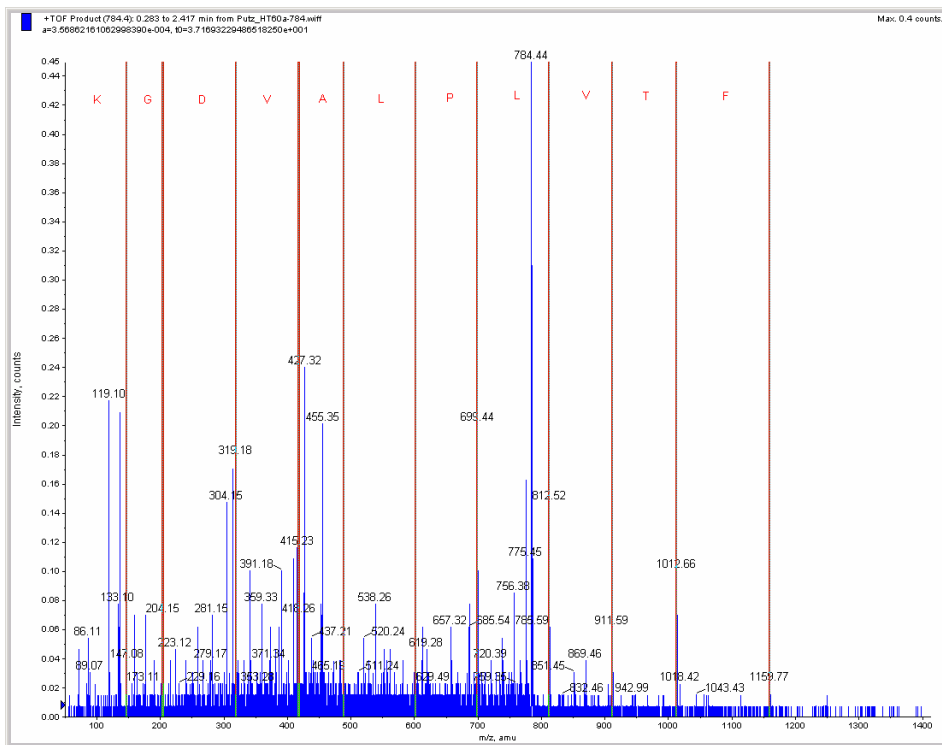
Sequence 1: (EP)LGTS GAETESR oder (EP)LGTS GAETEDK



Sequence 2: YSQLDELNVV.....



Sequence 3: ...FTVL(LP)AVDGK



Results of WU-Blast2 database search for homologous sequences (45 kDa protein)Internet site: <http://www.ebi.ac.uk/Tools/blast2/index.html>, date: 25/01/2009

Sequence searched for: VAPEEHPVLLTEAPLNPK

WU-BLAST2 Results

SUBMISSION PARAMETERS			
Title	Sequence	Database	uniprot
Sequence length	18	Sequence type	p
Program	WU-blastp	Version	2.0MP-WashU [04-May-2006]
Matrix	BLOSUM62	Number of scores	100
Number of alignments	5	Expected threshold	10
Filter	seg		

Alignment	DB-ID	Source	Length	Score	Identity%	Positives%	E()
1 <input type="checkbox"/>	UNIPROT:ACT1_ABSGL	Actin-1 (Fragment) OS=Absidia glauca GN=ACT1 PE=3 SV=1	140	95	100	100	0.0013
2 <input type="checkbox"/>	UNIPROT:ACT1_PSEMZ	Actin-1 (Fragment) OS=Pseudotsuga menziesii PE=1 SV=1	45	95	100	100	0.0013
3 <input type="checkbox"/>	UNIPROT:ACT_CHERU	Actin (Fragment) OS=Chenopodium rubrum PE=3 SV=1	85	95	100	100	0.0013
4 <input type="checkbox"/>	UNIPROT:A5Z2B9_PAXIN	Actin 1 (Fragment) OS=Paxillus involutus GN=actA PE=3 SV=1	84	95	100	100	0.0013
5 <input type="checkbox"/>	UNIPROT:A5Z2C0_PAXIN	Actin 1 (Fragment) OS=Paxillus involutus GN=actA PE=3 SV=1	84	95	100	100	0.0013

Sequence searched for: DLYANTVLSGGSTMYPGIADR

WU-BLAST2 Results

SUBMISSION PARAMETERS			
Title	Sequence	Database	uniprot
Sequence length	21	Sequence type	p
Program	WU-blastp	Version	2.0MP-WashU [04-May-2006]
Matrix	BLOSUM62	Number of scores	100
Number of alignments	5	Expected threshold	10
Filter	seg		

Alignment	DB-ID	Source	Length	Score	Identity%	Positives%	E()
1 <input type="checkbox"/>	UNIPROT:A3EYF0_9ASCI	Actin (Fragment) OS=Botrylloides leachi PE=2 SV=1	131	109	100	100	4.2e-05
2 <input type="checkbox"/>	UNIPROT:Q2LGN4_ANTEL	Beta-actin (Fragment) OS=Anthopleura elegantissima PE=2 SV=1	134	109	100	100	4.2e-05
3 <input type="checkbox"/>	UNIPROT:Q869B3_BOTSH	Cytoplasmic actin (Fragment) OS=Botryllus schlosseri PE=2 SV=1	172	109	100	100	4.2e-05
4 <input type="checkbox"/>	UNIPROT:Q9BMF8_NEMVE	Actin (Fragment) OS=Nematostella vectensis PE=2 SV=1	195	109	100	100	5.9e-05
5 <input type="checkbox"/>	UNIPROT:A9YYK3_ACRMI	Actin (Fragment) OS=Acropora millepora PE=3 SV=1	155	107	95	100	6.8e-05

Sequence searched for: TTGIVFDSGDGVSHTVPIYEGYALPHAILR

Title	Sequence	Database	uniprot			
Sequence length	30	Sequence type	p			
Program	WU-blastp	Version	2.0MP-WashU [04-May-2006]			
Matrix	BLOSUM62	Number of scores	100			
Number of alignments	5	Expected threshold	10			
Filter	seg					

Alignment	DB:ID	Source	Length	Score	Identity%	Positives%	E()
1 <input type="checkbox"/>	UNIPROT:B3XZG4_PSEDP	Actin (Fragment) OS=Pseudocentrotus depressus PE=2 SV=1	195	159	100	100	2.1e-10
2 <input type="checkbox"/>	UNIPROT:Q0QXC9_HELAT	Actin (Fragment) OS=Heliofungia actiniformis PE=3 SV=1	182	159	100	100	2.1e-10
3 <input type="checkbox"/>	UNIPROT:Q86N81_SPHGR	Putative actin protein (Fragment) OS=Sphaerechinus granularis GN=actin PE=2 SV=1	211	159	100	100	2.1e-10
4 <input type="checkbox"/>	UNIPROT:Q2TTE2_9METZ	Actin (Fragment) OS=Discodermia sp. ETS-2004 PE=3 SV=1	257	159	100	100	2.6e-10
5 <input type="checkbox"/>	UNIPROT:Q6ZYL2_9PULM	Actin (Fragment) OS=Arion lusitanicus GN=act PE=2 SV=1	212	156	96	100	4.4e-10

Results of WU-Blast2 database search for homologous sequences (60 kDa protein)Internet site: <http://www.ebi.ac.uk/Tools/blast2/index.html>, date: 01/03/2009

Sequence searched for: (EP)LGTSGAETESR

Alignment	DB:ID	Source	Length	Score	Identity%	Positives%	E()
1 <input type="checkbox"/>	UNIPROT:B0R9I0_HALS3	Putative uncharacterized protein OS=Halobacterium salinarum (strain ATCC 29341 / DSM 671 / R1) GN=OE6116R PE=4 SV=1	76	43	72	90	4.2e+02
2 <input type="checkbox"/>	UNIPROT:Q9HHF3_HALSA	Vng6431h OS=Halobacterium salinarium GN=VNG6431H PE=4 SV=1	76	43	72	90	4.2e+02
3 <input type="checkbox"/>	UNIPROT:A0LPJ1_SYNFM	Putative uncharacterized protein OS=Syntrophobacter fumaroxidans (strain DSM 10017 / MPOB) GN=Sfum_3673 PE=4 SV=1	94	41	100	100	7.8e+02

Sequence searched for: (EP)LGTSGAETEDK

Alignment	DB:ID	Source	Length	Score	Identity%	Positives%	E()
1 <input type="checkbox"/>	UNIPROT:B7QDP8_IXOSC	Putative uncharacterized protein OS=Ixodes scapularis GN=IscW_ISCW022317 PE=4 SV=1	112	45	75	75	4.0e+02
2 <input type="checkbox"/>	UNIPROT:A0LPJ1_SYNFM	Putative uncharacterized protein OS=Syntrophobacter fumaroxidans (strain DSM 10017 / MPOB) GN=Sfum_3673 PE=4 SV=1	94	41	100	100	7.8e+02
3 <input type="checkbox"/>	UNIPROT:B0R9I0_HALS3	Putative uncharacterized protein OS=Halobacterium salinarum (strain ATCC 29341 / DSM 671 / R1) GN=OE6116R PE=4 SV=1	76	40	58	83	8.8e+02
4 <input type="checkbox"/>	UNIPROT:Q9HHF3_HALSA	Vng6431h OS=Halobacterium salinarium GN=VNG6431H PE=4 SV=1	76	40	58	83	8.8e+02
5 <input type="checkbox"/>	UNIPROT:Q0UM81_PHANO	Putative uncharacterized protein OS=Phaeosphaeria nodorum GN=SNOG_07133 PE=4 SV=1	88	40	66	75	8.8e+02
6 <input type="checkbox"/>	UNIPROT:A5VEY3_SPHWW	Secretion protein HlyD family protein OS=Sphingomonas wittichii (strain RW1 / DSM 6014 / JCM 10273)	397	49	69	84	9.7e+02

Sequence searched for: YSQLDELNVV.....

WU-BLAST2 Results

SUBMISSION PARAMETERS			
Title	Sequence	Database	uniprot
Sequence length	10	Sequence type	p
Program	WU-blastp	Version	2.0MP-WashU [04-May-2006]
Matrix	BLOSUM62	Number of scores	100
Number of alignments	50	Expected threshold	1000
Filter	seg		

No significant hits found with the above parameters.

Sequence searched for: ...FTVL(LP)AVDGK

WU-BLAST2 Results

SUBMISSION PARAMETERS			
Title	Sequence	Database	uniprot
Sequence length	10	Sequence type	p
Program	WU-blastp	Version	2.0MP-WashU [04-May-2006]
Matrix	BLOSUM62	Number of scores	100
Number of alignments	50	Expected threshold	1000
Filter	seg		

No significant hits found with the above parameters.

Acknowledgments

I wish to thank Prof. P. Proksch for giving me the opportunity to conduct my PhD at his institute, for his patience, encouragement and steady support during the supervision of my first steps in the field of marine natural product research until the completion of this thesis.

I would further like to express my gratitude to Prof. L. Schmitt for the co-supervision of my work. Many thanks also go to all members of the Department of Biochemistry at the HHU Düsseldorf whose contribution in terms of advice, provision of biochemical equipment and the nice working atmosphere was essential for the outcome of this thesis. I especially thank Dr. N. Hanekop for his never-ending helpfulness, creativity and optimism during biochemical parts of my work, who was never tired to even answer my most stupid questions.

Special thanks are also attributed to Prof. F. Brümmer, Dr. M. Pfannkuchen, G. Fritz and A. Klöppel (Biological Institute, University of Stuttgart) for the great cooperation and help during field work in Rovinj, Croatia and provision of *A. aerophoba* samples for the biochemical work of this thesis. I especially thank Anne for the nice time in Rovinj, and her repeated rescue of “Thylli” from starving.

I deeply appreciate the assistance provided by Dr. R. Ebel and Dr. Edrada-Ebel for the structure elucidation of isolated compounds. I would further like to thank them for many interesting discussions, the nice cooperation during student courses PBI and PBIII, and various great recreational activities such as Christmas bakery...

I would like to express my special thanks to the working group of Prof. W. Müller (Physiological Chemistry and Pathobiochemistry, University of Mainz), to Dr. M. Kubbutat (ProQinase GmbH, Freiburg), and to the working group of PD Dr. W. Wätjen (Institute for Toxicology, HHU Düsseldorf) for the conduction of bioassays.

I further thank Dr. W. Peters and his coworkers for NMR measurements, and Dr. H. Keck and Dr. P. Tommes for conducting MS measurements (Institute for Anorganic and Structural Chemistry, HHU Düsseldorf). I greatly appreciate the help received from Dr. V. Wray (Helmholtz Center for Infection Research, Braunschweig) in terms of selected NMR measurements and discussion of spectra.

My great thanks are also attributed to Dr. Metzger from the BMFZ (Biologisch-Medizinisches Forschungszentrum, HHU Düsseldorf) who was always very helpful and motivated when solving problems encountered during the mass analysis of *Aplysina* proteins.

Dr. R. van Soest, Dr. N. de Voogd (Zoological Museum of the University of Amsterdam, The Netherlands) kindly identified sponges collected for the isolation of bioactive compounds.

Many thanks go to all present and former members I encountered during my time at the Institute for Pharmaceutical Biology. Katrin Rohde and Dieter Jansen gave me their valuable assistance during isolation of compounds. Waltraud Schlag, Katrin Rohde, Eva Müller and Simone Miljanovic always provided steady support and equipment required for this work, even if the organisation of particular chemicals was sometimes challenging. Special thanks are also attributed to Mareike Thiel and Claudia Eckelskemper for the smooth organisation of all administrative things, and for many nice conversations. I especially thank Nadine Weber, my former lab mate, for teaching me everything on the isolation of compounds, and moreover for her steady good mood and friendship. I am very grateful to my “Düsseldorf flat mate” Julia Kjer, with whom I had a lot of nice conversations and fun, and who was always open to listen to my complaints and problems. Many thanks also to the shopping-girls for the nice time! Thank you Dionex team (Dr. Sofia Ortlepp, Arnulf Diesel, Dr. Amal Hassan, Dr. Abdessamad Debbab and Simone Mejanovic) with whom I endured the most challenging Dionex problems. Arnulf, thanks a lot for the great diving lessons! My thanks also go to Clara Grüning whose work during her bachelor thesis lead to the start of the biochemical experiments during the last period of my thesis.

I would like to thank all people who improved first drafts of this thesis by their corrections: Karsten Loesing, Julia Kjer, and Dr. RuAn Edrada-Ebel.

I thank my husband for his steady support, encouragement and cheering-up during my thesis, especially during difficult times.

Finally I express my deep thanks for the Heinrich Heine University of Düsseldorf for granting the “Rektoratsstipendium” for the completion of my work.

Publications

- Putz A, Kloeppe A, Pfannkuchen M, Brümmer F, Proksch P (in press) Influence of depth on alkaloid patterns of Mediterranean *Aplysina* sponges. *Zeitschrift für Naturforschung C*
- Wätjen W, Putz A, Chovolou Y, Kampkötter A, Totzke F, Kubbutat M, Proksch P, Konuklugil B (in press) Hexa-, hepta- and nonaprenylhydroquinone isolated from marine sponges *Sarcotragus muscarum* and *Ircinia fasciculata* inhibit NF-κB signalling in H4IIE cells. *Journal of Pharmacy and Pharmacology*
- Gerce B, Schwartz T, Voigt M, Rühle S, Kirchen S, Putz A, Proksch P, Obst U, Sydatk C, Hausmann R (accepted) Effects of the long-term cultivation of *Aplysina aerophoba* under artificial conditions on the associated bacteria. *Microbial Ecology*
- Putz A, Proksch P (accepted) Chemical defense in marine ecosystems. In: Functions of Plant Secondary Metabolites and their Exploitation in Biotechnology Vol. 4, Ed. M. Wink. Annual Plant Reviews
- Kloeppe A, Pfannkuchen M, Putz A, Proksch P, Brümmer F (2008) *Ex situ* cultivation of *Aplysina aerophoba* close to *in situ* conditions: Ecological, biochemical and histological aspects. *Marine Ecology* 29, 259-272

Presentations

- Putz A, Hankop N, Schmitt L, Proksch P (2009) Biochemical characterisation of the wound-induced biotransformation of *Aplysina* alkaloids. Poster presentation during the symposium “21. Irseer Naturstofftage der DECHEMA e.V.” from 25. – 27.02.2009 in Irsee. The poster was awarded with the poster price.
- Putz A, Thoms C, Kloeppe A, Pfannkuchen M, Brümmer F, Proksch P (2007) Activated chemical defense and intraspecific chemical variation in *Aplysina* sponges. Presentation on the 37th meeting of the Gesellschaft für Ökologie (GfÖ) from 10.09. – 14.09.07 in Marburg.
- Putz A (2006) Intraspecific variation of alkaloids in *Aplysina aerophoba*. Presentation during the annual BIOTECmarin meeting in Mainz from 20. – 21.02.06.

Curriculum vitae

Name: Annika Putz
Address: Sankt-Augustinus-Strasse 18
53173 Bonn
Date of birth: 15.07.1980
Place of birth: Münster
Nationality: German
Civil status: Married

Education

Since July 2005 PhD at the HHU Düsseldorf
Institute for Pharmaceutical Biology and Biotechnology
August 2004 Diploma in biology
October 2001 Pre-diploma
October 1999 Studies of biology (Westfälische Wilhelms-Universität Münster)
1990 – 1999 Secondary school (Wilhelm-Hittorf-Gymnasium Münster)
1986 – 1990 Primary school (Peter-Wust-Schule Münster)

Stays abroad

November 2004 Trip to Australia and New Zealand, November / December 2004
- February 2005 work as field assistant in Australia, LIRS.
October 2003 Collection of data for diploma thesis in Australia, Lizard Island
- February 2004 Research Station (LIRS).

Stipends

01.01.08 - 31.12.08 Rektoratsstipendium (Heinrich Heine Universität
Düsseldorf, Graduiertenförderung)
25.10.03 - 22.02.04 Stipend of the German Academic Exchange Service
(DAAD, „Förderung zur Anfertigung von Abschluss-
arbeiten im Ausland“).

Düsseldorf, den

Erklärung

Ich versichere, dass ich die vorliegende Dissertation mit dem Titel “Secondary metabolites from marine sponges, with focus on the chemical ecology and biochemical characterisation of the stress-induced biotransformation of *Aplysina* alkaloids“ selbständig angefertigt habe und keine anderen als die angegebenen Quellen und Hilfsmittel verwendet habe. Die eingereichte Arbeit habe ich in dieser oder ähnlicher Form noch keinem anderen Prüfungsausschuss vorgelegt.

Düsseldorf, den

Annika Putz